UNIVERSIDAD AUTÓNOMA DE SAN LUIS POTOSÍ

FACULTAD DE CIENCIAS QUÍMICAS

Posgrado en Ciencias Farmacobiológicas

Efecto del extracto acuoso liofilizado de *Calea urticifolia* (Mill.) DC. en modelos *in vivo* de diabetes mellitus y neuropatía periférica diabética

Tesis para obtener el grado de:
Doctorado en Ciencias Farmacobiológicas

Presenta:
Segura Esparragoza Edgar Omar

Directora de Tesis
Dra. Erika García Chávez

Co-Director de Tesis
Dr. Ismael Jiménez Estrada

SAN LUIS POTOSÍ, S.L.P. AGOSTO 2025

Este proyecto se realizó en el Laboratorio de Recursos Bióticos del Instituto de Investigación de Zonas Desérticas, en el Bioterio de la Facultad de Medicina de la Universidad Autónoma de San Luis Potosí y en el Laboratorio de Fisiología del Desarrollo del Departamento de Fisiología, Biofísica y Neurociencias del Centro de Investigación y de Estudios Avanzados del Instituto Politécnico Nacional (CINVESTAV-IPN), en el periodo comprendido entre febrero 2018 y febrero 2022, bajo la dirección de la Dra. Erika García Chávez y el Dr. Ismael Jiménez Estrada y fue apoyado por recursos propios del grupo colaborativo de este proyecto y del Cuerpo Académico de Recursos Bióticos CA-206.

El programa de Doctorado en Ciencias Farmacobiológicas de la Universidad Autónoma de San Luis Potosí pertenece al Sistema Nacional de Posgrados de Calidad (SNP) del CONAHCyT, registro 003383. Número de registro de la beca otorgada por CONAHCyT: 589776, con número de CVU 705751.

Los datos del trabajo titulado “Efecto del extracto acuoso liofilizado de *Calea urticifolia* (Mill) DC en modelos *in vivo* de diabetes mellitus y neuropatía periférica diabética” se encuentran bajo el resguardo de la Facultad de Ciencias Químicas y pertenecen a la Universidad Autónoma de San Luis Potosí.

UNIVERSIDAD AUTÓNOMA DE SAN LUIS POTOSÍ
FACULTAD DE CIENCIAS QUÍMICAS

Posgrado en Ciencias Farmacobiológicas

05 de Junio de 2018, San Luis Potosí.

Asunto: **Registro de tema de tesis de Doctorado PCFB**

COMITÉ ACADÉMICO DEL POSGRADO EN CIENCIAS FARMACOBIOLÓGICAS
FACULTAD DE CIENCIAS QUÍMICAS. UASLP.
PRESENTE.-

Estudiante:
M.C. Segura Esparragoza Edgar Omar

Título:
"Efecto hipoglucemiante y antioxidante del extracto acuoso liofilizado de *Calea urticifolia* (MILL.) DC. en un modelo *in vivo* de neuropatía periférica diabética"

Línea de investigación en la que se inserta la tesis:
Desarrollo y Evaluación de Medicamentos
Subcomité Tutorial:

Integrantes	Firma
Dra. Erika García Chávez Directora de Tesis Profesora-Investigadora de IIZD-UASLP	
Dr. Ismael Jiménez Estrada Co-director Profesor-Investigador 3C de CINVESTAV-IPN Zacatenco	
Dra. Perla del Carmen Niño Moreno Asesor Profesor-Investigador de PCFB-FCQ-UASLP	
Dra. Claudia Castillo Martín del Campo Asesor externo Profesor-Investigador de PCBB-FM-UASLP	

III

UNIVERSIDAD AUTÓNOMA DE SAN LUIS POTOSÍ
FACULTAD DE CIENCIAS QUÍMICAS

Posgrado en Ciencias Farmacobiológicas

Trabajo de tesis vinculada con:

Convenio _____ Servicio _____ Proyecto_____ Grupo __X___ Artículo _____

Financiamiento de Tesis otorgado por

Institución, organismo o asociación:

Instituto de Investigación de Zonas Desérticas

Nombre del Proyecto en su caso: Caracterización del efecto hipoglucemiante del extracto acuoso de *Calea urticifolia* Mill (DC) sobre un modelo de hiperglucemia química y por alimentación rica en grasa

Monto: $ 50,000

Fecha de ejecución del proyecto:

13 de agosto de 2018

Objetivo del proyecto: Evaluar la co-administración de CuAqE con fármacos hipoglucemiantes en un modelo *in vivo* de diabetes mellitus tipo II; además se pretende valorar su posible efecto antioxidante en la neuropatía diabética por medio de estudios electrofisiológicos y de estrés oxidativo.

Participantes en el proyecto:

Dra. Erika García Chávez. Profesora-Investigadora de IIZD-UASLP

Dr. Ismael Jiménez Estrada. Profesor-Investigador 3C de CINVESTAV-IPN Zacatenco

Dra. Claudia Castillo Martín del Campo. Profesor-Investigador de PCBB-FM-UASLP

Atentamente

Dra. Erika García Chávez
Directora de Tesis

UASLP
Universidad Autónoma
de San Luis Potosí

Comité de Ética en Investigación y Docencia de la Facultad de Ciencias Químicas
Registro CONBIOÉTICA24CEI00820131212

10 de abril de 2019

DRA. ERIKA GARCÍA CHÁVEZ
PROFESORA INVESTIGADORA
INSTITUTO DE INVESTIGACIÓN DE ZONAS DESÉRTICAS
UNIVERSIDAD AUTÓNOMA DE SAN LUIS POTOSÍ
PRESENTE.

Con relación a su solicitud de revisión del protocolo titulado **"EFECTO HIPOGLUGEMIANTE Y ANTIOXIDANTE DEL EXTRACTO ACUOSO LIOFILIZADO DE *Calea urticifolia* (Mill.) DC. EN UN MODELO *IN VIVO* DE NEUROPATÍA PERIFÉRICA DIABÉTICA",** el Comité de Investigación y Docencia de la Facultad de Ciencias Químicas (CEID-FCQ) por mi conducto le informa que en la sesión del 10 de abril del año en curso, tomó la decisión de dictaminar este protocolo **APROBADO.** El dictamen cuenta con el registro **CEID2018015R2.**

Conforme al Reglamento del CEID-FCQ, todo protocolo registrado y aprobado queda sujeto al seguimiento señalado en el Art. 13, en particular al apartado 13.2.2:

El profesor o investigador responsable deberá entregar al CEID-FCQ un informe al término del proyecto ante la suspensión prematura del estudio o cuando le sea requerido. Si el proyecto no ha sido terminado en el lapso de un año deberá entregarse un informe anual que señale el grado de avance. Para la entrega de este informe se considerará un año transcurrido desde la fecha de emisión del dictamen de aprobación y un lapso no mayor de 10 días hábiles. El incumplimiento de lo anterior impedirá la revisión de un nuevo protocolo del investigador solicitante. El informe se enviará al CEID-FCQ con una carta de presentación dirigida al Presidente, así como el respectivo informe.

ATENTAMENTE

Dra. Rosa del Carmen Milán Segovia
Presidenta del CEID-FCQ

Ccp. Archivo

FACULTAD DE
CIENCIAS QUÍMICAS
Av. Dr. Manuel Nava Núm. 6
Zona Universitaria • CP 78210
San Luis Potosí, S.L.P.
tel. (444) 826 24 40 al 46
fax (444) 826 2372
www.uaslp.mx

UNIVERSIDAD AUTÓNOMA DE SAN LUIS POTOSÍ

FACULTAD DE CIENCIAS QUÍMICAS

Posgrado en Ciencias Farmacobiológicas

Efecto del extracto acuoso liofilizado de *Calea urticifolia* (Mill.) DC. en modelos *in vivo* de diabetes mellitus y neuropatía periférica diabética

Tesis para obtener el grado de:
Doctorado en Ciencias Farmacobiológicas

Presenta:
Segura Esparragoza Edgar Omar

SINODALES

Presidente: Dr. Gerson Alonso Soto Peña _____

Secretaria: Dra. Erika García Chávez _____

Vocal: Dr. Ismael Jiménez Estrada _____

Vocal: Dra. Claudia G. Castillo M. del Campo _____

Vocal: Dra. Perla del Carmen Niño Moreno _____

SAN LUIS POTOSÍ, S.L.P. AGOSTO 2025

INTEGRANTES DEL COMITÉ TUTORIAL ACADÉMICO

Dra. Erika García Chávez: Directora de tesis. Colaboradora del Posgrado en Ciencias Farmacobiológicas de la Universidad Autónoma de San Luis Potosí, San Luis Potosí, S.L.P. Adscrita al Instituto de Investigación de Zonas Desérticas (IIZD) de la UASLP.

Dr. Ismael Jiménez Estrada: Codirector de tesis. Asesor externo del Posgrado en Ciencias Farmacobiológicas de la Universidad Autónoma de San Luis Potosí, San Luis Potosí, S.L.P. Adscrito al Departamento de Fisiología, Biofísica y Neurociencias, del Centro de Investigación y de Estudios Avanzados del Instituto Politécnico Nacional (CINVESTAV-IPN), campus Zacatenco, CDMX.

Dra. Claudia Guadalupe Castillo Martín del Campo: Asesora de tesis. Colaboradora del Posgrado en Ciencias Farmacobiológicas de la Universidad Autónoma de San Luis Potosí, San Luis Potosí, S.L.P. Adscrita a Coordinación para la Innovación y Aplicación de la Ciencia y la Tecnología (CIACYT) de la UASLP.

Dra. Perla del Carmen Niño Moreno: Asesora de tesis. Núcleo Académico del Posgrado en Ciencias Farmacobiológicas de la Universidad Autónoma de San Luis Potosí, San Luis Potosí, S.L.P. Adscrita al Departamento de Genómica Médica del Centro de Investigación en Ciencias de la Salud y Biomedicina (CICSaB) de la UASLP.

Dr. Gerson Alonso Soto Peña: Tutor de tesis. Colaborador del Posgrado en Ciencias Farmacobiológicas de la Universidad Autónoma de San Luis Potosí, San Luis Potosí, S.L.P. Adscrito al Laboratorio de Análisis Químicos y Biológicos de la Facultad de Ingeniería, UASLP, México.

Formato D5

Carta Cesión de Derechos

San Luis Potosí, S.L.P. a 16 de junio del 2025

En la ciudad de **San Luis Potosí** el día 16 del mes de junio del año 2025, el que suscribe **M.C. Edgar Omar Segura Esparragoza**, estudiante del programa de **Posgrado en Ciencias Farmacobiológicas** adscrito a **Facultad de Ciencias Químicas** manifiesta que es *autor intelectual* del presente trabajo terminal, realizado bajo la dirección de: **Dra. Erika García Chávez e Ismael Jiménez Estrada** y *cede los derechos* del trabajo titulado **"Efecto del extracto acuoso liofilizado de *Calea urticifolia* (Mill.) DC. en modelos *in vivo* de diabetes mellitus y neuropatía periférica diabética**"; a la **Universidad Autónoma de San Luis Potosí**, para su difusión con fines académicos y de investigación.

Los usuarios de la información no deben reproducir de forma total o parcial texto, gráficas, imágenes o cualquier contenido del trabajo si el permiso expreso del o los autores. Éste, puede ser obtenido directamente con el autor o autores escribiendo a la siguiente dirección erika.garcía@uaslp.mx. Si el permiso se otorga, el usuario deberá dar el agradecimiento correspondiente y citar la fuente del mismo.

_____

M.C. Edgar Omar Segura Esparragoza

UNIVERSIDAD AUTÓNOMA DE SAN LUIS POTOSÍ
Facultad de Ciencias Químicas
Centro de Investigación y Estudios de Posgrado
Posgrado en Ciencias Farmacobiológicas
Programa de Doctorado

Formato D28

Carta de Análisis de Similitud

San Luis Potosí, S.L.P. A 04 de julio de 2025.

L.B. María Zita Acosta Nava
Biblioteca de Posgrado FCQ

Asunto: Reporte de porcentaje de similitud de tesis de grado

Por este medio me permito informarle el porcentaje de similitud obtenido mediante Ithenticate para la tesis titulada: “Efecto del extracto acuoso liofilizado de *Calea urticifolia* (Mill.) DC. en modelos *in vivo* de diabetes mellitus y neuropatía periférica diabética” presentada por el autor Segura Esparragoza Edgar Omar. La tesis es requisito para obtener el grado de Doctorado en el Posgrado en Ciencias Farmacobiológicas. El análisis reveló un porcentaje de similitud de 13% de Similitud excluyendo referencias y metodología.

Agradezco sinceramente su valioso tiempo y dedicación para llevar a cabo una exhaustiva revisión de la tesis. Quedo a su disposición para cualquier consulta o inquietud que pueda surgir en el proceso.

Sin más por el momento, le envío un cordial saludo.

A T E N T A M E N T E

_____
Dra. Claudia Escudero Lourdes
Coordinadora Académica del Posgrado
en Ciencias Farmacobiológicas

Dedicatoria

Hijo mío, si recibes mis palabras y guardas contigo mis mandamientos, prestando oído a la sabiduría e inclinando tu corazón al entendimiento; si llamas a la inteligencia y elevas tu voz hacia el entendimiento, si la buscas como si fuera plata y la exploras como un tesoro, entonces comprenderás el temor del Señor y encontrarás la ciencia de Dios. Porque el Señor da la sabiduría, de su boca proceden la ciencia y la inteligencia. Él reserva su auxilio para los hombres rectos, es un escudo para los que caminan con integridad; Él protege los senderos de la equidad y cuida el camino de sus fieles. (Cfr. Prov. 2:1-6).

A Dios

por ser el motor de mi vida y por sus innumerables bendiciones

A mis padres

Irene Segura Esparragoza Urbano Vázquez Hernández
Ma. Teresa Segura Esparragoza

Por su comprensión, apoyo y amor incondicional.
Así como al resto de mi familia y amigos por siempre sentirse orgulloso de mí, así mismo para aquellas personas que estuvieron colaborando con mi proyecto de vida y con cariño para mi pueblo Santa María del Río.

Agradecimientos

A la Universidad Autónoma de San Luis Potosí especialmente a la Facultad de Ciencias Químicas, por brindarme los conocimientos para mi formación y desarrollo profesional.

Al Instituto de Investigación de Zonas Desérticas de la Universidad Autónoma de San Luis Potosí; particularmente a Dra. Erika García Chávez por darme la oportunidad de trabajar en este proyecto bajo su dirección, así como por confiar en mí, por su apoyo, comprensión y amistad, así como por el interés en mi formación profesional.

Al Centro de Investigación y de Estudios Avanzados del Instituto Politécnico Nacional (CINVESTAV-IPN), campus Zacatenco, CDMX; concretamente al Dr. Ismael Jiménez Estrada por su colaboración en el proyecto, sus aportaciones y recomendaciones y a su equipo de trabajo del laboratorio por mostrarme un sentido humanista de la colaboración académica.

Así mismo a Dra. Claudia G. Castillo M. del Campo y Dra. Perla del Carmen Niño Moreno por su orientación y apoyo incondicional para desarrollar la parte experimental.

A Dra. Lucina Torres Rodríguez y Dra. Ma. de los Ángeles Zermeño Macías por su amistad, por compartir experiencias, locuras, consejos y sobre todo por su apoyo incondicional en el trabajo experimental.

A Dr. Vladimir Martínez Álvarez, M.C.A. Juan Francisco López Rodríguez y todo el equipo de trabajo del bioterio de la Facultad de Medicina de la UASLP, a QFB César Eduardo Padrón Flores por su apoyo durante el trabajo experimental.

A Teresa Huerta Mendoza, Dionisio Hernández Cadena, María Guadalupe González Tenorio, Pbro. Efraín Moreno Aguirre, QFB Olimpia Segura Hernández y QFB Julián Bueno Godoy; por su amistad y apoyo siempre y finalmente un agradecimiento a todas aquellas personas que de alguna manera contribuyeron para que la realización de este proyecto de investigación fuera concretada con éxito.

RESUMEN

La diabetes mellitus (DM) es una enfermedad crónica caracterizada por deficiencia en la producción o acción de la insulina, lo que genera hiperglucemia persistente y complicaciones como la neuropatía periférica diabética (DPN). En la medicina tradicional mexicana, particularmente en la comunidad Xi´iuy de San Luis Potosí, se utiliza *Calea urticifolia* (“negrito”) por sus propiedades terapéuticas contra la DM. demostrando efectos hipoglucemiantes, antiinflamatorios y antioxidantes. Este estudio evaluó el extracto acuoso liofilizado de sus hojas (CuAqE) en modelos in vivo de diabetes tipo 2 (inducida por dieta alta en grasas) y diabetes tipo 1 (generada por estreptozotocina), así como un modelo de DPN. Los resultados mostraron que CuAqE ejerce un efecto hipoglucemiante sinérgico con fármacos convencionales, mejora la conducción nerviosa en el nervio sural y reduce la alodinia mecánica, evidenciado por el aumento del umbral de retirada de la pata (PWT). Además, presentó actividad antioxidante al regular marcadores como de glucosa, insulina y aldosa reductasa y índice HOMA-IR. Estos hallazgos sugieren que CuAqE modula los desequilibrios metabólicos en la DM y posee un efecto neuroprotector en la DPN, respaldando su potencial como coadyuvante en el tratamiento de la diabetes y sus complicaciones. Los resultados refuerzan el valor terapéutico de esta planta en la medicina tradicional y abren nuevas perspectivas para su aplicación en el manejo integral de la DM.

Palabras clave: resistencia a la insulina, diabetes mellitus, neuropatía periférica, *Calea urticifolia*, hipoglucemiante, neuroprotector.

ABSTRACT

Diabetes mellitus (DM) is a chronic disease characterized by deficient insulin production or action, leading to persistence and complications such as diabetic peripheral neuropathy (DPN). In Mexican traditional medicine, particularly among the Xi'iuy community in San Luis Potosí, *Calea urticifolia* ("negrito") is used for its therapeutic against DM, demonstrating hypoglycemic, anti-inflammatory, and antioxidant effects. This study evaluated the lyophilized aqueous extract of its leaves (CuAqE) *in vivo* models of type 2 diabetes (induced by a high-fat diet) and type 1 diabetes (generated with streptozotocin), as well as in a DPN model. The results showed that CuAqE exerts a synergistic hypoglycemic effect with conventional drugs, improves nerve conduction in the sural nerve, and reduces mechanical allodynia, evidenced by an increased paw withdrawal threshold (PWT). Additionally, it exhibited antioxidant activity by regulating markers such as glucose, insulin, aldose reductase, and the HOMA-IR index. These findings suggest that CuAqE modulates metabolic imbalances in DM and has a neuroprotective effect in DPN, supporting its potential as an adjuvant in diabetes treatment and its complications. These results reinforce the therapeutic value of this plant in traditional medicine and open new perspectives for its application in the comprehensive management of DM.

Keywords: insulin resistance, diabetes mellitus, peripheral neuropathy, *Calea urticifolia*, hypoglycemic, neuroprotective.

Índice

1. INTRODUCCIÓN

Para 2030, se estima que la principal causa de muerte (80%) en nuestro país serán las enfermedades crónicas no transmisibles (OMENT, 2015). Dentro de este grupo se encuentra la diabetes mellitus (DM). De acuerdo con los resultados de la ENSANUT 2023, en México había 21.7 millones de adultos de 20 años o más con prediabetes y 4.5 millones con diabetes, pero desconocían su condición.

Esta evidencia epidemiológica refleja un mecanismo inadecuado de prevención y control de la DM en nuestro país, así como un problema emergente en la salud pública. A esto se suma que los pacientes bajo tratamiento no tengan una adherencia adecuada, presenten enfermedades concomitantes, enfrenten falta de abastecimiento de medicamentos y los altos costos de su tratamiento.

Lo anterior limita la eficacia de los programas institucionales, como la Estrategia Nacional para la Prevención y Control del Sobrepeso, la Obesidad y la Diabetes. A pesar de ello, el uso de terapias alternativas para el tratamiento de la DM está en aumento. A nivel mundial, se han implementado programas como la *Estrategia de la OMS sobre medicina tradicional 2014-2023* cuyo objetivo es validar su calidad, inocuidad y eficacia para su incorporación a los sistemas de salud de los países miembros (OMS, 2013).

En el caso particular de México, la medicina tradicional ha sido empleada desde tiempos ancestrales; sin embargo, el conocimiento científico y la validación de la medicina tradicional mexicana aún son limitados. Por ello, la investigación en plantas medicinales ofrece la oportunidad de utilizarlas con mayor seguridad y, sobre todo, de descubrir alternativas terapéuticas que mejoren la calidad de vida de las personas.

En San Luis Potosí, *Calea urticifolia* -conocida comúnmente como “negrito”- es una planta utilizada tradicionalmente por la etnia *Xi’iuy* con usos terapéuticos. El té preparado con sus hojas se emplea como remedio para tratar diabetes, úlceras

gástricas y procesos inflamatorios. Entre los efectos farmacológicos validados del extracto acuoso de esta especie destacan sus propiedades: antioxidantes (Torres *et al.,* 2015), anti-inflamatorias y reguladoras del metabolismo (Torres *et al.,* 2015; Segura *et al.,* 2017).

Pese a ello, el rigor científico de los efectos farmacológicos de *Calea urticifolia* aún deben ser explorado. Por lo tanto, existe interés en investigar:

1. El efecto hipoglucemiante del extracto acuoso liofilizado (CuAqE) con co-administración de fármacos hipoglucemiantes orales (OAD´s).
2. Su potencial antioxidante y neuroprotector en un modelo *in vivo* de neuropatía periférica diabética (DPN).

Estos estudios buscan contribuir al conocimiento científico de esta especie y sentar las bases para futuras investigaciones que permitan evaluar su aplicación clínica.

2. ANTECEDENTES

2.1 Diabetes mellitus (DM)

La DM puede ser conceptualizarse como una enfermedad sistémica, crónico-degenerativa, de carácter heterogéneo, con grados variables de predisposición hereditaria y con participación de diversos factores ambientales. Se manifiesta como un conjunto de trastornos metabólicos de la glucosa que se clasifican como "glucemia alterada en ayuno" e "intolerancia a la glucosa", lo que generalmente se identifica como hiperglucemia persistente o crónica. Esta condición resulta de una deficiencia en la producción o acción de la insulina, lo que afecta al metabolismo intermedio de hidratos de carbono, proteínas y grasas (NOM-015-SSA2-2010).

Dado que la DM es considerada una enfermedad endócrina, nutricional y metabólica, la Clasificación Internacional de Enfermedades y la Asociación Americana de Diabetes, la clasifican en cuatro grupos principales:

1. Diabetes tipo 2 (T2D, E10): Denominada anteriormente diabetes no insulinodependiente o del adulto. Se caracteriza por resistencia a la insulina acompañada de una deficiencia relativa o absoluta en su producción.

2. Diabetes tipo 1 (T1D, E11): Conocida previamente como diabetes insulinodependiente o juvenil. En este tipo se produce una destrucción de más del 90% de las células β pancreáticas, lo que genera una deficiencia absoluta de insulina (insulinopenia).

3. Diabetes gestacional: Desarrollada durante el embarazo en mujeres sin diagnóstico previo de diabetes.

4. Otros tipos de diabetes (E12-13): Incluye defectos genéticos, enfermedades pancreáticas, diabetes inducida por infecciones o por fármacos o químicos.

2.2 Diagnóstico y tratamiento de la DM

El diagnóstico de DM se establece cuando se cumple cualquiera de los criterios señalados en la Tabla 1.

Tabla 1. Criterios de diagnóstico de la DM

Estadio	Glucosa anormal en ayunas (GAA)	Intolerancia a la glucosa (ITG)
	Pruebas de laboratorio	
	Prueba de glucosa sanguínea en ayuno (FBG)	Prueba de tolerancia oral a la glucosa (PTOG)
Prediabetes	≥100 mg/dL y ≤ 125 mg/dL	≥140 mg/dL y ≤ 199 mg/dL
Diabetes	>126 mg/dL	>200 mg/dL
Todo esto acompañado del resultado de una glucemia en cualquier momento del día ≥200mg/dL, sin relación con el tiempo transcurrido desde la última comida.		

El tratamiento de la diabetes mellitus tiene como propósito fundamental aliviar los síntomas, mantener el control metabólico, prevenir tanto las complicaciones agudas como crónicas, mejorar la calidad de vida del paciente y reducir la mortalidad asociada a la enfermedad y sus complicaciones. Para lograr estos objetivos, las metas

terapéuticas básicas incluyen alcanzar niveles adecuados de glucosa en sangre, perfil lipídico (colesterol total, LDL, HDL y triglicéridos), presión arterial, parámetros antropométricos (índice de masa corporal y circunferencia abdominal), así como niveles óptimos de hemoglobina glicosilada (HbA1c).

En el caso específico de diabetes de tipo 1, el tratamiento con insulina está indicado desde el momento del diagnóstico, complementándose con medidas no farmacológicas que incluyen un plan alimenticio personalizado y un programa de actividad física regular. Por otro lado, en la diabetes tipo 2, el manejo farmacológico se inicia según el criterio del médico, incluso desde el diagnóstico.

De acuerdo con la Guía de tratamiento farmacológico para el control de DM y la Guía de recomendaciones para la promoción de la salud, prevención, detección, diagnóstico, tratamiento y control de la prediabetes y diabetes, actualmente se dispone de diversos agentes terapéuticos para el manejo de esta condición.

Tabla 2. Características farmacológicas de agentes farmacológicos en el tratamiento de T2D

Hipoglucemiante	Dosis (mg)		Indicación
	inicial	máxima	
Metformina (Biguanida)	500-850	2550	Inhibe selectivamente la gluconeogénesis hepática (LaMoia & Shulman, 2021).
Glibenclamida (sulfonilurea)	5	20	Estimula la secreción de insulina por células ß del páncreas (Batiha et. al., 2023).
Pioglitazona (Tiazolidinediona)	15	30	Activa al receptor nuclear específico (PPAR-γ), produciendo un aumento de sensibilidad a insulina (Lebovitz, 2019).
Acarbosa (Inhibidores de alfa glucosidasa)	20-50	100	Inhibe las disacaridasas intestinales por lo que no hay absorción de monosacáridos en el borde en cepillo (Dalsgaard et. al., 2023).
Sitagliptina	100	100	Inhibidores de la dipeptidil peptidasa 4 (DPP-4) (Rosenstock, et. al., 2019).

Cabe destacar que mientras la insulinoterapia pueda utilizarse en ambos tipos de diabetes (T1D y T2D), los agentes orales (OAD´s) están indicados exclusivamente para el tratamiento de la T2D, como se detalla en la Tabla 2.

El uso de insulina en el paciente con T2D tiene dos tipos de indicaciones: descontrol grave, ya sea que se espere un uso permanente o temporal de esta hormona, o falla a OAD´s. En el caso de T1D su indicación es absoluta. Existen diferentes preparaciones comerciales de insulina y sus análogos comerciales, como lo muestra la tabla 3 (O'Neill et. al., 2017).

Tabla 3. Características de las preparaciones de insulina

Insulina		Inicio	Pico	Duración
Insulina aspart (Fiasp, NovoLog), insulina glulisina (Apidra) e insulina lispro (Admelog, Humalog, Lyumjev).	acción rápida	15min	1h	3-4h
Insulina regular humana (Humulin R, Novolin R, Velosulin R)	regular o de acción corta	15-30min	2-3h	6-8h
neutral protamine Hagedorn o NPH (Humulin N, Novolin N, ReliOn)	acción intermedia	2-4h	4-12h	12-18h
degludec (Tresiba), detemir (Levemir) y glargina (Basaglar, Lantus)	acción prolongada	1-3h	20h	24h
glargina U-300 (Toujeo)	acción ultra prolongada	6h	---	36h

El inicio es el tiempo que transcurre antes de que la insulina llegue al torrente sanguíneo y comience a reducir la glucosa en sangre. El momento pico es el momento durante el cual la insulina tiene su máxima potencia en términos de reducción de glucosa en sangre. La duración es el tiempo durante el cual la insulina continúa reduciendo la glucosa en sangre.

2.3 Complicaciones vasculares de la DM

La hiperglucemia crónica se considera el principal factor de riesgo para el desarrollo de complicaciones vasculares en la DM. Estas surgen como consecuencia de las alteraciones metabólicas y las reacciones bioquímicas desencadenadas por el exceso de glucosa en sangre.

Las complicaciones vasculares asociadas a la DM se clasifican en dos categorías principales: Complicaciones macrovasculares, también denominadas enfermedades cardiovasculares, que incluyen cardiopatía isquémica, insuficiencia cardíaca, la enfermedad vascular cerebral y la insuficiencia arterial periférica en los miembros inferiores. Las complicaciones microvasculares, que afectan a los pequeños vasos sanguíneos y comprenden; retinopatía diabética (que puede progresar hasta la ceguera), nefropatía diabética (que deriva en insuficiencia renal crónica) y neuropatía periférica (asociada al desarrollo de pie diabético, condición que en casos severos puede requerir amputación debido a infecciones graves) (Cole & Florez, 2020).

La neuropatía diabética constituye un conjunto de alteraciones morfológicas y funcionales del sistema nervioso periférico, tanto somático como autonómico, que se manifiesta frecuentemente como dolor neuropático (Cashman y Höke, 2015). Esta condición puede presentarse como consecuencia de diversos factores, incluyendo enfermedades sistémicas (como la diabetes), deficiencias nutricionales Puede ocurrir como una secuela o síntoma de muchas afecciones, como enfermedades sistémicas (diabetes), deficiencia de vitaminas (particularmente de vitamina B12), insuficiencia renal, infecciones (como el VIH), exposición a toxinas ambientales (organofosforados), enfermedades neoplásicas (linfomas), alcoholismo crónico y como efecto adverso de ciertos fármacos, especialmente algunos agentes quimioterapéuticos (Prior et. al., 2017).

La tabla 4 muestra la clasificación fisiopatológica actual de la neuropatía. Las neuropatías metabólico-microvasculares son las más frecuentes. La DPN es una

polineuropatía distal que se caracteriza por disminución de la sensibilidad termoalgésica, más acentuada en las zonas distales de las extremidades y cuya severidad se correlaciona directamente con el grado de descontrol glicémico (Olmos et. al., 2012). Los pacientes con DPN expresan síntomas que pueden incluir dolor neuropático, alodinia o entumecimiento, parestesias (cosquilleo", "alfileres y agujas") hiperestesias e hiperalgesia, lo que aumenta el riesgo a complicaciones secundarias.

Tabla 4. Clasificación de la Neuropatía

Subtipo clínico de neuropatía	Fisiopatología
-Polineuropatía distal (DPN) **-Neuropatía autonómica (DAN)**	Metabólico microvascular-hipóxica
-Radículo-plexopatía lumbosacra **-Radículo-plexopatía cervical** **-Radiculopatía torácica** **-Neuropatía craneal** **-Neuropatía dolorosa + baja de peso**	Inflamatorio-autoinmune
-Síndrome del canal carpiano **-Neuropatía ulnar del codo** **-Neuropatía peronea**	Compresiva
-N. por Ketoacidosis **-N. por insuficiencia renal** **-N. por isquemia de grandes vasos**	Secundarias a complicaciones de la diabetes

La DM genera anormalidades en la excitabilidad axonal, incluidas las reducciones en el umbral de electrotonus y superexcitabilidad, así como la prolongación del periodo refractario, por lo que la velocidad y amplitud de la conducción nerviosa son significativamente reducidas (Landowski et. al., 2016; Quiroz et al., 2016).

El manejo de la DPN se fundamenta en el control de la glucemia como medida basal y el abordaje sintomático del dolor neuropático. Si bien los analgésicos convencionales y los fármacos neuromoduladores pueden proporcionar alivio sintomático, estos no modifican la historia natural de la enfermedad.

Dentro de las opciones terapéuticas disponibles, el ácido lipoico (antioxidante) de alta liberación a dosis de 600 mg dos o tres veces al día ha demostrado ser el único tratamiento etiopatogénico de leve a moderado (NOM-015-SSA2-2010).

2.4 Etiología de la neuropatía periférica diabética (DPN)

Los procesos que conllevan a la neuropatía periférica incluyen microangiopatía con isquemia, deficiencia en factores neurotróficos y/o sus receptores, excesiva formación de productos finales de glicación avanzada, estrés oxidativo, disfunción mitocondrial, desregulación de factores tróficos y susceptibilidad genética (Sytze et. al., 2013).

La neuropatía causa un daño a las fibras nerviosas sensoriales, motoras y autonómicas, asociado con atrofia axonal, desmielinización, regeneración atenuada del potencial de acción, inflamación y pérdida progresiva de nervio periférico (Zempoalteca et. al., 2017).

Los mecanismos por los cuales la hiperglucemia genera la neuropatía periférica son: acumulación y acción de productos de glicación avanzada, incremento en la actividad de la vía del sorbitol, aumento en la vía de las hexosaminas, activación de diversas isoformas de la proteína cinasa C, y aumento en el estrés oxidativo (Sytze et. al., 2013). Además de los efectos dañinos directos sobre la neurona, estos cambios celulares también influyen en el transporte del impulso eléctrico en el axón, degeneración axonal y limitando la capacidad regenerativa (Quiroz et al., 2016).

En los tejidos que no requieren de la insulina para captar glucosa (lo hacen por difusión facilitada) y que contienen la enzima aldosa reductasa (como en el riñón, tejido nervioso y vascular, así como el cristalino del ojo); el flujo de este monosacárido al interior de sus células está limitado a las condiciones de normoglucemia. Sin embargo, en la condición de hiperglucemia; el metabolismo de la glucosa se desvía a la vía del sorbitol, también conocida como la vía de los polioles (Watcho et. al., 2010). En esta

vía, la aldosa reductasa cataliza la reducción de las hexosas (glucosa) a sorbitol (Ding et.al., 2014).

El sorbitol se oxida a fructosa por acción de la enzima sorbitol deshidrogenada (SDH), enzima totalmente dependiente de NAD+ como aceptor de equivalentes de reducción que da lugar a su forma reducida NADH. La disminución del NAD+, provoca la inhibición de la actividad de la enzima gliceraldehído-3-fosfato deshidrogenada (GAPDH), frenándose con ello la vía metabólica de la degradación de la glucosa (la glucólisis) (Zhang et al., 2010).

El sorbitol no difunde extracelularmente con facilidad a través de las membranas, por lo que su aumento dentro de la célula contribuye a incrementar la presión osmótica intracelular que causa edema y daño celular. Por otro lado, la disminución del NADPH por la vía del sorbitol debido a su consumo excesivo, limita la acción de las enzimas antioxidantes, catalasa y glutatión reductasa, y de la enzima óxido nítrico sintasa (NOS), las cuales también utilizan a la coenzima para sus funciones. La consecuencia es la presencia de estrés oxidativo, debido a una caída en las concentraciones intracelulares del glutatión (GSH), mioinositol y del óxido nítrico, así como el aumento de las especies reactivas de oxígeno.

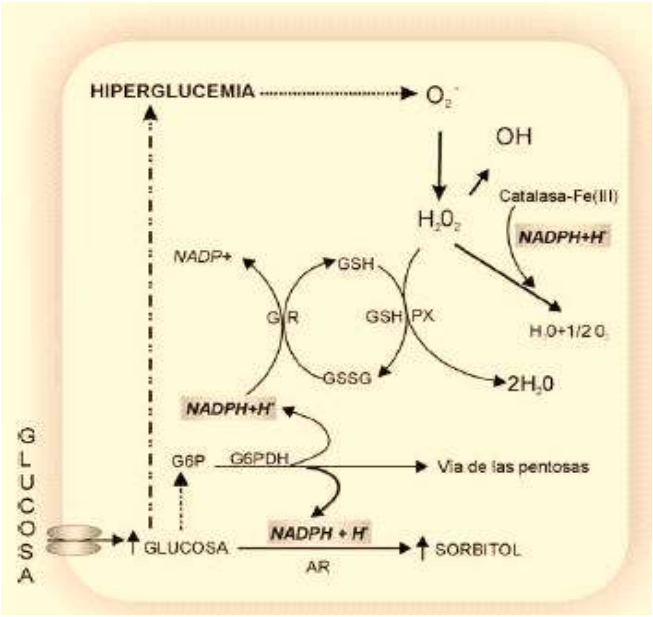

Figura 1.
Formación de especies reactivas de oxígeno y disminución de los mecanismos antioxidantes por falta de NADPH/NADH por la vía del sorbitol.
Aldosa reductasa (AR), nicotinamida adenina dinucleótido fosfato reducido (NADPH), glutatión forma oxidada (GSSG), glutatión forma reducida (GSH).

2.5 La medicina tradicional Xi’iuy de San Luis Potosí

La alta prevalencia de DM en México, principalmente T2D, tiene graves consecuencias para la economía, tanto individual como colectiva (Salas-Zapata et. al., 2018), ya que estos pacientes precisan atención médica constante, monitoreo farmacoterapéutico y polimedicación (Rodríguez Bolaños et. al., 2010). Por lo tanto, la población mexicana en general recurre a plantas medicinales en forma de té o infusiones de sus hojas, raíces o tallos como tratamiento alternativo para tratar la T2D (Acosta-Recalde et. al., 2018).

La medicina herbolaria o tradicional en ocasiones se denomina medicina alternativa o complementaria y se define como el conjunto de conocimientos, aptitudes y prácticas basados en teorías, creencias y experiencias indígenas de las diferentes culturas, sean o no explicables, que son empleados para el mantenimiento de la salud, así como para la prevención, el diagnóstico, la mejora o el tratamiento de enfermedades físicas o mentales (Jaradat et. al., 2016; Kamsu et al., 2013).

Los pueblos originarios de México tienen un extenso conocimiento sobre plantas medicinales, que ha trascendido por generaciones como parte de su cultura tradicional. La etnia Xi'ói o Xi’iuy en San Luis Potosí abarca cuatro regiones territoriales: Santa María Acapulco, Alaquines, Ciudad del Maíz y la región de La Palma (Rayón-Tamasopo); de tales localidades, esta última se caracteriza por ser la de menor densidad poblacional en comparación con los otros núcleos, pero de mayor conocimiento en el manejo y uso de plantas debido a su privilegiada ubicación geográfica (Guzmán et al., 2010).

De acuerdo con un estudio etnobotánico realizado en la Región de La Palma, *Calea urticifolia* (Mill.) DC. conocida tradicionalmente como “negrito”, es una de las trece plantas con mayor frecuencia de uso por esta región étnica. Las partes vegetales utilizadas son sus hojas y estas se preparan en forma de té para el tratamiento de

diversas condiciones clínicas como: inflamación, gastritis, DM, hipertensión, diarrea, empacho, bilis, vómito, dolor de estómago, de cabeza (Guzmán et al., 2010).

El tratamiento tradicional de *Calea urticifolia* consiste en la infusión de dos hojas secas (en promedio 0.13 g) sumergidas en una taza con agua hirviendo bajo reposo de 3 a 5 minutos. Los pacientes toman esta infusión dos veces al día, por la mañana en ayunas y por la tarde, por 60 días o hasta tener mejoría (Guzmán-Guzmán, 2010).

Calea urticifolia, vegetativamente es un arbusto de la familia *Compositae*, comúnmente conocida en México como chilchaca, jarilla, tacote, jaral de castilla o negrito. Son arbustos que pueden medir hasta 2m de altura, poseen hojas ovaladas, a veces dentadas y lustrosas en ambos lados; con flores amarillas agrupadas en cabezuelas. Además, los frutos tienen las semillas con pelillos como escamitas. Se encuentra comúnmente en estados como Veracruz, Yucatán, San Luis Potosí, Durango, Jalisco e Hidalgo; habita en climas cálidos y semicálidos, entre los 22 y los 1800msnm. Se asocia a vegetación perturbada derivada de bosques tropicales caducifolio, subcaducifolio, subperennifolio y perennifolio, bosques de encino y de pino (Biblioteca Digital de la Medicina Tradicional Mexicana, 2013).

Figura 2. *Calea urticifolia*
Elaboración propia

Dentro de los aspectos farmacológicos que se tiene registrados de la especie, han sido en función de sus metabolitos secundarios en donde se destacan sus efectos: antifúngico (Gamboa-Angulo et al., 2005), inhibición de la diferenciación pre-adipocitaria por germacranólidos aislados de la especie (Matsuura et. al., 2005), citotóxico en células de cáncer de colon y leucemia por sus lactonas sesquitérpenicas (Ohguchi et. al., 2009), antioxidante (Umemura et. al., 2008), para tratamiento de gastritis y bactericida (Matsuura et. al., 2005).

Guzmán y colaboradores (2010), corroboraron la capacidad anti-inflamatoria del extracto etanólico de las hojas de la especie en dos modelos *in vivo* de inflamación (aguda y crónica); la inflamación aguda mediada por carragenina y crónico a través del proceso inflamatorio de bajo grado asociado con una alimentación rica en grasas. Los resultados demostraron la capacidad anti-inflamatoria del extracto vegetal, a través de la inhibición de la secreción de citocinas pro-inflamatorias como el TNF-α, IL-1 β e IL-6 tanto en ambos modelos de inflamación (aguda y crónica); en esta última además, se incrementó la secreción de adiponectina, adipocina asociada con efectos antidiabéticos, anti-inflamatorios entre otros. El efecto modulador de las citocinas pro-inflamatorias y adiponectina se asociaron con la disminución de la concentración de glucosa sérica y triglicéridos en el grupo de ratas con dieta rica en grasa y tratadas con el extracto etanólico.

Por otra parte, Torres y colaboradores (2015), evaluaron el efecto anti-inflamatorio y antioxidante del extracto acuoso liofilizado (CuAqE), en macrófagos RAW 264.7. Los resultados corroboraron su efecto anti-inflamatorio, el cual se asoció con la supresión de la vía del óxido nítrico (NO)/óxido nítrico sintetasa inducible (iNOS), a través de inhibición de la translocación de las subunidades p65 y p50 del factor nuclear kappa B (NF-κB). Recientemente, se demostró que CuAqE modula el desequilibrio en los procesos metabólicos e inflamatorios presentes en la obesidad y diabetes mellitus con una dosis efectiva de 11mg/kg en un modelo *in vivo* de inflamación de bajo grado, bajo el consumo de una dieta rica en grasa (Segura et al., 2017).

3. Justificación

La medicina tradicional mantiene una relevancia significativa como alternativa terapéutica en el primer nivel de atención a la salud, particularmente en contextos comunitarios (Pan et al., 2014). Además, este conocimiento y su corroboración científica proporciona indicios para nuevas áreas de investigación para la creación de fuentes invaluables de productos farmacéuticos (Ji et al., 2009).

Se estima que en México alrededor de 4 000 especies de plantas con flores (15% de la flora total) tienen atributos terapéuticos (Ocegueda et. al., 2005), y muchas de sus culturas nativas tienen una extensa farmacopea de plantas medicinales; tras el conocimiento que se ha transmitido de generación en generación (Biblioteca Digital de la Medicina Tradicional Mexicana, 2013). Durante los últimos años, ha habido un resurgimiento del interés popular en plantas que se utilizan para el tratamiento de diferentes enfermedades, como la DM (Giovannini et al., 2016).

Las plantas medicinales se han utilizado empíricamente (ya sea como parte de la dieta, infusiones o extractos) para tratar y mejorar los síntomas de T2D. A pesar de su uso empírico, la Organización Mundial de la Salud cuenta con directrices sobre la monitorización de la seguridad de los medicamentos a base de plantas medicinales en los sistemas de farmacovigilancia (WHO, 2004)

Actualmente, el proceso de validación científica ha permitido el reconocimiento formal de diversas especies vegetales con propiedades medicinales (Torres-Vanda & Gutiérrez, 2023), lo que no solo legitima el conocimiento tradicional indígena, sino que también identifica fuentes promisorias para el desarrollo de terapias innovadoras.

Cabe recalcar que los principios activos de las plantas medicinales pueden reaccionar con la administración conjunta con fármacos convencionales y pueden generar variaciones en la magnitud del efecto terapéutico deseado. En la literatura médica son

escasos los trabajos de investigación sobre los efectos adversos e interacciones entre las plantas medicinales y medicamentos.

En este contexto, en el grupo de trabajo se ha corroborado científicamente para *Calea urticifolia* efectos antiinflamatorio, antioxidante e hipoglucemiante. Además, se ha determinado su baja toxicidad, lo que la convierte en una planta medicinal de inusitado interés. Puesto que estos resultados son prometedores y sugieren su potencial uso como coadyuvante en el tratamiento de enfermedades crónicas no transmitibles relacionadas con la alimentación (ENT-RA) como lo es la DM; que ocasionan un alto impacto negativo económico en el sistema de salud pública en México (Picó-Guzmán, et. al. 2022).

La presente propuesta de trabajo se fundamenta en la relevancia el ofrecer perspectivas concretas para la implementación de terapias combinadas que podrían mejorar los resultados clínicos en pacientes diabéticos. Por lo que, la evaluación farmacológica de *Calea urticifolia* y su capacidad sinérgica del extracto acuoso liofilizado con OAD´s en modelos *in vivo* de DM, y con DPN por medio de estudios funcionales de nervios y determinación de la enzima aldosa reductasa.

4. Hipótesis

El extracto acuoso liofilizado de *Calea urticifolia* (CuAqE) un tipo de interacción farmacológica; logrando así un efecto en la regulación del metabolismo de la glucosa en T2D experimental inducida a través de obesidad inducida con dieta rica en grasas (DIO-HFD) y T1D por inducción química de múltiples dosis bajas de estreptozotocina (MLD-STZ); además tendrá un efecto neuroprotector en la DPN.

5. Objetivos

5.1 Objetivo general

Evaluar el efecto de la coadministración del extracto acuoso liofilizado de *Calea urticifolia* (CuAqE) con antidiabéticos orales (OAD´s) e insulina en modelos *in vivo* de

diabetes mellitus (DM), así como su potencial efecto neuroprotector y antioxidante en la neuropatía diabética periférica (DPN).

5.2 Objetivos específicos

Fase 1: Establecimiento de modelos *in vivo* de DM para la evaluación Fitofarmacológica

- Inducir un modelo *in vivo* de T1D mediante la administración de estreptozotocina en dosis múltiples bajas (MLD-STZ).
- Generar un modelo *in vivo* de T2D mediante dieta alta en grasas (DIO-HFD) e inducción de resistencia a la insulina.
-

Fase 2: Evaluación del efecto de CuAqE en modelos de diabetes mellitus

- Determinar el potencial hipoglucemiante de CuAqE en modelos *in vivo* de DM.
- Analizar el efecto de la coadministración de CuAqE con insulina en modelo *in vivo* de T1D por MLD-STZ y con OAD´s en modelo *in vivo* de T2D por DIO-HFD.

Fase 3: Evaluación del efecto de CuAqE en modelo *in vivo* de DPN

- Establecer un modelo *in vivo* de DPN asociada a DM.
- Evaluar la función del nervio periférico mediante estudios electrofisiológicos del nervio periférico sensorial sural.
- Determinar el efecto neuroprotector a través de pruebas conductuales y de dolor en modelo *in vivo* de DPN.
- Cuantificar la actividad antioxidante de CuAqE a través de la medición de la actividad de la enzima aldosa reductasa.

6. Estructura del trabajo experimental por capítulos

Para presentar de manera organizada y publicable los hallazgos de esta investigación, el trabajo se ha estructurado en tres capítulos principales, cada uno correspondiente a una fase experimental y desarrollado en formato de artículo científico**.**

6.1 Diabetes mellitus murine models using multiple low doses of streptozotocin (type 1), and diet-induced obesity by high-fat diet feed (type 2) in C57BL/6 male mice

ABSTRACT

Background: Hyperglycemia is a clinical manifestation of diabetes mellitus (DM). The prevalence of diabetes, a significant public health problem, is rapidly increasing worldwide. Type 1 diabetes (T1D) and Type 2 diabetes (T2D) are the two most frequent categories of diabetes. Different animal models of DM available, such as spontaneous, transgenic, or induced. For a long time, the most commonly used model to induce DM is C57BL/6 mouse. Nevertheless, the age of mouse, time and method of DM development determine the success rate and comparison between research.

Aim of the study: We aimed to generate and characterize an appropriate and stable model nongenetic mouse of T1D and T2D in C57BL/6 male mice.

Methods: For T1D mice were fed a standard diet for twelve weeks, followed by multiple low dose streptozotocin (MLD-STZ, 20 or 40 mg/kg) or thirty-six feeding, single high-dose of STZ injection (SHD-STZ, 150 mg/kg). For T2D mice were diet-induced obesity (DIO) by high fat diet (HFD) fed for thirty-six weeks. Additionally, a combined model was developed with DIO-HFD and STZ (50 mg/kg). Body weight, food and water intake was monitored weekly. Blood glucose and insulin were measured. HOMA-IR and HOMA-β were calculated as insulin resistance.

Results: After 8 weeks, both models presented hyperglycemia with values >200 mg/dL (T2D) and >300 mg/dL (T1D). Decreased body weight and increased HOMA-β (β cell failure) were observed in T1D. Body weight gain (obesity) and increased HOMA-IR (insulin resistance) in T2D ($p<0.001$).

Conclusions: T1D and T2D models are profitable, easy to make, stable, and with long-lasting hyperglycemia for testing drugs or herbal medicines with hypoglycemic properties.

Keywords: Type 1 diabetes (T1D), Type 2 diabetes (T2D), multiple low dose streptozotocin (MLD-STZ), high fat diet (HFD), hyperglycemia, obesity and insulin resistance.

1. Introduction

Recent prevalence estimates and projections for diabetes mellitus (DM) indicate a global prevalence of 10.5% (536.6 million people) among 20–79-year-old in 2021, expected to rise to 10.5% rising to 12.2% (783.2 million) by 2045 (Sun et. al., 2021). In Mexico, the prevalence of DM has gradually increased from 14.4 to 18.3% between 2006 to 2022, posing a significant challenge to the healthcare system and impacting the overall quality of life for the population (Basto-Abreu et. al., 2023).

Hyperglycemia, a prominent clinical manifestation of DM, arises from a relative or complete lack of insulin, which is a peptide hormone produced by the pancreatic β-cells located in the islets of Langerhans, plays a fundamental role in managing blood glucose (BG). Its primary function is to regulate BG within the normal physiological range by enhancing the absorption, uptake and storage in peripheral tissues through anabolic effects (King and Bowe, 2016).

Type 1 diabetes (T1D) and type 2 diabetes (T2D) are notable as the two most frequent categories of diabetes. T1D, is characterized by autoimmune destruction of pancreatic β-cells, leading to insulin deficiency, On the other hand, T2D is associated with non-autoimmune progressive loss of adequate β-cell insulin secretion, often occurring against a background of insulin resistance (IR) and metabolic syndrome (ElSayed et. al., 2023).

Persistently elevated BG levels and pancreatic β-cell dysfunction contribute to a more rapid functional deterioration, resulting in a non-compensatory hyperglycemic state is a key diagnostic feature of T2D. For the above, is the difference between metabolic syndrome and this disease (Morris et. al., 2016). Unfortunately, currently, there are no effective and efficient treatments available for these diseases that can cure them completely; despite numerous advances in the therapeutic field.

Consequently, a comprehensive understanding of the pathophysiology and the exploration of new preventative or therapeutic approaches to treating DM are urgently needed (Gheibi et. al., 2017). In response to the prevalence of DM and its complications, several rodent models have been developed (Sullivan et. al., 2008; Biessels et. al., 2014; O'Brien et. al., 2014; Jolivalt et. al., 2016).

Numerous animal models of diabetes are currently available, each classified based on the type of diabetes they simulate (T1D or T2D) and the method of generation: spontaneous, transgenic by genetic manipulations or induced (utilizing surgical models, administration of toxic substances, hyper-caloric diets, immunosuppressors, or even viral infections). Moreover, both surgical and non-surgical methods can be combined to replicate special or more complex types of DM, such as combining high-fat diet (HFD) with streptozotocin (STZ), or under specific physiological conditions, such as during pregnancy (Brito et. al., 2016).

According to King & Bowe, one of animal models of T1D involved protecting β cells from damage, with characteristic being the steady autoimmune destruction β-cells. The most commonly employed method for achieving this is the chemically-induced DM by multiple low dose streptozotocin (MLD-STZ), which causes a gradual autoimmune destruction of β-cells, in contrast to the rapid destruction stimulated by a single high-dose STZ injection (SHD-STZ).

In the case of T2D, understanding the pathogenesis is crucial, with a focus on the role of IR and/or obesity, which are key characteristics of IR and impaired glucose tolerance. The most commonly utilized method to develop DM is diet-induced obesity (DIO), achieved by feeding mice a high fat diet (HFD) (King & Bowe, 2016).

The aim of this research is to generate and characterize an appropriate and stable model nongenetic of DM in C57BL/6 mice, considering the main clinical and metabolic

manifestations considering its advantages and disadvantages. The goal is to provide a practical guide for evaluating drugs and biopharmaceuticals with therapeutic potential.

We developed MLD-STZ and SHD-STZ models for T1D and DIO-HFD to induce T2D. Additionally, a combined model was constructed to simulate the natural progression from obesity and impaired glucose tolerance to T2D; utilizing SHD-STZ to induce a greater degree of hyperglycemia in DIO-HFD mice.

2. Material and methods

2.1. Materials

The Rat/Mouse Insulin ELISA Kit was purchased from Millipore Corporation, USA. Pentobarbital sodium (Pisabental ®) was obtained from Pisa Agropecuaria (PiSA® Farmacéutica, México). Streptozotocin (STZ) and anhydrous glucose were acquired from Sigma Aldrich, St. Louis, MO, and test strips Accu-Chek Aviva bought in Roche, UK.

2.2. Animal procurement and housing

C57BL/6 male mice, aged four to six weeks, were acquired from Unidad de Producción y Experimentación de Animales de Laboratorio UPEAL-CINVESTAV-IPN (México City, México). Upon arrival, the mice were housed in a controlled environment (21±2◦ C, 50±10% humidity) with a 12 h light/dark cycles (7:00am to 7:00pm) and provided with standard rodent food (Chow 5001) and water ad libitum. After a 5-dy acclimatization period, the mice were randomly assigned to diet groups and individual housed in acrylic cages.

The animal study protocol underwent review and approval by the local Animal Ethical Review Committee (CE102018015R2. FCQ-UASLP, San Luis Potosí, México). All procedures were conducted in accordance with animal ethics guidelines outlined in the Mexican Norm for Animal Care and Handing (NOM-062-ZOO-1999).

2.3 DM models

For DM models, mice (similar body weight and fasting glucose) were categorized as follows: seemingly healthy (CTL-NOM) mice fed standard diet (SD), for T1D models, mice injected with MLS-STZ or SHD-STZ (STZ-T1D) and for T2D models, mice fed DIO-HFD (DIO-T2D) and DIO-HFD injected with SHD-STZ (DIO-STZ-T2D) to combined model.

All mice had ad libitum access to diets and water. The experimental design is illustrated in Figure 1, and the cut-off points of DM (12 or 36 weeks) simulate the ages at which DM occurs (Table 1S) (Roser et. al., 2013; Schofield et. al., 2017).

2.3.1 Type 1 diabetes mouse model

CTL-NOM mice were injected intraperitoneal with vehicle sodium citrate buffer (VB) and STZ-T1D mice were randomized for injections with containing 20,40 or 150mg/kg of STZ in VB with dose volume of 0.3 mL/kg IP. At 12 weeks, five consecutive doses (20 or 40 mg/kg) were administrated (STZ20-T1D and STZ40-T1D, respectively), and 36 weeks, a single dose was given (STZ150-T1D). STZ was freshly prepared a 10 mg/mL solution in VB (1.47 g $Na_3C_6H_5O_7$ per 50 mL ddH_2O, pH 4.5) using 1 mL disposable insulin syringes (BD Biosciences) in a fume hood. The mice were injected with STZ at approximately 4:00 p.m. after a 4-hour fasting period, one daily for five consecutive days by intraperitoneal injection. Subsequently, mice continued to receive their diet for next 8 weeks.

2.3.2 Type 2 diabetes mouse model

Following the acclimatization period, DIO-T2D and DIO-STZ-T2D mice were fed with HFD for 36 weeks. The composition and energy densities of the HFD are detailed in Table 1. Diets with animal fat, such as lard (20-40g/100g), known for their high saturated fat content, are more likely to induce obesity and diabetes in susceptible strains (Guo et. al., 2018). After 36 weeks, DIO-STZ-T2D mice was administered as previously described, single dose STZ (50mg/kg) for induction of combined T2D for

DIO-HFD and HSD-STZ (DIO-STZ50-T2D). Subsequently, all mice continued to receive their diet for next 8 weeks.

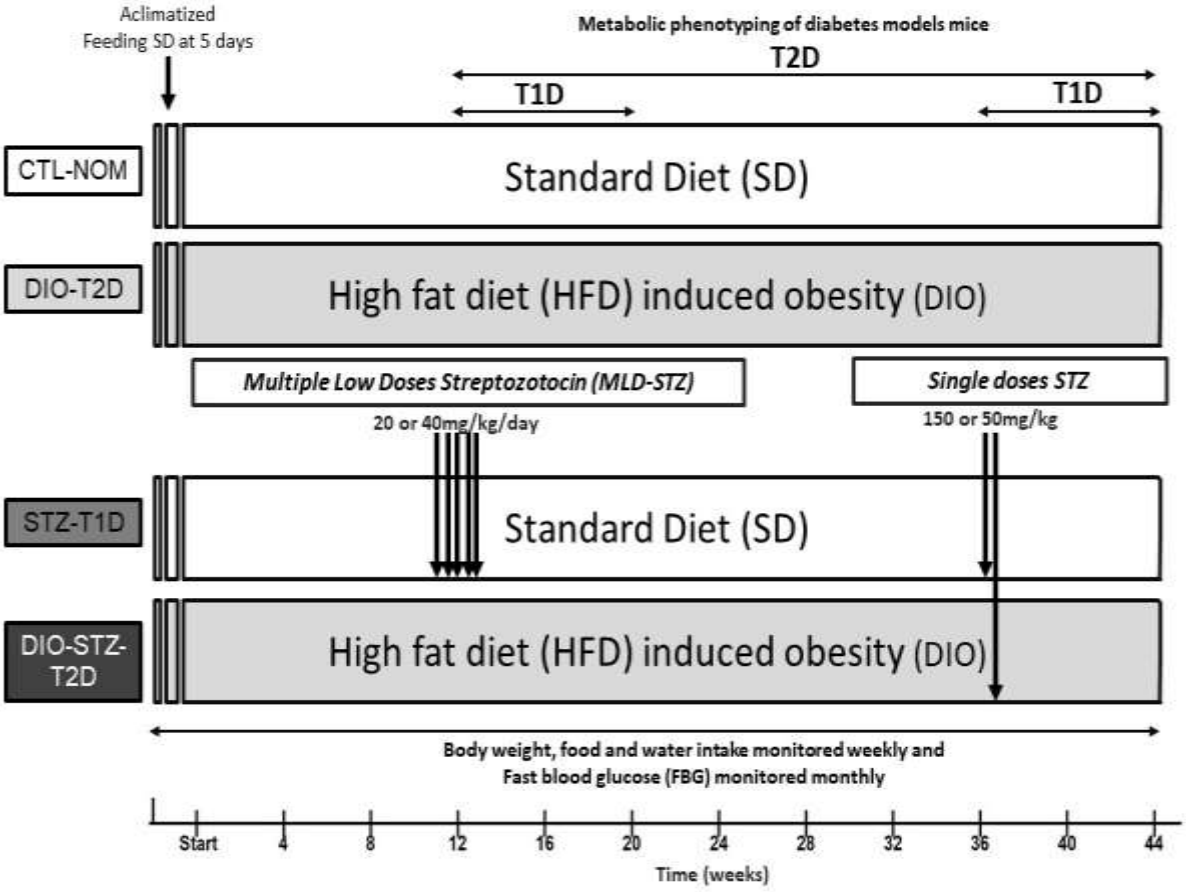

Figure 1. **Experimental design for DM murine models.**
Strategy to develop of Type 1 diabetes (T1D) and Type 2 diabetes (T2D) in C57BL/6 male mice.

2.4 Growth patterns (GW) and body composition (BC)

Individual body weight (BW) was measured weekly throughout the 44-weeks duration of the experiment with a precision 0.1g using an electronic balance. Additionally, BW variations at the cut-off points of each DM models were used to identify pathophysiological status of obesity (Table 2S). Body length (BL) was determined by measuring nasal-to-anal distance using a Vernier caliper when mice were anesthetized

with isoflurane inhalation to ensure good immobilization and positioning during a five-minute measure.

Table 1. Composition of the standard diet and the high fat diet.

Energy density		Diets		
		high-fat diet (HFD) Modified Chow 5008	Chow 5008	**standard diet (SD)** Chow 5001
Kcal provided %	**Protein**	32.21	26.85	28.50
	Fat	52.66	16.71	13.50
	Carbohydrate	15.18	56.44	58.00
Chemical Composition %	**Protein**	13.91	23.50	23.90
	Fat	40.58	6.50	5.00
	Carbohydrate	29.24	49.40	48.70
	Fiber	2.25	3.80	5.10
	Minerals	4.02	6.80	7.00
	Moisture	10.00	10.00	10.00
Kcal/g	**Gross energy**	5.93	4.15	4.07
	Metabolizable energy	5.12	3.31	3.02
	Physiological fuel value	5.38	3.50	3.36
Composition of HFD: 72.5g Chow 5008, 35g Lard, 10g Canola oil and water.				

Body surface area (BSA) was derived from the DuBois equation:

$$BSA = 0.20247 * BW^{0.425} * BL^{0.725}$$

Were BW in kg, BL is in m, and BSA in m^2. Body mass index (BMI) was calculated as the ratio between body weight and body surface (kg/m^2). The formulas to calculate these parameters specifically in mice were obtained from the investigation of Gargiulo *et. al.,* 2014. Body growth (BG) was identified as growth rate (GR) and total and monthly weight gain (WG_t and WG_m). GR defined as the weight increment per unit of time, was calculated from the formula: $GR= W_f/W_i$. For WG_t was defined as the subtraction of the final weight from the initial weight. $WG_m= WG_1 - WG_2/t_2-t_1$.

Additionally, to evaluate the degree of obesity in T2D model, body surface area (BSA_x) and Lee index were used. BSA_x (cm^2) was estimated using the Meeh formula: $BSA_x = k\ BW_{(g)}^{0.667}$, where k (Meeh constant) must be empirically determined by species. A Meeh constant of 10 is typically reported for mice; however, a value of k=9.85 reported by Cheung *et. al.,* 2008 was used. Lee Index was calculated according to Cao *et. al.* 2020 by the cube root of body weight (g)/naso-anal length (cm).

2.5 Energy metabolism (EM)

Water and food intake was also recorded weekly. Energy density data as seen in Table 1, were used to calculated gross energy, metabolizable energy (ME), loss energy (urine, feces, methane), and physiological fuel value for groups of mice fed both diets.

The relationship between basal metabolic rate (BMR) and body weight in different-sized mammals is described by the function: $BMR=cW^{0.75}$, where BMR is basal metabolic rate (kJ/day), W is body weight (kg), and c is basal metabolic rate per $kg^{0.75}$ per day, which is 300 $kJ/kg^{0.75}day$. Thus, the basal metabolic rate in different- sized species is proportional to the body weight raised to the 0.75 power, also known as metabolic weight (MW) which was also calculated (Terpstra, 2001).

The total daily expenditure of energy (TEE, TDEE, or DEE) can be partitioned into different components. These normally include the energy spent on basal metabolism, the thermic effect of food (the increase in energy expenditure following food intake which is also called the heat increment of feeding or the specific dynamic action), the energy spent on thermoregulation and the energy spent on physical activity (Speakman, 2013). If one assumes that the basal metabolic rate comprises 75% of the total energy expenditure, then the total daily expenditure of energy can be described by the function: $DEE=400kJ/kg^{0.75}day$ ($W^{0.75}$) and energy balance (EB) was a comparison between energy revenues and energy expenditures represented as: EB= ME- DEE. Food efficiency ratio (FER) was calculated as (gain body weight total/ Food intake total) *100.

2.6 Metabolic profile (MP)

2.6.1 Clinical Biochemistry

Blood samples from weekly cohorts of 12 or 36-week-old male mice, fasted overnight (12-18 h), were obtained by tail vein puncture for experimental BG measurement. A handheld blood glucose monitor (Accu-Check Aviva, Roche, UK) was used to determine BG.

Fasting blood glucose (FBG) and Postprandial blood glucose (PPBG) were measured every month to confirm hyperglycemia. Physiological reference range of FBG, we used to determine Cut-off levels: normoglycemic (≤150 mg/dL), prediabetes (≤200 mg/dL), DM (>200 mg/dL) (Table 4S), and Cut-off level PPBG: normoglycemic (≤185 mg/dL), prediabetes (≤235 mg/dL), and DM (>285 mg/dL) (Table 5S).

For the T1D model, FBG was measured before and after STZ administration by MLD-STZ model (5 days), and to monitor the course of the disease, it was determined for 8 weeks. For the T2D model, at 36 weeks, FBG was measured weekly throughout two months.

Mice were subjected to a fasting period of 10–12 hours before in vivo analysis, mice were anesthetized with intraperitoneal pentobarbital sodium doses adjusted according to the weight of each mouse (80mg/kg IP). Subsequently, mice were euthanized by cardiac puncture to collect blood for endpoint experimental procedures, including biochemical analyses. Plasma insulin levels were measured following the manufacturer's protocol. Microplate reading at 450nm was conducted using multiskan photometer with Ascent software (Thermo Fisher Scientific®, USA).

2.6.2 Blood glucose kinetics: **Oral glucose tolerance test (OGTT)**

For OGTT, glucose was prepared in dilution with isotonic solution according to the established dose (1g/kg) and administered by oral injection. After nine-hours fast (23:00–8:00), at time point 0, mice were injected with isotonic solution, and glucose

concentrations were measured at 0,15,30,60,90 and 120 minutes to assess the effects of handling on FBG. The trapezoidal approximation rule and plotted curve with chart trendline were used to determine the area under the curve (AUC) over the course of the glucose tolerance test. AUC_{OGTT} was used for evaluating IR.

2.6.3 Insulin resistance

To calculate Homeostatic Model Assessment insulin resistance (HOMA-IR), Homeostatic Model Assessment beta-cell function (HOMA-β or %β), Homeostatic Model Assessment insulin sensitivity (%S), insulin disposition index (DI), and quantitative insulin sensitivity check index (QUICKI), formulas for the single-pool first-order glucose kinetics were adapted from a previous method in mice (Van Dijk et. al. 2013). See Table 2.

2.7 Statistical analysis

Results are expressed as mean ± standard deviation (SEM). Data were subjected to analysis using one-way ANOVA, followed by Bonferroni post hoc test, where a significance level of $p<0.001$ value was employed to determine statistical significance. All analyses were conducted in at least three independent experiments, and each experiment was analyzed at least in triplicate. Statistical analysis was performed using the proc GLM procedures of SAS version 9.3 (SAS Inst. Inc., Cary, NC).

Table 2. **Formulas for calculated parameters for insulin resistance (IR)**

Eq. 1	**Homeostatic Model Assessment**	$\boldsymbol{HOMA-IR = (Glucose\ mmol/L)(Insulin\ mUI/L)/(BV\ mmol\ \mu UI/L^2)}$
Eq. 2	**Insulin sensitivity**	$\boldsymbol{\%S = (BV\ mmol\ \mu UI/L^2)/(Glucose\ mmol/L)(Insulin\ \mu UI/L) * 100\%}$
Eq. 3	**β-cell function**	$\boldsymbol{HOMA-\beta = \left[\left[\frac{1}{m}\ (Insulin\ \mu UI/L)\right]\ \right)/\left(Glucose\ \frac{mmol}{L}\right) - \frac{b}{m}\right] * 100\%}$
Eq. 4	**Disposition index**	$\boldsymbol{\%ID = (\%S)\ (\%\beta)\ /100\%}$
Eq. 5	**Quantitative Insulin Sensitivity Check Index**	$\boldsymbol{QUICKI = (\ 1\ )/(\log 10\ Glucose\ mmol/L) + (\log 10\ Insulin\ \mu UI/L)}$

Eq. 1. It was assumed that these lines intersect the median data point of the control group, for the research using average fasting glucose (5.99/6.97 mmol/L) and plasma insulin (28.13/ 139.58 mU/L) concentrations from the control mice fed with standard diet at 20/44 weeks. The basal value for HOMA-IR (BV) is the product of both values (168.65/ 972.39 mmol mU/L^2).

Eq. 2. %S represents whole body insulin sensitivity. Eq. 3. To deduce the lines representing 100% insulin sensitivity and 100% β-cell function (%B or HOMA-β) in the control group we used an empirical approach. The linear regression line through the data points of control group (m=12.19 and b=75.6 mmol μUIL^{2-}) was determined and data of the line were used for the calculation of %β in individual mice. Eq. 4. It has been shown that in normal situations changes in %S are adjusted by inverse effects in %B so that the relation between %B and %S can be described by a hyperbolic function and represents insulin disposition index. Eq. 5. QUICKI which is a HOMA modified, since it uses insulin and glucose but applying a logarithmic transformation.

3. Results

3.1 Growth patterns and body composition

At baseline, BW did not differ among any of the groups of mice (start). However, BW was expected to be reduced in the MLD-STZ/SHD-STZ models (T1D) and higher in HFD-DIO (T2D) (*p<0,001*). Within groups of SD fed mice (12 or 36 weeks), mice exposed to MLD-STZ/SHD-STZ treatments had a significantly lower BW compared to CTL-NOM at over time (8weeks). Post-STZ (8 weeks), BW differed between STZ20-T1D and STZ40-T1D (*p<0,001*).

In contrast, BW during generation of T2D was significantly greater in HFD-DIO versus CTL-NOM mice during 44 weeks (*p<0,001*). Moreover, HFD-DIO that received 50 mg/kg STZ (DIO-STZ50-T2D mice) lost a significant amount of BW and became severely underweight (*p<0,001* versus DIO-T2D mice) by end of investigation duration (Fig. 2).

The pathophysiological status of obesity in C57BL/6 male mice fed with HFD is shown in table 2S. STZ40-T1D mice were considered underweight at 8 weeks post-STZ (Fig. 3). From these cut-off points after 16 weeks, HFD produced obesity (*p<0,001)*, but after week 24 until the end of feeding, became more obese (p<0,001) classifying them with obesity class II (36 weeks). At 40 weeks, the increase in BW is not considerable (Fig. 4), so to make biological evaluations was considered the development of obesity from 20 to 36 weeks.

Due to increase in BW, BSA increase in DIO-T2D and DIO-STZ50-T2D mice from 4 weeks, although after STZ, BSA was lower in STZ20-T1D, STZ40-T1D, STZ50-T1D and DIO-STZ50-T2D mice (*p<0,001)* due to weight loss. The same effect is observed for BIM, and there were no considerable changes in body length (BL) (Table 3S).

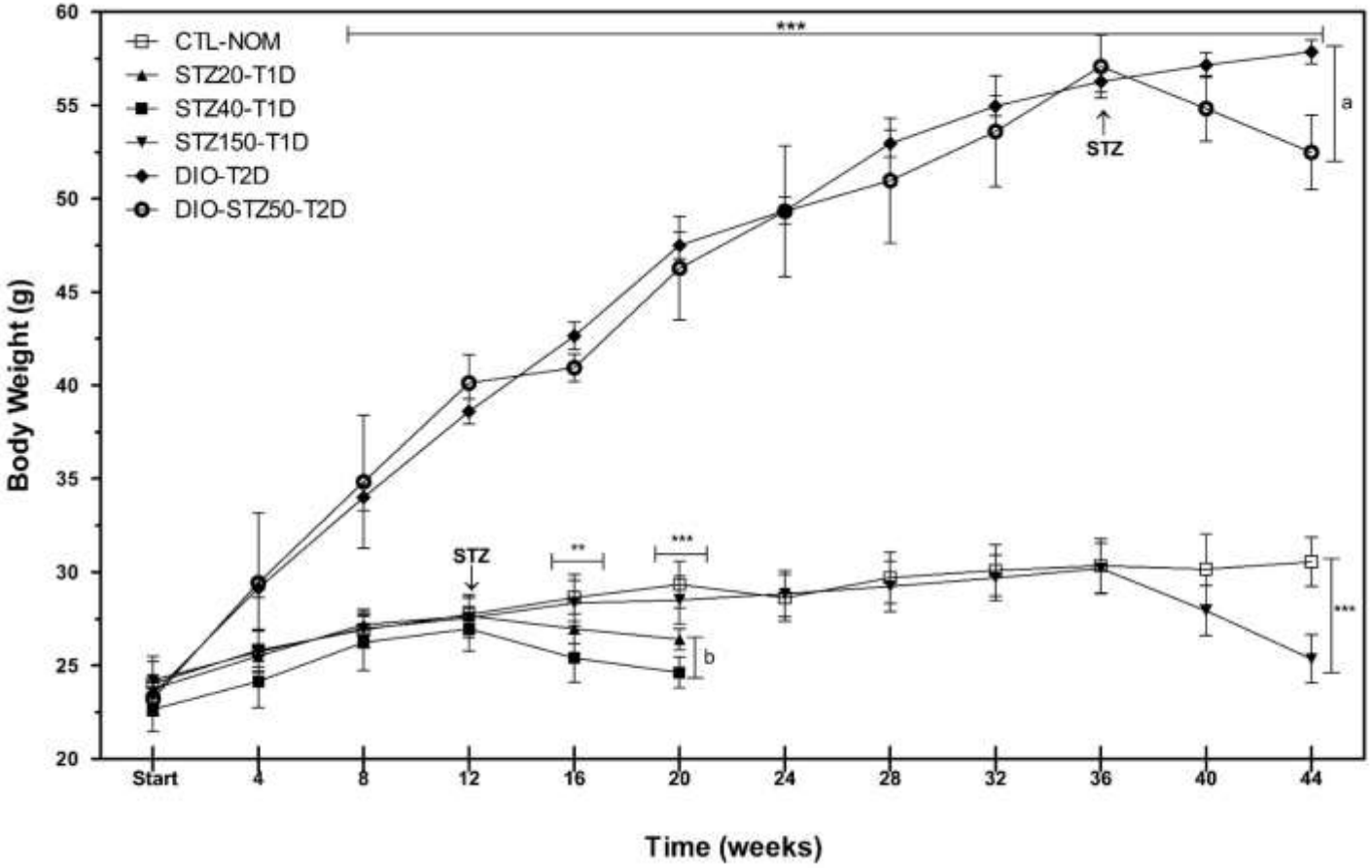

Figure 2. **Longitudinal variation of body weight in DM murine models.**

BW changes in C57BL/6 male mice fed with two dietary regimens: a HFD and SD to developed DM. Values represent means ± SEM of each group. Statistical analysis was performed using two-way ANOVA with Bonferroni multiple comparisons test. ***p<0,001; ** p<0.05 vs CTL-NOM and [a, b] p<0,001 DIO-T2D vs STZ20-T1D.

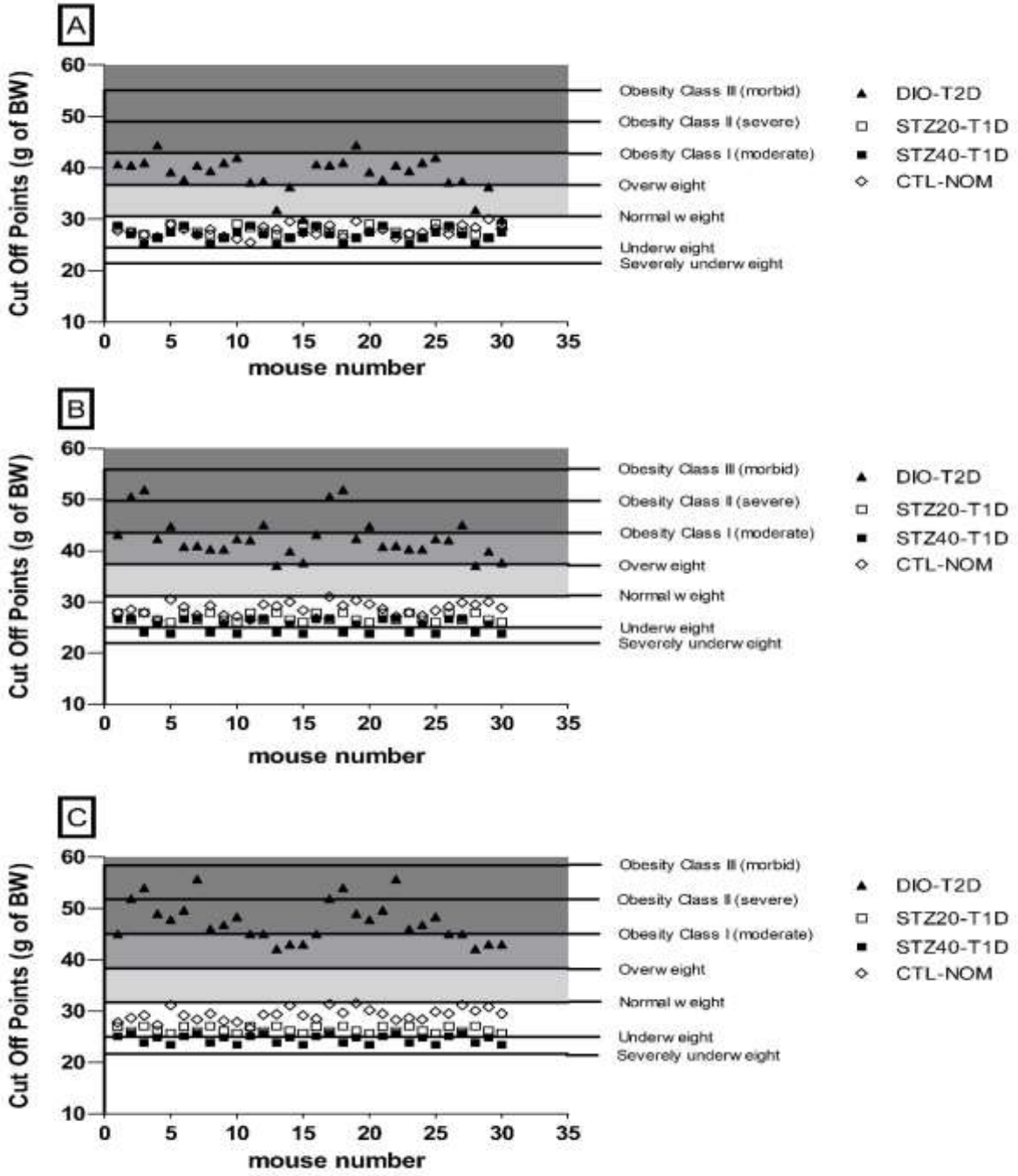

Figure 3. Body weight variations in C57BL/6 male mice on cut-off points of T1D. Individuals BW were used were graphically presented at cut-off points for identify the physical nutritional status of diabetic mice. (A) at 12 weeks before MLD-STZ (B) at 16 weeks and (C) at 20 weeks after MLD-STZ.

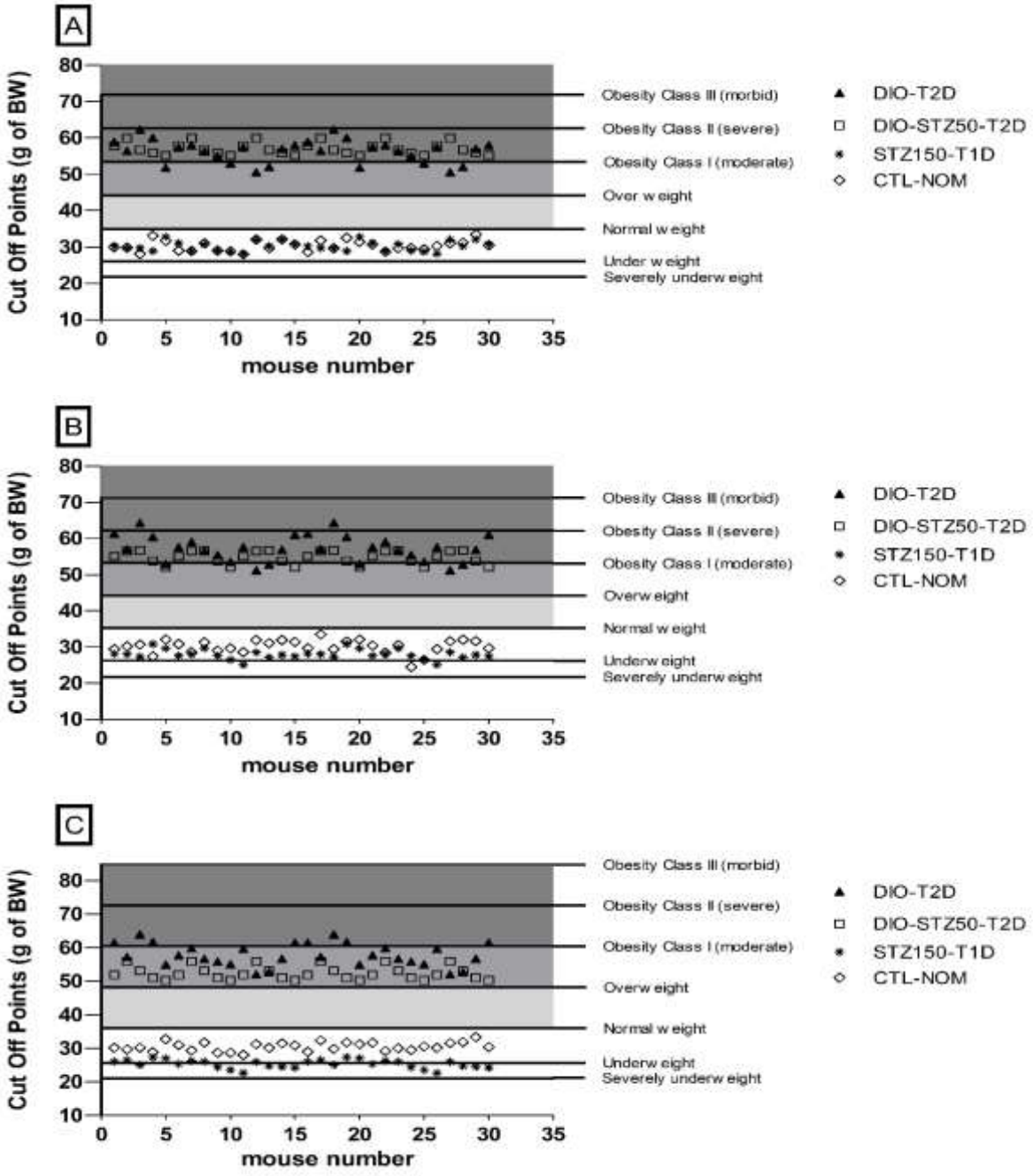

Figure 4. **Body weight variations in C57BL/6 male mice on cut-off points of T2D.** Individuals BW were used were graphically presented at cut-off points for identify the physical nutritional status of diabetic mice. (A) at 36 weeks (B) at 40 weeks and (C) at 44 weeks.

Weight gain or loss in each of DM models can be seen in table 3. Taking into account BW at week 44 of CTL-NOM mice (30.5g). DIO-T2D mice had a more than double WG and a loss for STZ20-T1D (5%), STZ40-T1D (8%), STZ50-T1D and DIO-STZ50-T2D mice (16%) (*p<0,001).* Additionally, parameters to estimate the degree of obesity in DIO-T2D mice were determined. At week 16, Lee index is constant, and BSA_x increases directly proportional to time (*p<0,001),* as shown by DIO-HFD mice (Fig. 1S).

Table 3. Body growth parameters in DM murine models.

T1D model						
	Before LDS (12 weeks)			**After LDS (20 weeks)**		
Parameters BG	**WGt**	**WGm**	**GR**	**WGt**	**WGm**	**GR**
CTL-NOM	3.71±1.05	1.24±0.35	1.16±0.05	1.60±0.64	0.80±0.32	1.06±0.02
STZ20-T1D	3.92±1.26	1.31±0.42	1.17±0.06	-1.26±1.34*	-0.63±0.67	0.96±0.05*
STZ40-T1D	3.72±0.93	1.24±0.31	1.19±0.07	-2.35±1.33*[b]	-1.18±0.66	0.91±0.05*[b]
	Before LDS (36 weeks)			**After LDS (44 weeks)**		
CTL-NOM	6.32±1.45	0.70±0.16	1.26±0.07	0.20±1.07	0.10±0.53	1.01±0.03
STZ150-T1D	5.98±1.38	0.66±0.15	1.25±0.06	-4.84±1.54*	-2.42±0.77	0.84±0.05*
T2D model						
DIO-T2D	32.79±3.15*	3.64±0.35*	2.40±0.16*	1.59±1.04*	0.79±0.52	1.03±0.02
DIO-STZ50-T2D	33.85±2.03*	3.76±0.23*	2.46±0.13*	-4.61±0.90*[a]	-2.31±0.45	0.92±0.02*[a]

Growth rate (GR) and weight gain total and monthly (WGt and WGm) in C57BL/6 male mice on cut-off points of DM. Values represent means ± SEM of each group. Statistical analysis was performed using two-way ANOVA with Bonferroni multiple comparisons test. *p<0,001 vs CTL-NOM and [a, b] p<0,001 vs DIO-T2D and STZ20-T1D respectively.

3.2 Energy metabolism

Feed consumption is reported as caloric intake (Gross energy). After STZ in T1D models, there is an increase in calories ingested by STZ20-T1D, STZ40-T1D, STZ50-T1D and DIO-STZ50-T2D mice (*p<0,001*). Until week 36 in DIO-T2D mice, there was a significant difference in high-calorie consumption compared to the CTL-NOM mice

(Fig. 5A; *p<0,001*). These data suggest the presence of polyphagia in DM models (see Fig. 2S). Metabolizable energy, loss energy as urine, fecal, methane and physiological fuel value of each DM model can be consulted in table 4S.

The daily volume drank of water was higher CTL-NOM mice compared to DIO-T2D mice ($p<0.001$); this difference could be attributed to DIO-HFD modifying the satiety center of animal. Conversely, after STZ induction in T1D models, there was a substantial increase in water consumption ($p<0.001$) (Fig. 5B). This indicates the presence of polydipsia, and a daily change of sawdust in the mouse's box was necessary due to the onset of polyuria.

Regarding the comparison between energy revenues and energy expenditures expressed as EB, it shows the same trend as gross energy (Fig. 6), indicating dysregulation of food intake. Metabolic Weight, basal metabolic rate, and total daily expenditure of energy, necessary for calculating EB, are shown Table 5S.

3.3 Metabolic profile

Fasting blood glucose levels in DM murine models can see in figure 7. In the development of T1D by MLD-STZ, a significant increase in FBG was observed. As anticipated, in each of DM model, FGB was significantly elevated compared to CTL-NOM mice ($p<0,001$). FBG increased two to threefold compared to basal concentration after STZ administration ($p<0,001$).

Subsequently, BG concentration increased significantly, reaching levels that are considered values for chronic diabetes. FBG increased significantly when mice received HFD for 36 weeks, while it remained almost unchanged in CTL-NOM mice ($p<0,001$). From weeks 12 to 32, with blood glucose levels greater than 150mg/dL, DIO-T2D mice were classified as having pre-diabetes, from week 36, acute diabetes; and at 44 weeks, chronic diabetes (Table 6S and 7S).

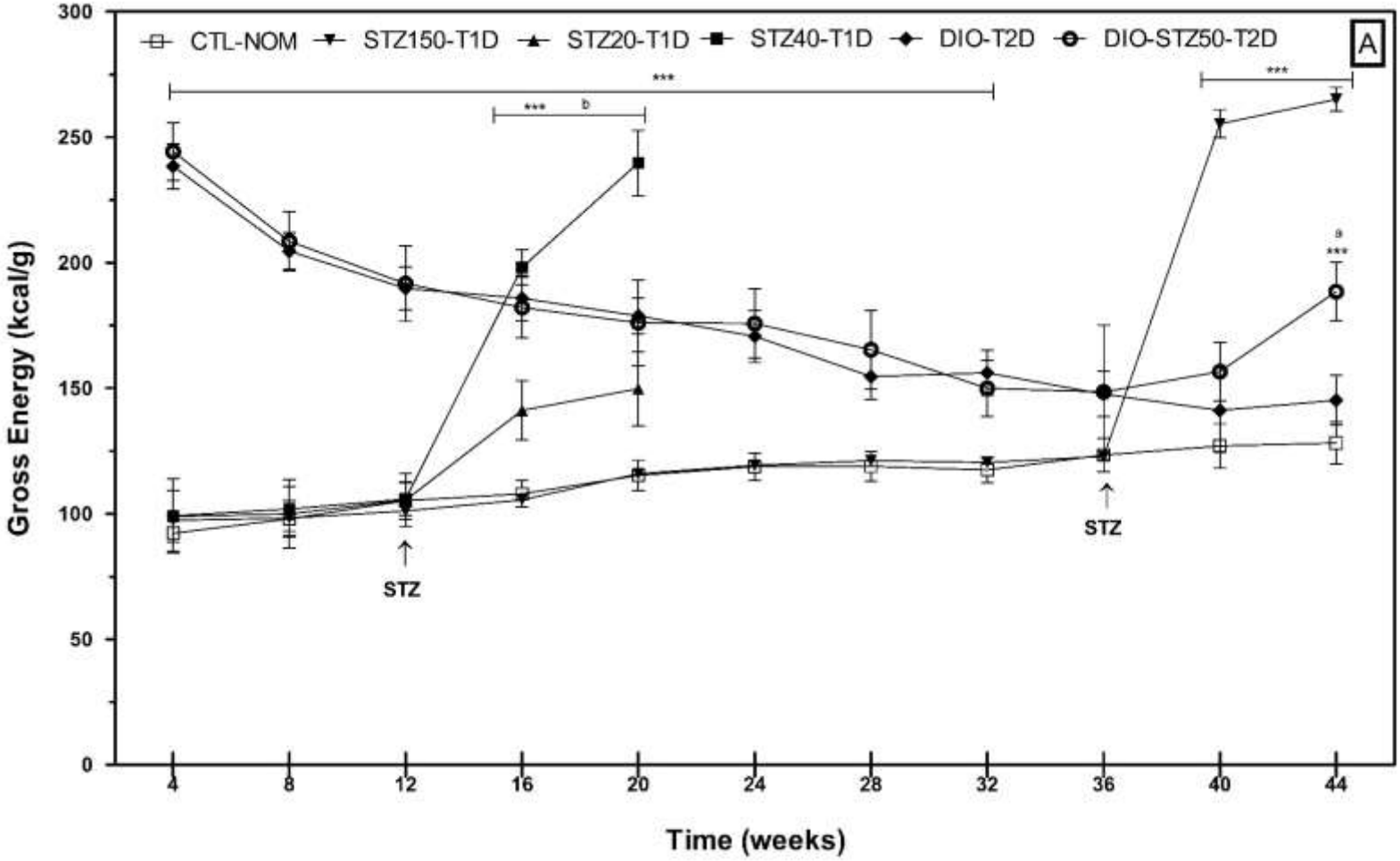
CTL-NOM
STZ150-T1D
STZ20-T1D
STZ40-T1D
DIO-T2D
DIO-STZ50-T2D
A
Gross Energy (kcal/g)
Time (weeks)
STZ
STZ
***
***
***
b
a
300
250
200
150
100
50
0
4
8
12
16
20
24
28
32
36
40
44

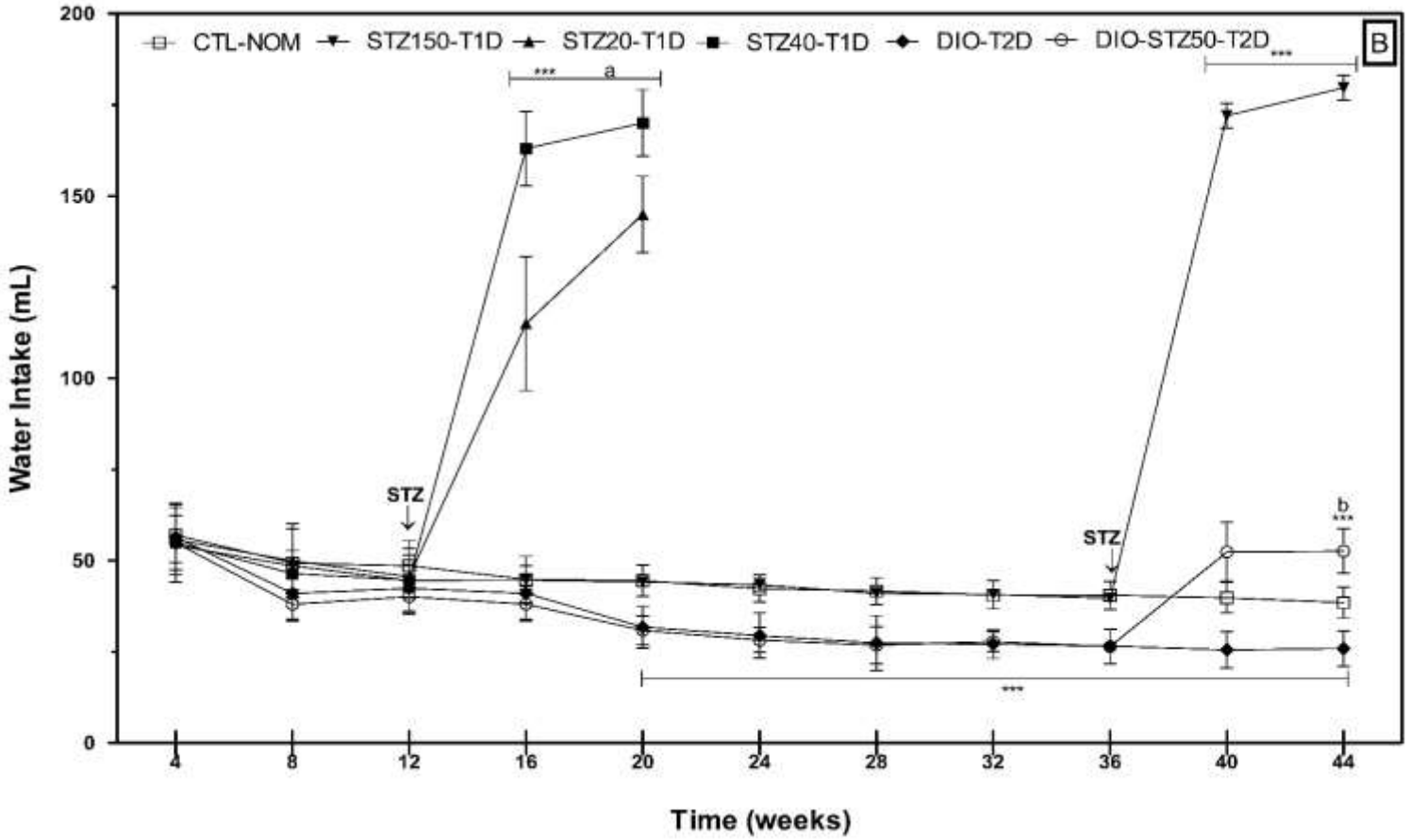

Figure 5. **Nutrient's intake in DM murine models**. (A) Food consumption expressed as gross energy o energy density and (B) Water intake in C57BL/6 male mice across the feeding time 44 weeks. Values represent means ± SEM of each group. Statistical analysis was performed using two-way ANOVA with Bonferroni multiple comparisons test. ***p<0,001 vs CTL-NOM and [a, b] p<0,001 vs DIO-T2D and STZ20-T1D respectively.

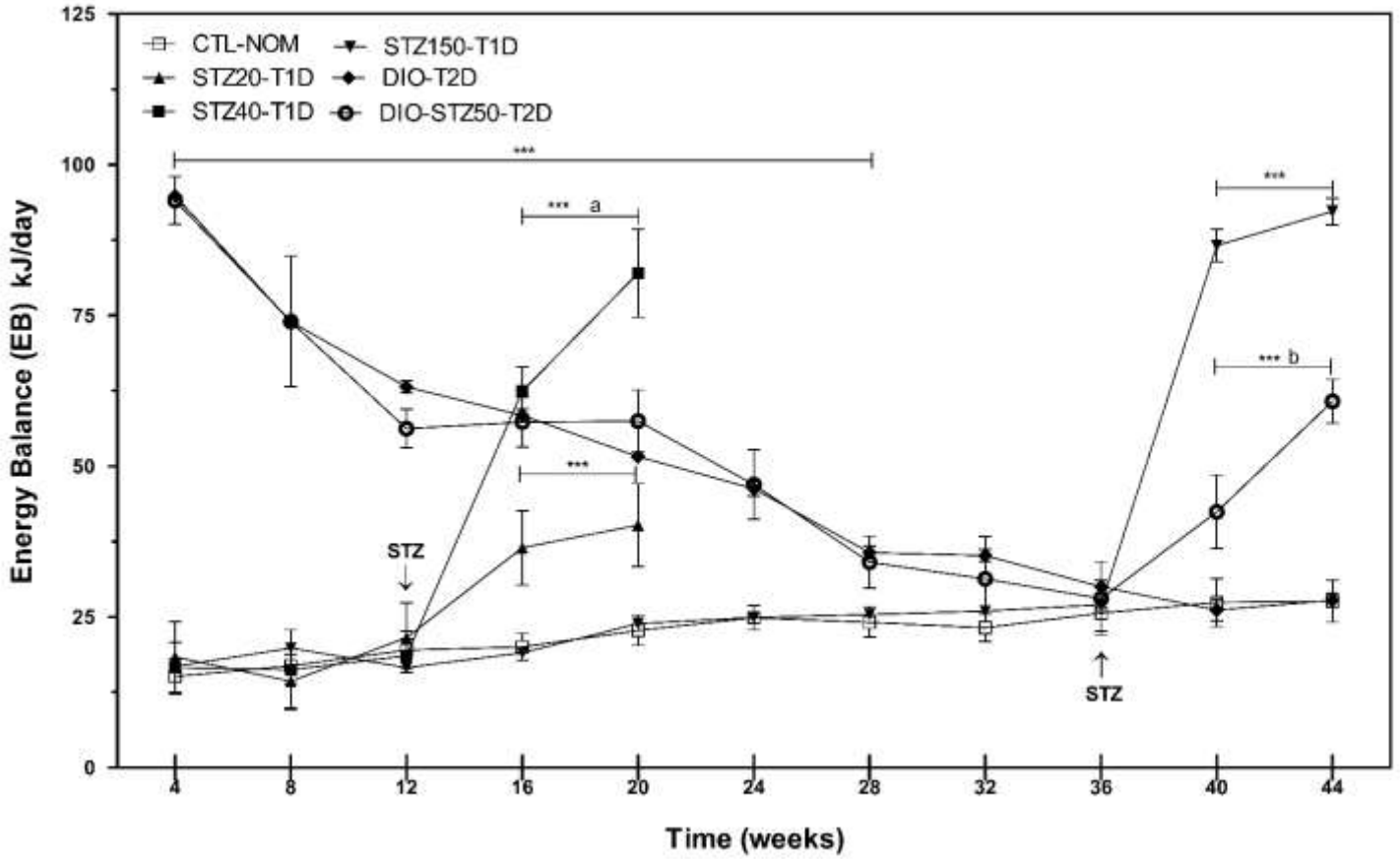

Figure 6. **Energy balance in DM murine models.** Comparison between energy revenues and energy expenditures in C57BL/6 male mice across the feeding time. Values represent means ± SEM of each group. Statistical analysis was performed using two-way ANOVA with Bonferroni multiple comparisons test. The symbols ***p<0,001 vs CTL-NOM. and [a, b] p<0,001 vs DIO-T2D and STZ20-T1D respectively.

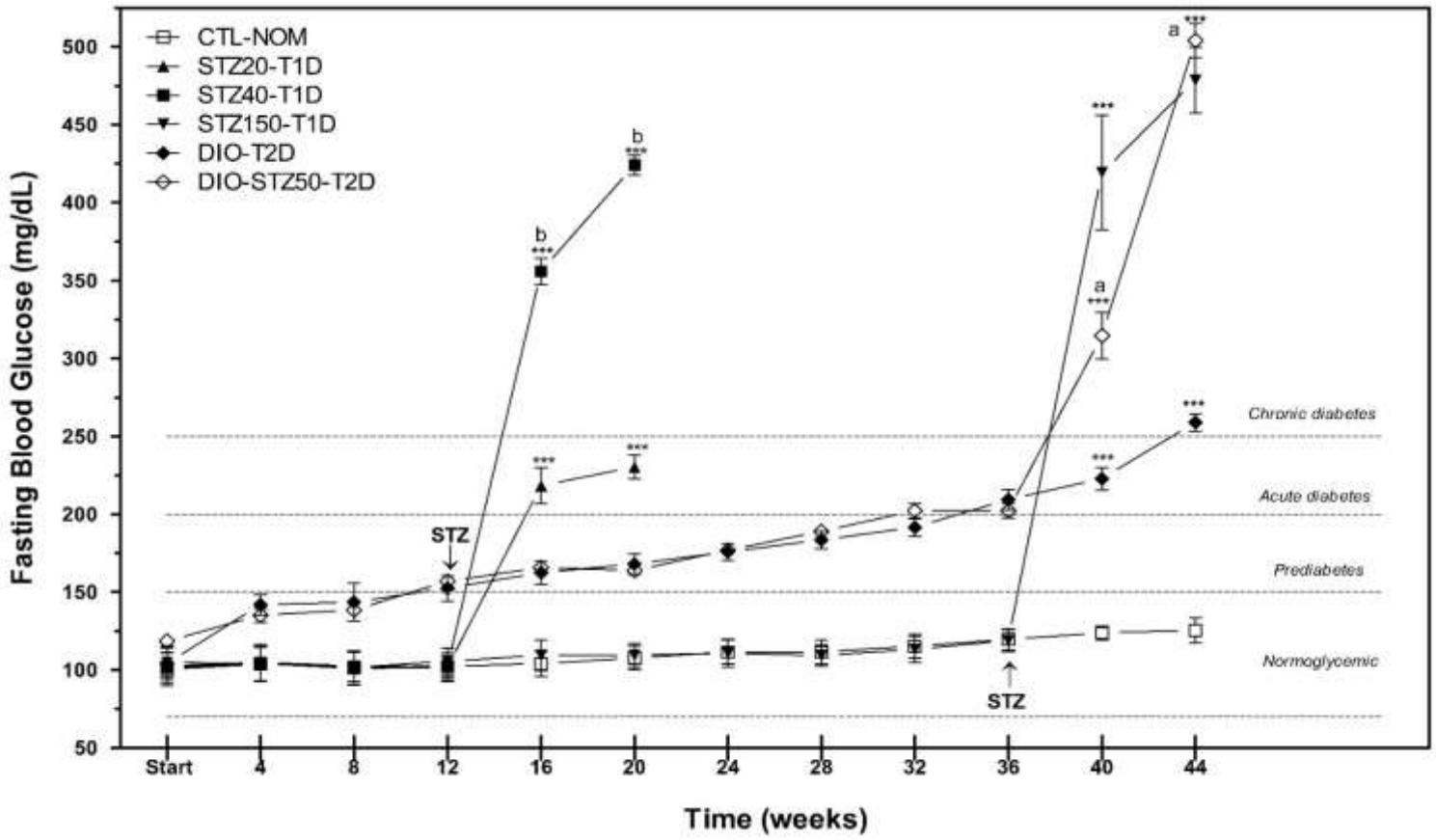

Figure 7. Fasting blood glucose levels in DM murine models. FBG (mg/dL) in C57BL/6 male mice across the feeding time. Values represent means ± SEM of each group. Statistical analysis was performed using two-way ANOVA with Bonferroni multiple comparisons test. ***p<0,001 vs CTL-NOM. and a, b p<0,001 vs DIO-T2D and STZ20-T1D respectively.

FBG values for STZ-injected mice were significantly elevated after the fourth injection and increased substantially during the subsequent weeks. In DIO-STZ50-T2D mice, FBG increase very rapidly from start of STZ administration (p<0,001), surpassing DIO-T2D and reaching classification as chronic diabetes. Interestingly, there were significant differences in FBG (p<0,001) between DM models (Figs. 3S and 4S). Similar differences in the increase and classification of DM are observed in PPBG (Fig. 8).

Figure 9 show the results of OGTT in two types DM, performed after 8 weeks of cut-off point (12 weeks for T1D and 36 weeks for T2D). In CTL-NOM mice, BG peaked at 15 min after glucose bolus; thereafter, a first-order kinetic of glucose elimination occurs until minute 120. In contrast, DIO-STZ50-T2D and DIO-T2D mice showed minimal glucose elimination between minute 15 and 120, suggesting severe glucose intolerance.

Figure 10 depicts plasma insulin levels in MLD-STZ/SHD-STZ models (STZ40-T1D and STZ150-T1D mice), which were significantly lower compared to CTL-NOM mice (*p<0,001)*, attributed to STZ-induced destruction of pancreatic β-cells similar to T1D. In DIO-T2D mice, there was evidence of hyperinsulinemia (p<0,001) compared to CTL-NOM mice.

3.4 Insulin resistance (IR)

Parametric models, such as HOMA-IR, are commonly used to assess the degree of IR and glucose intolerance. IR measured by HOMA-IR was increased in DIO-T2D and DIO-EZT50-T2D mice (p<0,001). There was no difference in insulin levels or HOMA-IR between MLD-STZ/SHD-STZ models (STZ20-T1D, STZ40-T1D and STZ150-T1D) and CTL-NOM mice, indicating the absence of IR but presence insulin deficiency, the main characteristic of T1D. Interestingly, plasma insulin and HOMA-IR were one-fold lower in DIO-EZT50-T2D compared to DIO-T2D mice, presumably as a consequence of single dose of STZ at week 36 (Fig. 11 A).

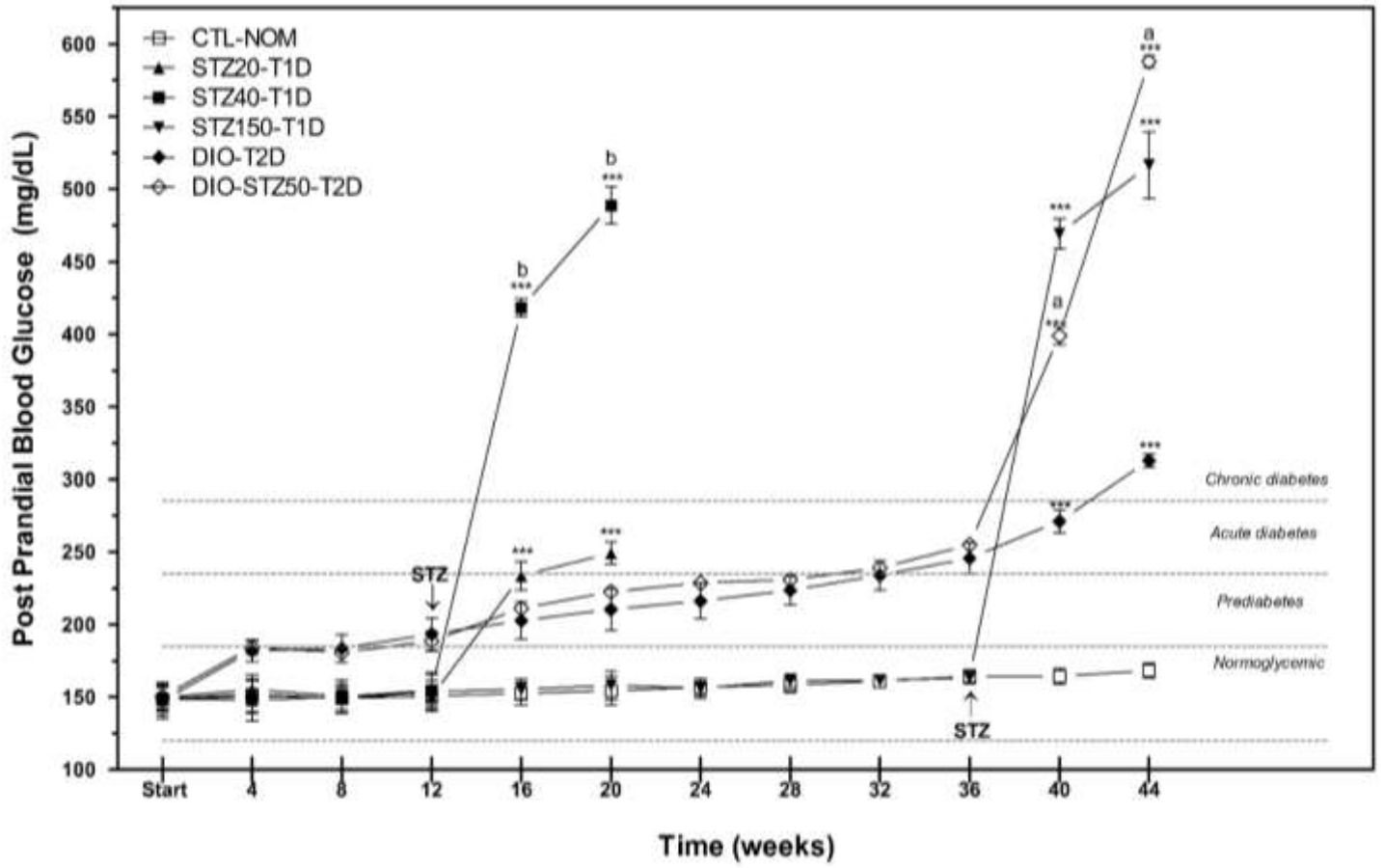

Figure 8. **Postprandial blood glucose levels in DM murine models.**

PPBG (mg/dL) in C57BL/6 male mice across the feeding time. Values represent means ± SEM of each group. Statistical analysis was performed using two-way ANOVA with Bonferroni multiple comparisons test. ***p<0,001 vs CTL-NOM. and [a, b] p<0,001 vs DIO-T2D and STZ20-T1D respectively.

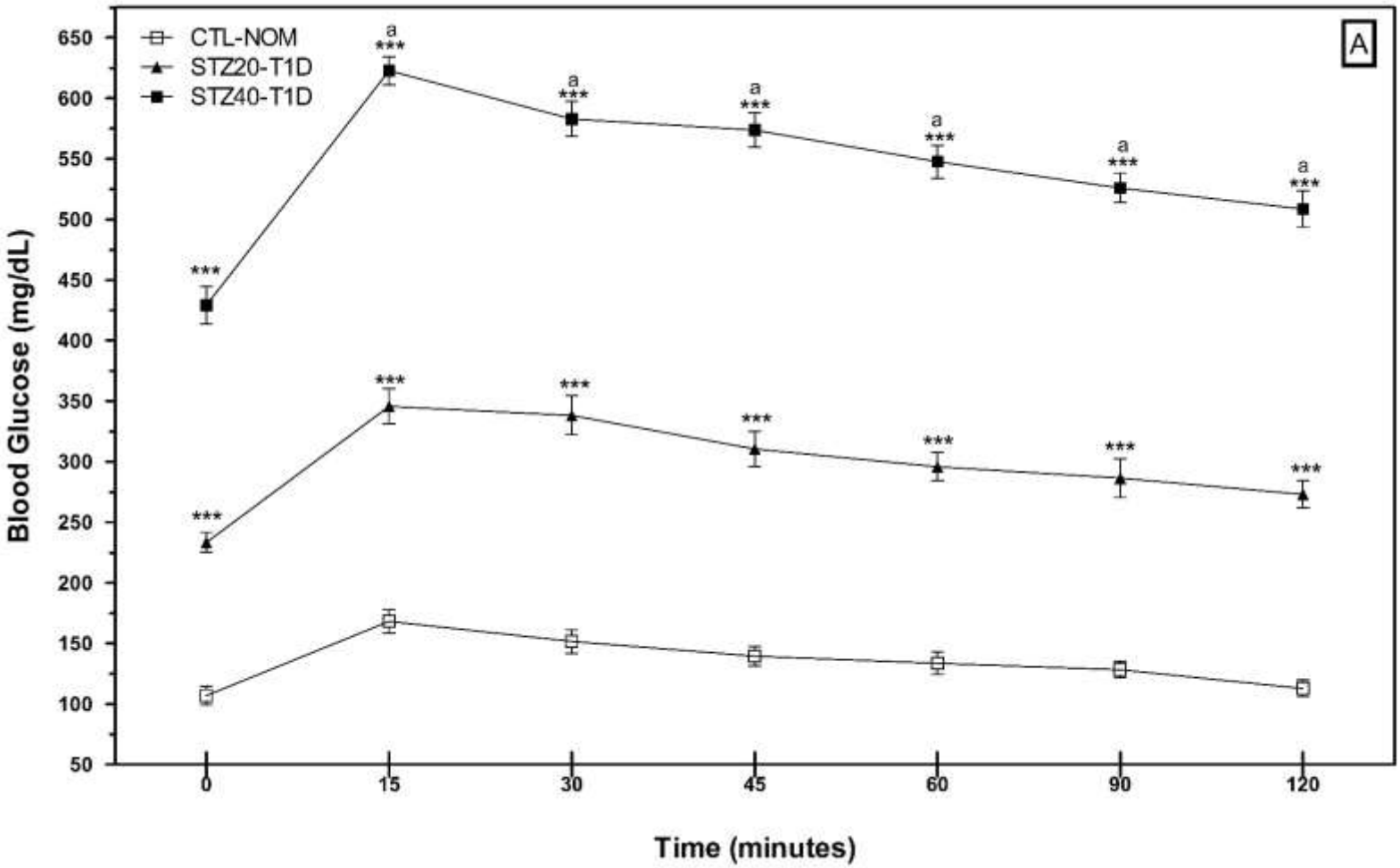
CTL-NOM
STZ20-T1D
STZ40-T1D
A
Blood Glucose (mg/dL)
650
600
550
500
450
400
350
300
250
200
150
100
50
0
15
30
45
60
90
120
Time (minutes)
***
a

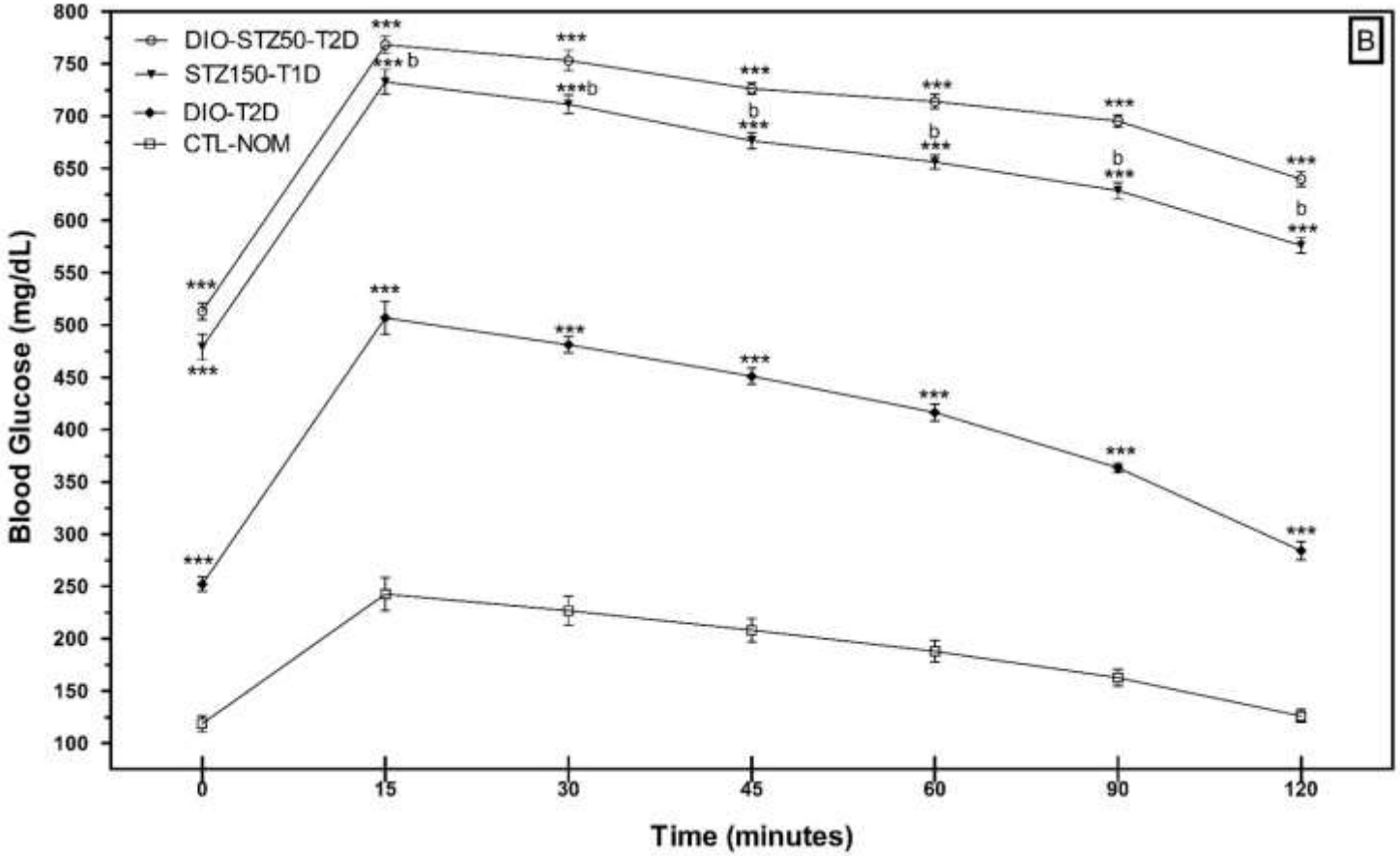

Figure 9. **Oral glucose tolerance test in DM murine models.** BG (mg/dL) during OGTT in C57BL/6 male mice. (A) T1D model (20 weeks) and (B)T2D model (44 weeks.). Data shown are means ± SEM of each group. Statistical analysis was performed using two-way ANOVA with Bonferroni multiple comparisons test. ***p<0,001 vs CTL-NOM. and [a,b] p<0,001 vs STZ20-T1D and DIO-T2D respectively.

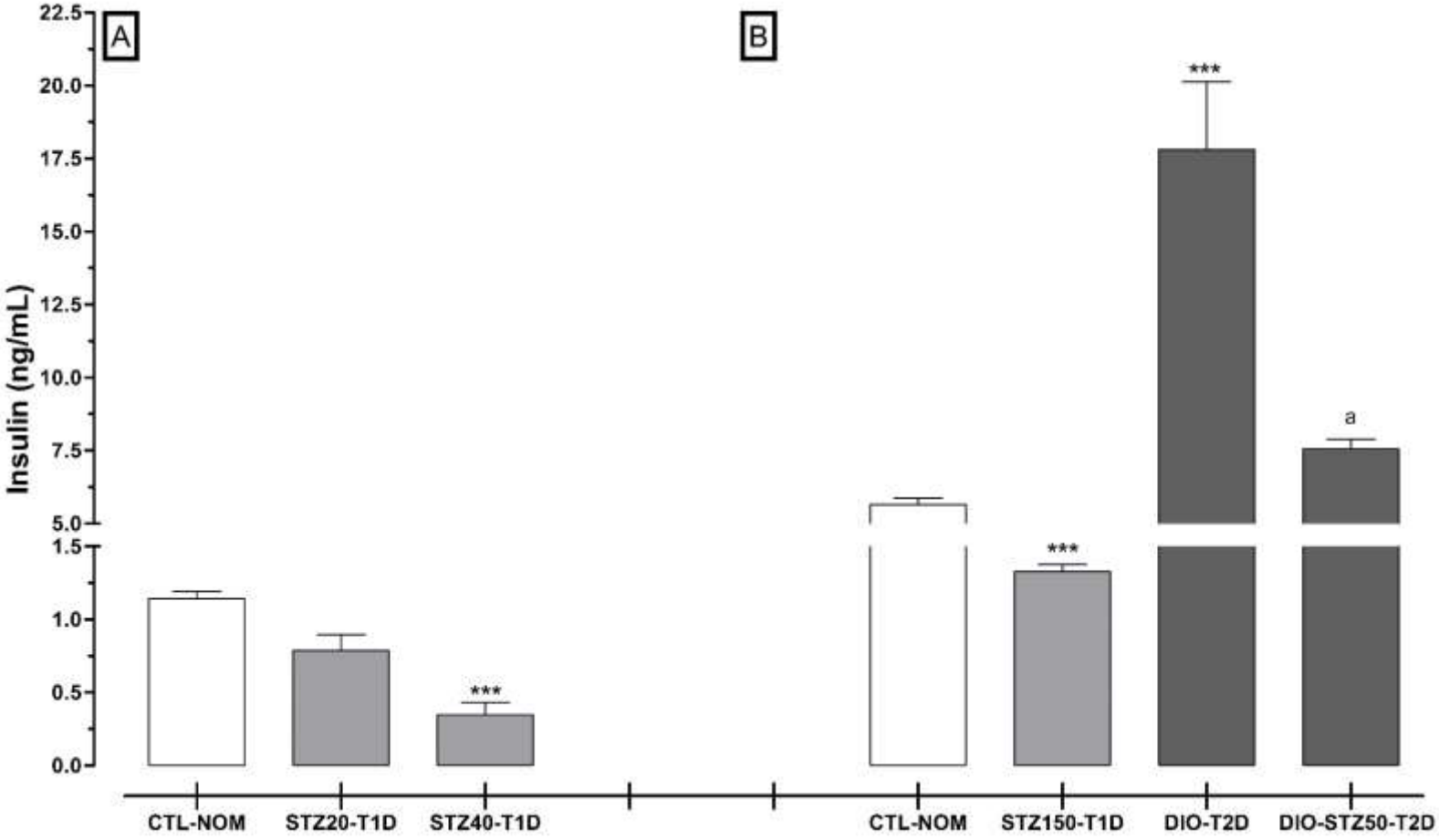

Figure 10. Plasma insulin levels in DM murine models. Insulin (ng/mL) in C57BL/6 male mice. (A) T1D model (20 weeks) and (B) T2D model (44 weeks). Data shown are means ± SEM of each group. Statistical analysis was performed using one-way ANOVA with Bonferroni multiple comparisons test. ***p<0,001 vs CTL-NOM. and [a] p<0,001 vs DIO-

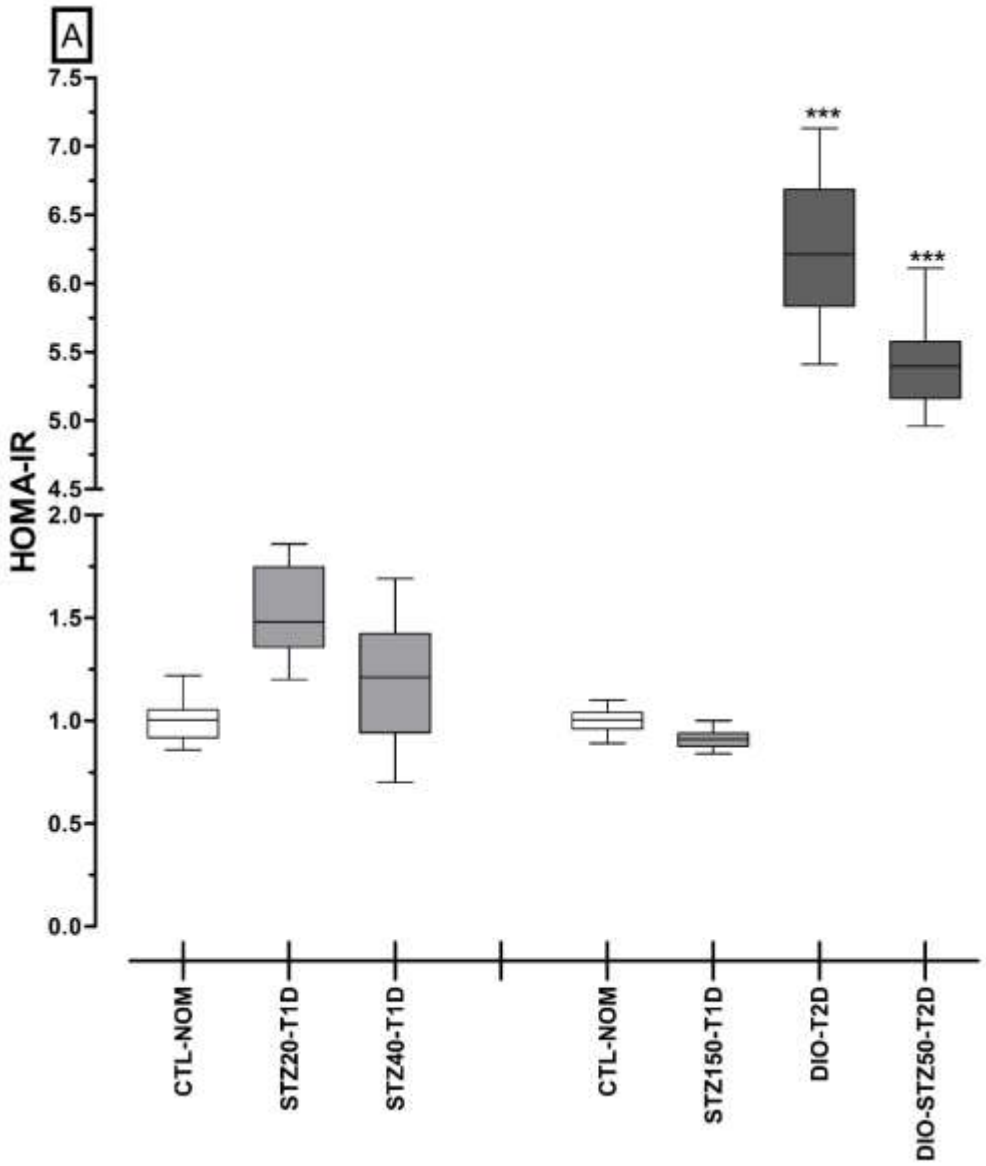
A
HOMA-IR
7.5
7.0
6.5
6.0
5.5
5.0
4.5
2.0
1.5
1.0
0.5
0.0
***
***
CTL-NOM
STZ20-T1D
STZ40-T1D
CTL-NOM
STZ150-T1D
DIO-T2D
DIO-STZ50-T2D

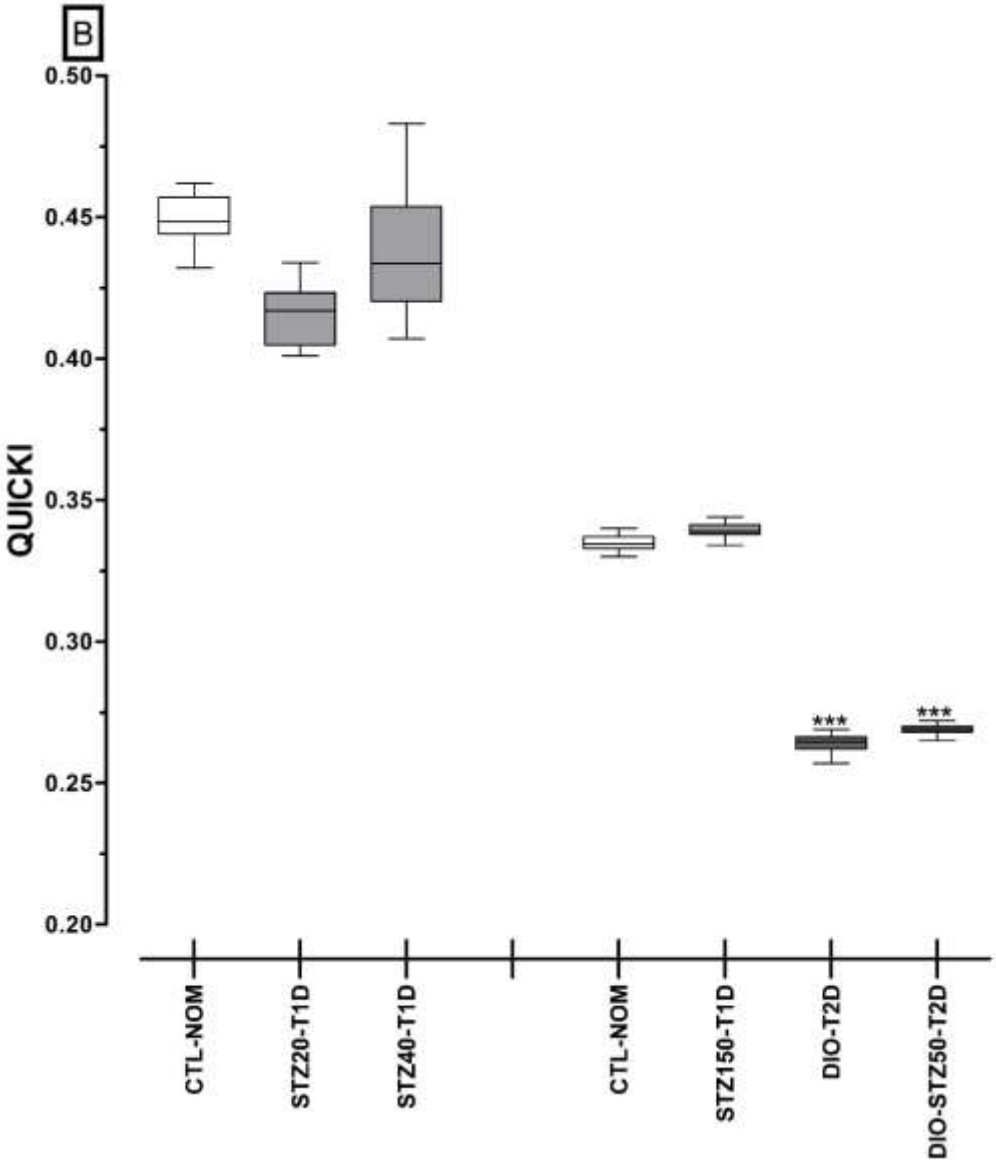
B
QUICKI
0.50
0.45
0.40
0.35
0.30
0.25
0.20
***
***
CTL-NOM
STZ20-T1D
STZ40-T1D
CTL-NOM
STZ150-T1D
DIO-T2D
DIO-STZ50-T2D

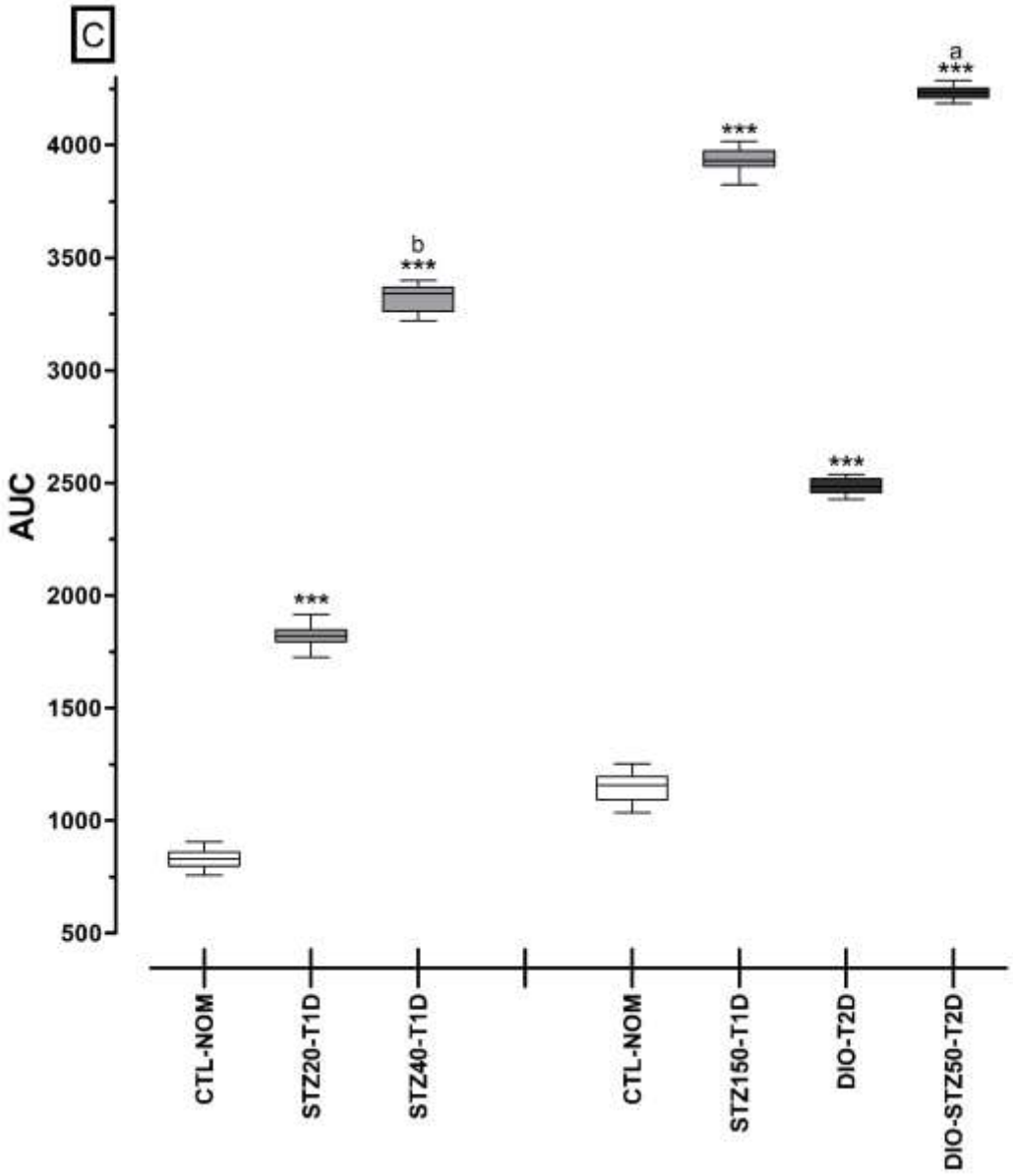

Figure 11. Insulin resistance in DM murine models. (A) HOMA-IR. (B) QUICKI and (C) AUC for OGTT. The left segment in each graph corresponds to T1D model (20weeks) and the right to T2D model (44 weeks). Data are presented as median with ranges in a Tukey box plot. Statistical analysis was performed using one-way ANOVA with Dunn's Multiple Comparison Test. ***p<0,05 vs CTL-NOM and a,b p<0,05 vs STZ20-T1D and DIO-T2D respectively.

Similar results were obtained when insulin sensitivity was determined using QUICKI. Furthermore, QUICKI evidenced a decrease in insulin sensitivity only in HFD-DIO mice (T2D) versus CTL-NOM (*p<0,001*). In mice fed with SD that received STZ (T1D), data revealed no difference in insulin sensitivity when were compared (Fig. 11 B). IR analyzed as AUC shown in figure 11 C was apparent in T2D mice (DIO-T2D and DIO-EZT-T2D mice) compared to CTL-NOM (*p<0,001*) post-glucose challenge, indicating impaired glucose clearance.

In addition, the %S and HOMA-β were calculated, with values of CTL-NOM mice representing 100% insulin sensitivity and 100% β-cell function. In Fig. 12 A, after 36 weeks %S was slightly but significantly reduced in DIO-T2D and DIO-STZ50-T2D mice (*p<0,001*). β-cell function (%B) in CTL-NOM mice remained unchanged but was increased in DIO-TD2 mice (*p<0,001*), implying compensation for reduced insulin sensitivity by increasing β-cell activity. In T1D models, function is diminished (*p<0,001*) due to chronic MLD-STZ and severe SHD-STZ destruction of the pancreas (Fig. 12 B). Shown in Fig. 12 C, DI, a measure for the ability of β-cells to compensate for reduced insulin sensitivity. Therefore, T1D groups have very low levels at the end of the experiment (*p<0,001*). Besides DI in DIO-T2D mice was greatly reduced compared with CTL-NOM mice (*p< 0,001*).

3.5 Phenotyping of DM murine models

In this study, C57BL/6 male mice received 20, 40, or 150 mg/kg STZ (T1D), induced significant body weight loss by eight weeks after STZ injections with decreased insulin levels and increased FBG and PPBG dependent on STZ concentration. T1D groups have low levels %S, HOMA-β and DI, indicating impaired β-cell function. Polyuria, polydipsia and polyphagia were also observed in this model. On the other side, C57BL/6 male mice consuming HFD generated obesity, hyperglycemia, insulin resistant (key characteristics of T12D). Alterations in FBG, PPBG and HOMA-IR, were observed, along with excessive increase in calorie consumption and weight gain.

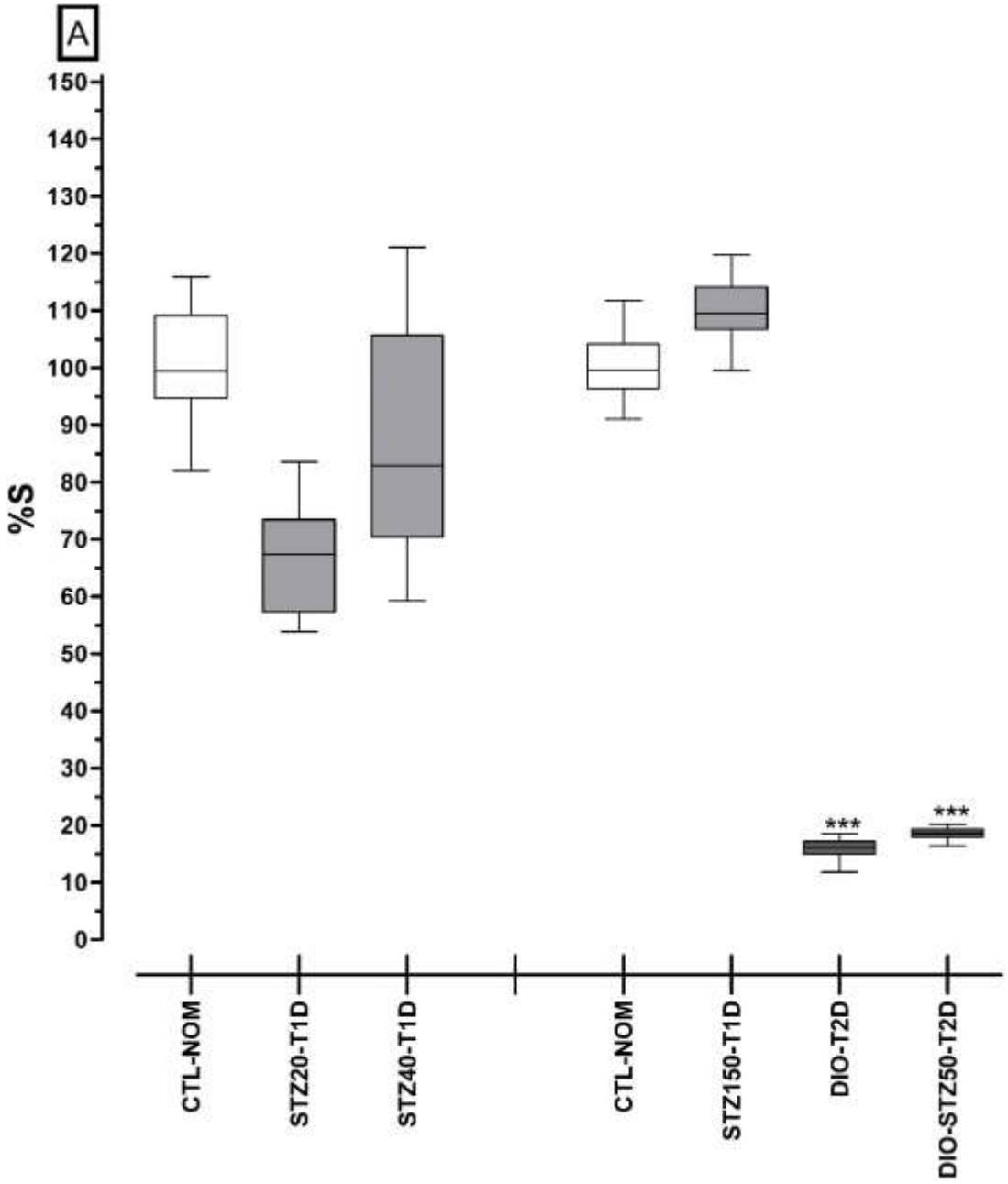
A
%S
150
140
130
120
110
100
90
80
70
60
50
40
30
20
10
0
***
***
CTL-NOM
STZ20-T1D
STZ40-T1D
CTL-NOM
STZ150-T1D
DIO-T2D
DIO-STZ50-T2D

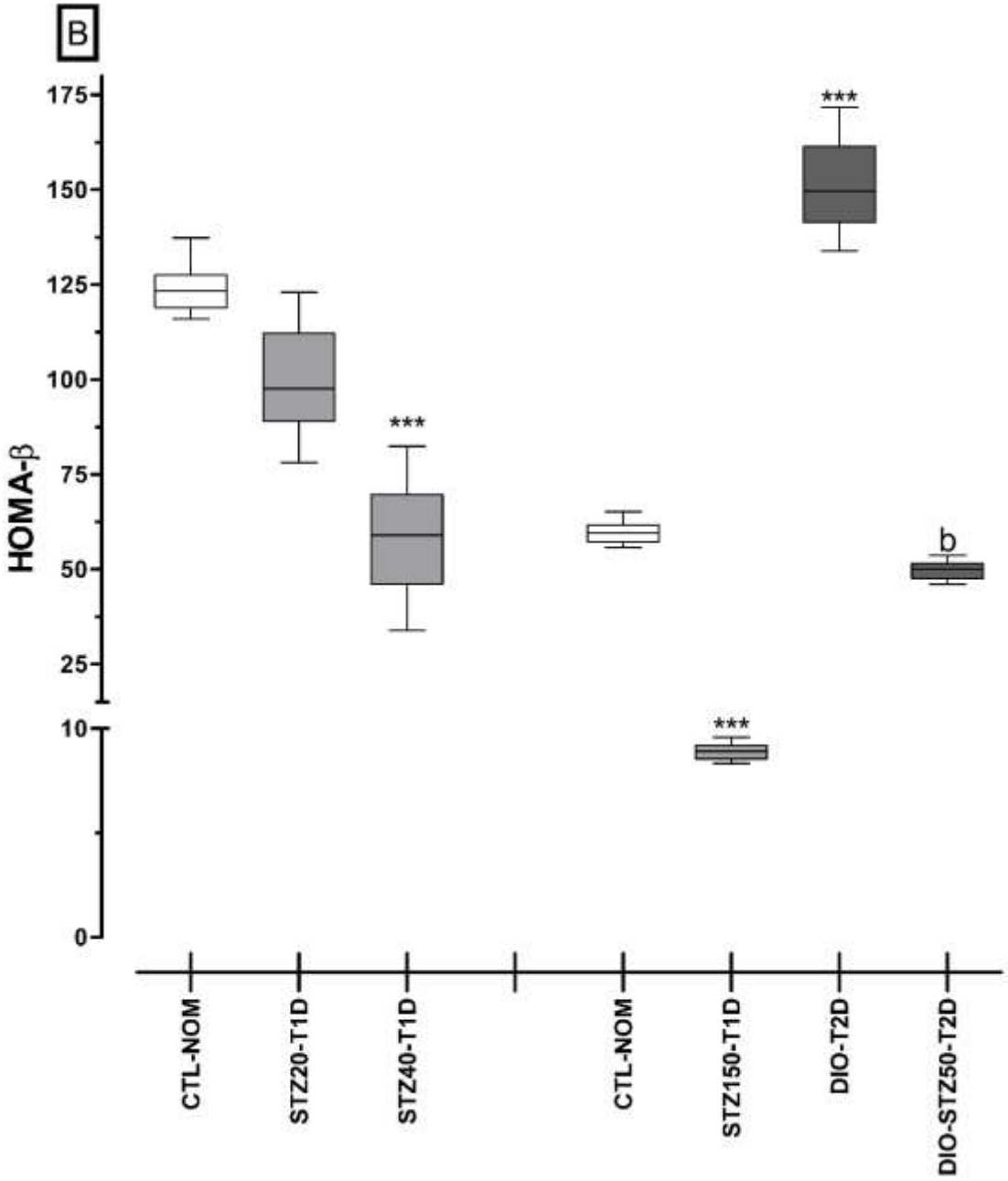
B
HOMA-β
175
150
125
100
75
50
25
10
0
***
***
***
b
CTL-NOM
STZ20-T1D
STZ40-T1D
CTL-NOM
STZ150-T1D
DIO-T2D
DIO-STZ50-T2D

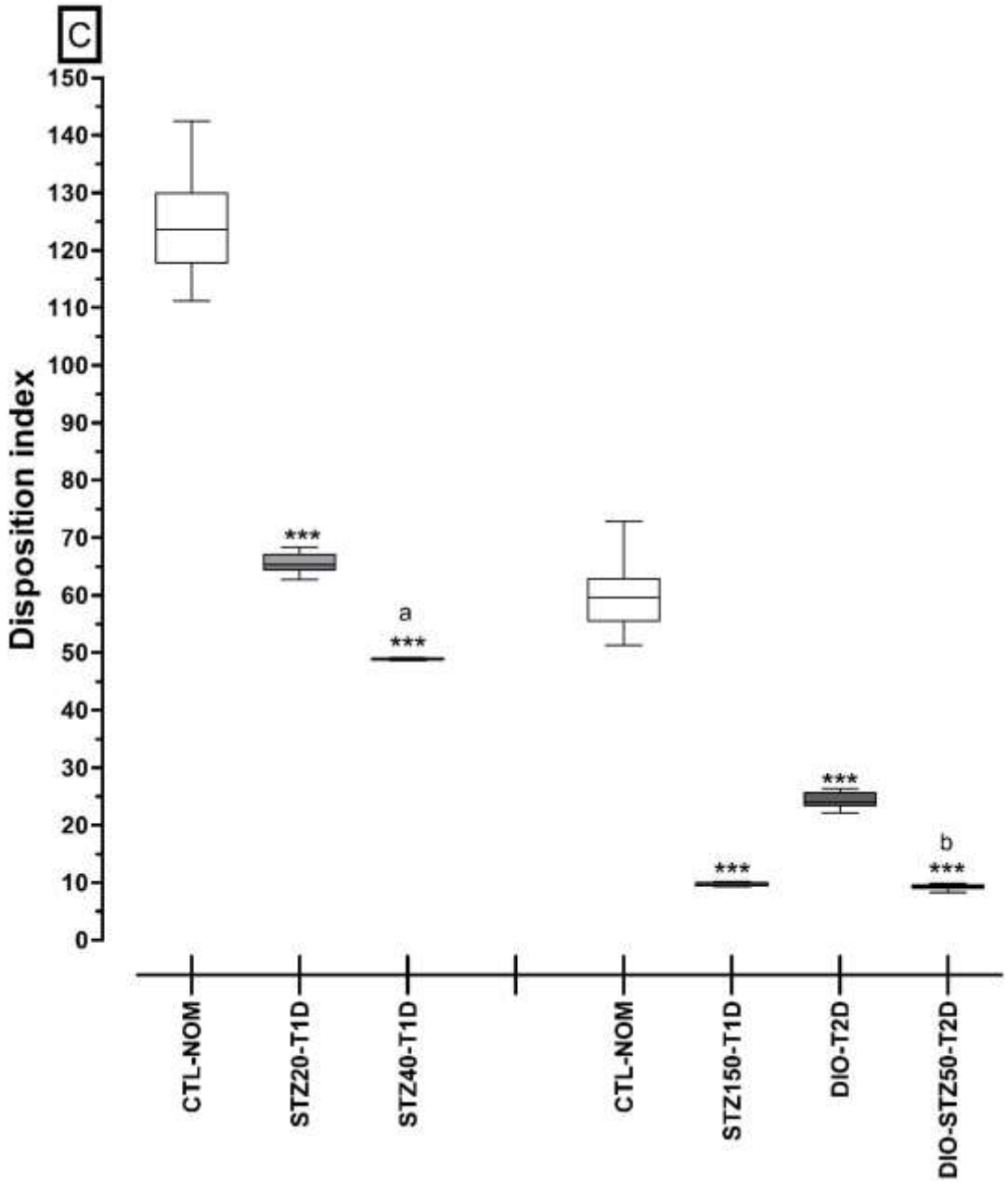

Figure 12. **Insulin sensitivity in DM murine models**. (A) Insulin sensitivity (%S). (B) β-cell function (HOMA-β) and (C) Disposition index (DI). The left segment in each graph corresponds to T1D model (20weeks) and the right to T2D model (44 weeks). Data are presented as median with ranges in a Tukey box plot. Statistical analysis was performed using one-way ANOVA with Dunn's Multiple Comparison Test. ***p<0,05 vs CTL-NOM and [a,b] p<0,05 vs STZ20-T1D and DIO-T2D respectively.

4. Discussion

4.1 T1D Model

The diabetes-inducing agent STZ is a monofunctional nitrosourea derivative isolated from *Streptomyces achromogenes*. It has broad-spectrum antibiotic activity and antineoplastic properties and is often used to induce DM in experimental animals through its toxic effects on pancreatic β cells. STZ is a potent alkylating agent known to directly methylate DNA and is highly genotoxic, producing DNA strand breaks, alkali-labile sites, unscheduled DNA synthesis, DNA adducts, chromosomal aberrations, micronuclei, sister chromatid exchanges, and cell death (Bolzán & Bianchi, 2002).

The destruction of pancreatic β-cells by STZ is associated with a huge release of insulin in their first phase, and then in the second phase, the destruction has led to deficiency of insulin causes hyperglycemia (Prog Drug Res, 2016). Several STZ dosing methods exist in the literature, depending on the type and severity of diabetes intended for the specific experimental protocol. The dose can vary greatly based on the species of the animal, the age of the animal, the route of administration, and the weight of the animal (Rais et. al., 2022).

Diabetogenic doses although variable, these dosing systems tend to fall into one of three categories: multiple small doses of STZ (MLD-STZ) over a period of several days (30-80mg/kg x 3–5 days), a single moderately sized dose (100-125 mg/kg), or a single large dose of the drug (150-300mg/kg) (Deeds et.al., 2011).

MLD-STZ are generally used in experiments attempting to mimic autoimmune insulitis and tends to produce T1D. C57BL/6 male mouse model of diabetes induced by MLD-STZ with 40 mg/kg for 5 days produce pancreatic insulitis, with progression to nearly complete β cell destruction and DM (Wang & Gleichmann, 1998; Friesen et. al., 2004).

The MLD-STZ model employed in this study using C57BL/6 male mice, adequately demonstrated the key features of T1D, including a lean phenotype, hypoinsulinemia,

and hyperglycemia, as demonstrated by both raised FBG and PPBG. Furthermore, the MLD-STZ/SHD-STZ models does not exhibit elevated HOMA-IR (evidence of IR), which is due to the suppressive effect of STZ on β-cell production of insulin, thereby preventing increased insulin secretion (Glastras et. al., 2016).

4.2 T2D Model

Studies have revealed that to induce DM by DIO-HFD in mice, 50-60 kcal% fat is commonly used. However, when screening the effects of drug or genetic manipulation, it may sometimes be necessary to use a 50% fat diet, as it could be more difficult to prevent or reverse the effects of this extreme 60% fat diet (Wang & Liao, 2012). It should be noted that different types of fats have different effects on glucose homeostasis and insulin sensitivity.

C57BL/6 mouse model is advantageous given its short gestational period, long lifespan, ease of availability, and the animal's tendency to over-consume HFD, thus mimicking human behavior and resulting in an obese phenotype. Furthermore, the wild type C57BL/6 mouse is particularly susceptible to weight gain when fed HFD compared to other genetically manipulated mouse models (Glastras et. al., 2016).

Both obesity and aging are characterized by a low-grade inflammatory state and endocrine changes. Obesity is accompanied by and accelerated with chronic inflammation in adipose tissue, especially visceral adipose tissue (VAT). This low-level inflammation predisposes the host to the development of metabolic disease, most notably T2D (Satoh et. al., 2022). Chronic inflammation in metabolic organs that affect IR and systemic energy metabolism is regulated by diverse com-ponents of the immune system (Zmora et. al., 2017).

Diet plays a crucial role in experimental animal nutrition, and understanding the relevant mechanisms of specific nutrients in creating an animal model is essential (Gheibi et. al., 2017). The first description of HFD inducing obesity through nutritional intervention

dates back to 1959 (Masek & Fabry, 1959). The C57BL/6 mouse model fed a high-fat diet (HFD), introduced by Surwit et. al. (1988), is used as a model of T2D due to altered glycemic response to ad libitum exposure to DIO-HFD. Obesity-associated insulin resistance is a major risk factor for T2D, and this group of mice may exhibit characteristic of T2D (Aigner et. al., 2008).

Mice fed a DIO-HFD gradually develop IR; showing impaired insulin sensitivity combined with greater insulin secretion, similar to characteristic observed in many obese humans. The progression to T2D in human with obesity is primarily attributed to insulin secretory dysfunction and a significant loss of functional pancreatic β cells (Gilbert et. al., 2011).

Furthermore, our dates suggest that a longer feeding time to DIO-HFD (36 weeks) may increase susceptibility to insulin sensitivity. Pancreatic β cell factors are thought to control glucose homeostasis by modulating insulin levels and insulin sensitivity, and further studies are needed to better define models of DM by means of impaired β-cell function, not solely relying on BG and insulin levels (Xu et. al., 2020).

DIO-HFD in C57BL/6 male mice significantly increased both insulin and BG, resulting in increased HOMA-IR and HOMA-β, decreased DI and %S (Van Dijk et. al., 2013). C57BL/6 male mice fed with DIO-HFD develop hyperglycemia, hyperinsulinemia, increased BW, central obesity, adiposity, hypertension, hyperlipidemia, glucose intolerance and IR, giving rise to T2D as complex metabolic disorder essentially characterized by these alterations (Collins et. al., 2004; Brito et. al., 2016; Glastras et. al., 2016).

Moreover, C57BL/6 male mice fed with HFD developed weight gain, elevated HOMA-IR compatible with the presence of IR, dyslipidemia, fat storage, and hepatic structural changes, and low-grade inflammation along with gut microbiota changes (Liu et. al., 2016). Most of these considerations were observed in our study.

Following the introduction of the DIO-HFD model, several modified models have been developed. Two most important modifications involved the additional use SHD-STZ and MLD-STZ with DIO-HFD; both are considered effective in inducing T2D (Radenković et. al., 2016).

Our study found that a single dose 50 mg/kg STZ administered to HFD-DIO (DIO-STZ50-T2D mice) induced a phenotype that was more akin to chronic diabetes, where plasmatic insulin levels were markedly diminished compared to DIO-HFD (DIO-T2D mice), resulting in low glucose-mediated insulin secretion. The addition of SHD-STZ together with DIO-HFD mitigates the effect of DIO-HFD on adiposity and hyperinsulinemia. These results suggest that the short-term effect of one dose of STZ in this model is sufficient to exacerbate the metabolic effects seen with DIO-HFD, but it appears to represent a T1D rather than T2D model.

Combining a DIO-HFD murine model with SHD-STZ-inducing destruction of pancreatic β-cells aims to expedite the development of overt DM symptoms. However, micro- and macro-vascular complications associated with clinical T2D require significant time to become established and cannot be achieved in a short-term treatment regime (Morris et. al., 2016). Therefore, we use a time of 36 weeks' timeframe to develop T2D, with the administration of STZ leading to a more severe state of DM, allowing for the evaluation of its complications.

4.3 Phenotyping of DM in C57BL/6 male mice

The C57BL/6 mouse model is extensively utilized due to its ability to replicate numerous aspects of DM. However, there is inherent heterogeneity among C57BL/6 mice in their response to an HFD-DIO in developing DM (Winzell & Ahrén, 2004; Hull et. al., 2017; Parilla et. al. 2018). Although different studies agree on the manifestation of hyperglycemia compared to normal controls, there is no consensus on a diagnostic or cut-off judgment.

In this study, we evidence two distinct DM models in C57BL/6 male mice that allow the reproduction of T1D and T2D. This is characterized by a remarkable loss of glucose-induced first-phase insulin release (FPIR), observed in the early stages of diabetes progression. The reduction of FPIR serves as a predictive marker for individuals at risk of developing DM, indicating a decline in β cell function and a consequential risk of DM onset. Histological assessments may provide insights into the slower progression to T2D compared to the rapid progression observed in T1D (Gordon & Bonner-Weir, 2021).

Considering the aging process, according to Liu et. al., 2016, mature life history stages in C57BL/6 male mice include mature adult (3-6 months old), middle age (10-15 months old), and old (18-24 months old). In our study, after the 44-week of HFD feeding, mice aged 48 weeks were at the early stages of old age, whereas T1D mice induced with MLD-STZ at 24 weeks were in the mature adult's stage. Interestingly, our findings suggest that aged mice can effectively mimic the signs of obesity and metabolic disorder in T2D, providing a valuable tool for understanding age-related aspects of diabetes.

Conclusion

In conclusion, our DM models offer an attractive avenue for research due to their relative cost-effectiveness and simplicity in induction compared to genetic models. Ensuring uniform conditions is crucial for consistent induction of diabetes. These models are easy to make, stable, and exhibit prolonged hyperglycemia, making them suitable for testing drugs or herbal medicines with hypoglycemic properties. However, it is imperative to acknowledge the limitations of these models, and researchers are encouraged to conduct studies using multiple animal models to obtain a comprehensive understanding. Further studies are necessary to evaluate the kind of metabolic, endocrine and morphologic alterations in pancreas, as well as the times in which these are manifest in diabetic animals.

References

1. Aigner, B., Rathkolb, B., Herbach, N., Hrabé de Angelis, M., Wanke, R., & Wolf, E. (2008). Diabetes models by screen for hyperglycemia in phenotype-driven ENU mouse mutagenesis projects. American journal of physiology. Endocrinology and metabolism, 294(2), E232–E240. https://doi.org/10.1152/ajpendo.00592.2007
2. Basto-Abreu, A., López-Olmedo, N., Rojas-Martínez, R., Aguilar-Salinas, C. A., Moreno-Banda, G. L., Carnalla, M., Rivera, J. A., Romero-Martinez, M., Barquera, S., & Barrientos-Gutiérrez, T. (2023). Prevalencia de prediabetes y diabetes en México: Ensanut 2022. Salud pública de México, 65, s163–s168. https://doi.org/10.21149/14832
3. Biessels, G. J., Bril, V., Calcutt, N. A., Cameron, N. E., Cotter, M. A., Dobrowsky, R., Feldman, E. L., Fernyhough, P., Jakobsen, J., Malik, R. A., Mizisin, A. P., Oates, P. J., Obrosova, I. G., Pop-Busui, R., Russell, J. W., Sima, A. A., Stevens, M. J., Schmidt, R. E., Tesfaye, S., Veves, A., … Zochodne, D. W. (2014). Phenotyping animal models of diabetic neuropathy: a consensus statement of the diabetic neuropathy study group of the EASD (Neurodiab). Journal of the peripheral nervous system: JPNS, 19(2), 77–87. https://doi.org/10.1111/jns5.12072
4. Bolzán, A. D., & Bianchi, M. S. (2002). Genotoxicity of streptozotocin. Mutation research, 512(2-3), 121–134. https://doi.org/10.1016/s1383-5742(02)00044-3
5. Brito-Casillas, Y., Melián, C., & Wägner, A. M. (2016). Study of the pathogenesis and treatment of diabetes mellitus through animal models. Endocrinologia y nutricion: organo de la Sociedad Espanola de Endocrinologia y Nutricion, 63(7), 345–353. https://doi.org/10.1016/j.endonu.2011.09.004
6. Candela, S., Hernandez, R. E., & Gagliardino, J. J. (1979). Circadian variation of the streptozotocin-diabetogenic effect in mice. Experientia, 35(9), 1256–1257. https://doi.org/10.1007/BF01963323

7. Cao, W., Chin, Y., Chen, X., Mi, Y., Xue, C., Wang, Y., & Tang, Q. (2020). The role of gut microbiota in the resistance to obesity in mice fed a high fat diet. International journal of food sciences and nutrition, 71(4), 453–463. https://doi.org/10.1080/09637486.2019.1686608
8. Cheung, M. C., Spalding, P. B., Gutierrez, J. C., Balkan, W., Namias, N., Koniaris, L. G., & Zimmers, T. A. (2009). Body surface area prediction in normal, hypermuscular, and obese mice. The Journal of surgical research, 153(2), 326–331. https://doi.org/10.1016/j.jss.2008.05.002
9. Chia-Yuan Liu, Ching-Wei Chang, Hung-Chang Lee, Yu-Jen Chen, Tung-Hu Tsai, Jen-Shiu Chiang Chiau, Tsang-En Wang, Ming-Chieh Tsai, Chun-Yan Yeung, Shou-Chuan Shih. (2016). Metabolic Damage Presents Differently in Young and Early-Aged C57BL/6 Mice Fed a High-Fat Diet. International Journal of Gerontology. 10 (2): 105-111. https://doi.org/10.1016/j.ijge.2015.10.004
10. Collins, S., Martin, T. L., Surwit, R. S., & Robidoux, J. (2004). Genetic vulnerability to diet-induced obesity in the C57BL/6J mouse: physiological and molecular characteristics. Physiology & behavior, 81(2), 243–248. https://doi.org/10.1016/j.physbeh.2004.02.006
11. Deeds, M. C., Anderson, J. M., Armstrong, A. S., Gastineau, D. A., Hiddinga, H. J., Jahangir, A., Eberhardt, N. L., & Kudva, Y. C. (2011). Single dose streptozotocin-induced diabetes: considerations for study design in islet transplantation models. Laboratory animals, 45(3), 131–140. https://doi.org/10.1258/la.2010.010090
12. Demir, S., Nawroth, P. P., Herzig, S., & Ekim Üstünel, B. (2021). Emerging Targets in Type 2 Diabetes and Diabetic Complications. Advanced science (Weinheim, Baden-Wurttemberg, Germany), 8(18), e2100275. https://doi.org/10.1002/advs.202100275
13. ElSayed, N. A., Aleppo, G., Aroda, V. R., Bannuru, R. R., Brown, F. M., Bruemmer, D., Collins, B. S., Hilliard, M. E., Isaacs, D., Johnson, E. L., Kahan, S., Khunti, K., Leon, J., Lyons, S. K., Perry, M. L., Prahalad, P., Pratley, R. E., Seley, J. J., Stanton, R. C., Gabbay, R. A., … on behalf of the American Diabetes

Association (2023). Classification and Diagnosis of Diabetes: Standards of Care in Diabetes-2023. Diabetes care, 46(Suppl 1), S19–S40. https://doi.org/10.2337/dc23-S002

14. Evaluation of Anti-diabetic Property on Streptozotocin-Induced Diabetic Rats. (2016). Progress in drug research. Fortschritte der Arzneimittelforschung. Progres des recherches pharmaceutiques, 71, 145–149.
15. Friesen, N. T., Büchau, A. S., Schott-Ohly, P., Lgssiar, A., & Gleichmann, H. (2004). Generation of hydrogen peroxide and failure of antioxidative responses in pancreatic islets of male C57BL/6 mice are associated with diabetes induced by multiple low doses of streptozotocin. Diabetologia, 47(4), 676–685. https://doi.org/10.1007/s00125-004-1367-x
16. Gargiulo, S., Gramanzini, M., Megna, R., Greco, A., Albanese, S., Manfredi, C., & Brunetti, A. (2014). Evaluation of growth patterns and body composition in C57Bl/6J mice using dual energy X-ray absorptiometry. BioMed research international, 2014, 253067. https://doi.org/10.1155/2014/253067
17. Gheibi, S., Kashfi, K., & Ghasemi, A. (2017). A practical guide for induction of type-2 diabetes in rat: Incorporating a high-fat diet and streptozotocin. Biomedicine & pharmacotherapy = Biomedecine & pharmacotherapie, 95, 605–613. https://doi.org/10.1016/j.biopha.2017.08.098
18. Gilbert, E. R., Fu, Z., & Liu, D. (2011). Development of a nongenetic mouse model of type 2 diabetes. Experimental diabetes research, 2011, 416254. https://doi.org/10.1155/2011/416254
19. Glastras, S. J., Chen, H., Teh, R., McGrath, R. T., Chen, J., Pollock, C. A., Wong, M. G., & Saad, S. (2016). Mouse Models of Diabetes, Obesity and Related Kidney Disease. PloS one, 11(8), e0162131. https://doi.org/10.1371/journal.pone.0162131
20. Guo, X. X., Wang, Y., Wang, K., Ji, B. P., & Zhou, F. (2018). Stability of a type 2 diabetes rat model induced by high-fat diet feeding with low-dose streptozotocin injection. Journal of Zhejiang University. Science. B, 19(7), 559–569. https://doi.org/10.1631/jzus.B1700254

21. Hull, R. L., Willard, J. R., Struck, M. D., Barrow, B. M., Brar, G. S., Andrikopoulos, S., & Zraika, S. (2017). High fat feeding unmasks variable insulin responses in male C57BL/6 mouse substrains. The Journal of endocrinology, 233(1), 53–64. https://doi.org/10.1530/JOE-16-0377
22. Jolivalt, C. G., Frizzi, K. E., Guernsey, L., Marquez, A., Ochoa, J., Rodriguez, M., & Calcutt, N. A. (2016). Peripheral Neuropathy in Mouse Models of Diabetes. Current protocols in mouse biology, *6*(3), 223–255. https://doi.org/10.1002/cpmo.11
23. King, A., & Bowe, J. (2016). Animal models for diabetes: Understanding the pathogenesis and finding new treatments. Biochemical pharmacology, 99, 1–10. https://doi.org/10.1016/j.bcp.2015.08.108
24. Masek, J., & Fabry, P. (1959). High-fat diet and the development of obesity in albino rats. Experientia, 15, 444–445. https://doi.org/10.1007/BF02157708
25. Max Roser, Esteban Ortiz-Ospina and Hannah Ritchie (2013) - "Life Expectancy". Published online at OurWorldInData.org. Retrieved from: https://ourworldindata.org/life-expectancy
26. Morris, J. L., Bridson, T. L., Alim, M. A., Rush, C. M., Rudd, D. M., Govan, B. L., & Ketheesan, N. (2016). Development of a diet-induced murine model of diabetes featuring cardinal metabolic and pathophysiological abnormalities of type 2 diabetes. Biology open, 5(8), 1149–1162. https://doi.org/10.1242/bio.016790
27. O'Brien, P. D., Hinder, L. M., Rumora, A. E., Hayes, J. M., Dauch, J. R., Backus, C., Mendelson, F. E., & Feldman, E. L. (2018). Juvenile murine models of prediabetes and type 2 diabetes develop neuropathy. Disease models & mechanisms, 11(12), dmm037374. https://doi.org/10.1242/dmm.037374
28. O'Brien, P. D., Sakowski, S. A. and Feldman, E. L. (2014). Mouse models of diabetic neuropathy. ILAR J. 54, 259-272. https://doi.org/10.1093/ilar/ilt052
29. Parilla, J. H., Willard, J. R., Barrow, B. M., & Zraika, S. (2018). A Mouse Model of Beta-Cell Dysfunction as Seen in Human Type 2 Diabetes. Journal of diabetes research, 2018, 6106051. https://doi.org/10.1155/2018/6106051

30. Radenković, M., Stojanović, M., & Prostran, M. (2016). Experimental diabetes induced by alloxan and streptozotocin: The current state of the art. Journal of pharmacological and toxicological methods, 78, 13–31. https://doi.org/10.1016/j.vascn.2015.11.004
31. Rais, N., Ved, A., Ahmad, R., Parveen, K., Gautam, G. K., Bari, D. G., Shukla, K. S., Gaur, R., & Singh, A. P. (2022). Model of Streptozotocin-nicotinamide Induced Type 2 Diabetes: a Comparative Review. Current diabetes reviews, 18(8), e171121198001. https://doi.org/10.2174/1573399818666211117123358
32. Satoh, M., Iizuka, M., Majima, M., Ohwa, C., Hattori, A., Van Kaer, L., & Iwabuchi, K. (2022). Adipose invariant NKT cells interact with CD1d-expressing macrophages to regulate obesity-related inflammation. Immunology, 165(4), 414–427. 165(4), 414–427. https://doi.org/10.1111/imm.13447
33. Schofield, S. E., Parkinson, J. R., Henley, A. B., Sahuri-Arisoylu, M., Sanchez-Canon, G. J., & Bell, J. D. (2017). Metabolic dysfunction following weight cycling in male mice. International journal of obesity (2005), 41(3), 402–411. https://doi.org/10.1038/ijo.2016.193
34. Sullivan, K. A., Lentz, S. I., Roberts, J. L., Jr, & Feldman, E. L. (2008). Criteria for creating and assessing mouse models of diabetic neuropathy. Current drug targets, 9(1), 3–13. Sullivan, K. A., Lentz, S. I., Roberts, J. L., Jr, & Feldman, E. L. (2008). Criteria for creating and assessing mouse models of diabetic neuropathy. Current drug targets, 9(1), 3–13. https://doi.org/10.2174/138945008783431763
35. Sun, H., Saeedi, P., Karuranga, S., Pinkepank, M., Ogurtsova, K., Duncan, B. B., Stein, C., Basit, A., Chan, J. C. N., Mbanya, J. C., Pavkov, M. E., Ramachandaran, A., Wild, S. H., James, S., Herman, W. H., Zhang, P., Bommer, C., Kuo, S., Boyko, E. J., & Magliano, D. J. (2022). IDF Diabetes Atlas: Global, regional and country-level diabetes prevalence estimates for 2021 and projections for 2045. Diabetes research and clinical practice, 183, 109119. https://doi.org/10.1016/j.diabres.2021.109119

36. Surwit, R. S., Kuhn, C. M., Cochrane, C., McCubbin, J. A., & Feinglos, M. N. (1988). Diet-induced type II diabetes in C57BL/6J mice. Diabetes, 37(9), 1163–1167. https://doi.org/10.2337/diab.37.9.1163
37. van Dijk, T. H., Laskewitz, A. J., Grefhorst, A., Boer, T. S., Bloks, V. W., Kuipers, F., Groen, A. K., & Reijngoud, D. J. (2013). A novel approach to monitor glucose metabolism using stable isotopically labelled glucose in longitudinal studies in mice. Laboratory animals, 47(2), 79–88. https://doi.org/10.1177/0023677212473714
38. Wang, C. Y., & Liao, J. K. (2012). A mouse model of diet-induced obesity and insulin resistance. Methods in molecular biology (Clifton, N.J.), 821, 421–433. https://doi.org/10.1007/978-1-61779-430-8_27
39. Wang, Z., & Gleichmann, H. (1998). GLUT2 in pancreatic islets: crucial target molecule in diabetes induced with multiple low doses of streptozotocin in mice. Diabetes, 47(1), 50–56. https://doi.org/10.2337/diab.47.1.50
40. Weir, G. C., & Bonner-Weir, S. (2021). Reduced glucose-induced first-phase insulin release is a danger signal that predicts diabetes. The Journal of clinical investigation, 131(12), e150022. https://doi.org/10.1172/JCI150022
41. Winzell, M. S., & Ahrén, B. (2004). The high-fat diet-fed mouse: a model for studying mechanisms and treatment of impaired glucose tolerance and type 2 diabetes. Diabetes, 53 Suppl 3, S215–S219. https://doi.org/10.2337/diabetes.53.suppl_3.s215
42. Xu, H., Du, X., Xu, J., Zhang, Y., Tian, Y., Liu, G., Wang, X., Ma, M., Du, W., Liu, Y., Dai, L., Huang, W., Tong, N., Wei, Y., & Fu, X. (2020). Pancreatic β cell microRNA-26a alleviates type 2 diabetes by improving peripheral insulin sensitivity and preserving β cell function. PLoS biology, 18(2), e3000603. https://doi.org/10.1371/journal.pbio.3000603
43. Zmora, N., Bashiardes, S., Levy, M., & Elinav, E. (2017). The Role of the Immune System in Metabolic Health and Disease. Cell metabolism, 25(3), 506–521. https://doi.org/10.1016/j.cmet.2017.02.006

Supplementary material

Table 1S. Age equivalences between human and mouse

Equalization of cut-off points simulate the ages at which DM occurs in humans.

Average lifespan for a C57BL/6 male mouse			
820 ± 20 days	2.24 years	117.1 weeks	
Global average life expectancy in humans for 2019			
72.6 years			
Each year of human person is equivalent to 1.61 weeks of mouse.			
Beginning of experiment	4-6 weeks old	2.5-3.7 years human life	
T1D		**T2D**	
Cut-off points	Equivalence	**Cut-off points**	Equivalence
12 weeks	10 years	**36 weeks**	26 years
20 weeks	15 years	**44 weeks**	31 years

Table 2S. Weight ranges to identify the physical nutritional status

Cut off points (g of BW) in C57BL/6 male mice as a function of age/sex and to determine the pathophysiological status of obesity. Levey-Jennings procedure was used in CTL-NOM to determine weight ranges that are closely related to degrees of obesity to identify a mouse as underweight, normal weight, overweight, or obese instead of comparing traditional weight versus weight plotting. Each week the mean BW was the control and the ranges were calculated with standard deviation up and down. The values represent the mean of the ranges calculated weekly.

	Cut Off Points (g of BW)						
Age (weeks)	**Severely underweight** (Less than)	**Underweight** (under)	**Normal weight** (Less than or equal to)	**Overweight** (Less than or equal to)	**Obesity Class I (moderate)** (Less than or equal to)	**Obesity Class II (severe)** (Less than or equal to)	**Obesity Class III (morbid)** (Less than or equal to)
4	18.17	21.65	28.64	35.63	42.61	49.59	56.57
8	20.73	23.56	29.25	34.94	40.62	46.30	51.99
12	21.42	24.47	30.61	36.74	42.87	49.00	55.13
16	21.92	25.00	31.20	37.38	43.56	49.75	55.93
20	21.64	24.98	31.68	38.37	45.06	51.75	58.44
24	21.90	25.43	32.52	39.60	46.67	53.75	60.83
28	21.96	25.58	32.87	40.14	47.42	54.69	61.96
32	21.56	25.92	34.67	43.41	52.15	60.89	69.63
36	21.75	26.04	34.94	44.16	53.39	62.61	71.84
40	21.73	26.22	35.22	44.21	53.20	62.19	71.18
44	21.10	25.70	36.05	48.28	60.50	72.73	84.95

Table 3S. Body composition parameters (BCP) in DM murine models.

Body length (BL), body surface area (BSA) and body mass index (BIM) in C57BL/6 male mice on cut-off points of DM. Values represent means ± SEM of each group. Statistical analysis was performed using two-way ANOVA with Bonferroni multiple comparisons test. The symbols *p<0,001 vs CTL-NOM and [a, b] p<0,001 vs DIO-T2D and STZ20-T1D respectively.

BCP	DM models	Feeding time (weeks)				
		4	8	12	16	20
BL (cm)	*CTL-NOM*	6.68±0.13	6.85±0.16	6.98±0.16	7.15±0.15	7.26±0.13
	STZ20-T1D	6.65±0.06	6.81±0.08	6.89±0.05	7.06±0.07	7.25±0.05
	STZ40-T1D	6.69±0.16	6.84±0.21	7.02±0.17	7.22±0.13	7.31±0.10
	STZ150-T1D	6.71±0.14	6.92±0.17	7.14±0.18	7.22±0.16	7.28±0.16
	DIO-T2D	6.66±0.13	6.83±0.11	7.07±0.10	7.22±0.15	7.40±0.14
	DIO-STZ50-T2D	6.72±0.04	6.87±0.05	7.30±0.15	7.12±0.08	7.44±0.16
BSA (cm^2)	*CTL-NOM*	60.16±1.88	62.38±1.95	64.04±2.03	66.04±2.06	66.94±1.92
	STZ20-T1D	59.74±0.97	61.64±1.21	63.04±0.91	64.48±0.66	63.82±1.09*
	STZ40-T1D	60.46±2.28	62.49±2.17	65.09±1.90	63.19±1.48*	62.93±1.06*
	STZ150-T1D	60.04±1.76	62.83±1.80	64.83±2.30	65.96±2.42	67.57±2.26
	DIO-T2D	63.15±2.59*	68.58±3.11*	74.30±3.24*	78.29±2.99*	83.89±3.08*
	DIO-STZ50-T2D	64.29±3.18*	68.68±3.56*	75.89±1.20*	78.24±1.47*	84.93±3.80*
BMI (kg/m^2)	*CTL-NOM*	4.26±0.13	4.27±0.06	4.27±0.09	4.29±0.07	4.29±0.05
	STZ20-T1D	4.28±0.04	4.29±0.04	4.33±0.04	4.22±0.08	4.09±0.06*
	STZ40-T1D	4.31±0.05	4.34±0.05	4.38±0.09	4.02±0.20*[b]	3.91±0.10*[b]
	STZ150-T1D	4.30±0.08	4.30±0.03	4.32±0.05	4.33±0.08	4.34±0.07
	DIO-T2D	4.60±0.28*	4.94±0.37*	5.41±0.34*	5.57±0.80*	5.65±0.29*
	DIO-STZ50-T2D	4.64±0.33*	4.89±0.40*	5.27±0.17*	5.27±0.10*	5.69±0.26*

BCP	DM models	Feeding time (weeks)					
		24	**28**	**32**	**36**	**40**	**44**
BL (cm)	***CTL-NOM***	7.29±0.13	7.47±0.19	7.54±0.17	7.61±0.16	7.64±0.15	7.67±0.16
	STZ20-T1D						
	STZ40-T1D						
	STZ150-T1D	7.30±0.16	7.47±0.20	7.54±0.18	7.59±0.16	7.63±0.15	7.67±0.15
	DIO-T2D	7.50±0.14	7.57±0.13	7.63±0.14	7.88±0.12*	8.10±0.14*	8.15±0.14*
	DIO-STZ50-T2D	7.53±0.15	7.62±0.16	7.66±0.16	7.87±0.07*	8.12±0.10*	8.20±0.08*
BSA (cm^2)	***CTL-NOM***	67.50±1.97	69.23±2.58	70.42±2.42	70.83±2.79	71.11±2.41	71.46±2.31
	STZ20-T1D						
	STZ40-T1D						
	STZ150-T1D	67.08±2.28	69.12±2.87	70.26±2.59	70.75±2.30	68.48±1.76	65.99±1.51*
	DIO-T2D	87.11±3.06*	91.80±3.26*	95.33±2.66*	97.92±2.85*	99.95±3.05*	100.95±3.0*
	DIO-STZ50-T2D	87.99±3.67*	91.21±2.56*	95.52±1.94*	98.06±2.24*	95.44±1.05*[a]	94.33±1.51*[a]
BMI (kg/m^2)	***CTL-NOM***	4.31±0.04	4.31±0.06	4.32±0.10	4.33±0.06	4.33±0.08	4.35±0.07
	STZ20-T1D						
	STZ40-T1D						
	STZ150-T1D	4.27±0.08	4.27±0.05	4.31±0.06	4.29±0.05	4.08±0.12*	3.84±0.14*
	DIO-T2D	5.66±0.29*	5.73±0.26*	5.76±0.18*	5.91±0.21*	6.01±0.22*	6.05±0.21*
	DIO-STZ50-T2D	5.68±0.25*	5.70±0.20*	5.75±0.11*	5.86±0.09*	5.74±0.15*[a]	5.56±0.15*[a]

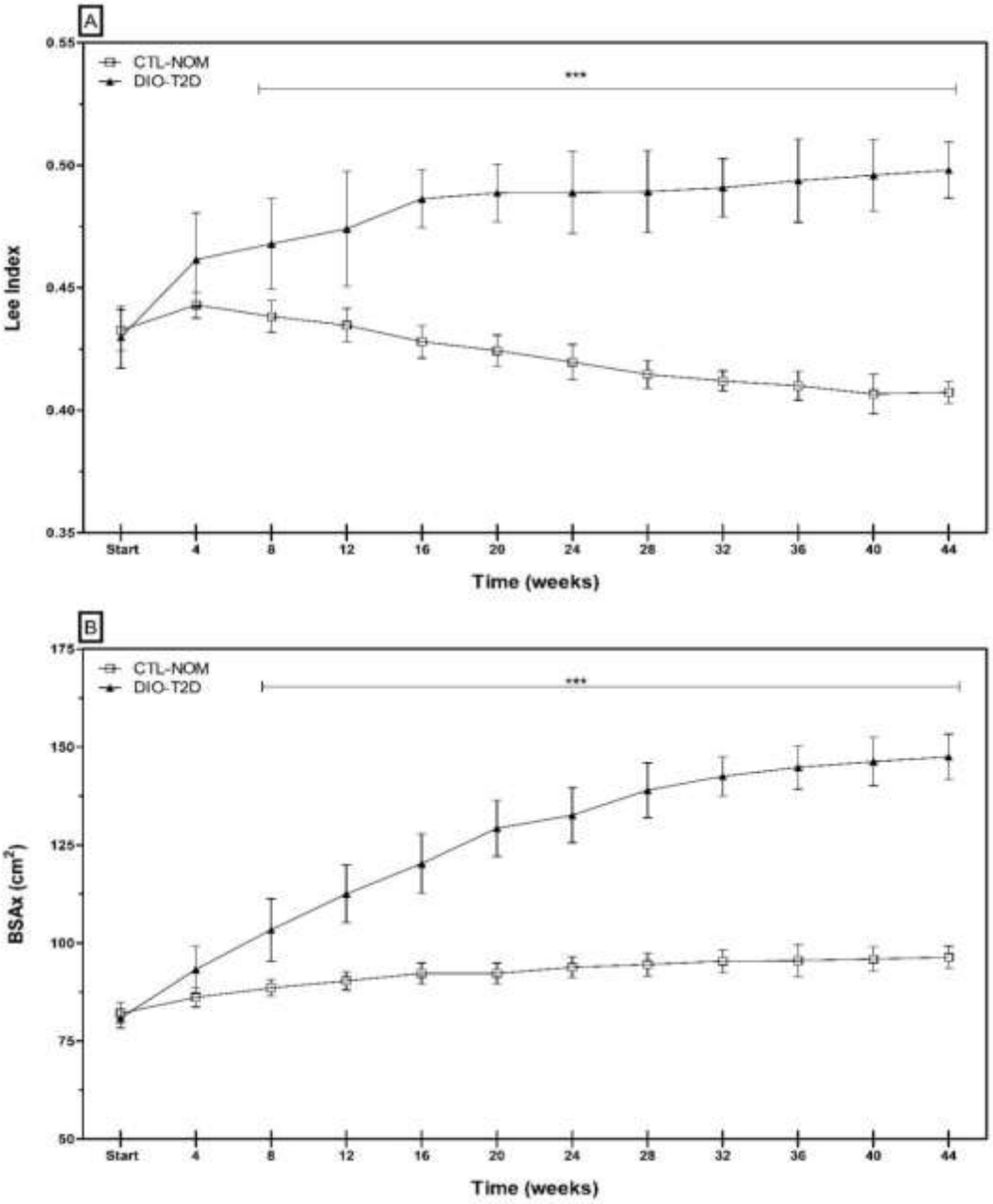

Figure 1S. **Parameters to estimate the degree of obesity in T2D murine model.** (A) Lee Index and (B) Body surface area (BSA_x) in C57BL/6 male mice across the feeding time to develop DM through HFD-DIO. Values represent means ± SEM of each group. Statistical analysis was performed using two-way ANOVA with Bonferroni multiple comparisons test. The symbols ***p<0,001 vs CTL-NOM.

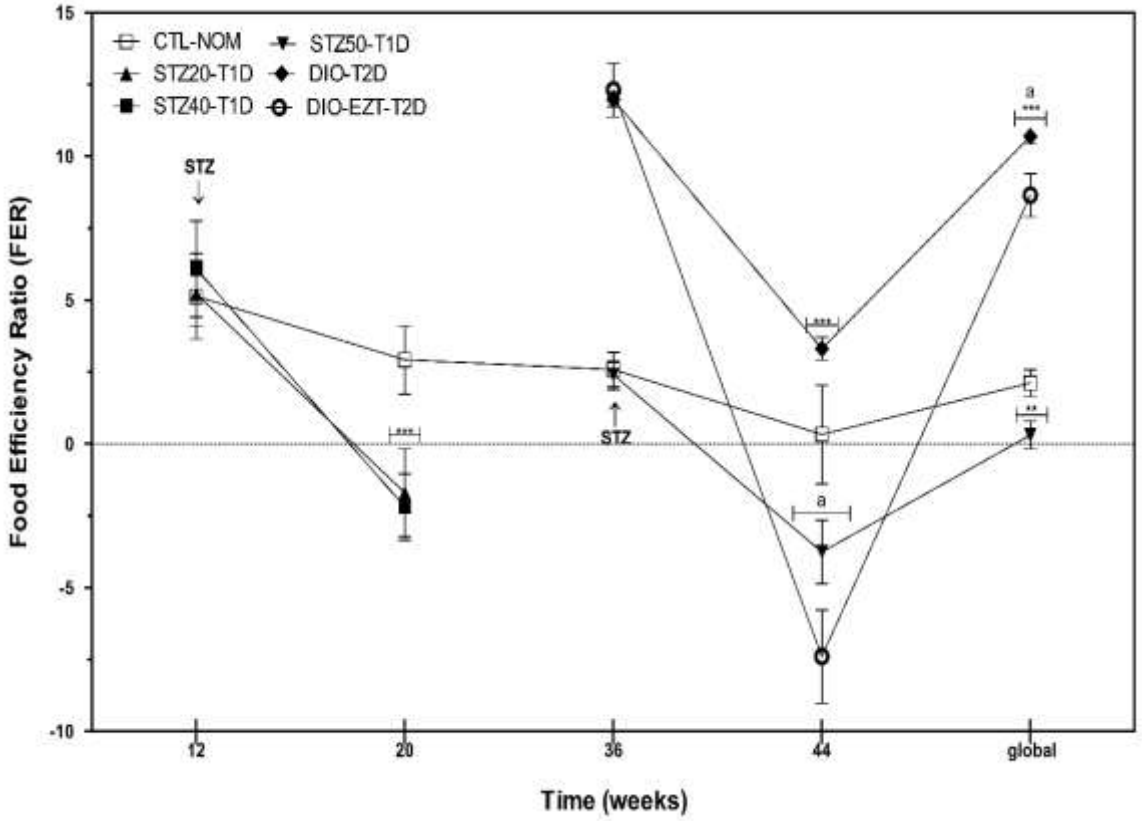

Figure 2S. **Food efficiency ratio in DM murine models**.Values represent means ± SEM of each group. Statistical analysis was performed using two-way ANOVA with Bonferroni multiple comparisons test. The symbols ***p<0,001 vs CTL-NOM. and [a] p<0,001 vs DIO-T2D.

Table 4S. Parameters of energy density in DM murine models.

Metabolizable energy, loss energy as urine, fecal, methane and physiological fuel value in C57BL/6 male mice on feeding time. Values represent means ± SEM of each group. Statistical analysis was performed using two-way ANOVA with Bonferroni multiple comparisons test. The symbols *p<0,001 vs CTL-NOM and [a, b] p<0,001 vs STZ20-T1D and DIO-T2D respectively.

Parameters	DM models	Feeding time (weeks)				
		4	8	12	16	20
Metabolizable Energy **kcal**	***CTL-NOM***	68.44±5.27	72.66±5.37	78.08±5.61	80.07±3.90	85.51±4.42
	STZ20-T1D	73.38±7.62	74.17±10.1	78.21±7.82	104.74±8.73*	111.10±10.9*
	STZ40-T1D	73.57±11.0	75.63±6.64	78.46±4.84	147.01±5.13*[a]	177.87±9.69*[b]
	STZ150-T1D	72.25±5.17	72.92±28.5	75.04±5.86	78.26±4.63	86.02±5.80
	DIO-T2D	205.80±7.78*	176.62±6.32*	163.82±7.38*	160.43±7.76*	154.35±6.07*
	DIO-STZ50-T2D	210.91±9.95*	180.03±10.2*	165.49±12.9*	157.22±10.5*	151.98±14.8*
Loss Energy (urine, fecal, methane) **kcal**	***CTL-NOM***	23.80±1.83	25.26±1.87	27.15±1.95	27.84±1.36	29.73±1.54
	STZ20-T1D	25.51±2.65	25.79±3.52	27.19±2.72	36.42±3.03*	38.63±3.80*
	STZ40-T1D	25.58±3.82	26.29±2.31	27.28±1.68	51.11±1.79*[a]	61.84±3.37*[b]
	STZ150-T1D	25.12±1.80	25.35±9.91	26.09±2.04	27.21±1.61	29.91±2.02
	DIO-T2D	32.56±1.23*	27.94±1.00	25.92±1.17	25.38±1.23*	24.42±0.96*
	DIO-STZ50-T2D	33.37±1.57*	28.48±1.62	26.18±2.04	24.87±1.66*	24.04±2.34*
Physiological Fuel Value **kcal**	***CTL-NOM***	76.15±5.86	80.84±5.98	86.87±6.25	89.08±4.34	95.14±4.91
	STZ20-T1D	81.65±8.47	82.52±11.3	87.01±8.70	116.53±9.71*	123.61±12.2*
	STZ40-T1D	81.86±12.2	84.14±7.39	87.30±5.39	163.56±5.71*[a]	197.90±10.8*[b]
	STZ150-T1D	80.38±5.75	81.13±31.7	83.49±6.52	87.07±5.16	95.70±6.45
	DIO-T2D	216.25±8.17*	185.59±6.65*	172.14±7.75*	168.58±8.15*	162.19±6.38*
	DIO-STZ50-T2D	221.62±10.5*	189.18±10.7*	173.89±13.6*	165.20±11.0*	159.69±15.6*

Parameters	DM models	Feeding time (weeks)					
		24	28	32	36	40	44
Metabolizable Energy kcal	*CTL-NOM*	88.15±3.99	88.19±4.40	87.11±3.73	91.53±4.89	94.19±6.58	95.07±6.22
	STZ20-T1D						
	STZ40-T1D						
	STZ150-T1D	88.47±3.87	89.85±4.97	89.40±5.42	91.12±9.16	189.45±22.4*	196.68±19.7*
	DIO-T2D	147.36±8.97*	133.48±7.73*	134.77±7.67*	127.44±7.76*	121.90±14.4*	125.37±8.67*
	DIO-STZ50-T2D	151.75±11.9*	142.71±13.6*	129.46±9.69*	128.20±23.1*	135.21±10.0*[a]	162.75±10.0*[a]
Loss Energy (urine, fecal, methane) kcal	*CTL-NOM*	30.65±1.39	30.66±1.53	30.29±1.30	31.82±1.70	32.75±2.29	33.05±2.16
	STZ20-T1D						
	STZ40-T1D						
	STZ150-T1D	30.76±1.35	31.24±1.73	31.08±1.89	31.68±3.18	65.87±7.77*	68.38±6.83*
	DIO-T2D	23.31±1.42*	21.12±1.22*	21.32±1.21*	20.16±1.23*	19.29±2.28*	19.83±1.37*
	DIO-STZ50-T2D	24.01±1.88*	22.58±2.16*	20.48±1.53*	20.28±3.65*	21.39±1.59*	25.75±1.58*[a]
Physiological Fuel Value kcal	*CTL-NOM*	98.07±4.44	98.12±4.90	96.92±4.15	101.83±5.44	104.80±7.32	105.77±6.92
	STZ20-T1D						
	STZ40-T1D						
	STZ150-T1D	98.43±4.31	99.96±5.53	99.47±6.03	101.38±10.2	210.78±24.9*	218.83±21.9*
	DIO-T2D	154.85±9.42*	140.26±8.12*	141.62±8.06*	133.91±8.15*	128.09±15.1*	131.73±9.11*
	DIO-STZ50-T2D	159.45±12.5*	149.96±14.3*	136.03±10.2*	134.71±24.2*	142.08±10.5*a	171.02±10.5*[a]

Table 5S. Parameters of energy metabolism in DM murine models.

Metabolic Weight, basal metabolic rate and total daily expenditure of energy in C57BL/6 male mice on feeding time. Values represent means ± SEM of each group. Statistical analysis was performed using two-way ANOVA with Bonferroni multiple comparisons test. The symbols *p<0,001 vs CTL-NOM.

Parameters	DM models	Feeding time (weeks)				
		4	8	12	16	20
Metabolic Weight (MW) $kg^{0.75}$	*CTL-NOM*	0.064±0.002	0.066±0.002	0.068±0.002	0.070±0.002	0.071±0.002
	STZ20-T1D	0.064±0.001	0.067±0.001	0.068±0.002	0.067±0.002	0.065±0.001*
	STZ40-T1D	0.061±0.003	0.065±0.003	0.067±0.002	0.064±0.003*	0.062±0.002*
	STZ150-T1D	0.064±0.002	0.067±0.002	0.068±0.002	0.069±0.002	0.069±0.002
	DIO-T2D	0.070±0.005	0.079±0.007*	0.087±0.006*	0.094±0.007*	0.102±0.006*
	DIO-STZ50-T2D	0.071±0.007	0.081±0.007*	0.090±0.003*	0.091±0.001*	0.100±0.005*
Basal metabolic rate (BMR) kJ/ day	*CTL-NOM*	19.32±0.63	19.93±0.53	20.39±0.60	20.87±0.68	21.26±0.67
	STZ20-T1D	19.14±0.34	20.08±0.27	20.35±0.58	19.96±0.49	19.65±0.35
	STZ40-T1D	18.37±0.88	19.55±0.91	19.96±0.72	19.08±0.81	18.64±0.51*
	STZ150-T1D	19.27±0.65	19.97±0.57	20.28±0.61	20.72±0.68	20.81±0.71
	DIO-T2D	21.14±1.52	23.73±2.06*	26.10±1.91*	28.12±2.00*	30.50±1.90*
	DIO-STZ50-T2D	21.28±2.24	24.17±2.07*	26.89±0.83*	27.31±0.40*	29.92±1.48*
Total daily expenditure of energy (TDEE) kJ/ day	*CTL-NOM*	25.76±0.84	26.57±0.71	27.18±0.79	27.83±0.91	28.35±0.90
	STZ20-T1D	25.52±0.46	26.78±0.36	27.13±0.77	26.61±0.65	26.20±0.46*
	STZ40-T1D	24.50±1.17	26.06±1.22	26.62±0.97	25.44±1.08*	24.86±0.68*
	STZ150-T1D	25.69±0.87	26.62±0.76	27.05±0.81	27.63±0.91	27.74±0.95
	DIO-T2D	28.19±2.03*	31.64±2.75*	34.81±2.55*	37.50±2.66*	40.67±2.53*
	DIO-STZ50-T2D	28.38±2.98*	32.22±2.77*	35.85±1.11*	36.41±0.54*	39.90±1.98*

Parameters	DM models	Feeding time (weeks)					
		24	28	32	36	40	44
Metabolic Weight (MW) **$kg^{0.75}$**	*CTL-NOM*	0.070±0.002	0.072±0.002	0.072±0.002	0.073±0.003	0.072±0.003	0.073±0.002
	STZ20-T1D						
	STZ40-T1D						
	STZ150-T1D	0.070±0.002	0.071±0.002	0.072±0.002	0.072±0.002	0.068±0.002	0.064±0.002*
	DIO-T2D	0.105±0.006*	0.110±0.006*	0.113±0.005*	0.116±0.005*	0.117±0.006*	0.118±0.005*
	DIO-STZ50-T2D	0.105±0.006*	0.107±0.006*	0.111±0.005*	0.117±0.003*	0.113±0.003*	0.110±0.003*
Basal metabolic rate (BMR) ***kJ/ day***	*CTL-NOM*	20.87±0.69	21.46±0.74	21.67±0.75	21.81±0.79	21.70±1.03	21.92±0.71
	STZ20-T1D						
	STZ40-T1D						
	STZ150-T1D	21.00±0.69	21.20±0.75	21.46±0.68	21.73±0.75	20.49±0.75	19.06±0.74*
	DIO-T2D	31.39±1.88*	33.09±1.88*	34.04±1.36*	34.65±1.48*	35.05±1.65*	35.38±1.56*
	DIO-STZ50-T2D	31.38±1.82*	32.16±1.72*	33.41±1.53*	35.03±0.86*	33.98±0.90*	32.89±1.02*
Total daily expenditure of energy (TDEE) ***kJ/ day***	*CTL-NOM*	27.83±0.91	28.61±0.99	28.89±1.00	29.07±1.05	28.93±1.38	29.22±0.95
	STZ20-T1D						
	STZ40-T1D						
	STZ150-T1D	27.99±0.92	28.27±1.00	28.61±0.90	28.97±1.00	27.33±1.00	25.41±0.99*
	DIO-T2D	41.86±2.50*	44.12±2.50*	45.39±1.81*	46.20±1.98*	46.74±2.20*	47.17±2.09*
	DIO-STZ50-T2D	41.84±2.43*	42.89±2.30*	44.55±2.05*	46.71±1.14*	45.31±1.20*	43.85±1.37*

Table 6S. Physiological range of blood glucose in C57BL/6 male mice

Owing to the fact that normal BG in mice is diagnostic for T2D in humans. Therefore, BG was measured in all C57BL/6 male mice before dietary intervention (HFD) to determine the physiological reference range of plasma glucose. Ranges of diabetic glycemic status were calculated with three standard deviations up and down (Mean ±3σ). For example, in the week 36 mean FBG was 119.57±6.79 mg/dL; the ranks are obtained like: Normoglycemic (FBG) 119.57 mg/dL, upper and lower limits FBG±3σ (99.21-139.92 mg/dL); prediabetes (FBG+6σ= 160.28 mg/dL), limits ±3σ (139.93-180.64 mg/dL) and DM (160.28 mg/dL+6σ=201.00 mg/dL), limits ±3σ (180.65-221.35 mg/dL).

Fasting blood glucose (mg/dL)							
Time (weeks)	**Mean ± σ**	**diabetic glycemic status**					
		normoglycemic	***prediabetes***	***DM***	**Min**	**Max**	**CV**
Start	100.4±10.7	79.0-132.4	≤196.3	up to 260.3	77	118	10.62
4	103.8±11.1	70.7-136.9	≤203.2	up to 269.5	82	120	10.64
8	101.5±10.6	69.7-133.4	≤197.1	up to 260.9	77	120	10.46
12	102.3±8.70	76.3-128.3	≤180.2	up to 232.2	84	119	8.46
16	103.9±8.10	79.5-128.3	≤177.0	up to 225.8	89	119	7.82
20	107.6±7.70	84.4-130.8	≤177.2	up to 223.6	92	122	7.19
24	111.4±7.60	88.7-134.2	≤179.7	up to 225.2	99	123	6.80
28	111.5±7.70	88.4-134.5	≤180.6	up to 226.7	99	128	6.89
32	115.2±7.70	92.3-138.2	≤184.1	up to 230.0	97	126	6.64
36	119.6±6.80	99.2-139.9	≤180.6	up to 221.4	100	129	5.68
40	125.5±6.40	106.2-144.8	≤183.3	up to 221.8	111	140	5.12
44	125.4±8.00	101.5-149.3	≤197.2	up to 245.1	106	142	6.36
Cut-off level general for normoglycemic: ≤150 mg/dL							
Cut-off level general for prediabetes: ≤200 mg/dL							
Cut-off level general for DM: >200 mg/dL							

Table 7S. Physiological range of post prandial blood glucose in C57BL/6 male mice

PPBG at 2 hours in C57BL/6 healthy male mice across intervention time. Ranges of diabetic glycemic status were calculated with three standard deviations up and down (Mean ±3 σ). For example, in the week 36 mean PPBG was 163.5±2.90 mg/dL; the ranks are obtained like: Normoglycemic upper and lower limits FBG±3σ (154.6-172.3mg/dL); prediabetes (FBG+6σ= 181.13 mg/dL), limits ±3σ (172.40-189.97 mg/dL) and DM (181.13 mg/dL+6σ=198.80 mg/dL), limits ±3σ (189.98-207.64 mg/dL).

Post prandial blood glucose (mg/dL)							
Time (weeks)	**Mean ± σ**	**Diabetic glycemic status**					
		Normoglycemic	***Prediabetes***	***DM***	**Min**	**Max**	**CV**
Start	147.6±10.3	126.7-178.7	≤240.7	up to 302.7	120	162	7.00
4	151.2±11.2	117.7-184.6	≤251.6	up to 318.5	124	170	7.38
8	149.1±8.20	124.4-173.8	≤223.3	up to 272.7	132	173	5.52
12	150.7±10.5	119.2-182.2	≤245.1	up to 308.1	128	170	6.97
16	152.6±7.90	128.9-176.4	≤223.8	up to 271.3	131	163	5.19
20	154.3±9.80	124.9-183.6	≤242.3	up to 301.0	131	173	6.34
24	156.8±5.90	139.3-174.4	≤209.5	up to 244.6	142	168	3.73
28	158.4±5.10	143.0-173.7	≤204.4	up to 235.1	150	168	3.23
32	160.9±3.80	149.6-172.2	≤194.9	up to 217.5	152	169	2.34
36	163.5±2.90	154.6-172.3	≤190.0	up to 207.6	159	169	1.80
40	163.5±4.10	151.3-175.7	≤200.1	up to 224.5	156	172	2.49
44	167.6±4.00	155.8-179.5	≤203.3	up to 227.1	161	178	2.36
Cut-off level general for normoglycemic: ≤185 mg/dL							
Cut-off level general for prediabetes: ≤235 mg/dL							
Cut-off level general for DM: >285 mg/dL							

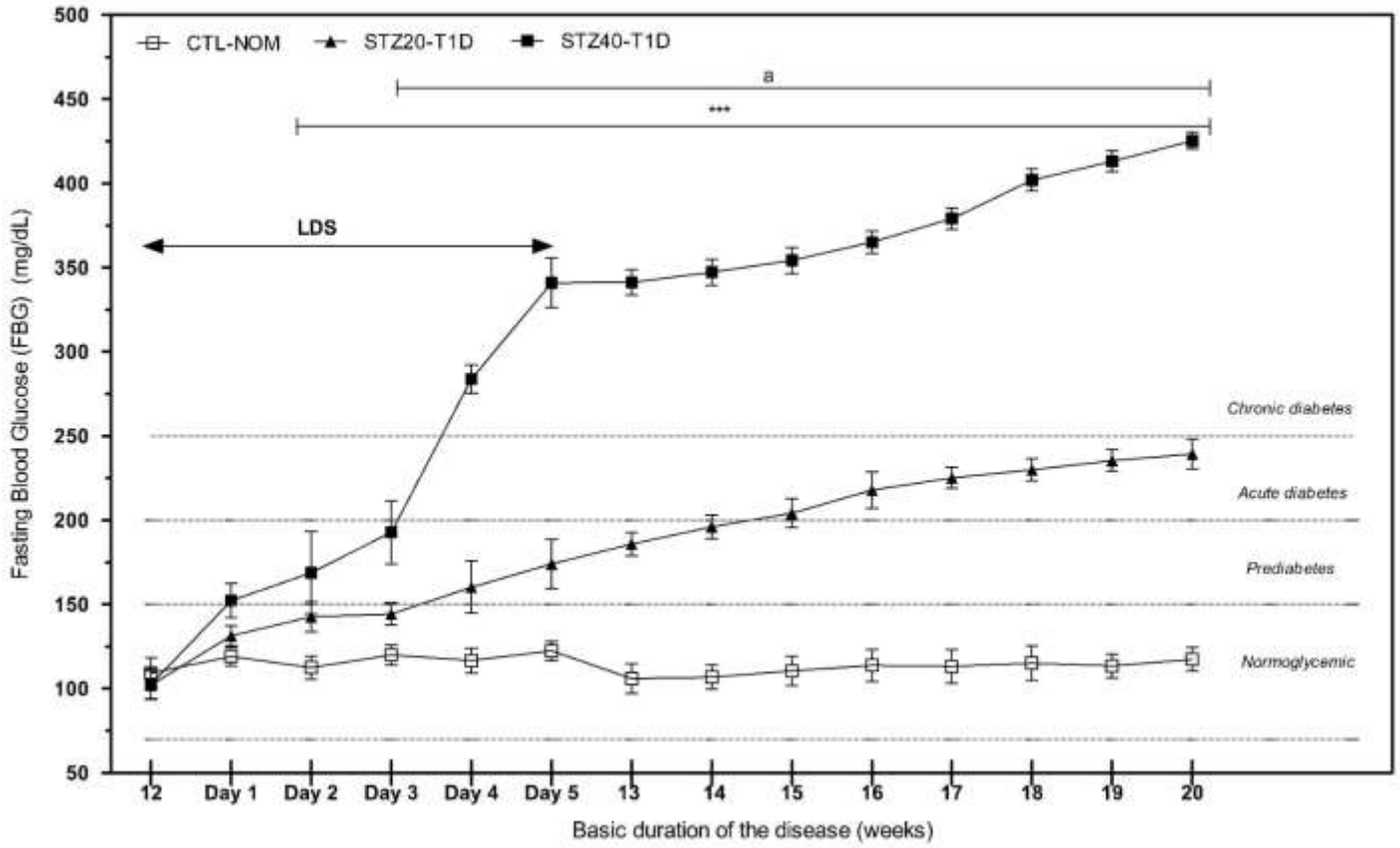

Figure 3S. **Monitoring across time fasting blood glucose in T1D murine models**.

FBG (mg/dL) in C57BL/6 male mice across the feeding time. Values represent means ± SEM of each group. Statistical analysis was performed using two-way ANOVA with Bonferroni multiple comparisons test. The symbols ***p<0,001 vs CTL-NOM. and [a] p<0,001 vs STZ20-T1D.

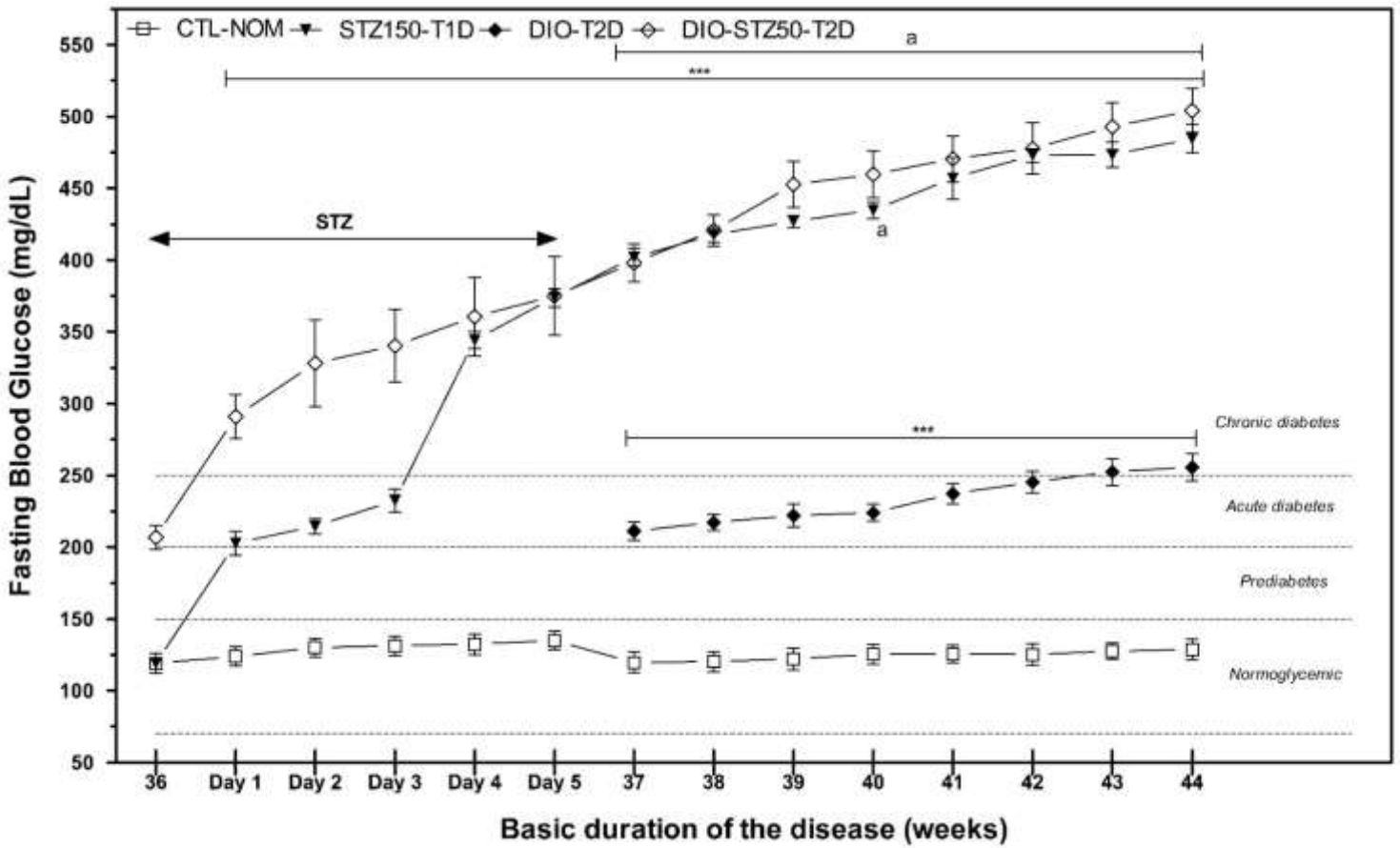

Figure 4S. **Monitoring across time fasting blood glucose in T2D murine models.**

FBG (mg/dL) in C57BL/6 male mice across the feeding time. Values represent means ± SEM of each group. Statistical analysis was performed using two-way ANOVA with Bonferroni multiple comparisons test. The symbols ***p<0,001 vs CTL-NOM. and [a] p<0,001 vs DIO-T2D.

6.2 Pharmacological evaluation of *Calea urticifolia* aqueous extract in diabetes mellitus: mechanistic interaction with oral hypoglycemic agents in murine models

1. Introduction

Diabetes mellitus (DM) is a chronic metabolic disorder characterized by persistent hyperglycemia resulting from insufficiency in insulin action or insulin secretion, or both (Dandekar et al. 2021). According to the American Diabetes Association (ADA), diabetes can be classified into the following general categories: 1. Type 1 diabetes (T1D), caused by autoimmune β-cell destruction, leading to absolute insulin deficiency. 2. Type 2 diabetes (T2D), resulting from a progressive loss of adequate β-cell insulin secretion, frequently on the background of insulin resistance and metabolic syndrome. 3. Specific types of diabetes due to other causes. 4. Gestational diabetes (ElSayed et. al., 2023).

Insulin resistance (IR) is defined as an impairment in insulin action that leads to reduced glucose uptake by muscles and increased hepatic glucose production (Gastaldelli, 2022). The International community, particularly Word Health Organization (WHO), has identified DM as threat to public health and healthcare systems worldwide. In 2021, the global prevalence of diabetes among individuals aged 20–79 years was estimated at 10.5% (536.6 million people), and this figure is projected to rise to 12.2% (783.2 million) by 2045 (Sun *et. al.,* 2022).

Since diabetes is a chronic multifactorial disease, current therapeutic approaches primarily focus on managing metabolic parameters (glycemic and lipid levels), to control or delay the onset of associated complications. A wide range of pharmacological options is available for managing DM. For instance, glycemic control in patients with T2D can be achieved using oral antidiabetics drugs (OADs), whereas exogenous insulin is required for T1D. However, despite this significant therapeutic arsenal, many

of these drugs have side effects that frequently compromise patient adherence to therapy (Andrade *et. al.,* 2020).

WHO recommends the use of medicinal plants in food items for the treatment of DM (Yedjou et. al., 2023). In recent years, there has been an increasing interest in the use of medicinal plants products for treating DM patients. Combinations conventional medications with medicinal plants may enhance the efficacy and safety of treatments through synergistic effects (Widjajakusuma et al., 2019).

Obesity, hypertension, and T2D have reached epidemic proportions worldwide. These conditions are common comorbidities associated with lifestyles characterized by physical inactivity, low energy expenditure, high caloric intake, and the excessive consumption of processed food.

These effects which are driven by rapid urbanization, industrialization, and globalization. Although research on this comorbidity and the use medicinal plants for their treatment has gained prominence in recent decades, the complex biological mechanisms regulating metabolism remain poorly understood. There is still an urgent need for new treatment modalities to prevent and manage these diseases effectively (Petrie et. al., 2018).

Herbal medicines and their phytochemicals exhibit significant pharmacological and biological activities. They are used for preventing, treating, or improving various metabolic illnesses like DM. Today, they continue to serve as an affordable alternative medication in many poorer and more remote regions (Elkomy *et al.,* 2023).

Traditional medicine (TM), refers to the knowledge, skills, and practices rooted in indigenous cultures that are used for health maintenance, as well as for the prevention, diagnosis, improvement, or treatment of illness (Choopani *et. al.,* 2015). When these practices are based on past experiences and observations passed down orally or in

writing from generation to generation and are native to a specific country, they are referred to indigenous traditional medicine (ITM) (WHO, 2019).

When such practices are adopted outside their country or origin, they are often termed complementary and alternative medicine (CAM) (Che *et al.,* 2017). TM encompasses a wide range of practices, including acupuncture, chiropractic, massage therapy, and herbal medicine, among others. Similarly, ITM includes practices such as bush medicine, traditional healers, singing/chanting, and the use of external remedies (Adams *et al.,* 2015).

In México, from an ethnopharmacological perspective, it is important to recognize that DM lies at intersection of modern science-based medicine and TM. In rural areas of the country, DM patients often use a combination of locally available plant species with hypoglycemic properties, either alongside or in place of prescribed conventional medications (Andrade *et. al.,* 2006).

Typically, patients are diagnosed in primary health centers, where doctors prescribe appropriate medications. However, after diagnosis, many patients turn to local healers or vendors of herbal and other healthcare products. This preference for spiritual rituals and plant-based treatments over conventional medical care is influenced by culture, ethnic, and religious factors, as well as the lack of adequate institutional health services, which significantly shapes their health-seeking behavior (Espinoza *et. al.,* 2022).

In México, at least 306 species from 235 genera and 93 families are used to treat diabetes (Andrade & Heinrich*,* 2005). However, at least 800 plants are currently used for treating DM (Escandón *et. al.,* 2020). Thus, Mexican traditional medicine (MTM) generally relies on botanically based herbal remedies administered by individuals recognized as qualified within their native community.

Xi'oi/Xi'uy (pame) ancient native community, located in municipalities Tamasopo-Rayon of San Luis Potosi, plays a variety of roles, including providing strong spiritual and social support often signifying a reconnection to land, ancestral and spiritual and social support. This often signifies a reconnection to the land, ancestral roots, and spiritual practices, which enhance overall well-being. In the Xi'uy region of La Palma, thirteen plants are used for the treatment of DM.

One of these is *Calea urticifolia* (Mill.) DC. known as "negrito". Traditionally, a decoction of its leaves (0.13 g of dry leaves per 250mL of water, twice daily) is used as a therapeutic remedy for diabetes, gastric ulcers, and inflammatory processes. This corresponds to an approximate dose of 0.5514 mg of dry aqueous extract per kg body weight per day (Torres et al., 2016).

Calea urticifolia (Mill.) DC. is widely distributed from México to Panama in semi-warm and warm climates, typically found in tropical and oak forest. It is a shrub 1–3 meters high with yellow flowers and belong to the *Asteraceae* family (syn. *Compositae*). It is known by various vernacular names, including hierba del negro, jaral de castilla, chilchaca and juanislama. Synonyms for this plant include *Calea urticifolia var. axillaris* (DC.) S.F. Blake and *Calea urticifolia var. urticifolia* (Gogineni et. al., 2019).

It is important to note that drugs or herbal extracts that produce similar effects often do so at different doses, which can be either desirable or undesirable. The main focus of this research is the study of interaction between two chemicals. The dose-response relationship of each agent provides this critical information and allows researchers to focus on a specific magnitude of the effect. Specifically, the interest lies in oral antidiabetic drugs (OAD´s) that act together to produce a similar effect, namely, a hypoglycemic effect.

Previously, our research group documented the dose-dependent regulation of freeze-dried aqueous extract of *Calea urticifolia* (CuAqE, up to 11 mg/kg) on glucose energy

metabolism in a T2D mouse model induced by a high-fat diet-induced obesity (DIO-HFD). Additionally, the hypoglycemic effect of CuAqE (41mg/kg) has been reported in a T2D rat model (induced by 65 mg/kg streptozotocin and 150 mg/kg nicotinamide) (Andrade *et. al.,* 2021 & Espinoza *et. al.,* 2022).

Despite these findings, scientific knowledge of CuAqE remains limited. Therefore, the objective of this investigation was to evaluate glycemic metabolic regulation of CuAqE (11 mg/kg) in a T1D murine model developed using multiple low doses of streptozotocin (MLD-STZ) and a T2D murine model by DIO-HFD in C57BL/6 male mice. Additionally, this aims to provide evidence the pharmacotherapeutic interaction of CuAqE with hypoglycemic drugs such as insulin, metformin, glibenclamide and sitagliptin.

2. Materials and Methods

2.1 Materials

The Rat/Mouse Insulin ELISA Kit was purchased from Millipore Corporation, USA. Pentobarbital sodium (Pisabental ®) from Pisa Agropecuaria (PiSA® Farmaceutica, Mexico). Streptozotocin (STZ) and anhydrous glucose were purchased from Sigma Aldrich, St. Louis, MO and Accu-Chek Aviva test strips were acquired from Roche, UK.

2.2 Herbal material harvest and preparation of freeze-dried aqueous extract of Calea urticifolia (CuAqE)

Fresh leaves of adult plants of *Calea urticifolia* were harvested in July 2022 from the Xi'uy ancient native community of Potrero del Carnero (21°52'27.6'' N y 099°27'00.6'', to 901 msnm, San Luis Potosi, Mexico). The plant material was authenticated by an herbalist of Isidro Palacios Herbarium (IIZD-UASLP, San Luis Potosí, México). The harvested material was separated, placed on absorbent paper for drying, and stored at room temperature until further use.

Dry leaves were ground using an electric mill (Osterizer Pulse Matic Blenders). A total of 100g of powdered leaves was mixture with 1L of distilled water and boiled for 5 min.

After cooling, the aqueous extract was filtered and freeze-dried (Freeze-dryer TFD5505, Ilshin®, Hialeah, FL, USA). The yield of the lyophilized extract was 19.88%, and the residue was stored at 4˚C until use.

2.3 Animal procurement, housing and bioethical considerations.

C57BL/6 male mice, aged 4-6 weeks, were purchased from the Laboratory animal production and experimentation unit (UPEAL, CINVESTAV-IPN. México City, México). Upon arrival, the mice were housed in a controlled environment (21±2◦ C, 50±10% humidity) with a 12 h light/dark cycles (7:00 am to 7:00 pm) and provided with standard rodent chow (Chow 5001) and water ad libitum.

Mice were acclimatized for 5 days before being randomly assigned to diet groups and housed in individual acrylic cages. Animal study protocol was reviewed and approved by local animal ethical review committee (CE102018015R2. FCQ-UASLP, San Luis Potosi, México). All procedures were conducted in accordance with the Mexican norm for animal care and handing (NOM-062-ZOO-1999).

2.5 Induction of DM mouse models and experimental design

2.5.1 *Induction of DM mouse models*

DM was induced in C57BL/6 male mice. For T1D model, chemically induced was achieved using MLD-STZ (40 mg/kg, IP) for 5 consecutive days at 12 weeks and for T2D model, was achieved using a DIO-HFD for 36 weeks, as previously described (Deeds *et. al.,* 2011 & Stancic *et. al.,* 2022).

2.5.2 Experimental design T1D mouse model for the evaluation of **CuAqE**

Mice were randomly assigned to 8 groups (n=5).

- **Group 1 (CTL-NOM):** Normoglycemic control (non-diabetic), receiving physiological solution (vehicle).
- **Group 2 (CTL-T1D):** Positive DM control (T1D-induced), receiving a physiological solution (vehicle).

Groups 3-4: Administrated *Calea urticifolia* aqueous extract (CuAqE 11 mg/kg/day).

- **Group 3 (NOM- CuAqE):** Normoglycemic control + CuAqE
- **Group 4 (T1D- CuAqE):** Experimental T1D + CuAqE

Groups 5-6: Experimental T1D mice receiving subcutaneous (SC) daily administration of insulin glargine, a long-acting insulin analog with a stable action profile.

- **Group 5 (T1D-InsN):** Lantus® (12.5 IU/kg/day).
- **Group 6 (T1D-InsR):** Lantus® (25 IU/kg/day).

Groups 7-8: Experimental T1D mice receiving CuAqE (11mg/kg/day) + insulin glargine.

- **Group 7 (T1D- CuAqE-InsN):** CuAqE + Lantus® (12.5 IU/kg/day).
- **Group 8 (T1D- CuAqE-InsR):** CuAqE + Lantus® (25 IU/kg/day).

The doses of insulin glargine were selected based on previous reports (Stammberger et. al., 2002 & Amein et. al.,2015). Treatment with Lantus® began 5 days after STZ injection and continued for 8 weeks.

2.5.3 Experimental design T2D mouse model for the evaluation of CuAqE

Mice were randomly assigned into 10 groups (n=5 per group).

- **Group 1 (CTL-NOM):** Normoglycemic control (non-diabetic), receiving a physiological solution (vehicle).
- **Group 2 (CTL-T2D):** Positive DM control (T2D-induced), receiving a physiological solution (vehicle).

Groups 3-4: Administered CuAqE (11 mg/kg/day).

- **Group 3 (NOM- CuAqE):** Normoglycemic control + CuAqE
- **Group 4 (T2D- CuAqE):** Experimental T2D + CuAqE

Groups 5-7: Experimental T2D mice receiving OAD´s. Doses were calculated based on human-equivalent do using pharmaceutical formulations (adjusted for a 70 kg body weight).

- **Group 5 (T2D-Met):** Dabex® Metformin (7.14 mg/kg/day).

- **Group 6 (T2D-GLI):** Glucoven® Glibenclamide (0.07 mg/kg/day).
- **Group 7 (T2D-SIT):** Januvia® (Sitagliptin 1.43 mg/kg/day).

Groups 8-10: Experimental T2D receiving CuAqE (11mg/kg/day) combined with OAD´s

- **Group 8 (T2D-CuAqE-Met):** CuAqE + Dabex® Metformin (7.14 mg/kg/day).
- **Group 9 (T2D-CuAqE-GLI):** CuAqE + Glucoven® Glibenclamide (0.07 mg/kg/day).
- **Group 10 (T2D-CuAqE-SIT):** CuAqE + Januvia® (Sitagliptin 1.43 mg/kg/day).

CuAqE and OAD´s solutions were orally-administrated daily via intragastric probe (0.1 mL/10 g body weight) at the same time and order for 8 weeks. Solutions were freshly prepared in physiological solution.

2.6 Mice profiles

2.6.1 Growth patterns (GW) and body composition (BC)

Individual body weight (BW) was measured weekly throughout the 44-weeks duration of the experiment with a precision 0.1g using an electronic balance. Body length (BL), body surface area (BSA), body mass index (BMI), growth rate (GR) and Lee index were calculated according to formulas previously established by the work team.

2.6.2 Energy metabolism (EM)

Water and food intake was also recorded weekly. Energy density was calculated as gross energy (GE), metabolizable energy (ME), loss energy (urine, feces, methane), physiological fuel value, basal metabolic rate (BMR), food efficiency ratio (FER), total daily expenditure of energy (DEE) and energy balance (EB) for groups of mice fed both models.

2.6.3 Clinical biochemistry

Blood samples were collected weekly from 12 or 36-week-old male mice fasted overnight (12-18 h) via tail vein puncture. Blood glucose (BG) were measured using a hand-held blood glucose monitor (Accu-Check Aviva, Roche, UK). Fasting Blood Glucose (FBG) and Postprandial Blood Glucose (PPBG) were assessed monthly. Serum Insulin (FSI) was quantified using a RAT/Mouse Insulin ELISA Kit (Millipore) following the manufacturer's protocol. Absorbance was measured at 450nm using a Multiskan photometer (Thermo Fisher Scientific®, USA).

2.6.4 Blood glucose and insulin kinetics

After 8 weeks of treatment, an oral glucose tolerance test (OGTT, 50 mg glucose) was performed on fasted mice for 6 hours. Blood samples were collected from the tail at 0,15,30,60,90 and 120 minutes post-glucose administration, and BG were measured as described by Kowalski et al. (2017). Area under the curve (AUC) for the glucose tolerance test was calculated using the trapezoidal rule, and a trendline was plotted to visualize the curve.

Additionally, an intraperitoneal insulin tolerance test (IITT: 0.75 IU/kg,) was performed, with blood samples collected at 0, 30, 60, and 120 minutes to measure plasma glucose levels, expressed as a percentage of initial value. An intraperitoneal glucose tolerance test (IPGTT; 50mg glucose) and an intravenous glucose tolerance test (IVGTT; 50mg) were also conducted. For the IPGTT and IVGTT, blood samples were collected at 0, 30, 60, and 120 minutes, and 0,2,5,10,20,30, and 45 minutes, respectively.

To minimize stress-related a fact in metabolic outcomes, all mice were acclimatized to handling procedures. For this purpose, two weeks prior to the glucose/insulin tolerance test (GITTs), mice were gently handled by the same experimenter every 2-3 days.

2.6.5 Insulin resistance and

To calculate Homeostatic Model Assessment insulin resistance (HOMA-IR), Homeostatic Model Assessment beta-cell function (HOMA-β or %β), Homeostatic Model Assessment insulin sensitivity (%S), insulin disposition index (DI), and quantitative insulin sensitivity check index (QUICKI) following formulas were applied based on single-pool first-order glucose kinetics adapted for mice (van Dijk et al., 2013). Additionally, the area under the curve from the oral glucose tolerance test (AUG-OGTT) was used to evaluate insulin resistance (IR).

2.7. Experimental Drug Dose-Effect Analysis

2.7.1 Hypoglycemic effect and dose-response curve

The hypoglycemic effect (E) was calculated using the equation:

$$E = \left[\frac{GlucT2D - Glucdrug}{GlucT2D - Glucnorm}\right] * Emax$$

Where:

E = Hypoglycemic effect,

$Gluc_{T2D}$ = BG in untreated diabetic mice,

$Gluc_{drug}$ = BG in drug-treated mice,

$Gluc_{norm}$ = BG in normoglycemic mice,

E_{max} = Maximum drug effect (typically 100%).

At the cut-off point for T2D generation, a hyperbolic dose-response curve was constructed using logarithmic transformations of model pharmacological data log dose [x] and glycemia [y]. Dose ranges were as follows:

- **Metformin:** 200-2800mg (2.86-40 mg/kg),
- **Glibenclamide**: 0.5-20mg (0.007-0.286 mg/kg),
- **Sitagliptin:** 10-200mg (0.14-2.86 mg/kg),
- **CuAqE:** 10-3500mg (0.14-50 mg/kg).

Five animals were tested per dose. A subset of mid-range data points (20 and 80% of the maximum effect) exhibited a linear trend when plotted as effect vs log(dose). These data were analyzed via linear regression ($E=a+b\ [\log C]$) to determine D50, standard error $\sigma_{(D_{50})} = 2.30 \times D_{50} \times \sigma(\log_{D50})$, and variance ($\sigma^2$). Doses are expressed as mg/kg of body mass.

2.8 Drug synergism: Combination Drug Analysis

2.8.1 Additivity and Relative Potency

Additivity assumes that drug combinations act proportionally to their relative potency (R), defined as R=A/B, where A and B are the doses of drug 1 and drug 2 required to achieve a specified effect (E_{50}). R >1 indicates higher potency of drug B.

Combination Index (CI)

Synergistic between CuAqE and OAD´s was evaluated using the combination index:

$$CI = \frac{Ca}{A} + \frac{Cb}{B}$$

Were:

- **Ca and Cb =** Doses of compounds A and B in combination,
- **A and B =** Doses required individually for the same effect.

Interpretation:

CI < 1: Synergism,

CI = 1: Additivity,

CI > 1: Antagonism (Zhao et al, 2005, 2010)

2.8.2 Isobolographic Analysis

According to the method described by Tallarida, the presence of synergy between two compounds can also be demonstrated through isobolographic analysis. The X- and Y-axis of the isobologram represent the concentrations of compounds A and B required individually or in combination to achieve the same effect. The straight line connecting these points is termed “line of additive”, defined by the individual drugs ED_{50} values.

The value f=0.5 was used to calculate the additive total, where the amounts in an additive combination are α=f A of drug A and β=(1–f) B of drug B. Total amount in the mixture, denoted, Z_{add}, represents the expected additive dose to achieve a 50% effect. Although the fraction f is assumed constant, uncertainty in Z_{add} due to variability in A and B. This uncertainty is quantity by the variance and standard error:

$$\sigma^2(Z_{add}) = f^2 * \sigma^2(A) + (1 - f)^2 * \sigma^2(B)$$

and $\sigma \log (Z_{add}) = \sigma Z_{add}/2.3*Z_{add}$ (Tallarida, 2012; Tallarida, 2010; Tallarida 2006 and Tallarida 2000).

For mixture, Z_{add} was reduced to half to determined other doses. Each total dose preserved the ratio of drug A to drug B, such that $\rho_A = fA/Z_{add}$ and $\rho_B = (1 - f)B/Z_{add}$. Using dose.effect data and linear regression, D_{50}, (denotes Z_{mix}) and its variance σ^2 (Zmix) were calculated. A significant difference between Z_{add} and Z_{mix} indicates nonadditivity: synergism if $Z_{mix} < Z_{add}$ or sub-additivity if $Z_{mix} > Z_{add}$.

2.9 Statistical analysis

Results are expressed as mean ± standard deviation (SEM). Data were analyzed using one way ANOVA followed by Bonferroni post hoc test, with $p<0.05$ considered statistical significance. All analyses were performed in at least three independent experiments and each analyzed in triplicate. To distinguish synergistic interactions from additive effects between experimental doses that cause 50% of hypoglycemic effect (Z_{mix}) and theoretical additive doses (Z_{add}), student t-test was applied, following isobolographic analysis protocols. Statistical analysis was conducted using the PROC GLM procedures of SAS version 9.3 (SAS Inst. Inc., Cary, NC).

3. Results

3.1 Hypoglycemic effect of CuAqE in DM murine models

Accordingly, to establish the antidiabetic potential of CuAqE, several in vivo tests were performed. The first experiment was a hypoglycemic test, compared to type DM. For

evaluated hypoglycemic activity of CuAqE, FBG and PPBG were measured during administration time (8 weeks).

In mice under normoglycemic conditions (CTL-NOM), CuAqE does not modify serum glucose concentrations at 20 weeks for T1D model and 44 weeks for T2D model (Fig. 1-2). Notwithstanding in T1D male mice treated with a therapeutic regimen of CuAqE (11mg/kg), this extract reduces hyperglycemia from the first week of treatment (-10%). A constant difference in BG (30-40 units) between T1D-CTL and T1D-CuAqE mice is maintained until the end of the experiment (Fig. 1, $p<0,001$).

For TD2, a hypoglycemic effect is also observed from week 2 of treatment (-16%). As time progresses, the difference in BG between T2D-CTL and T2D-CuAqE mice increases until reaching a decrease of 79% at the end of the administration of CuAqE (Fig. 2, $p<0,001$). In determination of BG after caloric intake, hypoglycemic action of CuAqE is similarly observed in both DM mice models (Fig. 1-2S).

During long-term treatment whit insulin glargine, BG of T1D-InsN mice (12.5 IU/kg/day) remained at 226 to 143mg/dL. Effectiveness of insulin in maintaining optimal levels of BG in T1D-InsN mice it is observed when drop to near normal level until 7 weeks post treatment ($p<0,001$). Moreover, BG of T1D-InsR (25 IU/kg/day) mice starting dropped to normal level within 1 week post treatment (140 to115 mmol/L BG) and were maintained in normoglycemic conditions throughout the experiment ($p<0,001$).

25 IU/kg and 12.5 IU/kg doses of insulin glargine had efficacy for provide for BG. Although, they had long-acting effects compared with CTL-T1D, therefore the long-acting effect of insulin glargine was not as potent with 12.5 IU/kg. When CuAqE is administered concomitantly with insulin no showed a synergistic or antagonist effects but rather additive effect not considerable (Fig. 3).

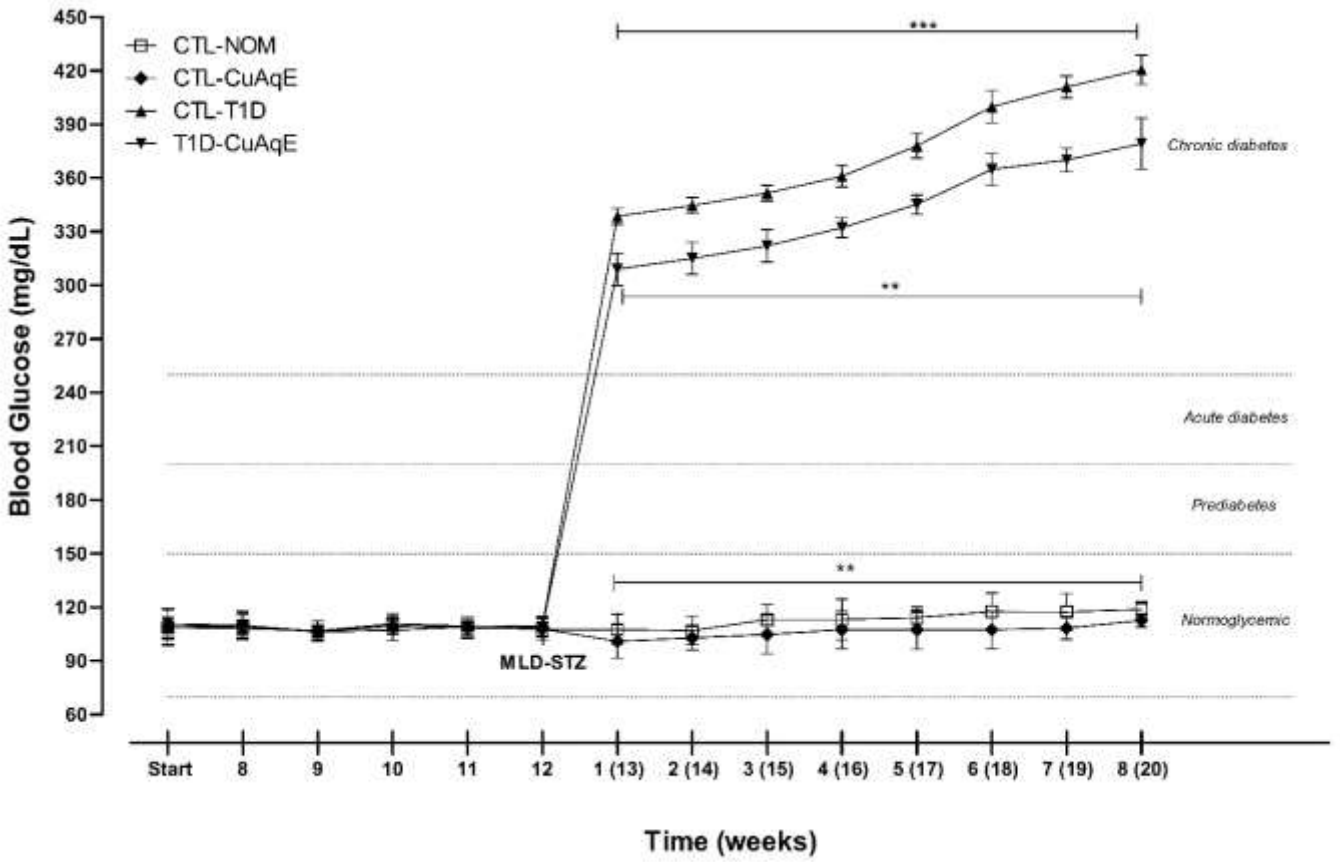

Figure 1. **Phytopharmacological evaluation of hypoglycaemic activity in T1D murine model with pharmacotherapeutic monitoring of CuAqE as treatment against T1D**. FBG (mg/dL) in C57BL/6 male mice ***p<0,001 vs CTL-NOM and ** p<0,001 vs CTL-T1D. Values represent means ± SEM of each group. Statistical analysis was performed using two-way ANOVA with Bonferroni multiple comparisons test.

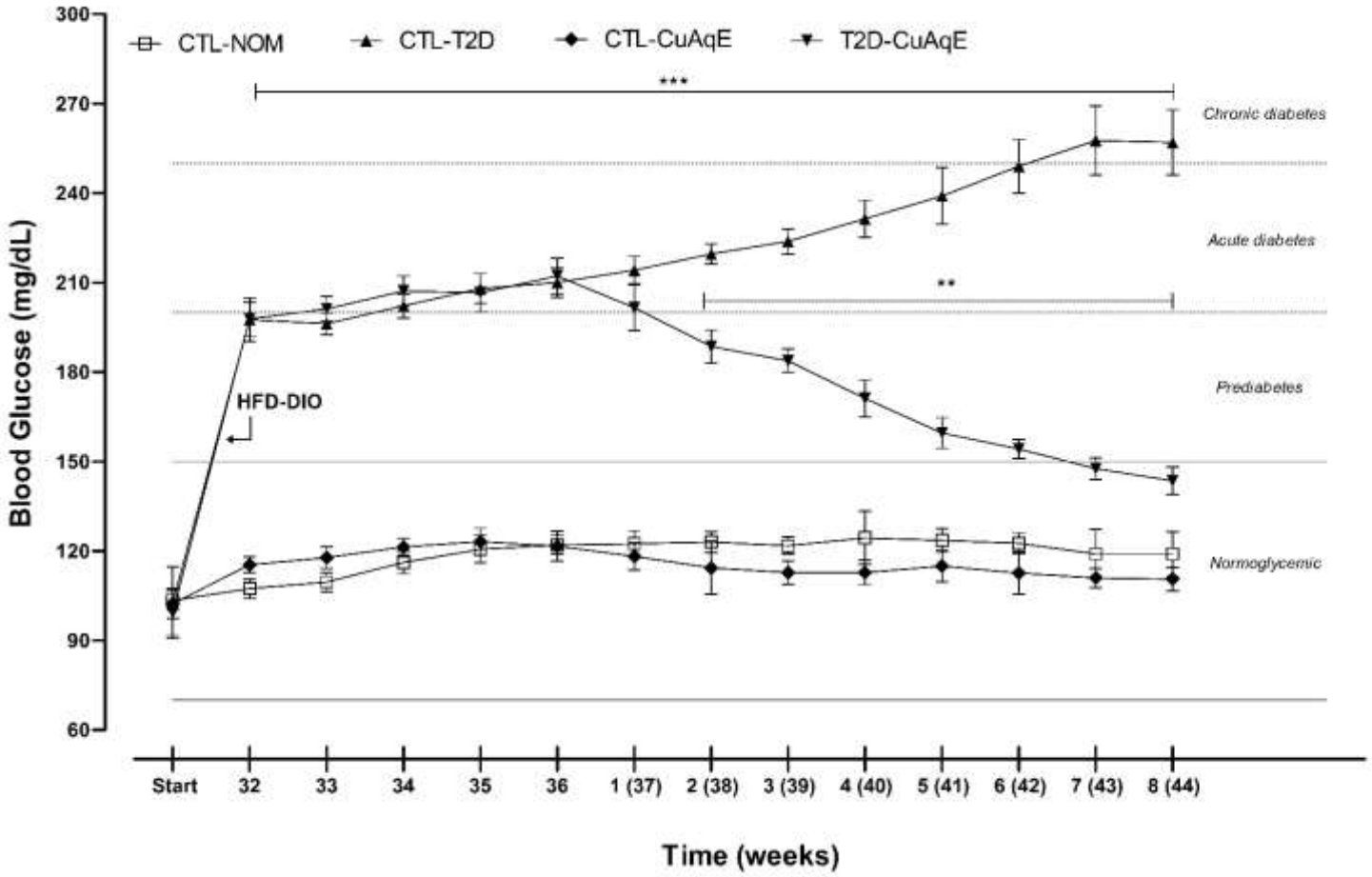

Figure 2. **Phytopharmacological evaluation of hypoglycaemic activity in T2D murine model with pharmacotherapeutic monitoring of CuAqE as treatment against T2D.** FBG (mg/dL) in C57BL/6 male mice ***p<0,001 vs CTL-NOM and **p<0,001 vs CTL-T2D. Values represent means ± SEM of each group. Statistical analysis was performed using two-way ANOVA with Bonferroni multiple comparisons test.

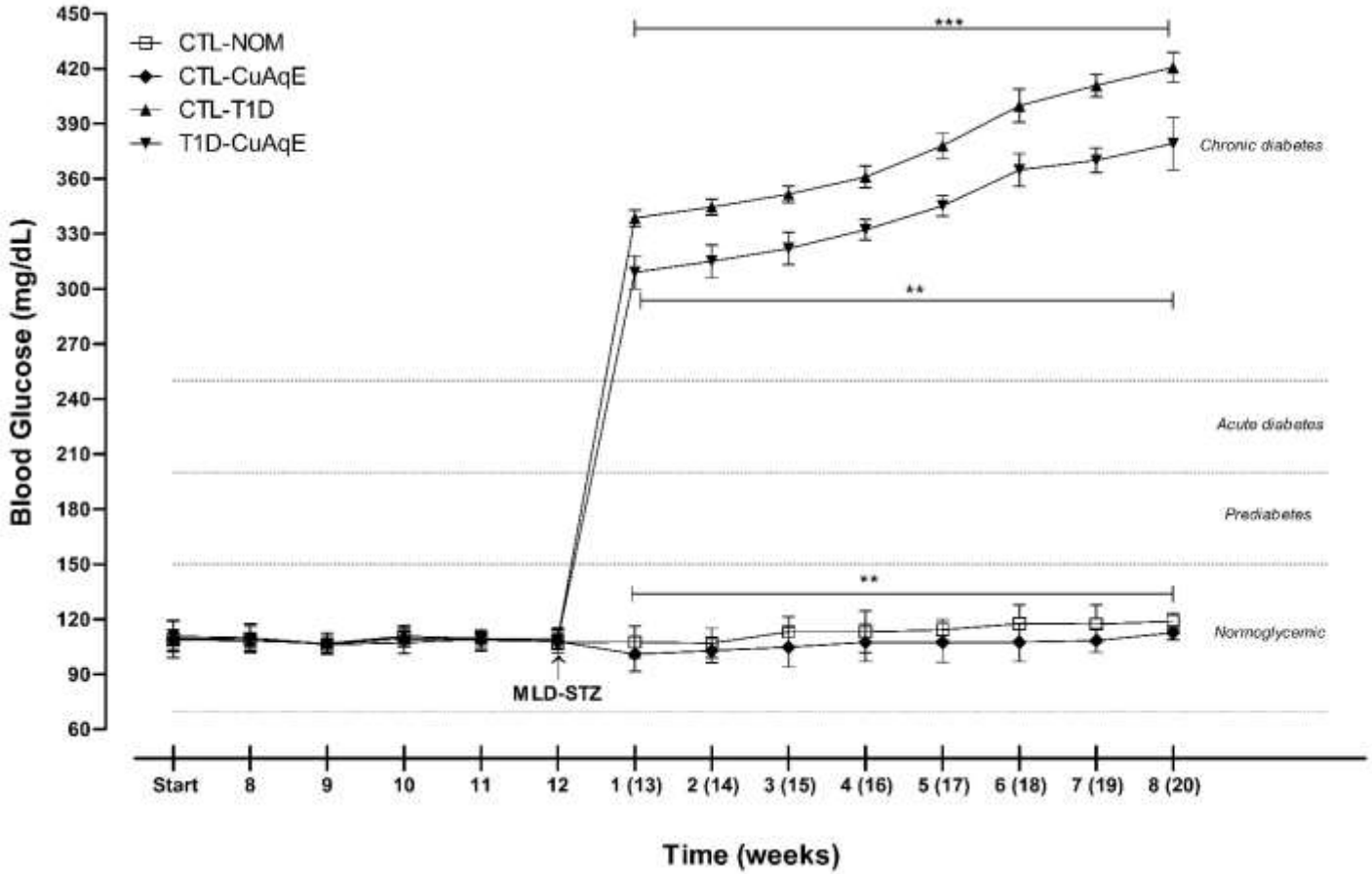

Figure 3. **Phyto-pharmacovigilance of hypoglycaemic activity in T1D murine model with pharmacotherapeutic monitoring of CuAqE and insulin for determining extract-drug interactions.** FBG (mg/dL) in C57BL/6 male mice. ***p<0,001 vs CTL-T1D and ** p<0,001 vs T1D-InsN. Values represent means ± SEM of each group. Statistical analysis was performed using two-way ANOVA with Bonferroni multiple comparisons test.

Some beneficial drugs associated as pharmaceutical employment of OAD´s to treat T2D have been tested in our model. OAD´s treatment in T2D mice it has a positive effect sustained over time until having a controlled normoglycemic state ($p<0,001$).

Metformin it has a hypoglycemic effect from the first week after treatment due to a 13.5% decrease in serum BG concentration in T2D-Met mice. Additionally, metformin shows trend to normoglycemic state at week 6 post-treatment (124-114 mg/dL) and it is important to notice that when CuAqE is administered with metformin in T2D-Met-CuAqE mice there is a considerable synergistic effect in regulation of BG from week 4 post-treatment (Fig. 4, $p<0,05$).

Glibenclamide it also has a hypoglycemic effect from the first week with a reduction in BG of up to 11% in T2D-Gli mice ($p<0,001$). Furthermore, it achieves a normoglycemic state up to the sixth week after treatment (137-117mg/dL). Concomitant administration of CuAqE and glibenclamide in T2D-CuAqE-Gli mice does not show any type of pharmacological interaction (Fig. 5).

When we administer sitagliptin to T2D-Sit mice, its hypoglycemic efficacy is also seen from the first week post-treatment with 12.6% of reduction of BG ($p<0,001$) and can lead to a normoglycemic state from week 5 until the end of the experiment (142-111 mg/dL). There is no pharmacological interaction that affects the hypoglycemic activity when CuAqE and sitagliptin are administered together in T2D-CuAqE-Sit mice (Fig. 6).

In determination of BG after caloric intake, hypoglycemic action of CuAqE with OAD´s is the same in both DM mice models (Fig. 3S). Finally, CuAqE decreased BG but its hypoglycemic activity is less effective and efficient to that produced by metformin, glibenclamide and sitagliptin.

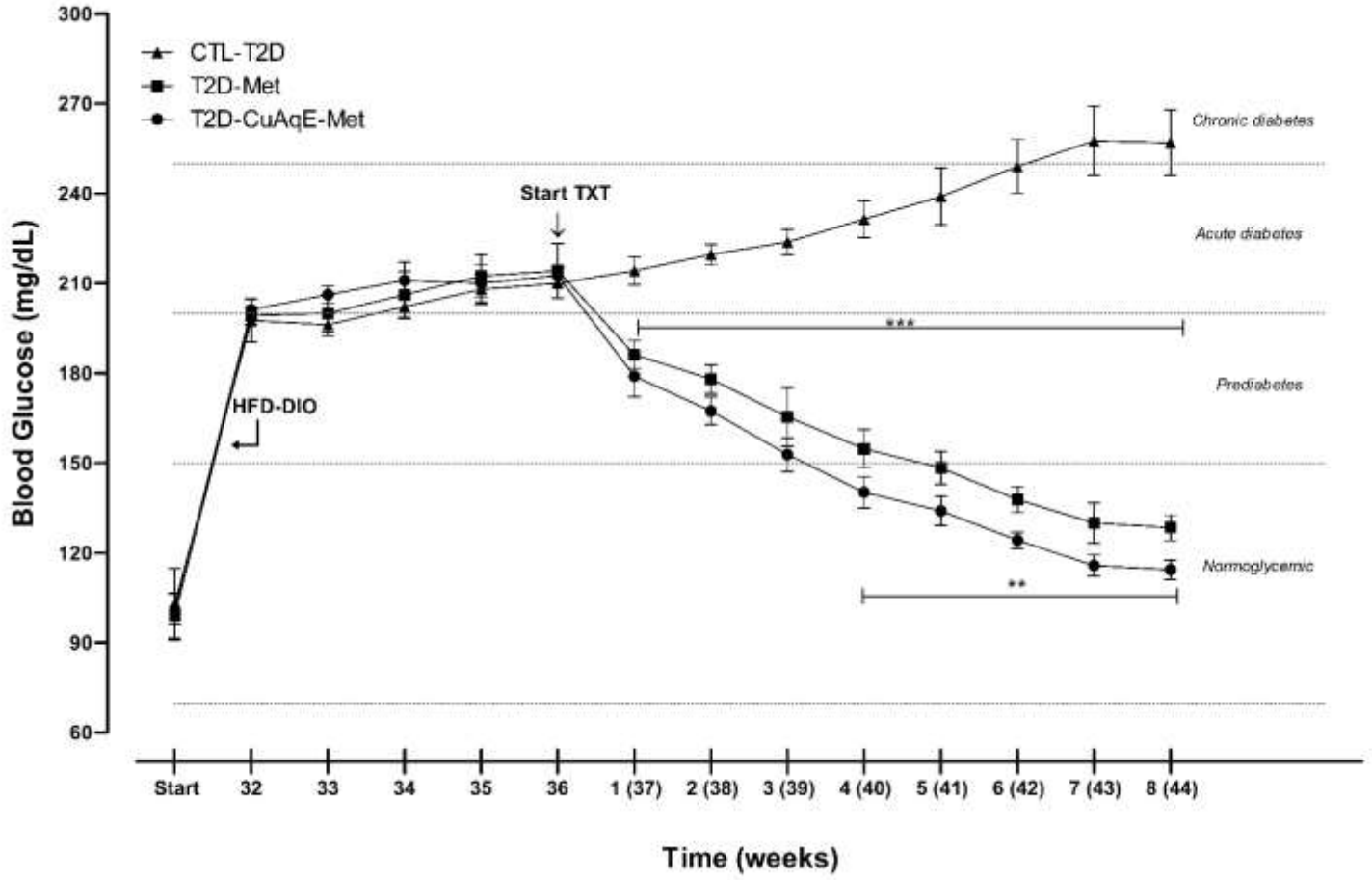

Figure 4. **Phyto-pharmacovigilance of hypoglycaemic activity in T2D murine model with pharmacotherapeutic monitoring of CuAqE and metformin for determining extract-drug interactions.** FBG (mg/dL) in C57BL/6 male mice. ***p<0,001 vs CTL-T2D and ** p<0,05 vs T2D-Met. Values represent means ± SEM of each group. Statistical analysis was performed using two-way ANOVA with Bonferroni multiple comparisons test.

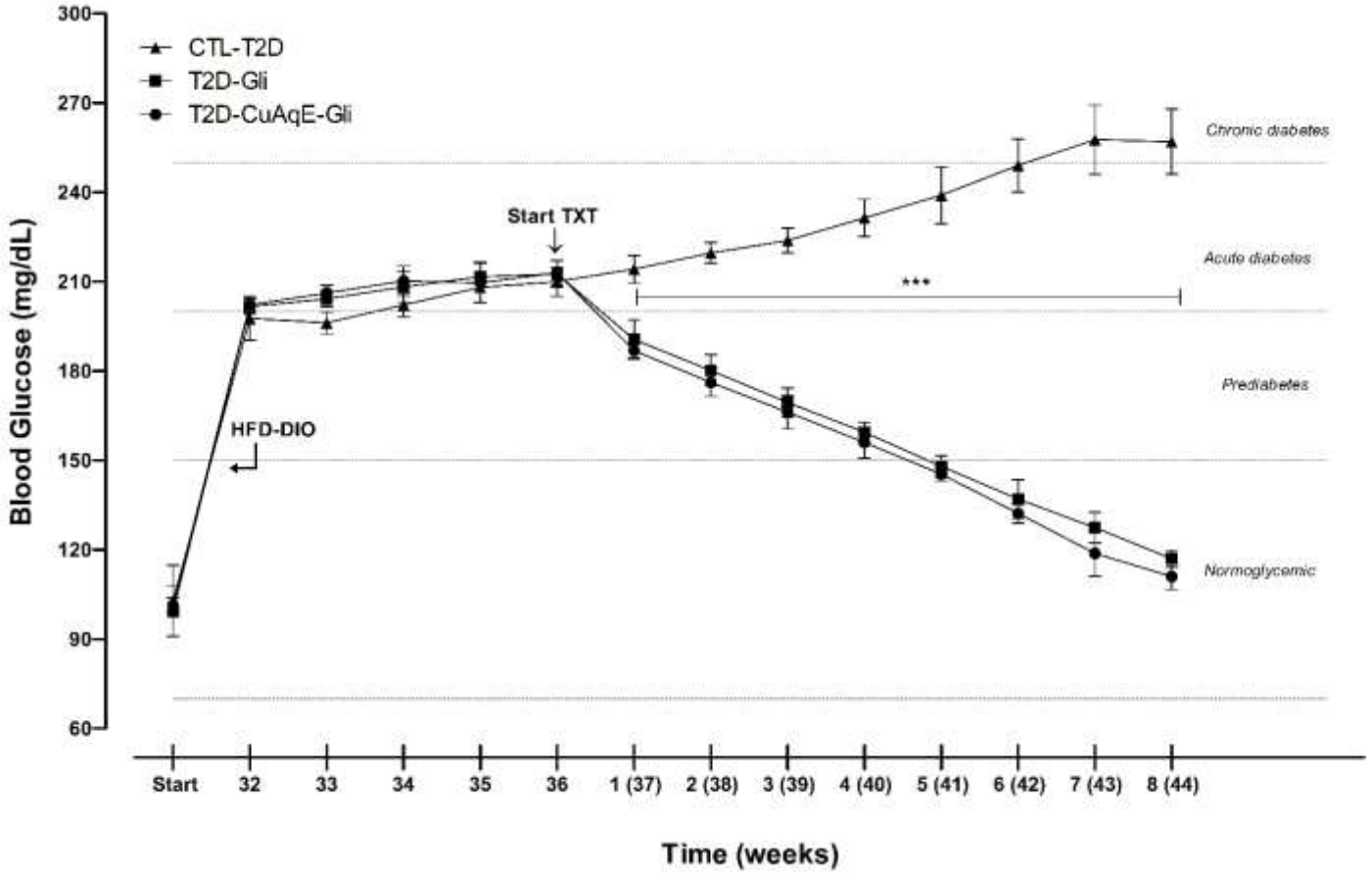

Figure 5. **Phyto-pharmacovigilance of hypoglycaemic activity in T2D murine model with pharmacotherapeutic monitoring of CuAqE and glibenclamide for determining extract-drug interactions.** FBG (mg/dL) in C57BL/6 male mice. ***p<0,001 vs CTL-T2D. Values represent means ± SEM of each group. Statistical analysis was performed using two-way ANOVA with Bonferroni multiple comparisons test.

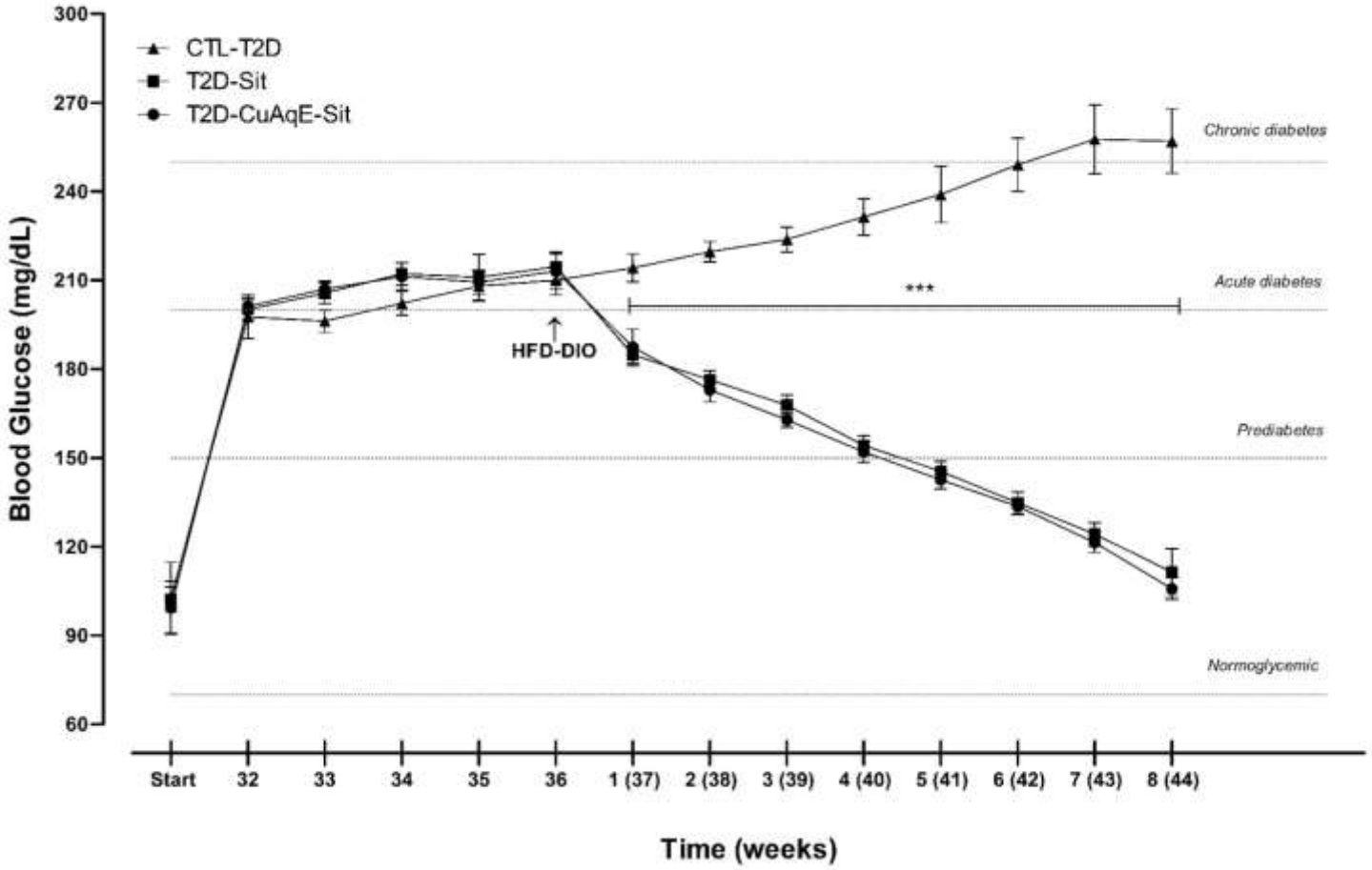

Figure 6. **Phyto-pharmacovigilance of hypoglycaemic activity in T2D murine model with pharmacotherapeutic monitoring of CuAqE and sitagliptin for determining extract-drug interactions.** FBG (mg/dL) in T2D C57BL/6 male mice. ***p<0,001 vs CTL-T2D. Values represent means ± SEM of each group. Statistical analysis was performed using two-way ANOVA with Bonferroni multiple comparisons test.

3.2 Regulation in growth patterns and body composition by CuAqE in DM murine models

The pathophysiological state of DM includes changes in BW, so we monitored growth patterns and body composition in both models. T1D mice tend to drastically lose BW (18%) after treatment with MLD-STZ, without reaching a state of underweight. At end of experiment, they had a 3% gain. T1D-CuAqE mice had a BW loss (12%), however, during the 8 weeks post-treatment with CuAqE they had a 5% gain, but not significant compared to CTL-NOM mice (Fig. 7). When insulin or CuAqE with insulin is administered, the BW loss is not as severe (Fig. 4S).

Moderate obesity is induced in T2D mice during HFD feeding. When extract is administered to T2D-CuAqE mice, their rate of weight gain is lower than that of T2D-CTL mice (Fig. 8, $p<0,001$). When OAD´s are administered to T2D mice, BW decreases, significantly regulating weight gain from week 5 post-treatment until the end of the experiment. If CuAqE is administered concomitantly with OADs, the rate of BW loss increases (Fig. 5S). For a better analysis of growth patterns and body composition, nutrient's intake, energy density parameters, energy metabolism parameters and water intake they can be consulted at supporting information.

3.3 Metabolic effects of CuAqE associated with altered glucose regulation and insulin resistance

GITT's were performed on a large cohort (8 weeks with DM) in male C57BL/6 mice to gain insight into glucose handling during DM mouse models for evaluated metabolic effect of CuAqE on hyperglycemia. Glucose administration led to a far higher glucose excursion/effective use in CTL-T2D mice than CTL-T1D mice. In both models, incremental AUC was significantly different respect to CTL-NOM ($p<0,05$). In OGTT, CuAqE reduced AUC by 17% in T1D-CuAqE and 53% in T2D-CuAqE mice (Tables 1-2). T1D model for groups of mice that received insulin without and with CuAqE was not significantly different among them.

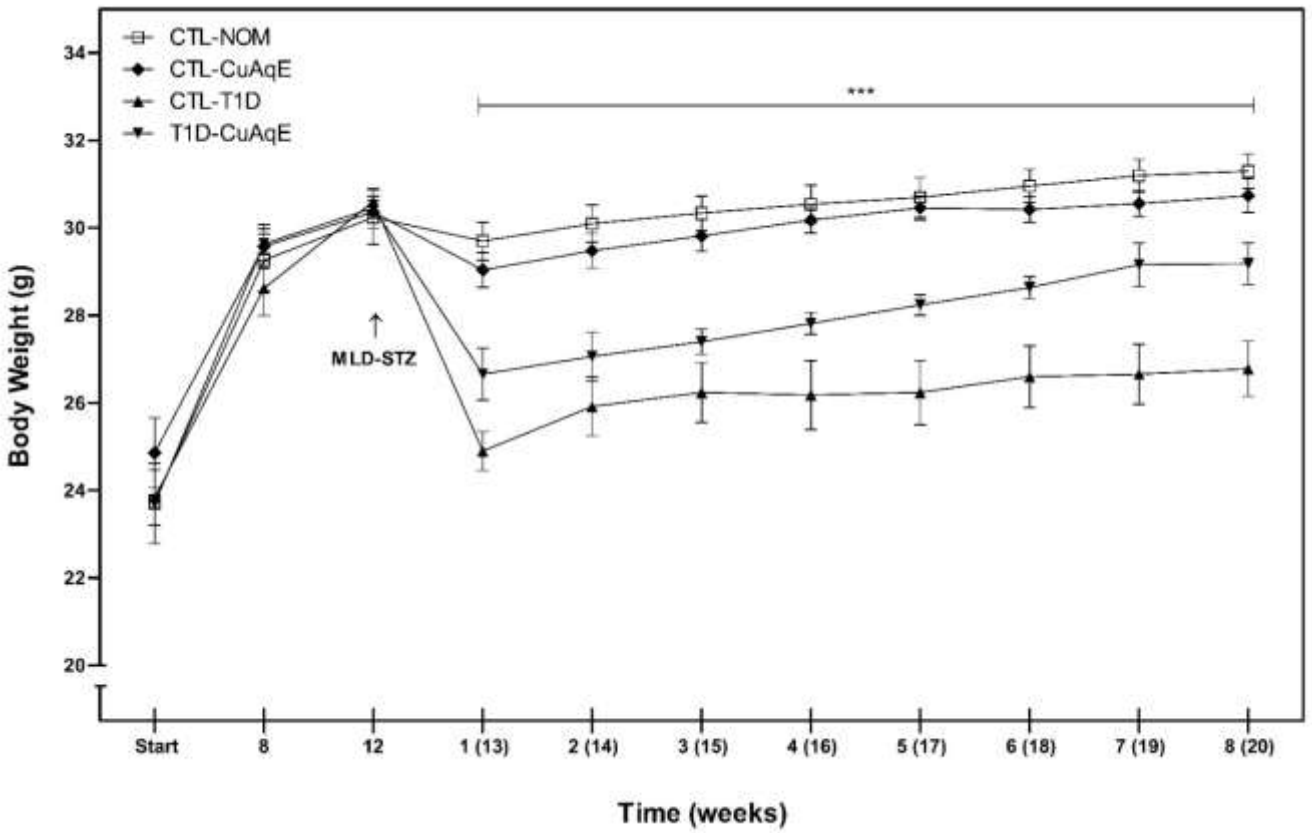

Figure 7. Longitudinal variation of body weight in T1D murine model with pharmacotherapeutic monitoring of CuAqE as treatment against T1D. Body weight changes in T1D C57BL/6 male mice that were treated with CuAqE. Values represent means ± SEM of each group (n=5). Statistical analysis was performed using two-way ANOVA with Bonferroni multiple comparisons test. ***p<0,001 vs CTL-T1D.

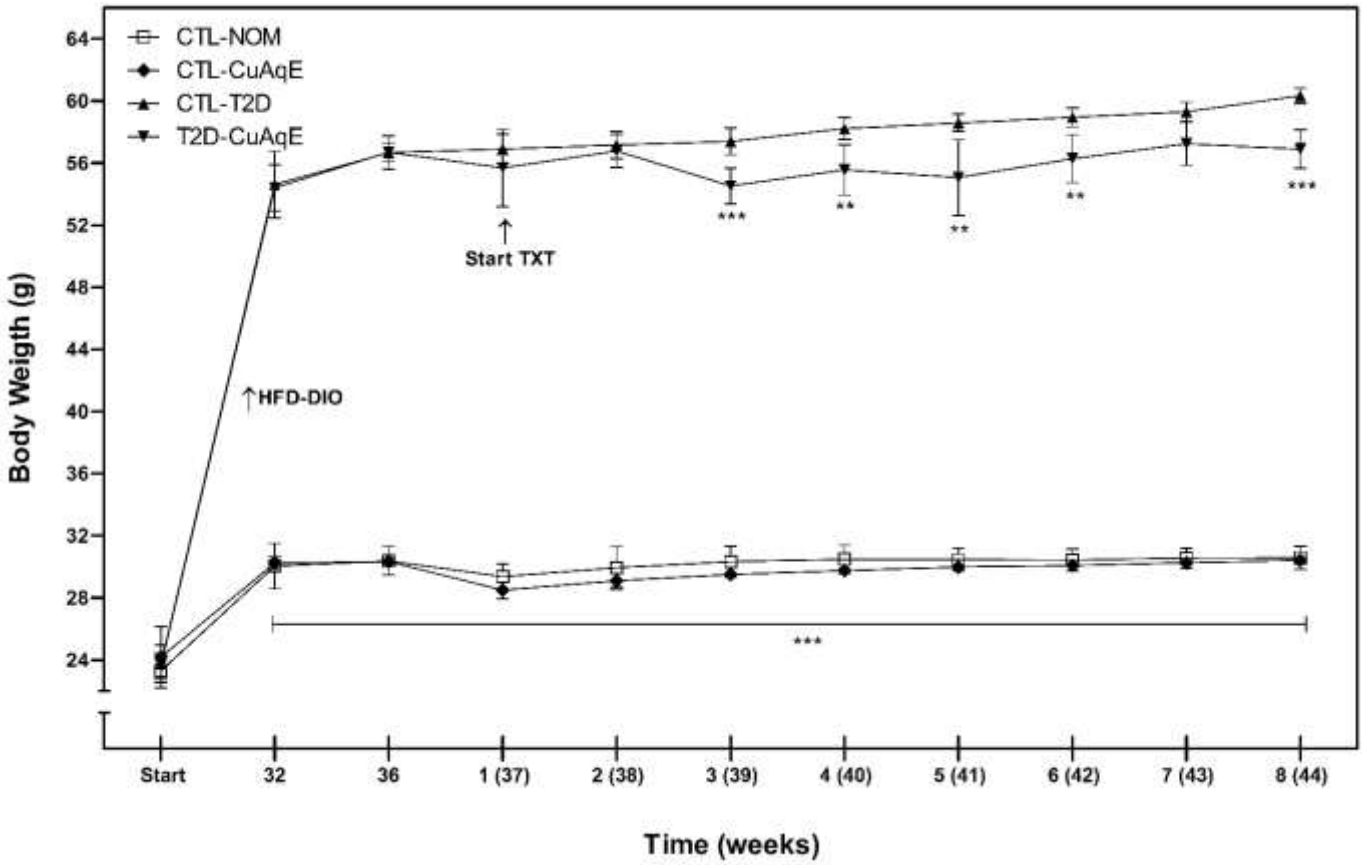

Figure 8. Longitudinal variation of body weight in T2D murine model with pharmacotherapeutic monitoring of CuAqE as treatment against T2D. Body weight changes in T2D C57BL/6 male mice that were treated with CuAqE. Values represent means ± SEM of each group (n=5). Statistical analysis was performed using two-way ANOVA with Bonferroni multiple comparisons test. ***p<0,001 vs CTL-T2D and **p<0,01 vs CTL-T2D.

Table 1. Areas under curve during glucose/insulin tolerance tests in T1D murine model with pharmacotherapeutic monitoring of CuAqE and therapeutic regimen against T1D for determining extract-drug interactions.

T1D models	OGTT*	ipGTT*	ITTS*	IVGTT*
CTL-NOM	22367±1062	19788±784	6510±713	22473±440
CTL-T1D	75882±2146*	64521±852*	24798±447*	62801±1103*
CTL-CuAqE	19659±872$^{\#}$	19809±851$^{\#}$	6900±320$^{\#}$	21761±538$^{\#}$
T1D-CuAqE	63051±2421*$^{\#\&}$	51180±2683*$^{\#\&}$	18933±1697*$^{\#\&}$	48290±2249*$^{\#\&}$
T1D-InsN	47691±2730*$^{\#\&\$}$	52107±4119*$^{\#\&}$	13923±486*$^{\#\&\$}$	43043±1322*$^{\#\&\$}$
T1D-InsR	32255±2451*$^{\#\&\$}$	35637±1445*$^{\#\&\$}$	11088±185*$^{\#\&\$}$	28209±463*$^{\#\&\$}$
T1D-CuAqE-InsN	46820±2422*$^{\#\&\$}$	50001±1517*$^{\#\&}$	15690±319*$^{\#\&\$a}$	41006±1056*$^{\#\&\$}$
T1D-CuAqE-InsR	30743±2443*$^{\#\&\$}$	35037±944*$^{\#\&\$}$	12144±132*$^{\#\&\$b}$	27080±324*$^{\#\&\$}$

Oral Glucose Tolerance Test (50mg, OGTT), Intraperitoneal Glucose Tolerance Test (50mg, ipGTT), Intraperitoneal Insulin Tolerance Test (0.75 IU/kg, IITT) and Intravenous Glucose Tolerance Test (50mg, IVGTT) in C57BL/6 male mice were treated with CuAqE and drugs against T1D. Values represent means ± SEM of each group (n=5). *Such as Area Under the Curve (AUC). Statistical analysis was performed using two-way ANOVA with Tukey multiple comparisons test for each intervention time. *p<0,05 vs CTL-NOM; # p<0,05 vs CTL-T1D; & p<0,05 vs CTL-CuAqE; $ p<0,05 vs T1D-CuAqE; ^{a} p<0,05 vs T1D-InsN and ^{b} p<0,05 vs T1D-InsR.

Table 2. Areas under curve during glucose/insulin tolerance tests in T2D murine model with pharmacotherapeutic monitoring of CuAqE and therapeutic regimen against T2D for determining extract-drug interactions.

T2D models	OGTT*	ipGTT*	ITTS*	IVGTT*
CTL-NOM	21515±1010	21354±552	8475±203	22658±190
CTL-T2D	52523±2321*	41169±589*	24888±197*	38649±299*
CTL-CuAqE	19268±596*#	20832±460#	8184±155#	21102±250#
T2D-CuAqE	24645±533*#&	26766±521*#&	11346±178*#&	27183±224#&
T2D-Met	20972±273#$	27201±378*#&	12975±143*#&$	24602±112#&$
T2D-GLI	20147±431#$	26610±295*#&	12609±215*#&$	23534±208#&$
T2D-SIT	19542±352#$	25809±303*#&$	11883±153*#&$	22799±139#&$
T2D-CuAqE-Met	19940±327#$	26301±273*#&a	11100±261*#&a	23522±100#&$a
T2D-CuAqE-GLI	19748±199#$	27501±264*#&b	11817±173*#&b	22616±164#&$b
T2D-CuAqE-SIT	18546±115*#$	25155±427*#&$	10734±450*#&$c	21891±169#&$c

.

Oral Glucose Tolerance Test (50mg, OGTT), Intraperitoneal Glucose Tolerance Test (50mg, ipGTT), Intraperitoneal Insulin Tolerance Test (0.75 IU/kg, IITT) and Intravenous Glucose Tolerance Test (50mg, IVGTT) in C57BL/6 male mice were treated with CuAqE and drugs against T1D. Values represent means ± SEM of each group (n=5). *Such as Area Under the Curve (AUC). Statistical analysis was performed using two-way ANOVA with Tukey multiple comparisons test for each intervention time. *p<0,05 vs CTL-NOM; # p<0,05 vs CTL-T2D; & p<0,05 vs CTL-CuAqE; $ p<0,05 vs T2D-CuAqE; a p<0,05 vs T2D-Met; b p<0,05 vs T2D-Gli and c p<0,05 vs T2D-Sit.

Glucose excursion/effective use was accompanied by a w2-fold increase in blood glucose concentration, peaking 15 min after glucose administration and returning to basal levels 120 min after in all groups, except for mice treated with CuAqE not having better efficiency than OAD´s mice ($p<0,05$).

In ipGTT, T1D model a less effective trend in glucose utilization is observed in all treatments compared to CTL-T1D ($p<0,05$), except with T1D-InsR andT1D-CuAqE-InsR, which shows a stable regulation during the test time with an additive effect between both drugs. There are differences in AUC of IITT between T1D-CuAqE mice and Ins/CuAqE or insulin alone (Table 1. $p<0,05$).

In IVGTT, through our finding, we observed that AUC in all treatments were significantly lower than those in T1D mice ($p<0,05$). There is difference in Ins/CuAqE or insulin alone with CuAqE treatments. These results together could indicate down-regulation of glucose homeostasis by CuAqE in this model (Table 1).

In ipGTT, T2D model increased BG was not significantly altered AUC by oral treatment with OAD´s with and without CuAqE, within 120 min after glucose loading. However, all treatments decrease AUC compared to CTL-T2D at 60 and 120 min. IITT was used to determine the degree of peripheral glucose utilization. CuAqE and OAD´s treatment improved insulin tolerance, as evidenced by lower plasma glucose levels and AUC when compared to T2D-CTL (Table 2. $p<0,05$).

IVGTT was performed to assess glucose tolerance. After receiving glucose in T2D-CuAqE mice reduced AUC ($p<0,05$), indicating that the test plant medicinal has the potential to improve glucose tolerance. Even when administered in conjunction with an OAD´s, it reduces AUC even more than when OAD´s are administered alone (Table 2).

In figure 9 depicts concentration of serum insulin in T1D mice. As expected, insulin levels in T1D mice were three-fold less than those of CTL-NOM ($p<0.001$).

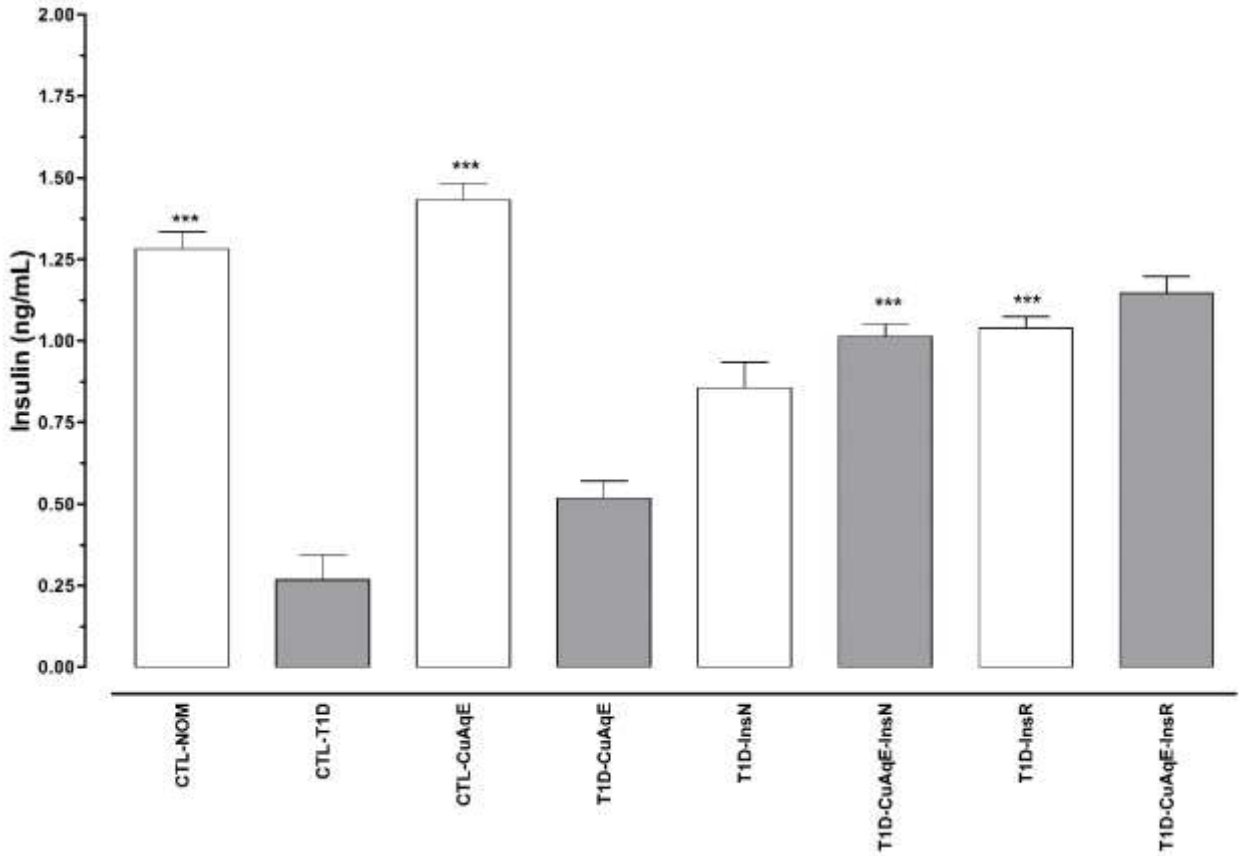

Figure 9. **Fasting serum insulin in T1D murine model with pharmacotherapeutic monitoring of CuAqE and therapeutic regimen against T1D for determining extract-drug interactions.** FSI (ng/dL) in C57BL/6 male mice that were treated with a therapeutic regimen against T1D and with CuAqE. Values represent means± SEM of each group. Statistical analysis was performed using two-way ANOVA with Bonferroni multiple comparisons test. ***p<0,001 vs CTL-T1D.

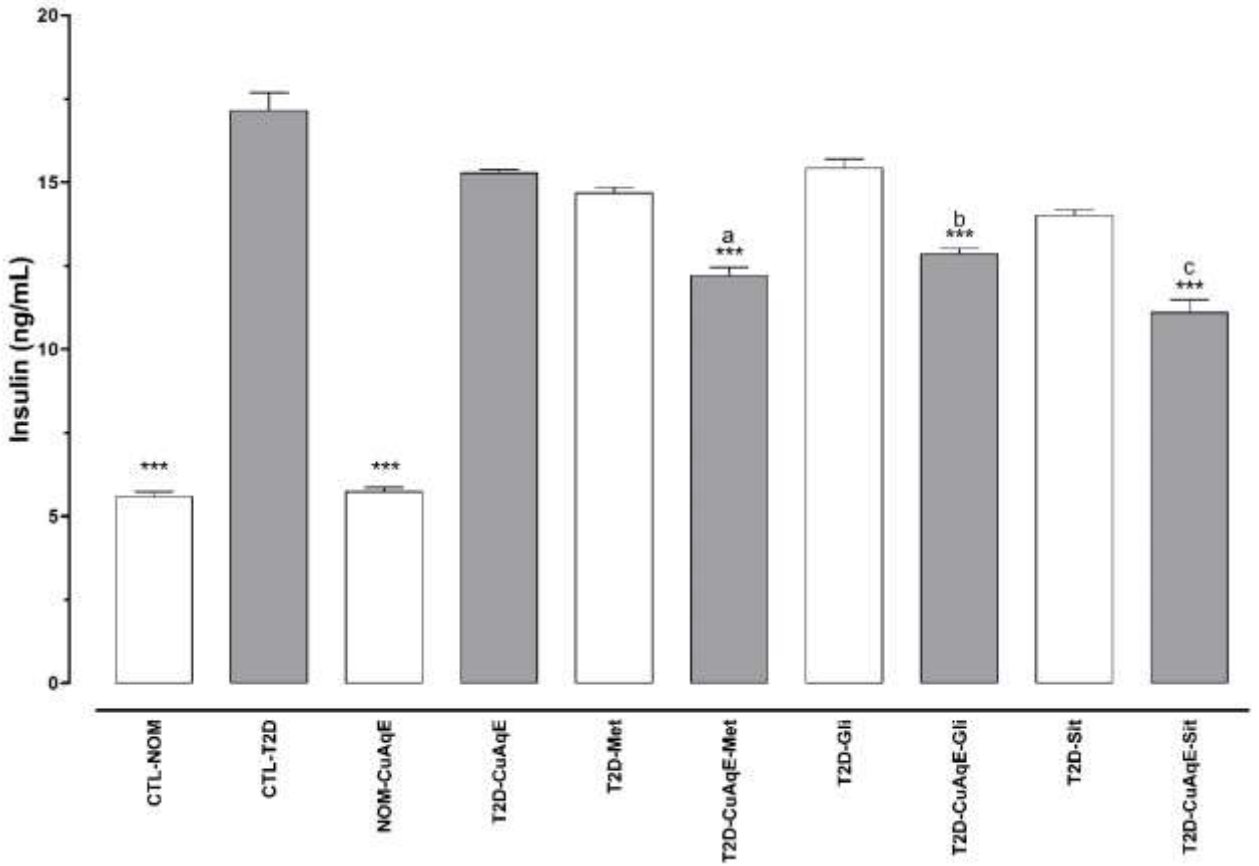

Figure 10. **Fasting serum insulin in T2D murine model with pharmacotherapeutic monitoring of CuAqE and therapeutic regimen against T2D for determining extract-drug interactions.** FSI (ng/dL) in C57BL/6 male mice that were treated with a therapeutic regimen against T2D and with CuAqE. Values represent means± SEM of each group. Statistical analysis was performed using two-way ANOVA with Bonferroni multiple comparisons test. ***p<0,001 vs CTL-T2D.

Insulin treated mice increased insulin levels compared to CTL-T1D and not by a regeneration effect but by the administration of exogenous insulin as a treatment. Furthermore, CuAqE increased too insulin levels in T1D-CuAqE mice significantly and also when administered concomitantly with insulin ($p<0,001$).

CTL-T2D mice have elevated insulin levels compared to CTL-NOM mice generating a state of hyperinsulinemia and consequently insulin resistance. In T2D-CuAqE mice, there was a decrease in insulin secretion, but it was not significant. However, in mice given CuAqE and OADs, the decrease in insulin concentration was considerable (Fig. 10, $p<0,001$).

Into the bargain GITT´s, other dynamic tests are used to estimate peripheral insulin resistance, fasting indexes are based on glucose and insulin values such as HOMA-IR, QUICKI, %S, HOMA-β and Index DI. In T2D model, HOMA-IR levels were reduced after treatment with OAD´s and with and without CuAqE, indicating a reduction in insulin resistance and improved glycemic management ($p<0,05$). Compared to T2D-CTL, mice receiving a CuAqE showed a remarkable improvement in metabolic indices similar to OAD´s (Table 3). The data generated for T1D model has no implication in insulin resistance and sensitivity (Table 3S).

3.4 Interaction of CuAqE in combination with OAD´s in T2D model mice

Dose-response curves in T2D murine model with pharmacotherapeutic monitoring were made for CuAqE and OAD´s and presented a dose-dependent effect. The efficacy of a drugs was indicated by the maximum of its dose-effect curve.

CuAqE dose to achieve a hypoglycemic effect in a single dose up to normoglycemic levels, was approximately 22 mg/kg. In the case of Metformin was necessary 28 mg/kg. For Sitagliptin and Glibenclamide were 0.86 and 0.071mg/kg respectively. Because of above CuAqE and OAD´S produce overtly similar effects were generally do so with different doses (Fig. 11).

Table 3. Insulin resistance and sensitivity in T2D murine model with pharmacotherapeutic monitoring of CuAqE and OAD´s for determining extract-drug interactions

T2D models	HOMA-IR	%S	HOMA-β	Index DI	QUICKI
CTL-NOM	0.99±0.03	100.94±2.92	50.80±1.59	51.26±1.52	0.335±0.001
CTL-T2D	6.24±0.39*	16.08±1.04*	123.89±3.72*	19.91±1.17*	0.264±0.002*
CTL-CuAqE	0.88±0.03$^{\#}$	113.91±3.27$^{\#}$	53.98±1.29$^{\#}$	61.47±1.66*$^{\#}$	0.341±0.001$^{\#}$
T2D-CuAqE	3.10±0.09*$^{\#\&}$	32.23±0.96*$^{\#\&}$	134.12±1.74*$^{\#\&}$	43.24±1.75*$^{\#\&}$	0.287±0.001*$^{\#\&}$
T2D-Met	2.55±0.07*$^{\#\&}$	39.25±1.05*$^{\#\&}$	134.10±2.68*$^{\#\&}$	52.65±2.42*$^{\#\&}$	0.295±0.001*$^{\#\&}$
T2D-Gli	2.55±0.04*$^{\#\&}$	39.21±0.59*$^{\#\&}$	142.46±3.44*$^{\#\&}$	55.86±1.67*$^{\#}$	0.295±0.001*$^{\#\&}$
T2D-Sit	2.21±0.15*$^{\#\&}$	45.49±3.25*$^{\#\&}$	130.92±3.02*$^{\#\&}$	59.61±5.48*$^{\#}$	0.300±0.003*$^{\#\&}$
T2D-CuAqE-Met	2.01±0.04$^{\#\&\$}$	49.79±1.06*$^{\#\&\$a}$	112.90±2.93*$^{\#\&\$a}$	56.21±1.72*$^{\#}$	0.304±0.001$^{\#\&\$}$
T2D-CuAqE-Gli	2.02±0.07$^{\#\&\$}$	49.59±1.64*$^{\#\&\$b}$	120.23±2.43*$^{\&\$b}$	59.65±2.87*$^{\#}$	0.304±0.001$^{\#\&\$}$
T2D-CuAqE-Sit	1.660.08$^{\#\&\$}$	60.35±3.04*$^{\#\&\$c}$	104.84±3.99*$^{\#\&\$c}$	63.21±2.57*$^{\#}$	0.312±0.002$^{\#\&\$}$

Homeostatic Model Assessment (HOMA-IR), Insulin sensitivity (%S), β-cell function (HOMA-β), Disposition index (DI) and Quantitative Insulin Sensitivity Check Index (QUICKI) in C57BL/6 male mice that were treated with a therapeutic regimen against T2D and with CuAqE. Values represent means ± SEM of each group (n=5). Statistical analysis was performed using two-way ANOVA with Dunn's Multiple Comparison Test. *p<0,05 vs CTL-NOM; # p<0,05 vs CTL-T2D; & p<0,05 vs CTL-CuAqE; $ p<0,05 vs T2D-CuAqE; ^{a} p<0,05 vs T2D-Met; ^{b} p<0,05 vs T2D-Gli and ^{c} p<0,05 vs T2D-Sit.

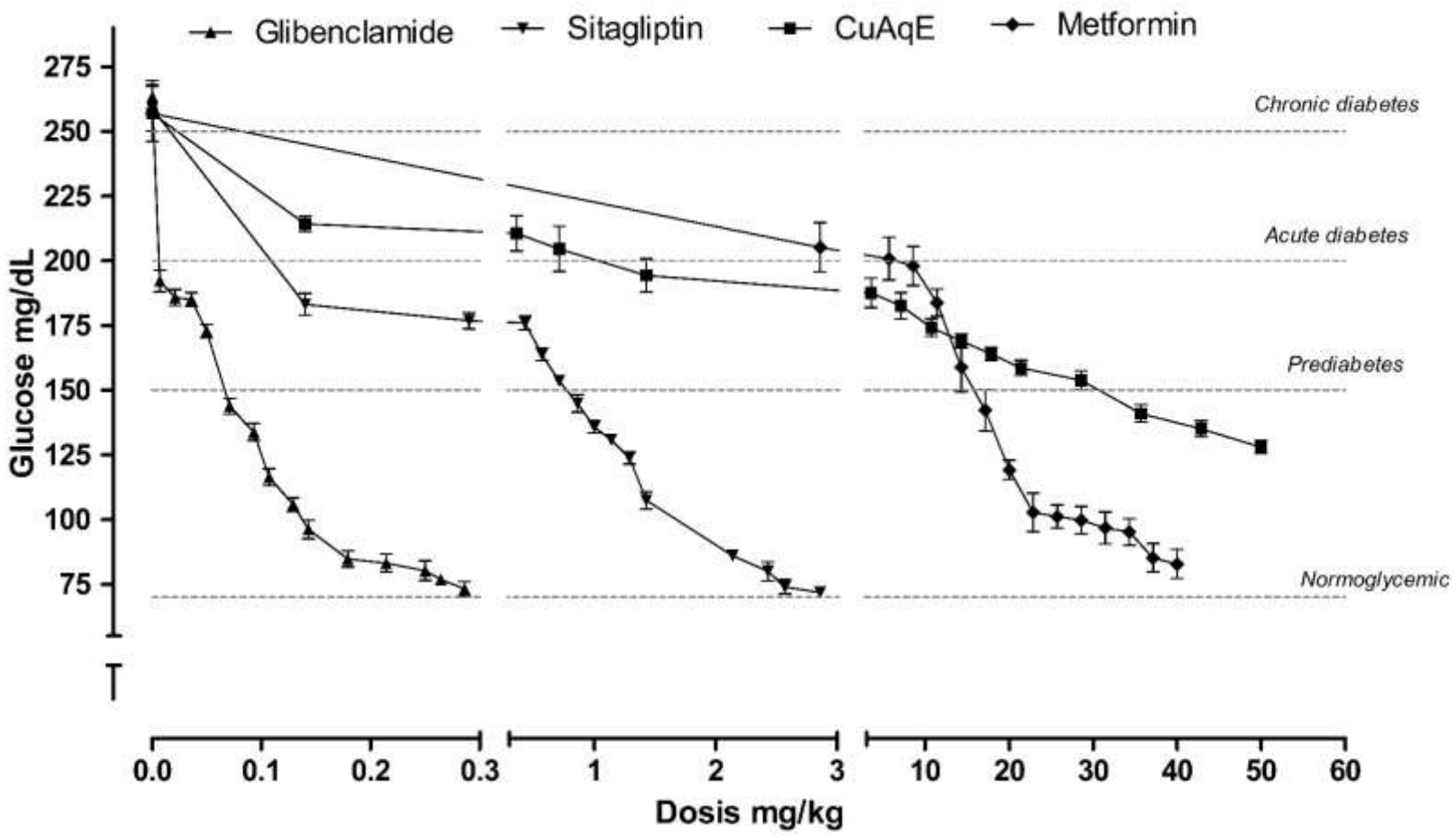

Figure 11. Comparation of dose-response curves in T2D murine model with pharmacotherapeutic monitoring. of CuAqE and OAD´s for determining extract-drug interactions. Blood glucose (mg/dL) in C57BL/6 male mice that were treated with oral hypoglycemic medications and with CuAqE

In dose-effect data that exhibit the hyperbolic shape (shown in Fig. 11) was taken on a different appearance if the effect is plotted against the logarithm of dose (shown in Figure 8S). The transformed plot is sigmoidal or S-shaped, yet it conveys the same kind of information. data points in the mid-range, this subset of points displays a nearly linear trend and whit this subset of points was used to get CuAqE or OAD´s D_{50} value.

In figure 12 shows D_{50} of CuAqE and OAD´s such as are indicators of drug potency therefore regarding to CuAqE relative potency was CuAqE (1) > Met (0.479) > Sit (0.027) > Gli (0.0022). Gli requires lower dose to achieve the half maximal effect is to be more potent than CuAqE.

For combination of CuAqE with each OAD´s, an isobologram was constructed with equieffective doses of the individual drugs when each is present alone. Z_{mix} of CuAqE with each OAD´s were calculated by the same method used to determine D_{50}. The generated additivity line represents all possible combinations that are equivalent in producing the effect (E_{50}).

To perform the isobolographic analysis of the interaction of CuAqE with each of the OADs, an additivity line was used and all the points on this line, which theoretically represent the pairs of additive doses (Z_{add}) of the drugs administered together that cause the same level of effect as the drugs alone.

When performing the combination experiment, the doses to cause the same effect (Z_{mix}) were lower than the theoretical additive doses (Z_{add}) so there is a superadditive or synergistic effect between both drugs with a statistically significant difference between them ($p<0.05$). All combinations were super-additive or synergistic (Figures 13-15).

D_{50} CuAqE	
Log D_{50}	1.51
D_{50}	32.618
Variance Log D_{50}	0.00012
σ Log D_{50}	0.0111
σ Log D_{50} (t)	0.0188
σ D_{50}	0.8364
D_{50}=32.618 ±0.8364 mg/kg	

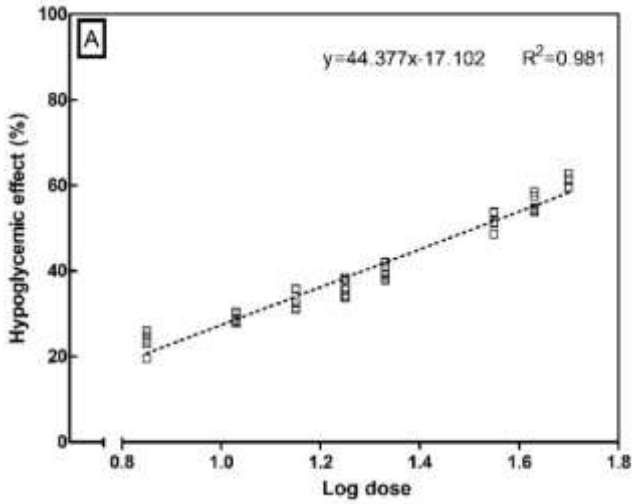

D_{50} Metformin	
Log D_{50}	1.19
D_{50}	15.640
Variance Log D_{50}	0.000057
σ Log D_{50}	0.0076
σ Log D_{50} (t)	0.0129
σ D_{50}	0.273
D_{50}=15.64 ±0.273 mg/kg	

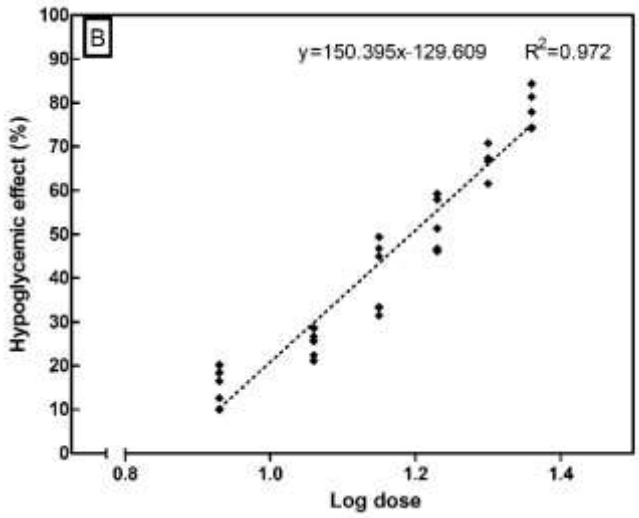

D_{50} Glibenclamide	
Log D_{50}	-1.12
D_{50}	0.075
Variance Log D_{50}	0.000024
σ Log D_{50}	0.0049
σ Log D_{50} (t)	0.0083
σ D_{50}	0.0009
D_{50}=0.075±0.0009 mg/kg	

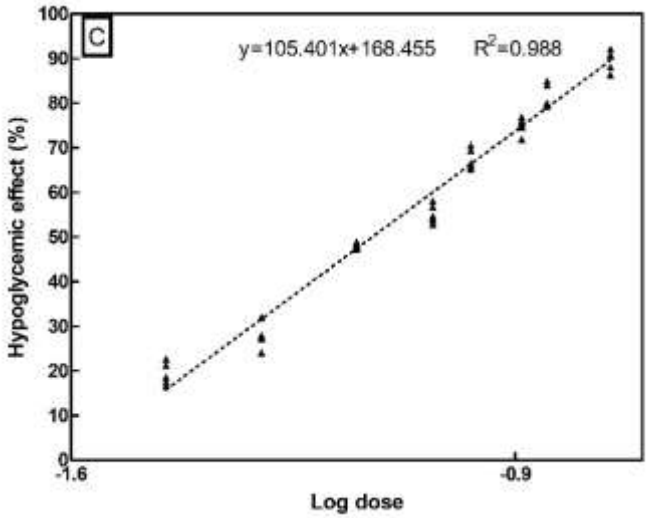

D_{50} Sitagliptin	
Log D_{50}	-0.051
D_{50}	0.889
Variance Log D_{50}	0.000027
σ Log D_{50}	0.0052
σ Log D_{50} (t)	0.0088
σ D_{50}	0.011
D_{50}=0.889±0.011 mg/kg	

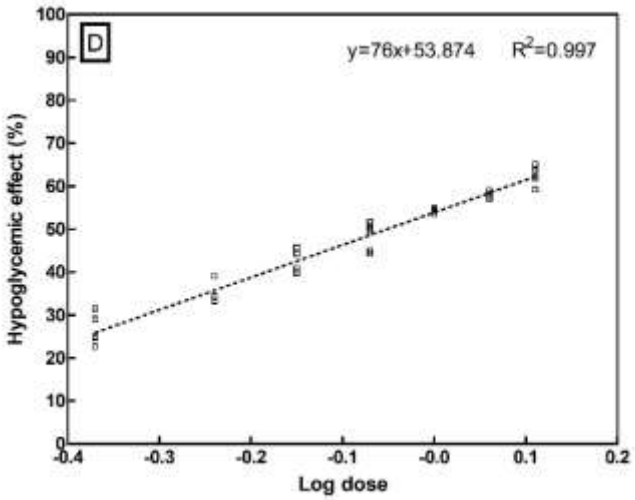

Figure 12. Dose-Response for drug alone

Hypoglycemic effect in C57BL/6 male mice that were treated with a therapeutic regimen against T2D or CuAqE. The drug was orally-administrated with intra-gastric probe (0.1 mL/10 g body weight).

(A) Determination D_{50} from of CuAqE

Slope=41.34 to 47.11; Y-intercept=-20.74 to -13.00; Goodness of Fit: coefficient of determination (r^2)=0.962. p< 0.0001, F=961.9; DFn=1.000 and DFd=38.00. n=40.

(B) Determination D_{50} of Metformin.

Slope= 134.5 to 166.3; Y-intercept= -148.4 to -110.9; Goodness of Fit: coefficient of determination (r^2)=0.9307. p< 0.0001, F=376.2; DFn=1.000 and DFd=28.00. n=30.

(C) Determination D_{50} of Glibenclamide.

Slope= 100.4 to 110.3; Y-intercept= 163.2 to 173.8; Goodness of Fit: coefficient of determination (r^2)=0.9798. p< 0.0001, F=1839; DFn=1.000 and DFd=38.00. n=40.

(D) Determination D_{50} of Sitagliptin.

Slope= 70.61 to 80.77; Y-intercept= 52.94 to 54.81; Goodness of Fit: coefficient of determination (r^2)=0.9654. p< 0.0001, F=920; DFn=1.000 and DFd=33.00. n=35.

Statistical analysis was performed using linear regression and one-way ANOVA by t-Test. p< 0.05.

Dose data of combination drug					
Metformin		**CuAqE**		**Combination**	
mg	mg/kg	mg	mg/kg	mg/kg	**CI***
547.41	7.82	1141.6	16.31	24.13	1
273.71	3.91	570.8	8.15	12.06	0.5
136.85	1.96	285.4	4.08	6.03	0.25
68.43	0.98	142.7	2.04	3.02	0.13
34.21	0.49	71.4	1.02	1.51	0.06
17.11	0.24	35.7	0.51	0.75	0.03
Z_{add}=24.13± 0.44 mg/kg					

D_{50} Mixture	
Log D_{50}	1.28
D_{50} (Z_{mix})	18.97
Variance Log D_{50}	0.0169
σ Log D_{50}	0.1299
σ Log D_{50} (t)	0.0088
σ D_{50}	0.2301
Z_{mix}=18.97±0.23 mg/kg	

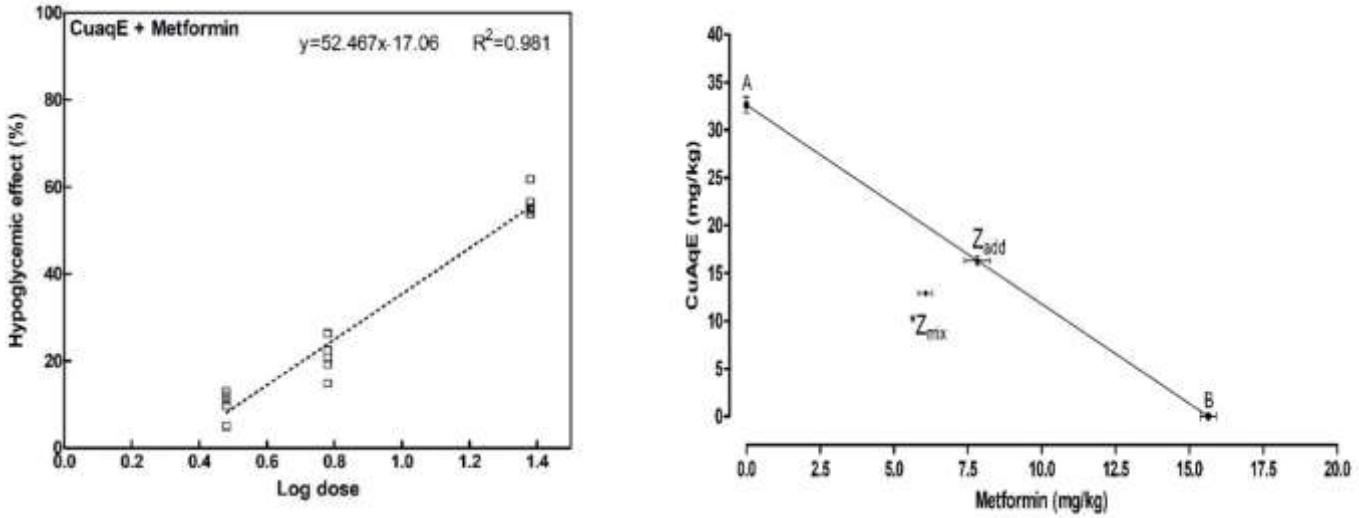

Figure 13. Combination drug analysis metformin with CuAqE. Hypoglycemic effect in mouse in C57BL/6 male mice that were treated with metformin and CuAqE. The mixture was orally-administrated with intra-gastric probe (0.1 mL/10 g body weight). **Table Left. Dose data of combination drug.** Combination dose is the sum of be individual doses. Proportion ρ_{met}=0.32 and ρ_{CuAqE}=0.68. *Combination index. Reducing total dose by half determined another dose and so on until achieving 6 doses by dilution. **Figure Left. Dose-Response for combination drugs.** Slope=46.25 to 58.69; Y-intercept=-23.01 to -11.12; Goodness of Fit: coefficient of determination (r^2) =0.962. p< 0.0001, F=331.9; DFn=1.000 and DFd=13.00. n=15. **Table right. D_{50} mixture.** Using linear regression. **Figure right. Line of additivity of the isobologram. Equieffective dose pairs or isoboles (A, 0), (0, B). A=D_{50} CuAqE and B D_{50} Metformin.** Statistical analysis was performed and one-way ANOVA by t-Test. p<0.05.

Dose data of combination drug					
Glibenclamide		**CuAqE**		**Combination**	
mg	mg/kg	mg	mg/kg	mg/kg	**CI***
2.63	0.038	1141.6	16.31	16.35	1
1.32	0.019	570.8	8.15	8.17	0.5
0.66	0.009	285.4	4.08	4.09	0.25
0.33	0.005	142.7	2.04	2.04	0.13
0.16	0.002	71.4	1.02	1.02	0.06
0.08	0.001	35.7	0.51	0.51	0.03
Z_{add}=16.35±0.42 mg/kg					

D_{50} Mixture	
Log D_{50}	1.15
D_{50} (Z_{mix})	14.25
Variance Log D_{50}	0.00053
σ Log D_{50}	0.23
σ Log D_{50} (t)	0.0394
σ D_{50}	0.7542
Z_{mix}=14.25±0.75mg/kg	

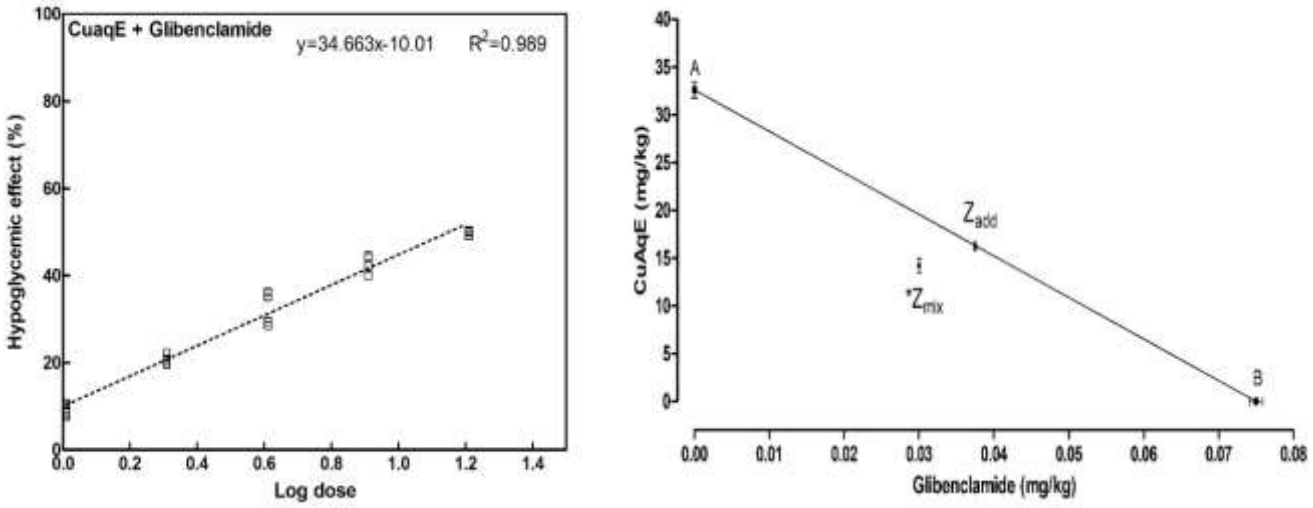

Figure 14. Combination drug analysis glibenclamide with CuAqE. Hypoglycemic effect in C57BL/6 male mice that were treated with glibenclamide and CuAqE. The mixture was orally-administrated with intra-gastric probe (0.1 mL/10 g body weight). **Table Left. Dose data of combination drug.** Combination dose is the sum of be individual doses. Proportion ρ_{Gli}=0.002 and ρ_{CuAqE}=0.998. *Combination index. Reducing total dose by half determined another dose and so on until achieving 6 doses by dilution. **Figure Left. Dose-Response for combination drugs.** Slope=32.38 to 37.19; Y-intercept=8.196 to 11.77; Goodness of Fit: coefficient of determination (r^2) =0.975. p< 0.0001, F=879.9; DFn=1.000 and DFd=23.00. n=25.

Table right. D_{50} mixture. Using linear regression. **Figure right. Line of additivity of the isobologram. Equieffective dose pairs or isoboles (A, 0), (0, B). A=D_{50} CuAqE and B D_{50} Glibenclamide.** Statistical analysis was performed and one-way ANOVA by t-Test. p<0.05.

Dose data of combination drug					
Sitagliptin		**CuAqE**		**Combination**	
mg	mg/kg	mg	mg/kg	mg/kg	**CI***
31.12	0.445	1141.6	16.31	16.75	1
15.56	0.222	570.8	8.15	8.38	0.5
7.78	0.111	285.4	4.08	4.19	0.25
3.89	0.056	142.7	2.04	2.09	0.13
1.94	0.028	71.4	1.02	1.05	0.06
0.97	0.014	35.7	0.51	0.52	0.03
Z_{add}=16.75±0.42 mg/kg					

D_{50} Mixture	
Log D_{50}	1.17
D_{50} (Z_{mix})	14.86
Variance Log D_{50}	0.00189
σ Log D_{50}	0.0435
σ Log D_{50} (t)	0.0740
σ D_{50}	1.488
Z_{mix}=14.86±1.49mg/kg	

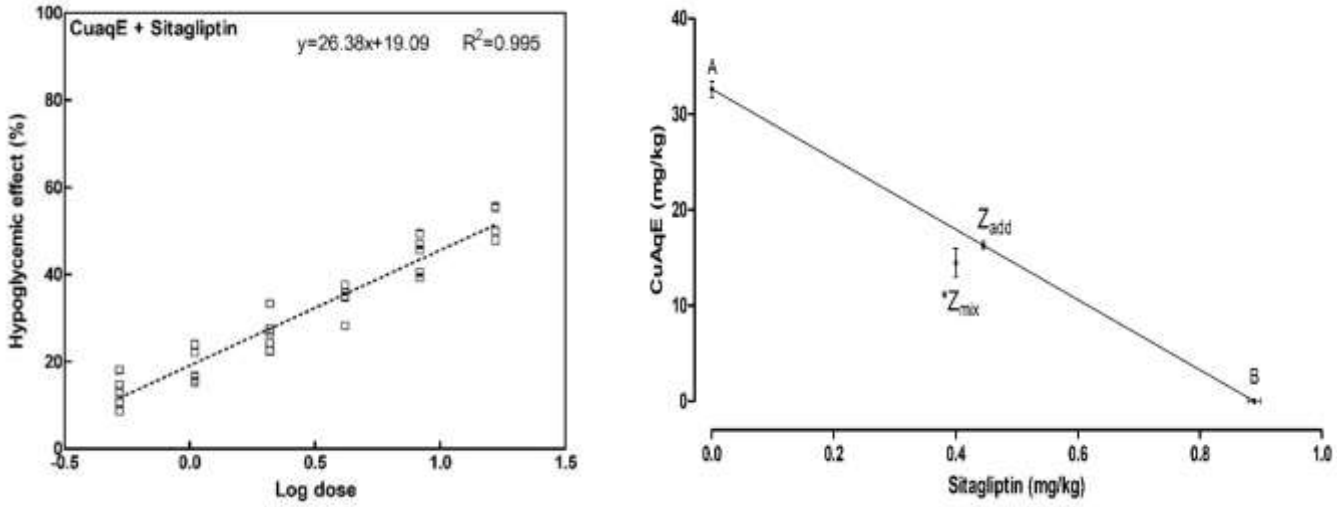

Figure 15. Combination drug analysis sitagliptin with CuAqE. Hypoglycemic effect in C57BL/6 male mice that were treated with sitagliptin and CuAqE. The mixture was orally-administrated with intra-gastric probe (0.1 mL/10 g body weight). **Table Left. Dose data of combination drug.** Combination dose is the sum of be individual doses. Proportion ρ_{Sit}=0.027 and ρ_{CuAqE}=0.973. *Combination index. Reducing total dose by half determined another dose and so on until achieving 6 doses by dilution. **Figure Left. Dose-Response for combination drugs.** Slope=23.75 to 29.18; Y-intercept=17.20 to 20.97; Goodness of Fit: coefficient of determination (r^2) =0.934. p< 0.0001, F=398.6; DFn=1.000 and DFd=28.00. n=30.

Table right. D_{50} mixture. Using linear regression. **Figure right. Line of additivity of the isobologram. Equieffective dose pairs or isoboles (A, 0), (0, B). A=D_{50} CuAqE and B D_{50} Glibenclamide.** Statistical analysis was performed and one-way ANOVA by t-Test. p<0.05.

4. Discussion

A wide range of animal models DM such as genetic, nutritional or experimental induction. Have been proven to be excellent tools to study the molecular mechanisms as well as its accompanying illnesses (Nagy & Einwallner, 2018). STZ-induced diabetes in rodents simulates the immunological and clinical signs of T1DM in humans, and is a suitable model for studying the molecular and immunological mechanisms when evaluating medicinal plants or new drugs (Li et. al., 2021).

Besides C57BL/6 mouse model used in the present study is considered to very closely mimic the progression of T2D when fed with HFD ad libitum, develop obesity, hyperglycemia, and hyperinsulinemia along with hypertension, however, they remain lean without metabolic abnormalities when fed normal chow diet ad libitum (Mahesh et.al., 2018).

Due to metabolic changes present in DM, treatment involves lifestyle changes, oral medications, and in some cases, injectable drugs. Despite these therapeutic alternatives, the WHO estimates that 80% of the world's population uses traditional medicine to treat diseases such as T2D, and in recent years, studies have increased on plants with potential antidiabetic activity, their main bioactive compounds, and their possible mechanisms of action involved (Rey et. al., 2024).

Such is the case of *Xiao Bopi* from traditional Chinese medicine (up to 1.5 g/kg) has been evaluated in a murine model of diabetic retinopathy and after 8 weeks of administration of the aqueous extract effectively increased glucose tolerance and insulin sensitivity, although CuAqE has the same hypoglycemic effect, but it was evaluated in different models of diabetes and its underlying mechanisms remain unclear (Ai, et. al., 2022).

The use of herbal drugs (alone or in combination with allopathic medications) to treat the symptoms of DM is common in Mexico. There are at least 800 Mexican plants used

for treating diabetes nowadays. Unfortunately, only a few of these species (40) have been analyzed to confirm their efficacy as antidiabetic agents like plants of family *Asteraceae* (Escandón et. al., 2020). People consider that herb preparations are less toxic, more efficacious and less expensive than allopathic products.

With same use as CuAqE in the treatment of DM we found *Calea ternifolia* (prodigiosa, zacachichi and amula) and its aqueous extract (up to 316 mg/kg) made from aerial parts of the plant. Which was effective in controlling fasting and postprandial blood glucose levels in mice with experimental T2D (STZ, 100 mg/kg and NAD, 40 mg/kg), but not in a DIO-HFD model.

We use this model to generate DM, so we cannot compare the results, but we can compare the effect and which is due to flavonoids, chromenes and sesquiterpene lactones with potent inhibitory activity against α-glucosidase (Escandón et. al., 2012 and 2017). Both plants represent good phytotherapeutic agents.

Overall, which demonstrated the ability of CuAqE to substantially reduce the blood glucose levels of diabetic mice. To determine the role of insulin secretion and insulin sensitivity, additional tests are required to assess each of these factors such as HOMA.

Since insulin resistance contributes greatly to the metabolic syndrome and is the major cause of type 2 diabetes mellitus, treatment with insulin sensitizers may ameliorate these pathophysiological abnormalities; CuAqE can be natural drug very helpful for this. Moreover, our findings are consistent with hypoglycemic evaluations of medicinal plants (Liu et. al., 2017; Alshabi et. al., 2022; Ghanbari et. al., 2022; Rey et. al. 2024; Reza et. al., 2024).

Glucose tolerance test is an important tool to diagnose with impaired glucose metabolism, a key characteristic of diabetes. However, GTT protocol in mice is not standardized and can vary widely between research teams, inasmuch as can intervene

several variables in mouse GTT protocol including time of glucose dosing, fasting duration, handling stress, anesthesia, and the timing of experimentation from the standpoint of assessing murine glucose metabolism (Small et. al., 2022).

Alternatively, fasting time may play a role whereby a decrease in glucose level can potentiate/drop AUC during an OGTT. Therefore, not recommend overnight fasting before a GTT but it is important to consider that even shorter fasts, such as the 6-h fast used in this study, can be ideal duration for discriminating differences in glucose tolerance between Chow- and HFD-fed mice (Small et. al., 2022).

The glucose tolerance test (GTT) is a cornerstone technique that assesses whole-body glucose homeostasis following the administration of a glucose load. It is not only used in clinical practice but is also widely used in animal-based biomedical and pharmaceutical research.

In this context, the GTT (oral, intraperitoneal, or intravenous) is frequently used in laboratory mice as an integrative readout of whole-body glucose handling and, when combined with blood insulin measurements, is thought to provide some additional readout of β-cell function and insulin action (Bruce et. al., 2021).

CuAqE regulated glucose and insulin metabolism in both models, even though results for OGTT, IVGTT, and IPGTT was different because the underlying physiological mechanisms are unique (Hahn et. al., 2024).

Considering DM is a multifactorial chronic disease, further research is needed to better understand the possible mechanism of the hypoglycemic action of this plant by exploring the effect of CuAqE on the hepatic glucose production, intestinal glucose absorption, and peripheral glucose uptake in the muscle and adipose tissues whit a bioactivity-guided approach to further investigate the hypoglycemic activity as like other anti-diabetic medicinal plants (Widyawati et al., 2022).

For the treatment DM is a need for new hypoglycemic agents which will have therapeutic efficacy as well as less side effects. There are shapeless to manage diabetes with medicinal plants which is having less side effects, better effectiveness, multiple target sites and are of relatively low cost (Prabhakar et. al., 2011).

Also, if the therapeutic doses of ODA´s could be reduced by replacing it with a phytochemicals or medicinal plants, the side effects caused by OAD´s such as diarrhea, lactic acidosis, hepatic failure, weight gain, tachycardia and hypothyroidism could be reduced to a large extent (Alam et. al., 2022).

For such therapeutic strategy one has to consider interaction between OAD and phytochemicals and on the metabolism as well as the bioavailability of the phytochemicals. In this study we focus on interactions of combination CuAqE with OAD´s, it would be necessary to delve deeper into the ADME processes.

Compared to the pharmacological effects observed with OAD´S, better results are obtained with OAD´S/CuAqE due to the presence of various bioactive compounds of plant that can work in synergy by targeting either the same or different pathways to reduce glucose that OAD´S.

The results of indicate that combination of CuAqE with OAD´s could provide an opportunity to reduce the dose of OAD´s, which may help in minimizing the adverse effects of these commercial drugs as well as achieve enhanced therapeutic effects. At the same time, proper precaution and care should be taken to avoid the severe hypoglycemia that may occur due to combination of CuAqE and OAD´s.

Finally, we provide guidelines for experimental design of DM in mice for evaluation medicinal plants such as CuAqE and can be tools to investigate influence pharmacological in glucose metabolism when medicinal plants and drugs are used. Even though outside of the scope of this research, many other downstream applications

can be performed as well as detailed analysis of metabolic markers for understand better disease pathogenesis and developing new therapies based on natural extracts.

CuAqE at the present study showed the ability to reduce BG to be within the hypoglycemic range in the model DM which validated its activity as a hypoglycemic drug. Besides it is necessary to investigate further possible antidiabetic mechanisms of action of CuAqE. For subsequent studies, it is recommended to design a formulation through which to administer CuAqE and carry out studies in humans.

Conclusions

Altogether results of this inquiry suggest that CuAqE is promising as a complementary or adjuvant treatment for DM, since they are not only limited to controlling FBG, PPBG and FSI in MLD-STZ and DIO-HFD in C57BL/6 male mice but also modifies the glucose metabolism observed in GTT´s, HOMA-IR and QUICKI. Likewise, it has a synergistic behavior with the OAD´s. It is uppermost to highlight that this would be the first time that CuAqE of has been determined to have a positive effect on several relevant outcomes in the control of DM.

References

1. Adams, J., Valery, P. C., Sibbritt, D., Bernardes, C. M., Broom, A., & Garvey, G. (2015). Use of Traditional Indigenous Medicine and Complementary Medicine Among Indigenous Cancer Patients in Queensland, Australia. Integrative cancer therapies, 14(4), 359–365. https://doi.org/10.1177/1534735415583555
2. Ai, X., Yu, P., Luo, L., Sun, J., Tao, H., Wang, X., & Meng, X. (2022). *Berberis dictyophylla F*. inhibits angiogenesis and apoptosis of diabetic retinopathy via suppressing HIF-1α/VEGF/DLL-4/Notch-1 pathway. Journal of ethnopharmacology, 296, 115453. https://doi.org/10.1016/j.jep.2022.115453
3. Alam, S., Sarker, M. M. R., Sultana, T. N., Chowdhury, M. N. R., Rashid, M. A., Chaity, N. I., Zhao, C., Xiao, J., Hafez, E. E., Khan, S. A., & Mohamed, I. N. (2022). Antidiabetic Phytochemicals From Medicinal Plants: Prospective Candidates for New Drug Discovery and Development. Frontiers in endocrinology, 13, 800714. https://doi.org/10.3389/fendo.2022.800714
4. Alshabi, A. M., & Shaikh, I. A. (2022). Antidiabetic and antioxidant potential of *Gardenia latifolia* in type-2 diabetic rats fed with high-fat diet plus low-dose streptozotocin. Saudi medical journal, 43(8), 881–890. https://doi.org/10.15537/smj.2022.43.8.20220258
5. Amein K. A., Hamdy M.M., Abd El-Emam R.A. & Osman F.H., (2015). Assessment of Genetic Damage in Diabetic Rats Treated with Insulin Glargine. Med. J. Cairo Univ., 83(1): 651-661.
6. Andrade, C., Gomes, N. G. M., Duangsrisai, S., Andrade, P. B., Pereira, D. M., & Valentão, P. (2020). Medicinal plants utilized in Thai Traditional Medicine for diabetes treatment: Ethnobotanical surveys, scientific evidence and phytochemicals. Journal of ethnopharmacology, 263, 113177. https://doi.org/10.1016/j.jep.2020.113177
7. Andrade-Cetto, A., & Heinrich, M. (2005). Mexican plants with hypoglycaemic effect used in the treatment of diabetes. Journal of ethnopharmacology, 99(3), 325–348. https://doi.org/10.1016/j.jep.2005.04.019

8. Andrade-Cetto, A., Becerra-Jiménez, J., Martínez-Zurita, E., Ortega-Larrocea, P., & Heinrich, M. (2006). Disease-Consensus Index as a tool of selecting potential hypoglycemic plants in Chikindzonot, Yucatán, México. Journal of ethnopharmacology, 107(2), 199–204. https://doi.org/10.1016/j.jep.2006.03.005
9. Andrade-Cetto, A., Espinoza-Hernández, F., & Mata-Torres, G. (2021). Hypoglycemic Effect of Calea urticifolia (Mill.) DC. Evidence-based complementary and alternative medicine: eCAM, 2021, 6625009. https://doi.org/10.1155/2021/6625009
10. Basto-Abreu, A., López-Olmedo, N., Rojas-Martínez, R., Aguilar-Salinas, C. A., Moreno-Banda, G. L., Carnalla, M., Rivera, J. A., Romero-Martinez, M., Barquera, S., & Barrientos-Gutiérrez, T. (2023). Prevalencia de prediabetes y diabetes en México: Ensanut 2022. Salud pública de México, 65, s163–s168. https://doi.org/10.21149/14832
11. Bhatt A. (2016). Phytopharmaceuticals: A new drug class regulated in India. Perspectives in clinical research, 7(2), 59–61. https://doi.org/10.4103/2229-3485.179435
12. Bruce, C. R., Hamley, S., Ang, T., Howlett, K. F., Shaw, C. S., & Kowalski, G. M. (2021). Translating glucose tolerance data from mice to humans: Insights from stable isotope labelled glucose tolerance tests. Molecular metabolism, 53, 101281. https://doi.org/10.1016/j.molmet.2021.101281
13. Che, C.T., George, V., Ijinu, T.P., Pushpangadan, P., Andrae-Marobela, K. (2017). Traditional medicine. Pharmacognosy. Academic Press, 15–30. https://doi.org/10.1016/B978-0-12-802104-0.00002-0
14. Choopani, R., Sadr, S., Kaveh, S., Kaveh, N., & Dehghan, S. (2015). Pharmacological treatment of catarrh in Iranian traditional medicine. Journal of traditional and complementary medicine, 5(2), 71–74. https://doi.org/10.1016/j.jtcme.2014.08.001
15. Dandekar P., Ramkumar S., RaviKumar A. (2021). Chapter 12—Structure–Activity Relationships of Pancreatic α-Amylase and α-Glucosidase as Antidiabetic Targets. In: Atta-ur-Rahman, editor. Studies in Natural Products

Chemistry. Elsevier; Amsterdam, The Netherlands. pp. 381–410. https://doi.org/10.1016/B978-0-12-819489-8.00014-4

16. Deeds, M. C., Anderson, J. M., Armstrong, A. S., Gastineau, D. A., Hiddinga, H. J., Jahangir, A., Eberhardt, N. L., & Kudva, Y. C. (2011). Single dose streptozotocin-induced diabetes: considerations for study design in islet transplantation models. Laboratory animals, 45(3), 131–140. https://doi.org/10.1258/la.2010.010090
17. Elkomy, N. M. I. M., El-Shaibany, A., Elnagar, G. M., Abdelkhalek, A. S., Al-Mahbashi, H., Elaasser, M. M., Raweh, S. M., Aldiyarbi, M. A., & Raslan, A. E. (2023). Evaluation of acute oral toxicity, anti-diabetic and antioxidant effects of *Aloe vera* flowers extract. Journal of ethnopharmacology, 309, 116310. https://doi.org/10.1016/j.jep.2023.116310
18. ElSayed, N. A., Aleppo, G., Aroda, V. R., Bannuru, R. R., Brown, F. M., Bruemmer, D., Collins, B. S., Hilliard, M. E., Isaacs, D., Johnson, E. L., Kahan, S., Khunti, K., Leon, J., Lyons, S. K., Perry, M. L., Prahalad, P., Pratley, R. E., Seley, J. J., Stanton, R. C., Gabbay, R. A., … on behalf of the American Diabetes Association (2023). 2. Classification and Diagnosis of Diabetes: Standards of Care in Diabetes-2023. Diabetes care, 46(Suppl 1), S19–S40. https://doi.org/10.2337/dc23-S002
19. Escandón-Rivera, S. M., Mata, R., & Andrade-Cetto, A. (2020). Molecules Isolated from Mexican Hypoglycemic Plants: A Review. Molecules (Basel, Switzerland), 25(18), 4145. https://doi.org/10.3390/molecules25184145
20. Escandón-Rivera, S., González-Andrade, M., Bye, R., Linares, E., Navarrete, A., & Mata, R. (2012). α-glucosidase inhibitors from Brickellia cavanillesii. Journal of natural products, 75(5), 968–974. https://doi.org/10.1021/np300204p
21. Escandón-Rivera, S., González-Andrade, M., Bye, R., Linares, E., Navarrete, A., & Mata, R. (2017). Correction to α-Glucosidase Inhibitors from *Brickellia cavanillesii*. Journal of natural products, 80(1), 233. https://doi.org/10.1021/acs.jnatprod.6b01120

22. Espinoza-Hernández, F. A., & Andrade-Cetto, A. (2022). Chronic Antihyperglycemic Effect Exerted by Traditional Extracts of Three Mexican Medicinal Plants. Evidence-based complementary and alternative medicine: eCAM, 2022, 5970358. https://doi.org/10.1155/2022/5970358
23. Gastaldelli A. (2022). Measuring and estimating insulin resistance in clinical and research settings. Obesity (Silver Spring, Md.), 30(8), 1549–1563. https://doi.org/10.1002/oby.23503
24. Ghanbari, M., Lamuki, M. S., Habibi, E., & Sadeghimahalli, F. (2022). Artemisia annua L. Extracts Improved Insulin Resistance via Changing Adiponectin, Leptin and Resistin Production in HFD/STZ Diabetic Mice. Journal of pharmacopuncture, 25(2), 130–137. https://doi.org/10.3831/KPI.2022.25.2.130
25. Gogineni, V., Nael, M. A., León, F., Núñez, M. J., & Cutler, S. J. (2019). Computationally aided stereochemical assignment of undescribed bisabolenes from Calea urticifolia. Phytochemistry, 157, 145–150. https://doi.org/10.1016/j.phytochem.2018.10.022
26. Guzmán G., P.; García Ch., E.; Juárez, B.I. and Fortanelli, M.J. (2010). Exploración, aprovechamiento y validación experimental de plantas con efecto anti-inflamatorio de la Sierra Madre Oriental de San Luis Potosí. Tesis de maestría. Programa Multidisciplinario de Posgrado en Ciencias Ambientales, UASLP. San Luis Potosí, SLP, México. 79p. https://repositorioinstitucional.uaslp.mx/xmlui/handle/i/3593
27. Hahn, M. K., Giacca, A., & Pereira, S. (2024). In vivo techniques for assessment of insulin sensitivity and glucose metabolism. The Journal of endocrinology, 260(3), e230308. https://doi.org/10.1530/JOE-23-0308
28. Harreiter, J., & Roden, M. (2023). Diabetes mellitus – Definition, Klassifikation, Diagnose, Screening und Prävention (Update 2023) [Diabetes mellitus: definition, classification, diagnosis, screening and prevention (Update 2023)]. Wiener klinische Wochenschrift, 135(Suppl 1), 7–17. https://doi.org/10.1007/s00508-022-02122-y

29. Hull, R. L., Hackney, D. J., Giering, E. L., & Zraika, S. (2020). Acclimation Prior to an Intraperitoneal Insulin Tolerance Test to Mitigate Stress-Induced Hyperglycemia in Conscious Mice. Journal of visualized experiments: JoVE, (159), 10.3791/61179. https://doi.org/10.3791/61179
30. Kowalski, G. M., Kraakman, M. J., Mason, S. A., Murphy, A. J., & Bruce, C. R. (2017). Resolution of glucose intolerance in long-term high-fat, high-sucrose-fed mice. The Journal of endocrinology, 233(3), 269–279. https://doi.org/10.1530/JOE-17-0004
31. Li, P., Chen, Y., Luo, L., Yang, H., & Pan, Y. (2021). Immunoregulatory Effect of *Acanthopanax trifoliatus (L.) Merr.* Polysaccharide on T1DM Mice. Drug design, development and therapy, 15, 2629–2639. https://doi.org/10.2147/DDDT.S309851
32. Liu, L., Tang, D., Zhao, H., Xin, X., & Aisa, H. A. (2017). Hypoglycemic effect of the polyphenols rich extract from *Rose rugosa Thunb* on high fat diet and STZ induced diabetic rats. Journal of ethnopharmacology, 200, 174–181. https://doi.org/10.1016/j.jep.2017.02.022
33. Mahesh Kumar, P., Venkataranganna, M. V., Manjunath, K., Viswanatha, G. L., & Ashok, G. (2018). *Momordica cymbalaria* fruit extract attenuates high-fat diet-induced obesity and diabetes in C57BL/6 mice. Iranian journal of basic medical sciences, 21(10), 1083–1090. https://doi.org/10.22038/IJBMS.2018.29354.7095
34. Medina-Gómez, O. S., & Peña, J. E. (2023). Inequalities in diabetes mortality in Mexico: 2010-2019. Desigualdades en la mortalidad por diabetes en México: 2010-2019. Gaceta medica de Mexico, 159(2), 110–115. https://doi.org/10.24875/GMM.22000298
35. Nagy, C., & Einwallner, E. (2018). Study of In Vivo Glucose Metabolism in High-fat Diet-fed Mice Using Oral Glucose Tolerance Test (OGTT) and Insulin Tolerance Test (ITT). Journal of visualized experiments: JoVE, (131), 56672. https://doi.org/10.3791/56672

36. Petrie, J. R., Guzik, T. J., & Touyz, R. M. (2018). Diabetes, Hypertension, and Cardiovascular Disease: Clinical Insights and Vascular Mechanisms. The Canadian journal of cardiology, 34(5), 575–584. https://doi.org/10.1016/j.cjca.2017.12.005
37. Prabhakar, P. K., & Doble, M. (2011). Interaction of phytochemicals with hypoglycemic drugs on glucose uptake in L6 myotubes. Phytomedicine: international journal of phytotherapy and phytopharmacology, 18(4), 285–291. https://doi.org/10.1016/j.phymed.2010.06.016
38. Rey, D. P., Echeverry, S. M., Valderrama, I. H., Rodriguez, I. A., Ospina, L. F., Mena Barreto Silva, F. R., & Aragón, M. (2024). Antidiabetic Effect of *Passiflora ligularis* Leaves in High Fat-Diet/Streptozotocin-Induced Diabetic Mice. Nutrients, 16(11), 1669. https://doi.org/10.3390/nu16111669
39. Rey, D. P., Echeverry, S. M., Valderrama, I. H., Rodriguez, I. A., Ospina, L. F., Mena Barreto Silva, F. R., & Aragón, M. (2024). Antidiabetic Effect of Passiflora ligularis Leaves in High Fat-Diet/Streptozotocin-Induced Diabetic Mice. Nutrients, 16(11), 1669. https://doi.org/10.3390/nu16111669
40. Reza Seyedi Moqadam, S. M., Lamuki, M. S., Sadeghimahalli, F., & Ghanbari, M. (2024). The effect of *Artemisia annua L.* aqueous and methanolic extracts on insulin signaling in liver of HFD/STZ diabetic mice. Journal of complementary & integrative medicine, 21(2), 215–221. https://doi.org/10.1515/jcim-2024-0011
41. Schwartz, J. I., Ramaiya, K., Warren, M., Yadav, P., Castillo, G., George, R., & McGuire, H. (2023). Carpe DM: The First Global Diabetes Targets. Global health, science and practice, 11(2), e2200403. https://doi.org/10.9745/GHSP-D-22-00403
42. Small, L., Ehrlich, A., Iversen, J., Ashcroft, S. P., Trošt, K., Moritz, T., Hartmann, B., Holst, J. J., Treebak, J. T., Zierath, J. R., & Barrès, R. (2022). Comparative analysis of oral and intraperitoneal glucose tolerance tests in mice. Molecular metabolism, 57, 101440. https://doi.org/10.1016/j.molmet.2022.101440
43. Stammberger, I., Bube, A., Durchfeld-Meyer, B., Donaubauer, H., & Troschau, G. (2002). Evaluation of the carcinogenic potential of insulin glargine (LANTUS)

in rats and mice. International journal of toxicology, 21(3), 171–179. https://doi.org/10.1080/10915810290096306

44. Stancic, A., Saksida, T., Markelic, M., Vucetic, M., Grigorov, I., Martinovic, V., Gajic, D., Ivanovic, A., Velickovic, K., Savic, N., & Otasevic, V. (2022). Ferroptosis as a Novel Determinant of β-Cell Death in Diabetic Conditions. Oxidative medicine and cellular longevity, 2022, 3873420. https://doi.org/10.1155/2022/3873420
45. Sun, H., Saeedi, P., Karuranga, S., Pinkepank, M., Ogurtsova, K., Duncan, B. B., Stein, C., Basit, A., Chan, J. C. N., Mbanya, J. C., Pavkov, M. E., Ramachandaran, A., Wild, S. H., James, S., Herman, W. H., Zhang, P., Bommer, C., Kuo, S., Boyko, E. J., & Magliano, D. J. (2022). IDF Diabetes Atlas: Global, regional and country-level diabetes prevalence estimates for 2021 and projections for 2045. Diabetes research and clinical practice, 183, 109119. https://doi.org/10.1016/j.diabres.2021.109119
46. Tallarida R. J. (2006). An overview of drug combination analysis with isobolograms. The Journal of pharmacology and experimental therapeutics, 319(1), 1–7. https://doi.org/10.1124/jpet.106.104117
47. Tallarida R. J. (2012). Revisiting the isobole and related quantitative methods for assessing drug synergism. The Journal of pharmacology and experimental therapeutics, 342(1), 2–8. https://doi.org/10.1124/jpet.112.193474
48. Tallarida R. J. (2016). Drug Combinations: Tests and Analysis with Isoboles. Current protocols in pharmacology, 72, 9.19.1–9.19.19. https://doi.org/10.1002/0471141755.ph0919s72
49. Tallarida, R. J., Stone, D. J., Jr, & Raffa, R. B. (1997). Efficient designs for studying synergistic drug combinations. Life sciences, 61(26). https://doi.org/10.1016/s0024-3205(97)01030-8
50. Tallarida, R.J. (2000). Drug Synergism and Dose-Effect Data Analysis, pp 65–66, Chapman & Hall/CRC, Inc., Boca Raton, FL. https://doi.org/10.1201/9781420036107

51. Tallarida, R.J. (2010). Combination Analysis. In: Raffa, R.B., Tallarida, R.J. (eds) Chemo Fog. Advances in Experimental Medicine and Biology, vol 678. Springer, New York, NY. https://doi.org/10.1007/978-1-4419-6306-2_17
52. Torres-Rodríguez, M. L., García-Chávez, E., Berhow, M., & de Mejia, E. G. (2016). Anti-inflammatory and anti-oxidant effect of *Calea urticifolia* lyophilized aqueous extract on lipopolysaccharide-stimulated RAW 264.7 macrophages. Journal of ethnopharmacology, 188, 266–274. https://doi.org/10.1016/j.jep.2016.04.057
53. Widjajakusuma, E. C., Jonosewojo, A., Hendriati, L., Wijaya, S., Ferawati, Surjadhana, A., Sastrowardoyo, W., Monita, N., Muna, N. M., Fajarwati, R. P., Ervina, M., Esar, S. Y., Soegianto, L., Lang, T., & Heriyanti, C. (2019). Phytochemical screening and preliminary clinical trials of the aqueous extract mixture of *Andrographis paniculata (Burm. f.) Wall. ex Nees and Syzygium polyanthum (Wight.) Walp* leaves in metformin treated patients with type 2 diabetes. Phytomedicine: international journal of phytotherapy and phytopharmacology, 55, 137–147. https://doi.org/10.1016/j.phymed.2018.07.002
54. Widyawati, T., Yusoff, N. A., Bello, I., Asmawi, M. Z., & Ahmad, M. (2022). Bioactivity-Guided Fractionation and Identification of Antidiabetic Compound of *Syzygium polyanthum (Wight.)'s Leaf* Extract in Streptozotocin-Induced Diabetic Rat Model. Molecules (Basel, Switzerland), 27(20), 6814. https://doi.org/10.3390/molecules27206814
55. World Health Organization. (2013). WHO Traditional Medicine Strategy 2014-2023. Geneva, Switzerland. Available in: https://www.who.int/publications/i/item/9789241506096
56. World Health Organization. (2019). WHO Global Report on Traditional and Complementary Medicine 2019. Geneva, Switzerland. Available in: https://www.who.int/publications/i/item/978924151536
57. World Health Organization. Implementation roadmap 2023–2030 for the Global action plan for the prevention and control of NCDs 2013–2030. (2021). 1-18.

Available in: https://www.who.int/teams/noncommunicable-diseases/governance/roadmap

58. Yedjou, C. G., Grigsby, J., Mbemi, A., Nelson, D., Mildort, B., Latinwo, L., & Tchounwou, P. B. (2023). The Management of Diabetes Mellitus Using Medicinal Plants and Vitamins. International journal of molecular sciences, 24(10), 9085. https://doi.org/10.3390/ijms24109085
59. Yuan, S., Merino, J., & Larsson, S. C. (2023). Causal factors underlying diabetes risk informed by Mendelian randomisation analysis: evidence, opportunities and challenges. Diabetologia, 66(5), 800–812. https://doi.org/10.1007/s00125-023-05879-7
60. Zhao, L., Au, J. L., & Wientjes, M. G. (2010). Comparison of methods for evaluating drug-drug interaction. Frontiers in bioscience (Elite edition), 2(1), 241–249. https://doi.org/10.2741/e86
61. Zhao, Z., Egashira, Y., & Sanada, H. (2005). Phenolic antioxidants richly contained in corn bran are slightly bioavailable in rats. Journal of agricultural and food chemistry, 53(12), 5030–5035. https://doi.org/10.1021/jf050111n

Supplementary material

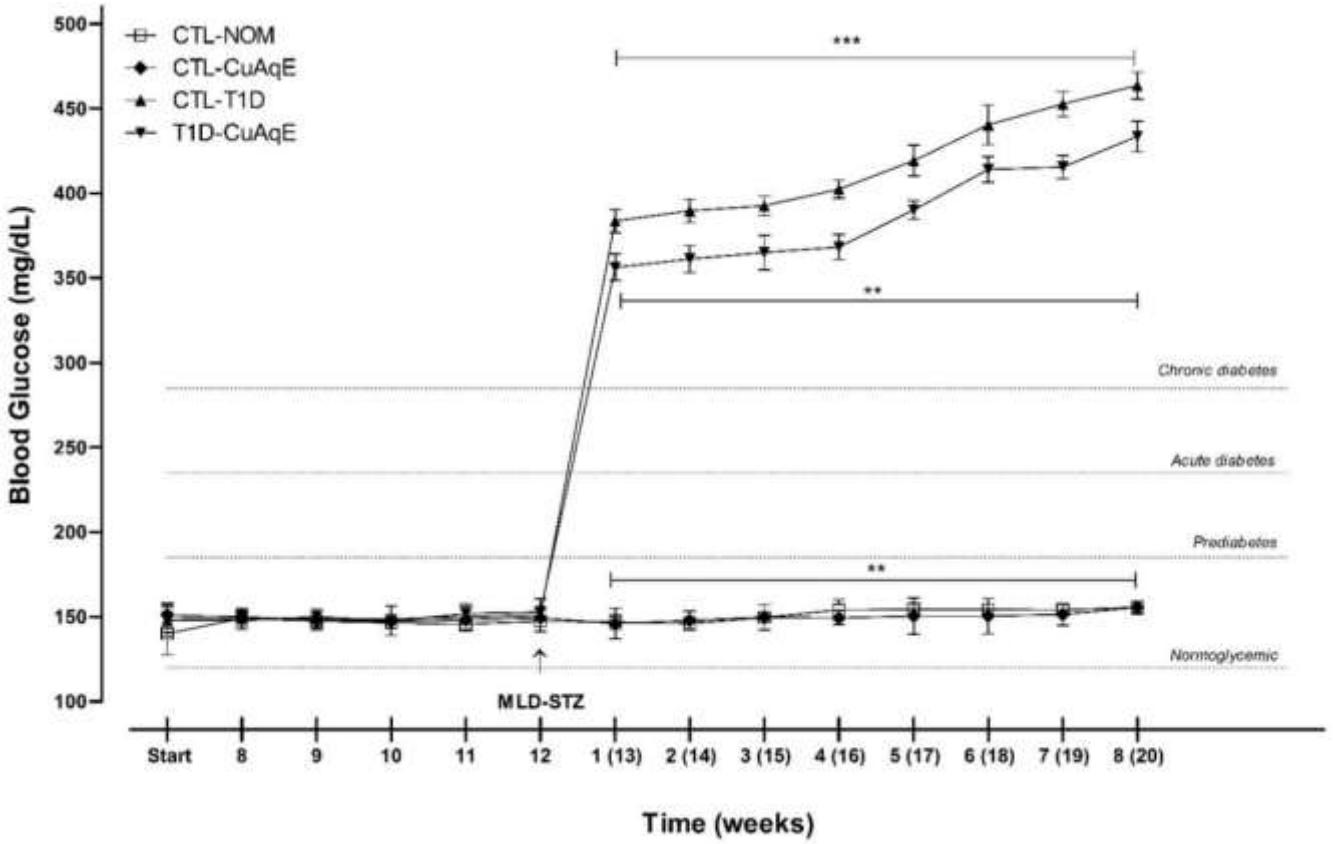

Figure 1S. **Phytopharmacological evaluation of postprandial hypoglycaemic activity in T1D murine model with pharmacotherapeutic monitoring of CuAqE as treatment against T1D.** PPBG (mg/dL) in T1D C57BL/6 male mice ***p<0,001 vs CTL-NOM and ** p<0,001 vs CTL-T1D. Values represent means ± SEM of each group. Statistical analysis was performed using two-way ANOVA with Bonferroni multiple comparisons test.

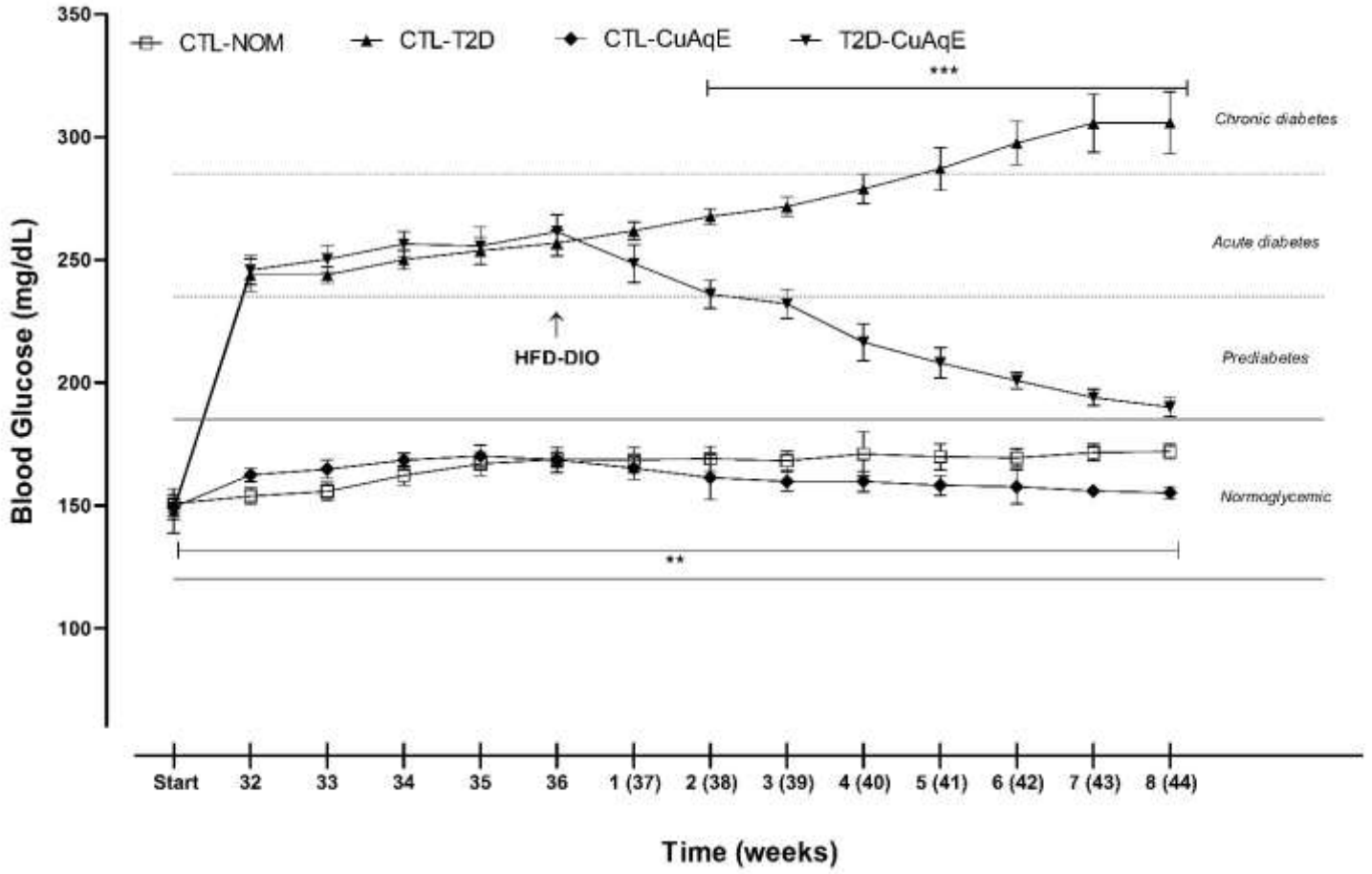

Figure 2S. **Phytopharmacological evaluation of postprandial hypoglycaemic activity in T2D murine model with pharmacotherapeutic monitoring of CuAqE as treatment against T2D.** PPBG (mg/dL) in T2D C57BL/6 male mice ***p<0,001 vs CTL-NOM and **p<0,001 vs CTL-T2D. Values represent means ± SEM of each group. Statistical analysis was performed using two-way ANOVA with Bonferroni multiple comparisons tes

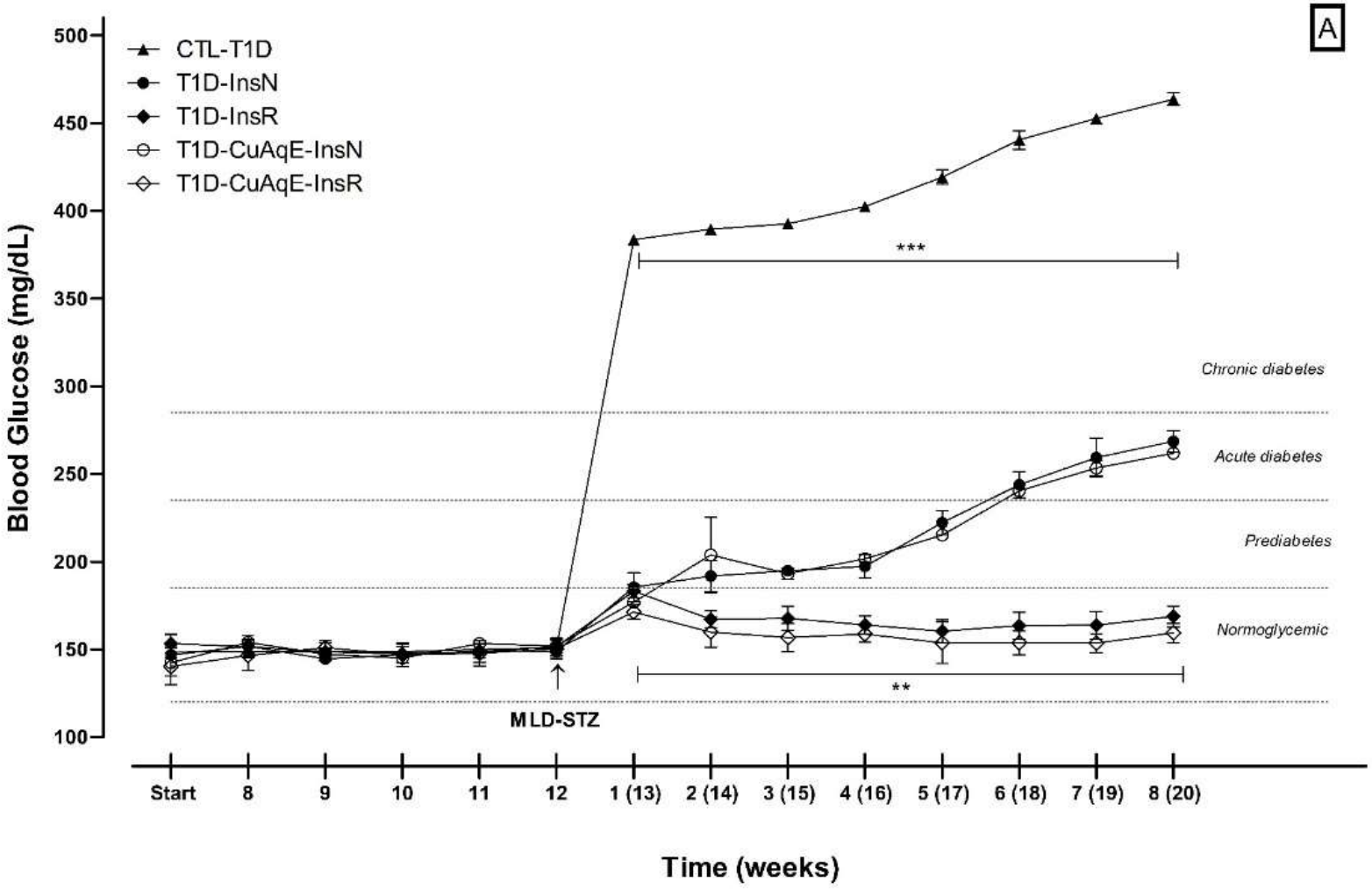
A
CTL-T1D
T1D-InsN
T1D-InsR
T1D-CuAqE-InsN
T1D-CuAqE-InsR
Blood Glucose (mg/dL)
500
450
400
350
300
250
200
150
100
***
**
Chronic diabetes
Acute diabetes
Prediabetes
Normoglycemic
MLD-STZ
Start
8
9
10
11
12
1 (13)
2 (14)
3 (15)
4 (16)
5 (17)
6 (18)
7 (19)
8 (20)
Time (weeks)

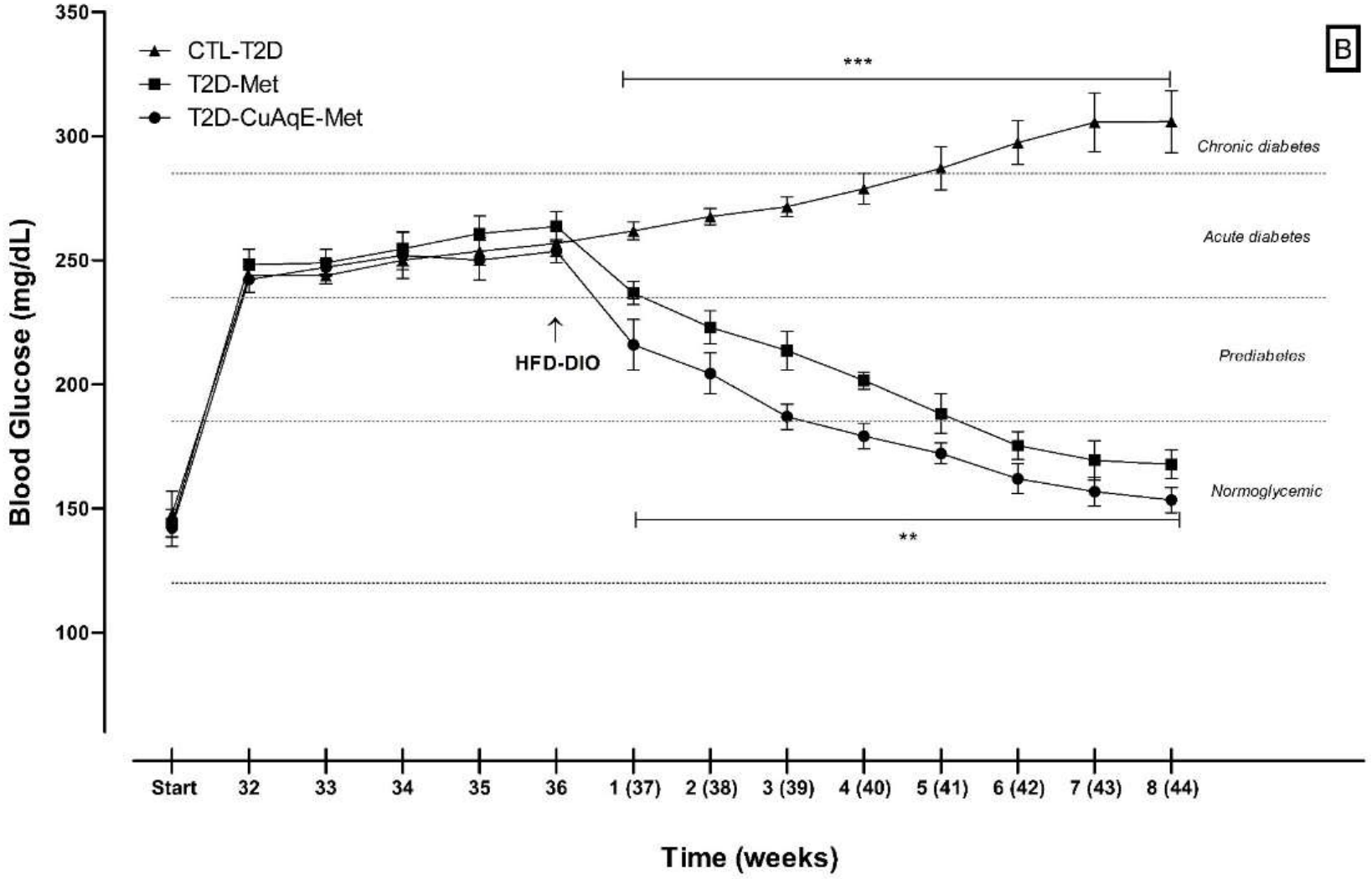
B
CTL-T2D
T2D-Met
T2D-CuAqE-Met
***
**
HFD-DIO
Chronic diabetes
Acute diabetes
Prediabetes
Normoglycemic
Blood Glucose (mg/dL)
350
300
250
200
150
100
Start
32
33
34
35
36
1 (37)
2 (38)
3 (39)
4 (40)
5 (41)
6 (42)
7 (43)
8 (44)
Time (weeks)

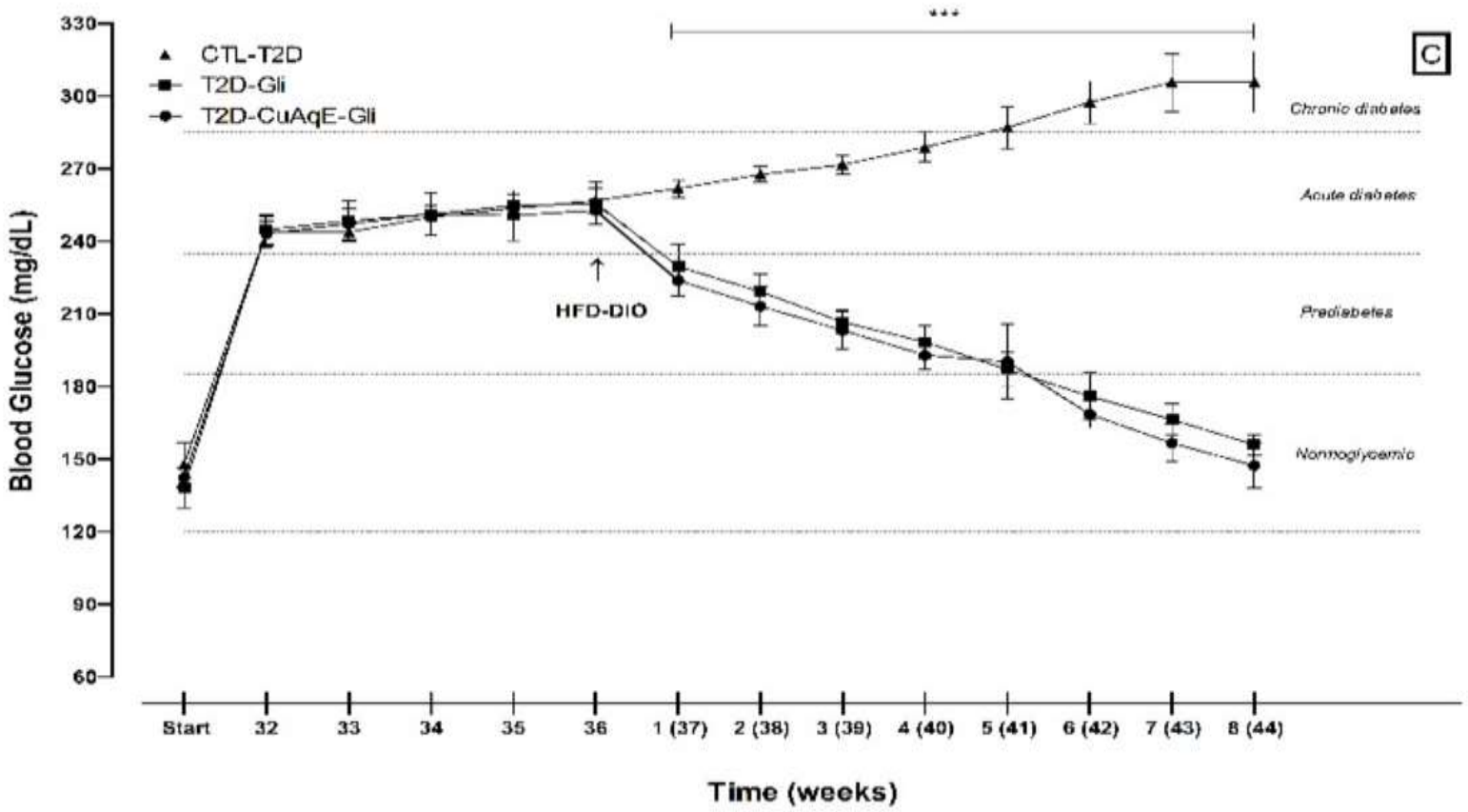
***
C
CTL-T2D
T2D-Gli
T2D-CuAqE-Gli
Chronic diabetes
Acute diabetes
Prediabetes
Normoglycemic
HFD-DIO
Blood Glucose (mg/dL)
330
300
270
240
210
180
150
120
90
60
Start
32
33
34
35
36
1 (37)
2 (38)
3 (39)
4 (40)
5 (41)
6 (42)
7 (43)
8 (44)
Time (weeks)

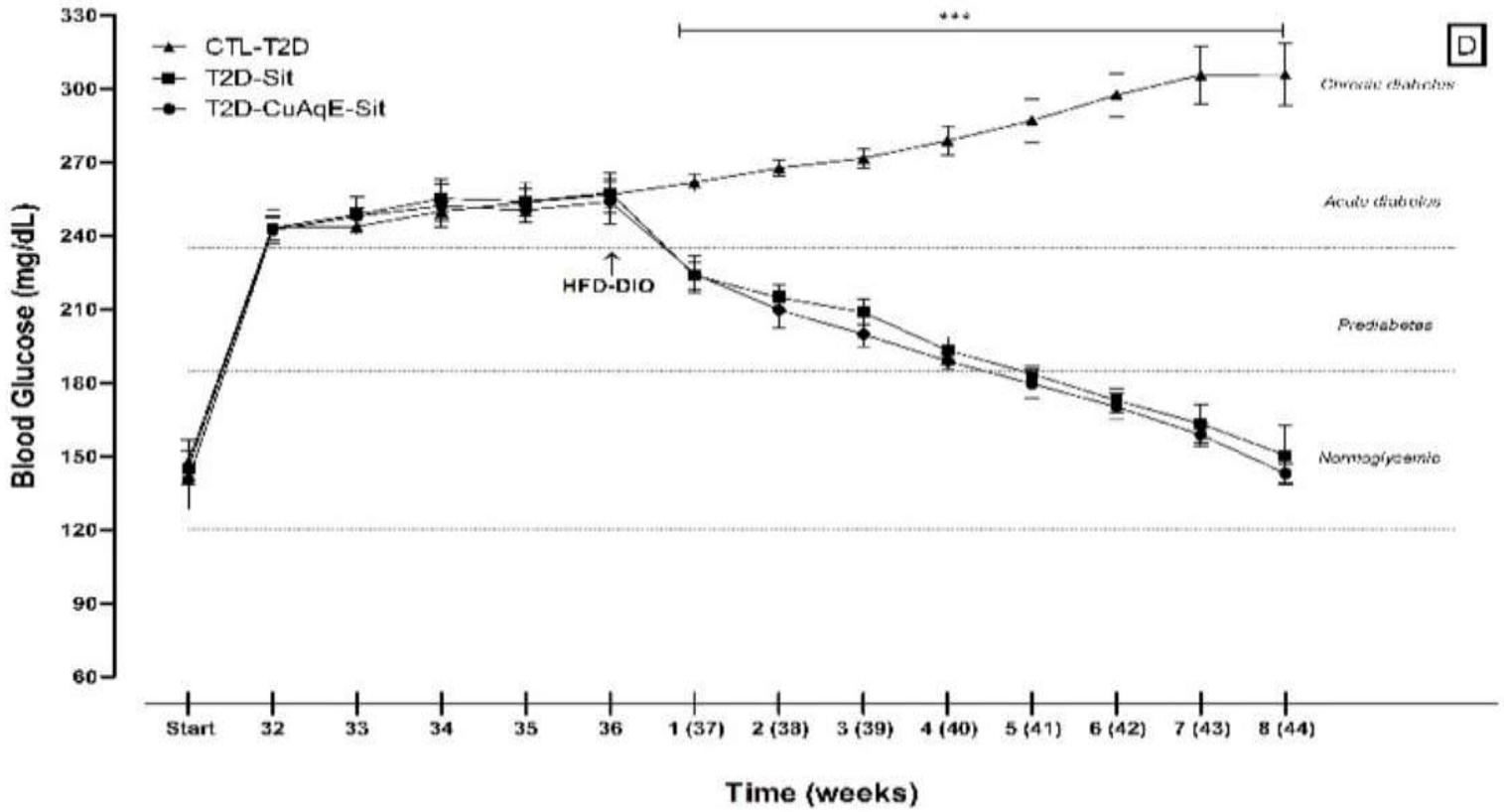

Figure 3S. Phyto-pharmacovigilance of postprandial hypoglycaemic activity in DM murine models with pharmacotherapeutic monitoring of CuAqE and treatment against DM for determining extract-drug interactions. PPBG (mg/dL) in DM C57BL/6 male mice. (A) CuAqE with insulin. ***p<0,001 vs CTL-T1D and ** p<0,001 vs T1D-InsN. (B) CuAqE with metformin. (C) CuAqE with glibenclamide and (D) CuAqE with sitagliptin. ***p<0,001 vs CTL-T2D and ** p<0,05 vs T2D-Met. Values represent means ± SEM of each group. Statistical analysis was performed using two-way ANOVA with Bonferroni multiple comparisons test.

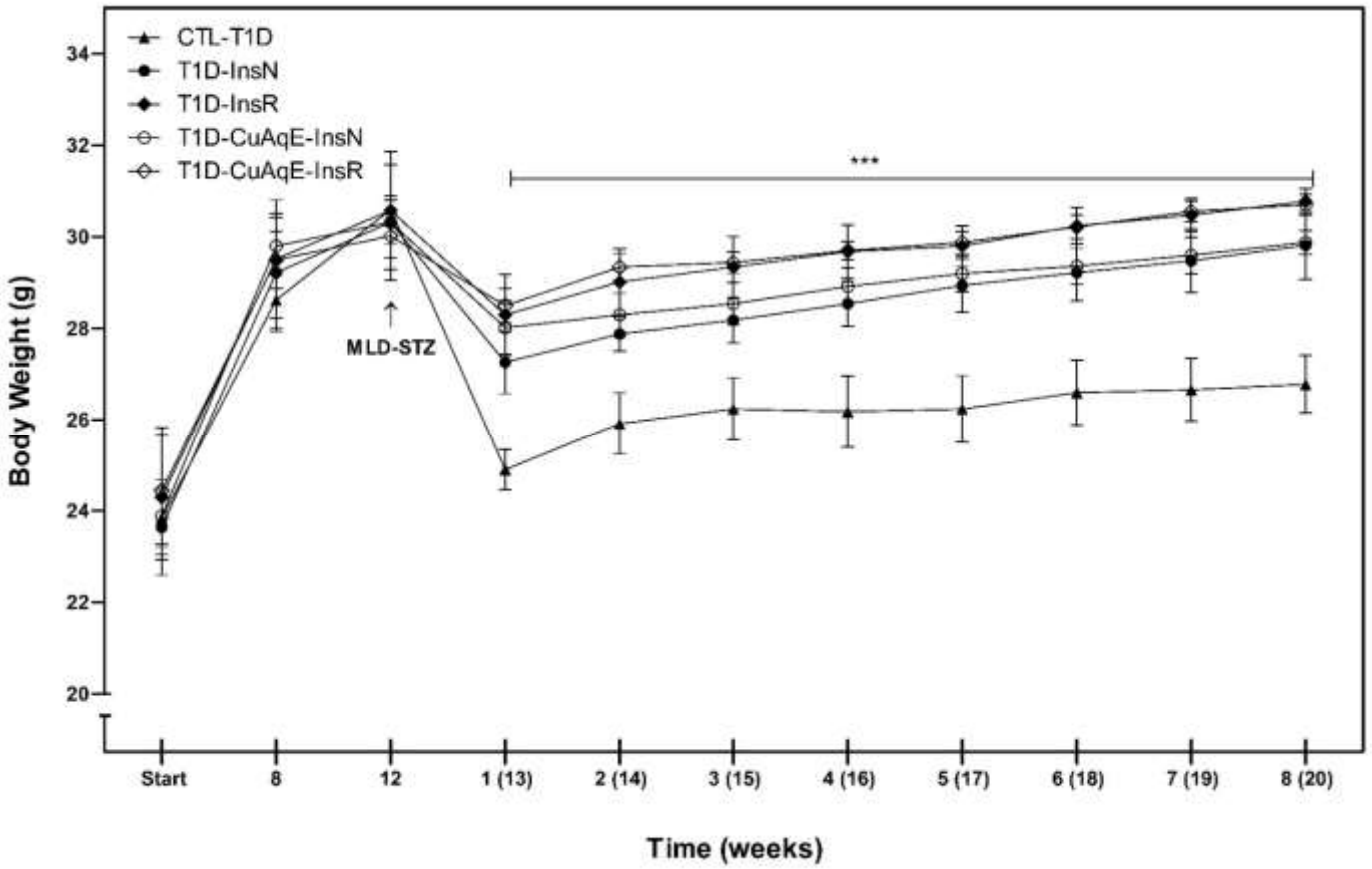

Figure 4S. Longitudinal variation of body weight in T1D murine model with pharmacotherapeutic monitoring of CuAqE and insulin for determining extract-drug interactions. Body weight changes in T1D C57BL/6 male mice that were treated with CuAqE and insulin. Values represent means ± SEM of each group (n=5). Statistical analysis was performed using two-way ANOVA with Bonferroni multiple comparisons test. ***p<0,001 vs CTL-T1D.

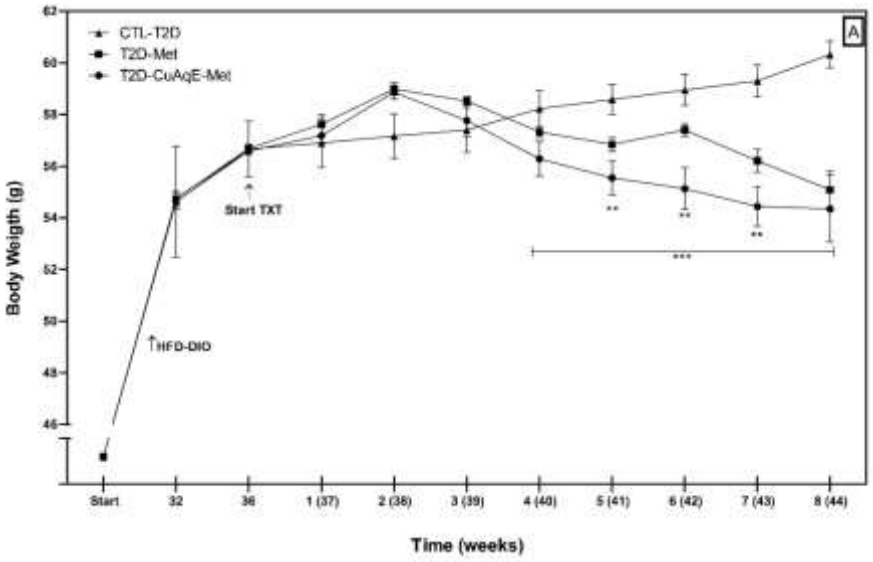

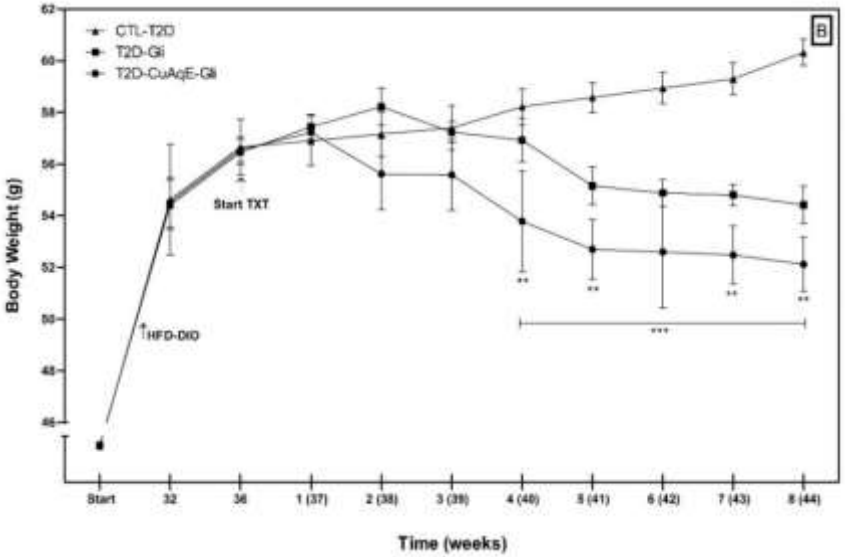

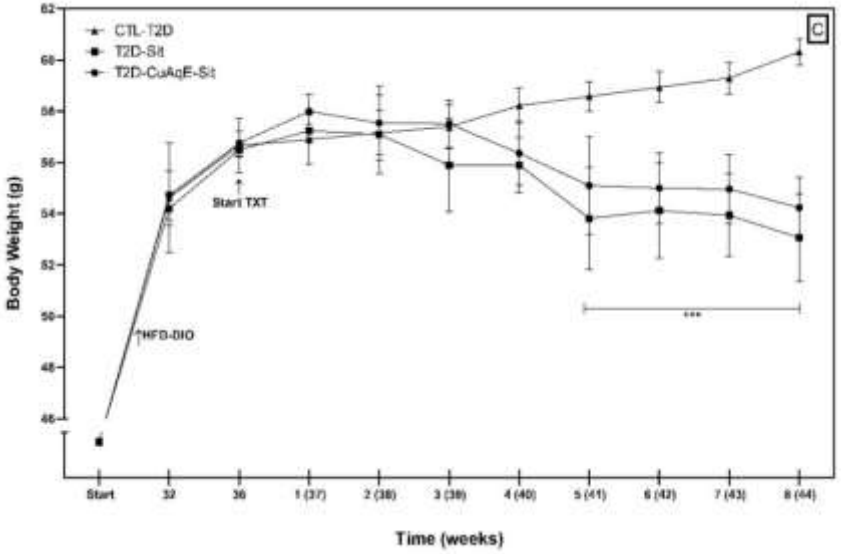

Figure 5S. Longitudinal variation of body weight in T2D murine model with pharmacotherapeutic monitoring of CuAqE and OAD´s for determining extract-drug interactions. Body weight changes in T2D C57BL/6 male mice that were treated with CuAqE and OAD´s. (A) CuAqE with metformin. (B) CuAqE with glibenclamide and (C) CuAqE with sitagliptin. Values represent means ± SEM of each group (n=5). Statistical analysis was performed using two-way ANOVA with Bonferroni multiple comparisons test. ***p<0,001 vs CTL-T2D. **p<0,01 vs T2D-Met and T2D-Gli.

Table 1S. Body growth (BG) and body composition (BC) parameters in DM murine models with pharmacotherapeutic monitoring of CuAqE and treatment against DM for determining extract-drug interactions. Weight gain total (WGt), growth rate (GR), body length (BL), body surface area (BSA) and body mass index (BIM) in DM C57BL/6 male mice that were treated with CuAqE and therapeutic regimen against DM. (A) T1D murine model and (B) T2D murine model**.** Values represent means ± SEM of each group (n=5). Statistical analysis was performed using one-way ANOVA with Bonferroni's Multiple comparisons test for each intervention time. *p<0,001 vs CTL-NOM, **p<0,001 vs CTL-T1D or CTL-T2D.

A	**Without pharmacological administration scheme**					**With pharmacological administration scheme**				
	Before MLD-STZ (12 weeks)					**After MLD-STZ (8 weeks)**				
	BG		**BC**			**BG**		**BC**		
T1D models	**WGt**	**GR**	**BL (cm)**	**BSA (cm^2)**	**BMI (kg/m^2)**	**WGt**	**GR**	**BL (cm)**	**BSA (cm^2)**	**BMI (kg/m^2)**
CTL-NOM	6.50±1.55	1.27±0.07	6.98±0.24	66.41±1.74	4.55±0.18	0.86±1.06	1.03±0.04	7.26±0.19	69.16±1.98	4.50±0.13
CTL-T1D	6.98±1.26	1.30±0.06	6.96±0.21	66.63±1.75	4.59±0.09	-3.84±2.14*	0.88±0.07*	7.04±0.17	63.65±1.46*	4.24±0.20*
NOM-CuAqE	5.50±1.91	1.23±0.10	7.00±0.26	66.68±2.26	4.55±0.11	0.38±0.37**	1.01±0.01**	7.26±0.19	68.84±2.07**	4.47±0.05
T1D-CuAqE	6.76±1.04	1.29±0.06	7.08±0.36	67.32±2.58	4.53±0.16	-1.48±0.19**	0.95±0.01**	7.26±0.33	67.12±2.15**	4.32±0.14
T1D-InsN	6.68±1.08	1.28±0.05	6.96±0.15	66.35±0.69	4.57±0.17	-0.50±0.71**	0.98±0.02**	7.24±0.11	67.81±0.40**	4.40±0.11
T1D-InsR	6.32±1.58	1.26±0.08	7.08±0.16	67.43±1.59	4.53±0.14	0.16±1.06**	1.01±0.03**	7.26±0.19	68.87±1.50**	4.47±0.08
T1D-CuAqE-InsN	6.44±0.29	1.27±0.02	7.04±0.22	66.92±1.91	4.53±0.07	-0.44±0.63**	0.99±0.02**	7.26±0.21	68.00±1.31**	4.40±0.10
T1D-CuAqE-InsR	5.58±1.19	1.23±0.06	6.98±0.25	66.22±1.88	4.54±0.11	0.68±0.61**	1.02±0.02**	7.24±0.17	68.66±1.18**	4.47±0.08

B	Without pharmacological administration scheme					With pharmacological administration scheme				
	Before MLD-STZ (12 weeks)					After MLD-STZ (8 weeks)				
	BG		BC			BG		BC		
T2D models	**WGt**	**GR**	**BL (cm)**	**BSA (cm^2)**	**BMI (kg/m^2)**	**WGt**	**GR**	**BL (cm)**	**BSA (cm^2)**	**BMI (kg/m^2)**
CTL-NOM	7.08±1.28	1.31±0.07	7.56±0.15	70.51±1.82	4.31±0.04	0.20±0.46	1.01±0.02	7.58±0.14	70.89±1.63	4.31±0.03
CTL-T2D	32.92±1.52*****	2.39±0.12*	7.84±0.08*	94.41±1.33*	6.00±0.04*	3.66±0.80*	1.06±0.02*	8.14±0.06*	99.63±0.59*	6.05±0.04*
NOM-CuAqE	6.14±2.23**	1.26±0.11**	7.44±0.18**	69.63±1.38**	4.36±0.07**	0.10±0.37**	1.00±0.01**	7.59±0.12**	70.76±0.82**	4.30±0.05**
T2D-CuAqE	33.08±1.12	2.40±0.10	7.88±0.12	94.77±1.17	5.98±0.07	2.20±1.36	1.04±0.02	8.19±0.13	98.99±0.92	5.95±0.12
T2D-Met	32.74±1.13	2.37±0.10	7.88±0.08	94.78±0.76	5.98±0.04	-1.60±1.45**	0.97±0.03**	8.21±0.06	96.38±1.53	5.71±0.08
T2D-GLI	32.16±2.01	2.33±0.15	7.88±0.12	94.61±0.87	5.97±0.11	-2.04±1.83**	0.96±0.03**	8.05±0.13	94.56±1.54**	5.75±0.12
T2D-SIT	32.72±1.53	2.38±0.13	7.89±0.12	94.72±1.17	5.97±0.07	-4.24±4.42**	0.92±0.08**	8.22±0.10	94.24±3.11**	5.54±0.34**
T2D-CuAqE-Met	33.35±0.92	2.44±0.11	7.89±0.08	94.79±0.76	5.97±0.04	-2.04±2.92**	0.96±0.05**	8.20±0.12	95.85±1.39	5.69±0.23**
T2D-CuAqE-GLI	33.11±2.13	2.42±0.17	7.88±0.08	94.69±1.34	5.97±0.04	-4.44±2.58**	0.92±0.05**	8.09±0.14	93.18±2.83**	5.59±0.09**
T2D-CuAqE-SIT	33.04±1.55	2.40±0.15	7.89±0.06	94.90±0.99	5.98±0.07	-2.52±2.37**	0.96±0.04**	8.20±0.05	95.71±1.98	5.66±0.16**

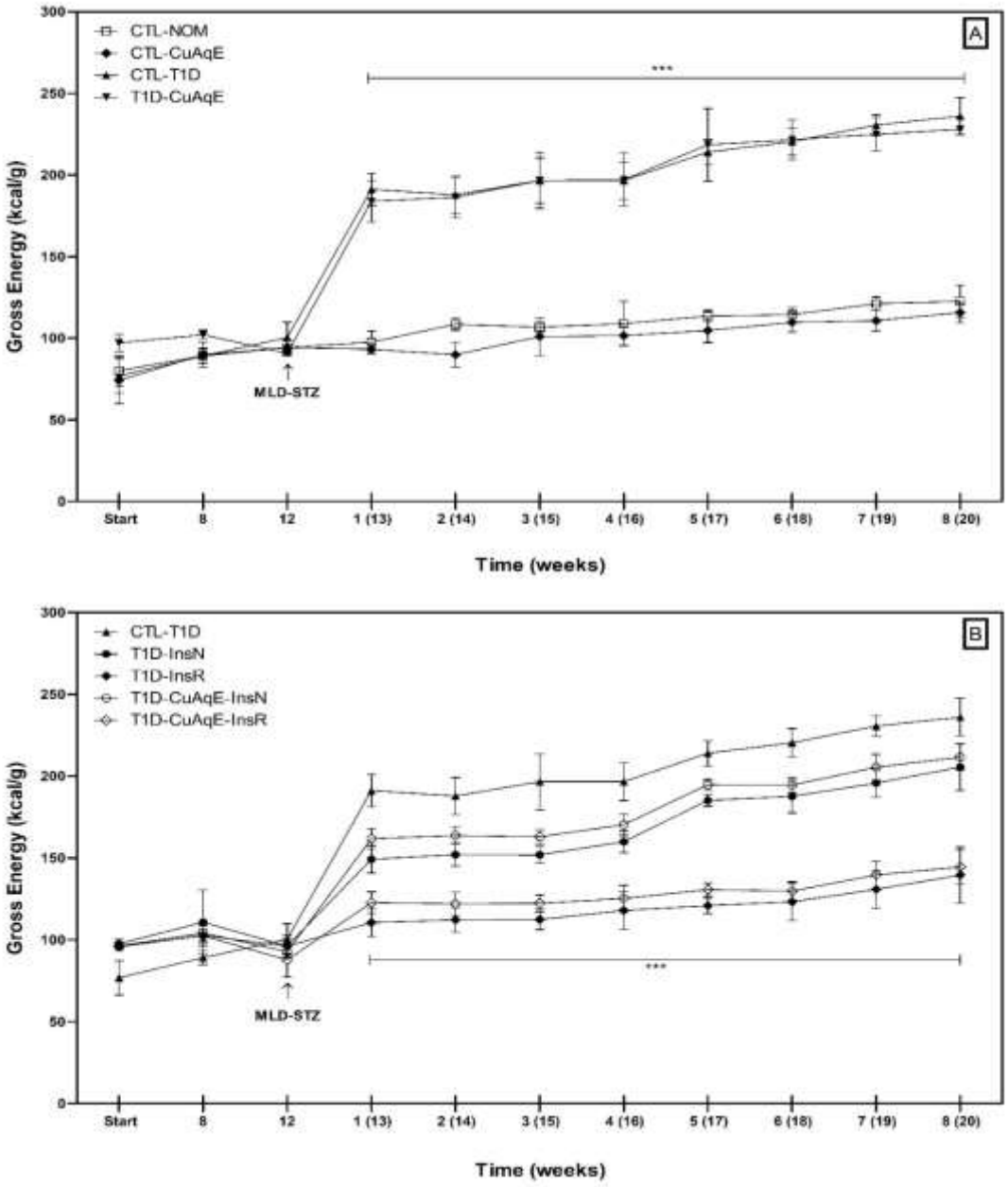

Figure 6S. **Nutrient's intake in T1D murine model with pharmacotherapeutic monitoring of CuAqE and insulin for determining extract-drug interactions.** Food consumption expressed as gross energy o energy density in T1D C57BL/6 male mice across the feeding time 20 weeks. (A) CuAqE as a treatment against T1D, ***p<0,001 vs CTL-NOM. (B) CuAqE and insulin ***p<0,001 vs CTL-T1D. Values represent means ± SEM of each group (n=5). Statistical analysis was performed using two-way ANOVA with Bonferroni multiple comparisons test.

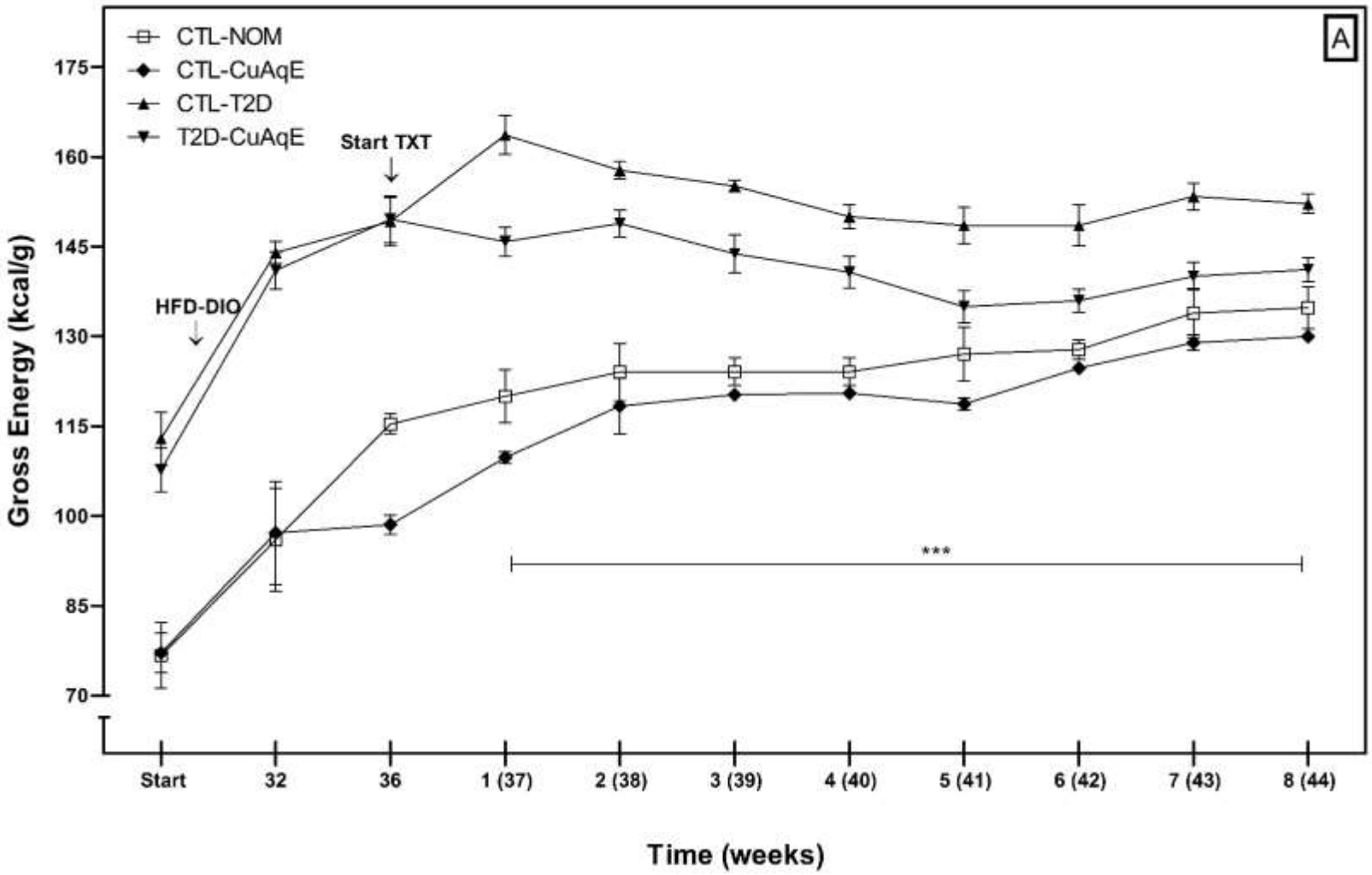
A
CTL-NOM
CTL-CuAqE
CTL-T2D
T2D-CuAqE
Start TXT
HFD-DIO
***
Gross Energy (kcal/g)
175
160
145
130
115
100
85
70
Start
32
36
1 (37)
2 (38)
3 (39)
4 (40)
5 (41)
6 (42)
7 (43)
8 (44)
Time (weeks)

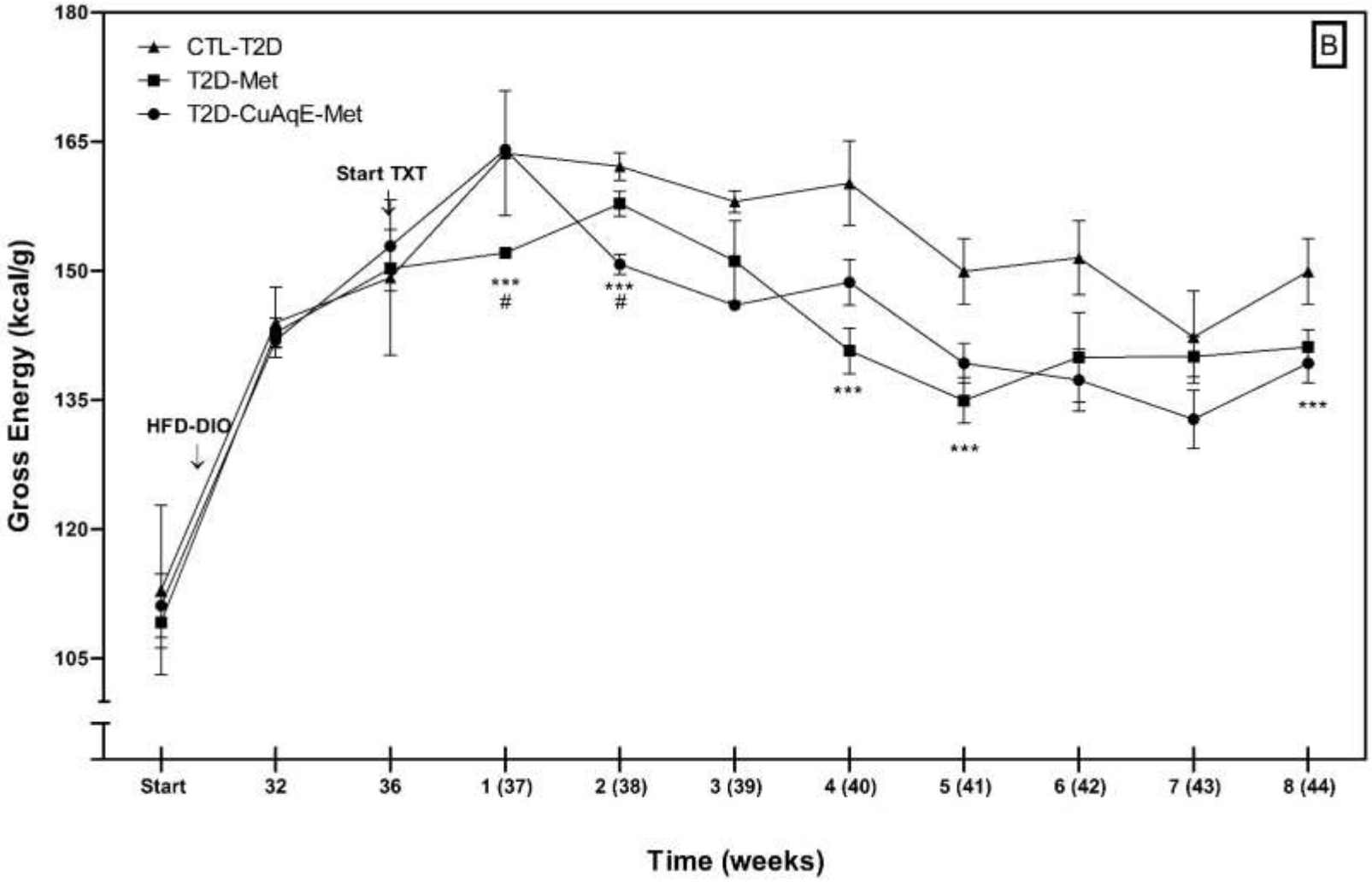
B
CTL-T2D
T2D-Met
T2D-CuAqE-Met
Start TXT
HFD-DIO
Gross Energy (kcal/g)
180
165
150
135
120
105
***
#
***
#
***
***
***
Start
32
36
1 (37)
2 (38)
3 (39)
4 (40)
5 (41)
6 (42)
7 (43)
8 (44)
Time (weeks)

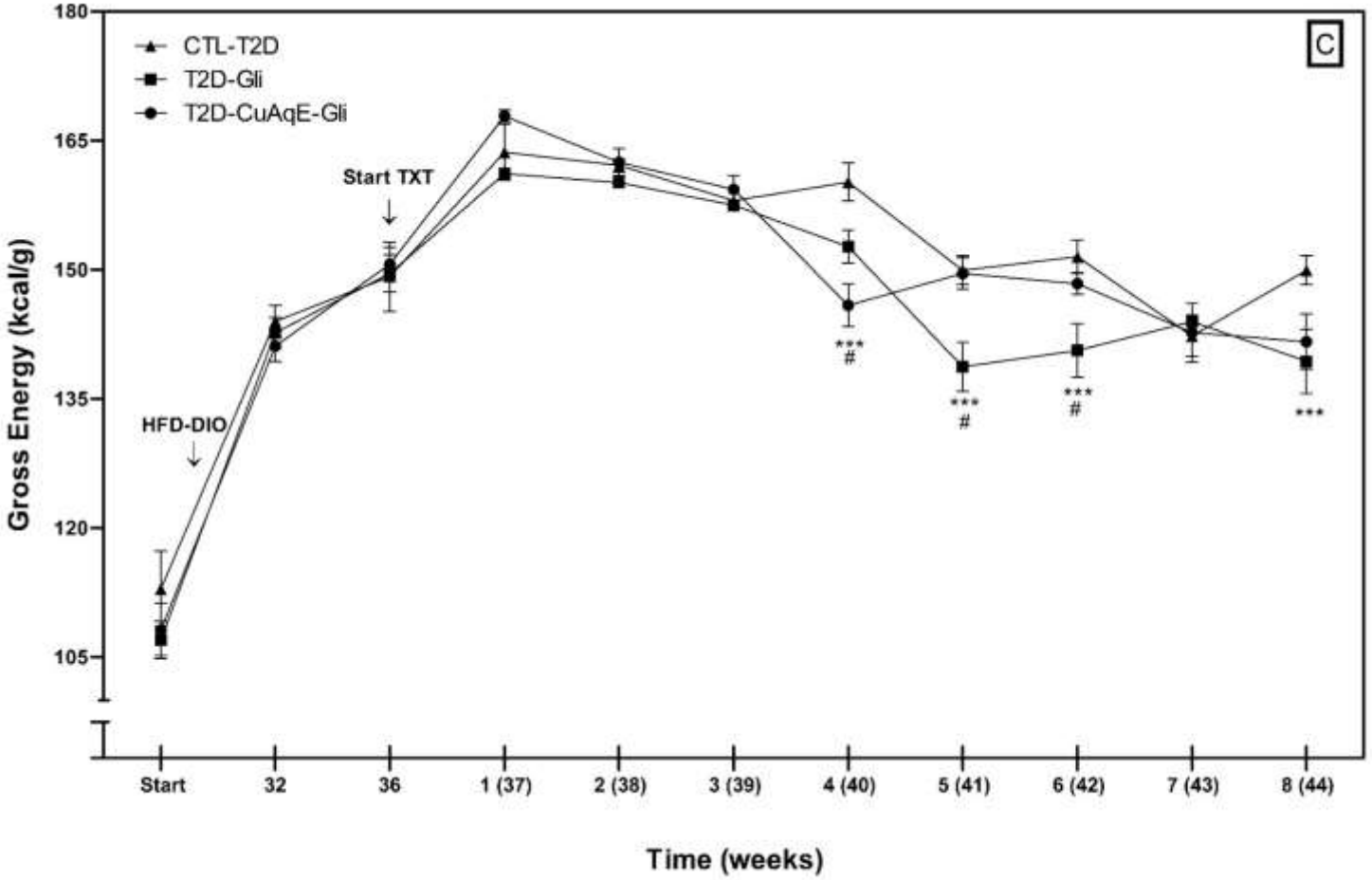
C
CTL-T2D
T2D-Gli
T2D-CuAqE-Gli
Start TXT
HFD-DIO
Gross Energy (kcal/g)
180
165
150
135
120
105
***
#
Start
32
36
1 (37)
2 (38)
3 (39)
4 (40)
5 (41)
6 (42)
7 (43)
8 (44)
Time (weeks)

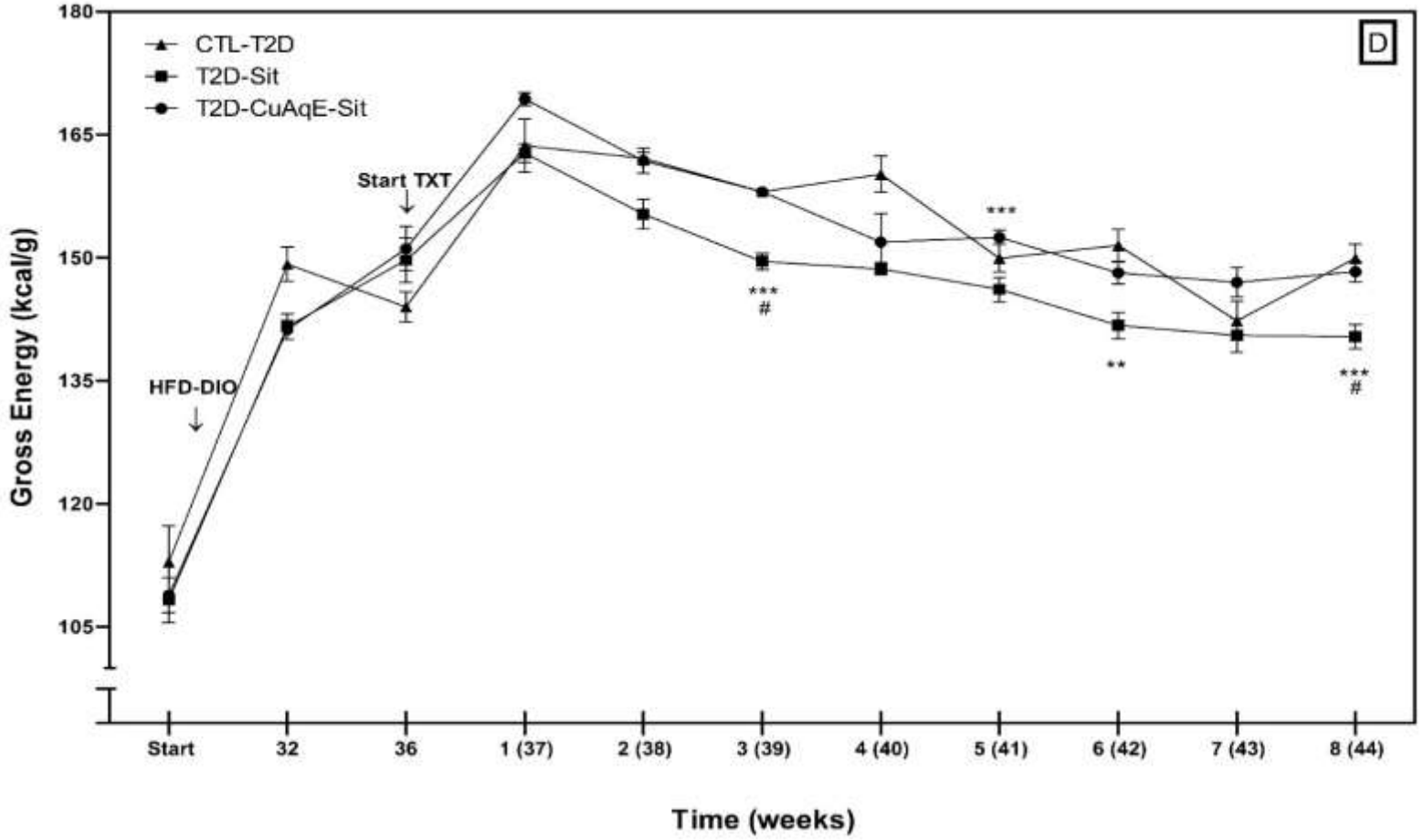

Figure 7S. Nutrient's intake in T2D murine models with pharmacotherapeutic monitoring of CuAqE and OAD´s for determining extract-drug interactions. Food consumption expressed as Gross energy o energy density in male C57BL/6 diabetic mice across the feeding time 44 weeks. (A) Biological Evaluation of CuAqE as a treatment against T2D. (B) CuAqE with metformin. (C) CuAqE with Glibenclamide. (D) CuAqE with Sitagliptin. Values represent means ± SEM of each group (n=5). Statistical analysis was performed using two-way ANOVA with Bonferroni multiple comparisons test. ***p<0,001 vs CTL-T2D and # vs formulation of Oral Hypoglycemic Drugs and CuAqE.

Table 3S. Insulin resistance and sensitivity in T1D murine model with pharmacotherapeutic monitoring of CuAqE and insulin for determining extract-drug interactions

T1D models	HOMA-IR	%S	HOMA-β	Index DI	QUICKI
CTL-NOM	1.02±0.02	98.40±2.19	33.05±1.77	32.51±1.56	0.431±0.002
CTL-T1D	0.76±0.23*	163.2±41.48*	3.72±1.11*	4.92±0.10*	0.461±0.030*
CTL-CuAqE	1.08±0.05$^{\#}$	92.99±4.72$^{\#}$	37.56±1.47$^{\#}$	34.90±1.57$^{\#}$	0.426±0.004$^{\#}$
T1D-CuAqE	1.33±0.15$^{\#}$	75.90±9.21$^{\#}$	7.63±0.80*$^{\&}$	5.73±0.07*$^{\&}$	0.411±0.009$^{\#}$
T1D-InsN	0.81±0.06*$^{\&\$}$	123.38±8.86*$^{\&\$}$	20.69±2.23*$^{\&}$	25.38±1.23*$^{\&}$	0.450±0.006*$^{\&\$}$
T1D-InsR	0.80±0.03*$^{\&\$}$	125.51±4.96*$^{\&\$}$	27.11±1.03$^{\#\&\$}$	34.01±1.30$^{\#\$}$	0.451±0.003*$^{\&\$}$
T1D-CuAqE-InsN	0.89±0.04$^{\&\$}$	112.33±4.62$^{\&\$}$	25.23±1.15*$^{\#\&}$	28.32±1.30$^{\#\&}$	0.442±0.003$^{\&\$}$
T1D-CuAqE-InsR	0.92±0.04$^{\&\$}$	109.26±4.56$^{\$}$	29.47±1.68$^{\#\&\$}$	32.17±1.94$^{\#\$}$	0.440±0.004$^{\&\$}$

Homeostatic Model Assessment (HOMA-IR), Insulin sensitivity (%S), β-cell function (HOMA-β), Disposition index (DI) and Quantitative Insulin Sensitivity Check Index (QUICKI) in C57BL/6 male mice that were treated with a therapeutic regimen against T1D and with CuAqE. Values represent means ± SEM of each group (n=5). Statistical analysis was performed using two-way ANOVA with Dunn's Multiple Comparison Test. *p<0,05 vs CTL-NOM; # p<0,05 vs CTL-T1D; & p<0,05 vs CTL-CuAqE and $ p<0,05 vs T1D-CuAqE.

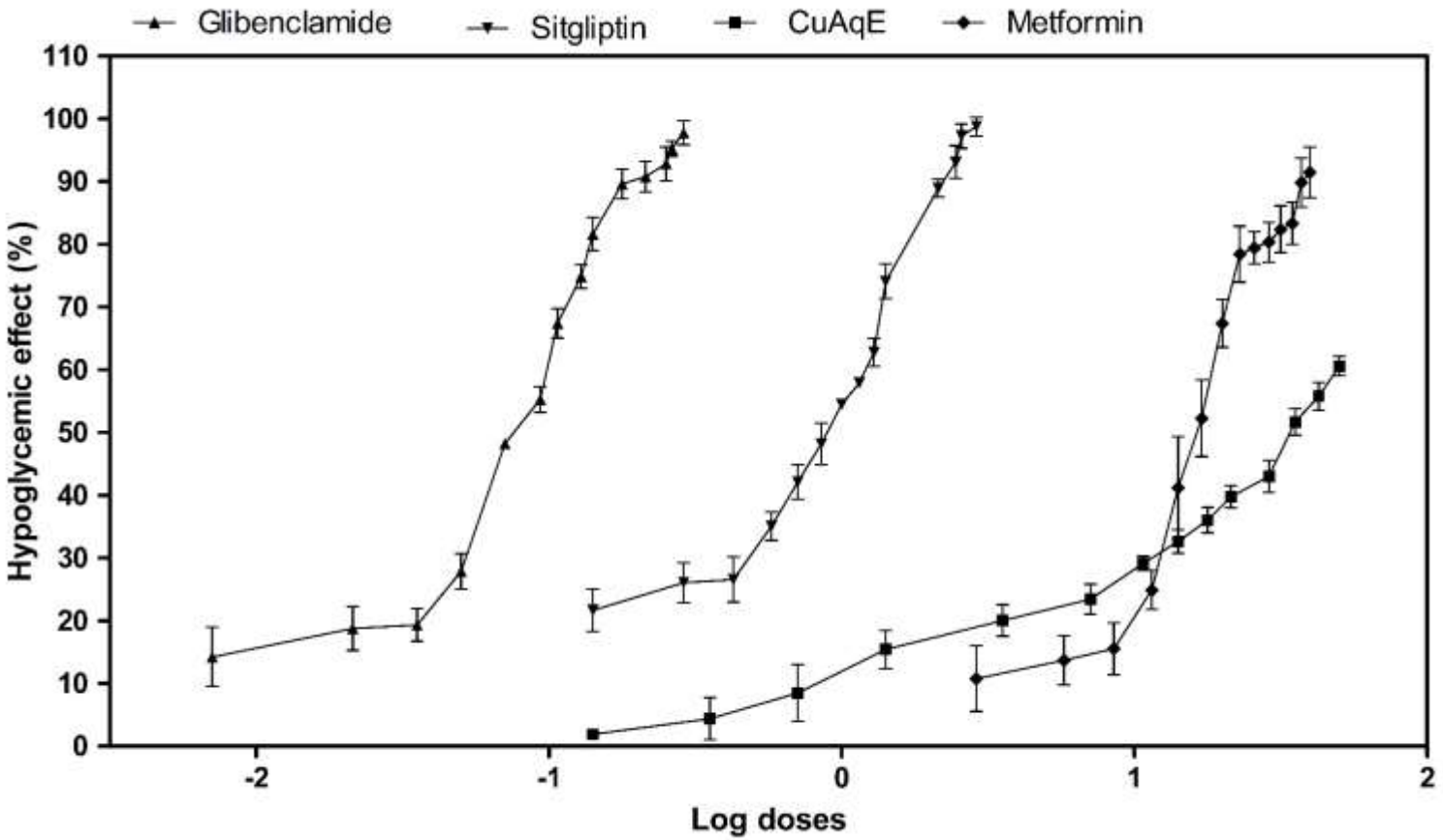

Figure 8S. Hyperbolic dose-response curve in T2D murine model with pharmacotherapeutic monitoring. of CuAqE and OAD´s for determining extract-drug interactions. Hypoglycemic effect (as a percentage) in C57BL/6 male mice that were treated with oral hypoglycemic medications and with CuAqE.

6.3 Pharmacotherapeutic evaluation of the aqueous extract of *Calea urticifolia* in diabetic peripheral neuropathy murine models

1. Introduction

Diabetes mellitus (DM), is a chronic metabolic disorder of endocrine system diagnosed by high blood glucose levels (hyperglycemia, BG). Concerning the pathogenesis of disease, two major mechanisms have been proposed. Autoimmune destruction of the pancreatic β- cells with consequent insufficient insulin production as well as endogenous resistance of the body cells to insulin action or both (Goyal et. al., 2023).

DM has been classified mainly into three types: (a) juvenile/childhood-onset diabetes, insulin-dependent diabetes or type 1 (T1D), defined by the deficiency of insulin production in human body and its treatment requires regular administration of insulin analogues. (b) adult-onset diabetes, non-insulin dependent diabetes or type 2 (T2D). Finally (c) gestational (GD), is condition of HBG during pregnancy in women without a previous history of DM (Lovic et. al., 2020). Additional clinically recognizable subtypes exist, such Maturity-onset Diabetes of the Young (MODY) or late-onset autoimmune form (latent autoimmune diabetes in the adult or LADA) but in Mexico is unknown (Alemán-Contreras, et. al., 2024).

In Mexico, DM is the second leading cause of death and has an estimated prevalence of 15.2% (12.8 million adults); furthermore, over the past three decades, mortality attributable to diabetes increased by an alarming 77%. This is reflected in that Mexico is the fourth country in the world with the highest burden of disease associated with T2D. (Bello-Chavolla et. al., 2022). At the state level, the most pronounced increases occurred in the poorest states of the country. The disproportionate and unequal burden of T2D is result of the confluence of factors such as genetic predisposition, a high prevalence of risk factors and comorbidities as well as insufficient coverage of health services, which reflects serious limitations for early detection and proper control of the disease that increase the risk of cardiovascular, neurological, and renal diseases and other complications such as blindness and amputations (Montoya et. al., 2023).

Although in Mexico current pharmacological treatments for DM such as insulin and oral hypoglycemics are available, the Mexican population continues to use, and sometimes prefers, medicinal plants in the treatment of DM. In terms of traditional medicinal knowledge, Mexico is recognized as the second most important country in the world, with a great ancestral tradition and richness in the use of medicinal plants, just after China. Inside the Mexican territory, which is characterized by a wide range of environmental conditions, approximately 4500 species are used by the 56 ethnic groups that occupy it. The ancestral presence of these ethnic groups and their interactions with their surrounding environments have allowed the development of multiple local forms of knowledge and uses of natural resources to satisfy different needs (Lucía et al., 2021).

According to ethnobotanical knowledge sheltered by Mexican Traditional Medicine (MTM) botanical families with the largest number of plant species used for control of DM are from the following families: *Asteraceae, Leguminosae, Cactaceae, Euphorbiaceae, Labiatae, Rubiaceae, Solanaceae, Cucurbitaceae, and Rosaceae* (Huerta-Reyes et. al., 2022). Among these families, *Calea urticifolia* (Asteraceae) is highlighted due to endemic species in the country and wild species, continuous common use by Xi'uy ethnic group in San Luis Potosí, Mexico as an herbal remedy for DM in their rudimentary health system, and also was reported Aerial parts of the plant for its hypoglycemic and antioxidant activity (Torres-Rodríguez et al., 2016). While *Calea urticifolia* have clinical data in research that approach its hypoglycemic effect. Have no safety or efficacy data available of the protective and antioxidant effect in microvascular complications of DM such as Diabetic Neuropathy (DN).

High clinical suspicion and early recognition of diabetic microvascular complications (DMC) are mandatory, as it is estimated that up to 25% of newly diagnosed patients with T2DM have already developed one or more. DM and DMC pose a major global health threat (Zheng et. al., 2018). It is important to note that chronic intracellular hyperglycemia, genetic predisposition in synergy with the other metabolic disorders in patients with DM can affect the macro and microvasculature and therefore cause

damage to various organ systems, leading to the development of disabling and life-threatening health complications. Most prominent of which are mainly from kidneys (Diabetic Nephropathy is the leading cause of end-stage renal disease, ESRD), eyes (Diabetic Retinopathy is the main cause of blindness) and nervous system (Diabetic Neuropathy is the major risk factor for amputation and foot ulceration) and finally, sexual dysfunction (Faselis et. al., 2020). In conjunction with (cardiovascular disease, CVD) are the leading cause of morbidity and mortality in individuals with DM carrying enormous financial burden with unequal healthcare expenditure and access to treatment between developed and developing countries (Cole & Florez, 2020).

DM damage to the peripheral and autonomic nervous system, causing several patterns of peripheral nerve injury, including radiculoplexus neuropathy, radiculopathy, mononeuropathy and Diabetic Peripheral Neuropathy (DPN) refers to development of peripheral nerve dysfunction. DPN is a distal-to-proximal loss of peripheral nerve function causing physical disability and pain, lowering quality-of-life. Symptoms of DPN are a predominantly sensory such as encompass numbness attributable to injury of large, myelinated nerves, known as large. Fibers tingling and pain (burning, stinging, shooting, deep aching) attributable to injury of unmyelinated nerves, known as small fibers. Although there are often motor features with advancing disease (Elafros et. al., 2022).

Patients with DPN usually experience symmetrical pain and numbness in the limbs, particularly in the distal end. The most typical manifestation is the gloves-and-socks sensation (Yang et. al., 2022). With loss of sensation identifying, it as Diabetic distal Symmetric Polyneuropathy (DSPN) and is the most frequently encountered form of the disease, accounting for 75% of DN. (Zhu et. al., 2024).

For diagnosis of DPN is recommends evaluating in patients with T2D at diagnosis and patients with T1D five years after diagnosis and then annually thereafter. Screening should comprise: a detailed clinical history (higher HbA1C). Examination physical of sensations positive: tingling, burning, pain, prickling sensations (paresthesia),

disordered sensory processing may evoke pain when the feet are touched (allodynia) and increase sensitivity to noxious stimuli (hyperalgesia).

But also, negative sensations (numbness symmetric distal-to-proximal). Including assessment of temperature or pinprick sensation (small fiber), vibratory sensation (large fiber), and ability to perceive pressure using a 10-gram monofilament assesses ulcer risk, (large fiber). Electrodiagnostic testing is rarely needed such as measures nerve conduction velocities (NCVs) in sensory (sural, peroneal, tibial) and motor (peroneal, tibial) nerves using surface or needle electrodes (Elafros et. al., 2022 and Selvarajah et.al., 2019).

Peripheral nervous system (PNS) is formed by motor, sensory, and autonomic nerves that connect tissues and organs to the central nervous system (CNS). Nerves are formed by axons, long cytoplasmic protrusions of neurons located in or aside the spinal cord, and specialized glial cells named Schwann cells (SCs). SCs can be divided into three main classes, myelinating SCs, non-myelinating SCs, and terminal SCs. Myelinating SCs associate one-to-one with axons, ensheath, and form a compact myelin sheath around large caliber axons (> 1 μm). In this way, they provide electrical insulation which allows rapid, saltatory conduction of action potentials over long distances. Myelination proceeds longitudinally to form internodes nodes of Ranvier (Previtali, 2021).

The presence of myelin allows the neuronal electrical signals to achieve 20–100-fold higher speeds compared with nonmyelinated axons. Under influence of oxidative stress, and inflammatory reactions metabolic disorders (hyperglycemia, insulin resistance, and hyperlipidemia), through special signal transduction pathways entail mitochondrial dysfunction, whence destroy normal structure and function of nerve cells and lead to neuronal demyelination (SCs apoptosis) and neuronal damage (Wallerian degeneration), which are the main causes of DPN usually manifests as demyelination by SCs apoptosis. (Liu, et. al., 2020 and Zhu et. al., 2024).

Hyperglycemia and dyslipidemia are the most common two factors that can trigger Oxidative and metabolic pathways for example: PKC pathway, polyol pathway, AGE pathway, hexosamine pathway, and PARP pathway such as bioenergetic mechanisms of nerve injury. In Polyol pathway excess glucose is converted to sorbitol by aldose reductase; this results in osmotic imbalance in the cell secondary to increased sorbitol, with resultant osmotic stress and compensatory efflux of myoinositol and taurine.

In turn, loss of myoinositol, an essential component of sodium/potassium (Na/K) ATPase, impairs normal nerve physiology. A second set of neuronal insults occur as aldose reductase activity depletes cellular stores of NADPH, needed for nitric oxide (NO) generation and regeneration of the essential antioxidant glutathione. The resulting generation of cytoplasmic ROS leads to ROS-mediated intracellular injury and cellular dysfunction (Feldman et. al., 2017).

Current management of DPN focuses on controlling diabetes: Glucagon-like peptide 1 receptor agonists and neurotropic B vitamin supplementation, B1, B6, and B12 (Beshyah et. al., 2024) and neuropatic pain: antidepressants, antiepileptics and brain neuromodulation techniques (Attal & Bouhassira, 2020). Lack of efficacy and the side effects of drugs that are used to prevent and treat DPN also present serious clinical problems. Thus, use of medicinal plants with antioxidant properties for the treatment of DPN is increasing (Ahmadzadeh et. al., 2024).

There are no scientific studies carried out regarding the effect of aerial parts of *Calea urticifolia* in DPN to substantiate their traditional therapeutic claim. Hence, the aim of this study was to assess effect of a Lyophilized Aqueous Extract of *Calea urticifolia* (CuAqE) in DPN mice model through measurement of behavioral tests, Compound Action Potential (CAP) and aldose reductase activity.

Materials and Methods

2.1 Materials

Mouse Akr1b1 (aldose reductase) ELISA Kit was purchased from MyBioSource, USA. Monofilaments (or Von Frey hairs) based on the Semmes Weinstein monofilament set (from 0.008 to 300 grams) from Bioseb, USA. Isofloran (Soflorant Vet ®) from Pisa Agropecuaria (PiSA® Farmacéutica, México). Streptozotocin (STZ) and test strips Accu-Chek Aviva bought in Roche, UK. Compound of Krebs solution were purchased from Sigma-Aldrich (St.Louis, MO, USA).

2.2 Herbal material harvest and preparation of lyophilized aqueous extract (CuAqE)

Fresh leaves of adult plants of *Calea urticifolia* were harvested in Xi'uy ancient native community of Potrero del Carnero (21°52'27.6'' N y 099°27'00.6'', to 901 msnm, San Luis Potosí, Mexico) in July 2023. It was authenticated by an herbalist of Isidro Palacios Herbarium (IIZD-UASLP, San Luis Potosí, México). Herbal material was separated and transferred to absorbent paper for drying and stored at room temperature until use.

Dry leaves were crushed in an electric mill (Osterizer Pulse Matic Blenders) before extraction. 100g were mixture with 1L of distilled water and boiled for 5 min. Once the aqueous extract was cooled down, it was filtered and freeze-dried (Freeze-dryer TFD5505, Ilshin®, Hialeah, FL, USA). Residue was stored at 4˚C until use.

2.3 Animal procurement, housing and bioethical considerations.

Four to six weeks old C57BL/6 male mice were purchased from the CINVESTAV-IPN. (México City, México). Upon arrival, the mice were maintained in a controlled environment (21±2◦ C, 50±10% humidity) with a 12 h light/dark cycles (7:00am to 7:00pm) and were given access to standard rodent food (Chow 5001) and water ad libitum. The mice were acclimatized for 5 days prior to use, then randomly assigned to diet groups and were housed in individual acrylic cages. Animal study protocol were reviewed and approved by the local Animal Ethical Review Committee

(CE102018015R2. FCQ-UASLP, San Luis Potosí, México) and the mice were handled in agreement with animal ethics guidelines as the Mexican Norm for Animal Care and Handing (NOM-062-ZOO-1999).

2.4 Experimental Design: DPN mice model

DM was induced in C57BL/6 male mice, for T1D model according to Chemically-Induced Diabetes by Multiple Low Dose Streptozotocin (40 mg/kg, MLD-STZ), at twelve weeks were given intraperitoneally for five consecutive days and to T2D model in accord with Diet-Induced Obesity (DIO-HFD) for thirty-six weeks.

It has previously been shown that C57BL/6 mice with MLD-STZ-induced diabetes develop motor and sensory nerve conduction deficits, thermal and mechanical hypoalgesia, tactile allodynia, intraepidermal nerve fiber loss, oxidative-nitrosative stress, and accumulation of sorbitol pathway intermediates in nerve fibers (Watcho, et.at., 2011). Thus, characterizing a model of Type 1 Diabetic Peripheral Neuropathy (T1D-DPN).

In addition, DIO-HFD in C57BL/6 mice develops nerve fiber damage and displays increased sorbitol pathway activity, oxidative-nitrosative stress, and proinflammatory changes in peripheral nervous system (Watcho, et. al., 2010). Thus, generating Type 2 Diabetic Peripheral Neuropathy (T2D-DPN). To evaluate CuAqE in DPN models, we decided to measure FBG, neuropathic pain, CAP and aldose reductase.

2.5 Treatments

Mice were randomly assigned into eight groups (n=5). For T1D model: Group 1 (CTL-NOM), Group 2 (T1D-DPN), Group 3 (CTL-CuAqE), Group 4 (T1D/DPN- CuAqE). For T2D model: Group 5 (CTL-NOM), Group 6 (T2D-DPN), Group 7 (CTL-CuAqE), Group 8 (T2D/DPN-CuAqE). Groups 3, 4, 7 and 6 were treated with CuAqE (11 mg/kg/day) orally-administrated daily using an intra-gastric probe (0.1 mL/10 g body weight) to

each of the mice in the same timing and order for 8 weeks. CuAqE was dissolved and prepared fresh in physiological solution.

2.6 Biochemical parameters

Severity of the induced diabetic state was assessed by monitoring Fasting Blood Glucose (FBG) with a Hand-held Blood Glucose Monitor (Accu-Check Aviva, Roche, UK). Mice whose blood glucose level exceeded 250 mg/dL were considered as diabetic. After surgical procedures, mice were euthanized by cardiac puncture for to collect blood sample. Aldose reductase was measured according to the manufacturer's protocol, for microplate reading at 450nm was run on Multiskan photometer with software Ascent (Thermo Fisher Scientific®, USA).

2.7 Evaluation pain behaviors

2.7.1 non-stimulus evoked nociception

An overall assessment of the health and welfare of mice included an evaluation of the animal in its home cage and a hands-on exam. Changes in body weight, water and food consumption were recorded every week. Body Condition Score (BCS) was evaluated by palpating sacroiliac bones (spine and hip bones) and assigning a score from one to five. A score of one indicates extreme thinness, while a score of five indicated obesity. Mice with an optimal body condition, scored a three, the bones are palpable but not prominent (Burkholder et. al., 2012).

We follow a standardized behavioral coding system, Mouse Grimace Scale (MGS), consisting of five facial features (action units), intensity of each feature was coded on a three-point scale (Langford et. al., 2010). Mice were individually placed on a table top in cubicles (9 × 5 × 5 cm) with two walls of transparent Plexiglas and two side walls of removable stainless steel. Mice were acclimated for 30min and tested by to MGS for 20min.

2.7.2 stimulus-evoked pain-like behaviors

To assess neuropathic pain, mechanical and cold allodynia were measured. Mice were placed in elevated plexiglas cages (15 × 10 × 10 cm) with a wire mesh floor and allowed to acclimatize for 10–30 min prior to testing. To assess mechanical allodynia, the paw withdrawal threshold (PWT) to mechanical stimulation of the left hind paw was assessed using von Frey hairs (North Coast Medical, San Jose, USA). A series of von Frey hairs were pressed perpendicularly (for 2 s) onto the plantar surface of the hind paw (four times for each hair).

A positive response was recorded if brisk withdrawal or paw flinching occurred. Flinching immediately upon removal of the filament was also considered a positive response. Pain-like behaviors such as flinching, licking, shaking, biting, jumping, stretching or squashing the abdomen, guarding of the hind paw, and changes in posture were assessed for their presence or absence. To determine mechanical sensitivity were employed four methods: Up-down method, Simplified Up-Down method (SUDO), Ascending stimulus method and Dixon method using threshold tracking algorithm: PWT=log X+ (k) [δ], where X = represents the value (in log units) of the final Von Frey filament used; k = is a tabular value, and δ is the mean difference (in log units) between stimuli (Adamson et. al., 2016; Bonin et al., 2014; Watcho *et al.,* 2010).

2.8 Surgical procedures, stimulation and recording of CAP

At day of experiment, mice were anesthetized with isoflurane (exposure to long-term) and sural nerve (3–6 mm, depending on the animal size) of both hind-limbs was removed carefully during microscope-assisted visualization and placed on a recording chamber filled with oxygenated Krebs buffer solution: (NaCl, 128 mM; NaH_2PO_4, 0.5 mM; $CaCl_2$, 1.5 mM; $MgSO_4$, 1.0 mM; $NaHCO_3$, 21 mM; glucose, 35 mM) which was gassed with 95% O_2 and 5% CO_2. The pH and temperature of the buffer were maintained at 7.4 and room temperature (22–24°C), respectively.

Electrophysiological procedures for stimulation and recording of the CAP in the peripheral sural nerves were performed as described in previous studies (Zempoalteca et. al., 2018 and Quiroz-González et. al., 2016). In short, both ends of each sural nerves were drawn into suction electrodes to record and evoke CAP. Stimulating electrode consisted of a fine silver wire inserted into a glass micropipette filled with the bath saline solution, which was wrapped around with an isolated silver wire (except at the tip) and connected to a pulse generator (Digitimer DS3), and recording electrodes consisted of a pair of chlorinated silver wires. One wire was inserted in a glass micropipette and the other was located in the bath saline solution, and both were connected to a low-noise, high-gain differential amplifier (band pass filters 0.3–1.0 kHz; Grass Model 7P511), to an oscilloscope (Tektronix Model TDS2024) and to a computer for capture and analysis of potentials.

Once both extremes of the nerves segment were installed, the electrophysiological responses of the nerve were evoked by applying single square current pulses (0.05 ms duration). The resistance of the recording electrode (Rp) was determined by measuring the voltage drop that occurs when a constant voltage pulse (1–2 V, 5 ms) was passed across the stimulating electrode with the nerve inserted on it. The system was previously calibrated.

Maximal CAP amplitude was evoked at two times the stimulus current strength needed to evoke a barely discernible response in the nerve (threshold, xT). The CAP was obtained by average samples a 1 Hz. CAP parameters determined were following: Electrical threshold (T), peak-amplitude, area, half-width, initial latency (Li), peak-latency, and the length of the nerves was measured (D). Subsequently, Nerve Conduction Velocity (NVC) was determinate by NVC=D/ Li.

2.9 Statistical analysis

Multiple comparisons were performed among experimental groups by one-way ANOVA analysis, followed by Dunnett's post hoc test. The data are expressed as means ±

standard deviation (SD) and $p < 0.05$ was considered statistically significant Statistical analysis was performed using GraphPad Prism Version 6.0 (GraphPad Software Inc., La Jolla, CA, USA).

3. Results

3.1 Generation of DPN in DM mice model and hypoglycemiant activity of CuAqE

FBG after MLD-STZ in T1D-DPN had an accelerated increase ~2.7-fold higher compared with CTL-NOM 20-week final time point ($p<0.001$). CuAqE treatment did affect FBG with a percentage reduction of 11.9 respect T1D-DPN in 8 weeks (Figure 1). Besides T1D-DPN triggered polydipsia and polyuria (data no showed).

A 44-week HFD-DIO in T2D-DPN resulted in an increase on FBG ~1.2-fold higher with CTL-NOM ($p<0.001$). CuAqE treatment reduced by half FBG in T2D/DPN-CuAqE compared with baseline level to T2D-DPN (Figure 1). For mice that acquired T2D-DPN, we can state that they presented the disease due to excessive consumption of calories in the diet (data not shown) for 44 weeks during which they developed DIO-HFD as BW and FBG increased (Figure 2).

Initial (MLD-STZ or DIO-HFD) BW were similar in all experimental groups (data no showed). BW at the end of 8-week period after MLD-STZ administration had significant reduction (15.3%) ending in underweight in T1D-DPN mice compared to CTL-NOM ($p<0.001$). CuAqE treatment for 8 weeks did affect weight gain (5.8%) in T1D-DPN-CuAqE respect to T1D-DPN. Thus, preventing excessive BW loss but not a normal BW maintenance (Figure 2).

After 36-week HFD-DIO resulted in T2D-DPN a progressive increase in BW compared with CTL-NOM (data no showed). Similar differences between the two groups maintained at the end of the study (44 weeks). This diet showed a two-fold gain in BW in T2D-DPN ($p<0.001$), resulting in a status of Obesity Class II (severe) in mice. An 8-week CuAqE treatment did affect body weights in T2D-DPN-CuAqE showing a 2.5% decrease BW compared with T2D-DPN (Figure 2).

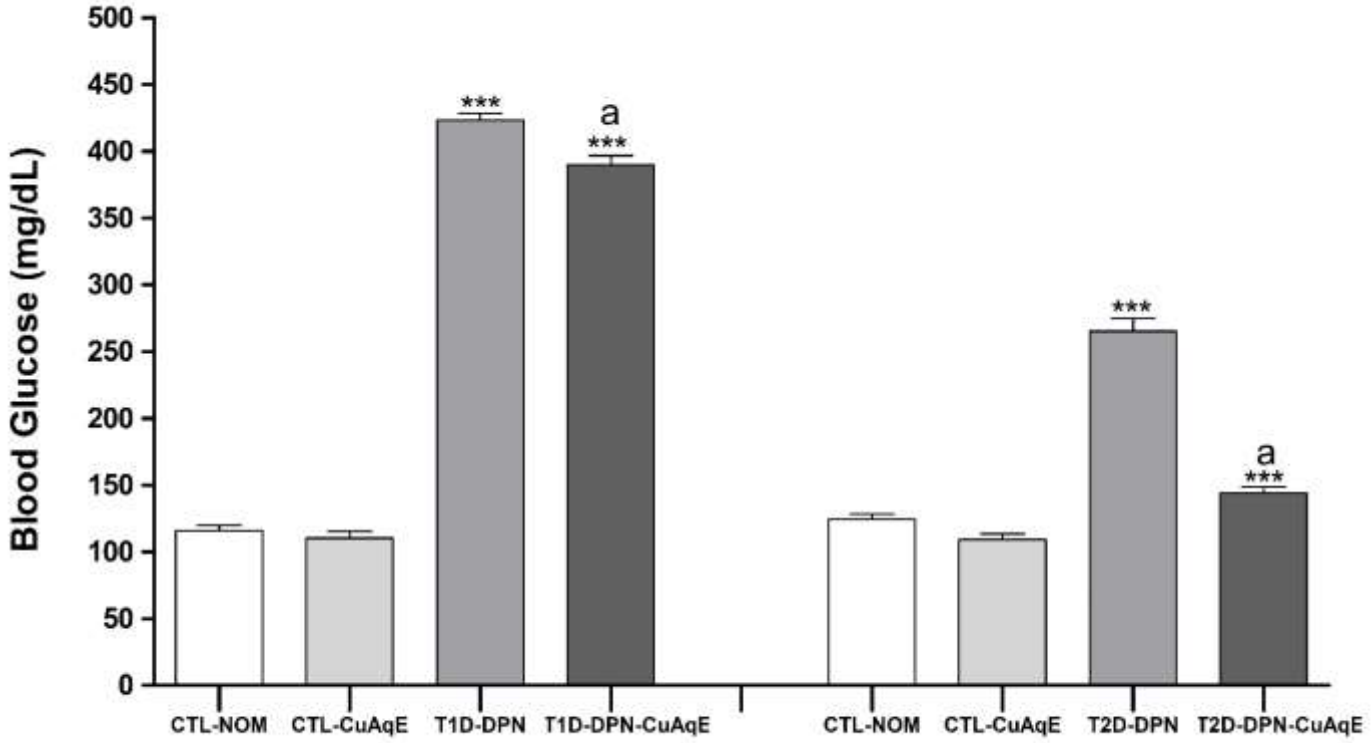

Figure 1. Fasting Blood Glucose in DPN murine model with phyto-pharmacotherapeutic monitoring of CuAqE. FBG (mg/dL) in C57BL/6 male mice that were treated with CuAqE. Biological evaluation for 8 weeks of CuAqE as a treatment against T1D-DPN (left) and Biological evaluation for 8 weeks of CuAqE as a treatment against T2D-DPN (right). Values represent means ± SD of each group (n=5). Statistical analysis was performed using two-way ANOVA with Tukey's multiple comparisons test. and ***p<0,001 vs CTL-NOM and a p<0,001 vs CTL-T1D or CTL-T2D.

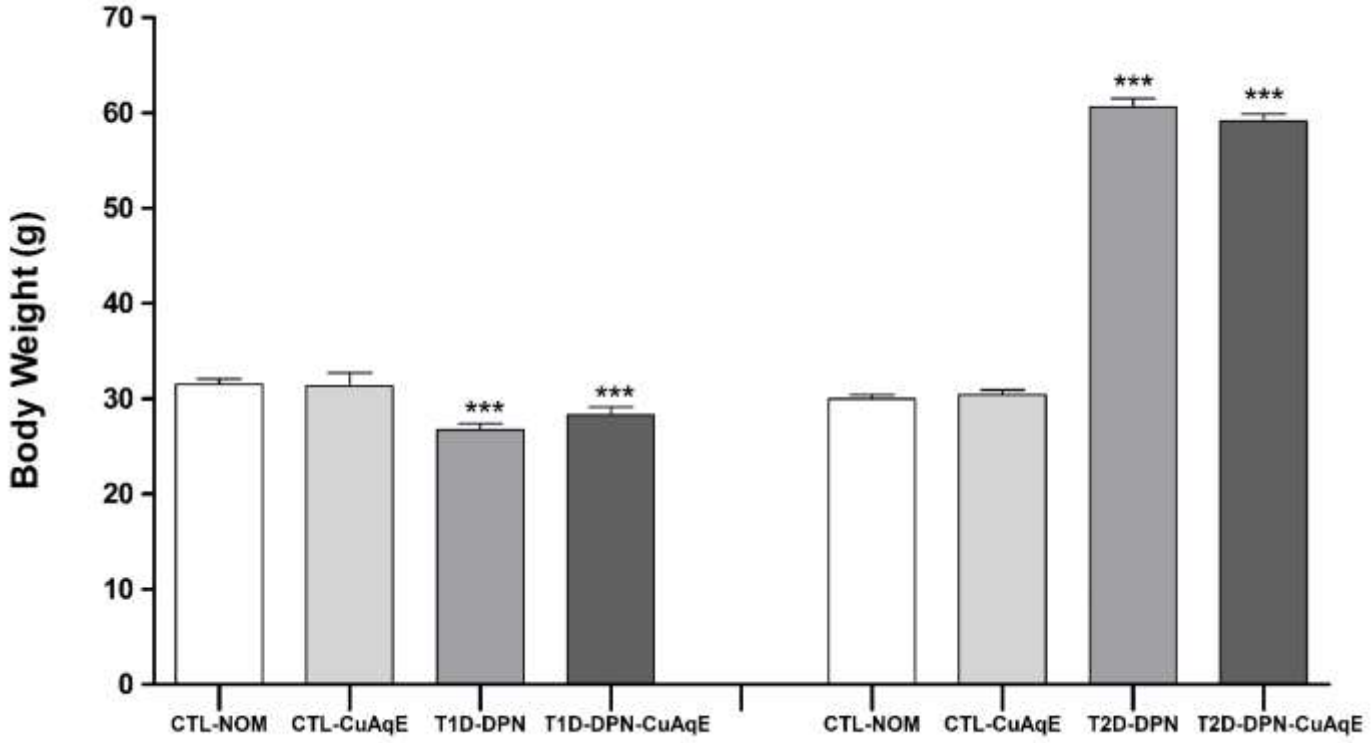

Figure 2. Body weight in DPN murine model with phyto-pharmacotherapeutic monitoring of CuAqE.

Body weight (g) in C57BL/6 male mice that were treated with CuAqE. Biological evaluation for 8 weeks of CuAqE as a treatment against T1D-DPN (left) and Biological evaluation for 8 weeks of CuAqE as a treatment against T2D-DPN (right). Values represent means ± SD of each group (n=5). Statistical analysis was performed using two-way ANOVA with Bonferroni multiple comparisons test. and ***p<0,001 vs CTL-NOM.

BCS is a fast, easy and reliable method to assess the health of mice. T1D-DPN mice had a condition of 2, the others maintained the optimal condition. This is reflected in the decrease in BSA where there are significant differences with respect to the normal control ($p< 0.001$). With the CuAqE treatment, although DPN mice do not recover their optimal BSA, the BMI and Lee index remain unchanged. This reflects the protective impact that CuAqE can have on sudden changes in weight loss in T1D-DPN mice. In addition, T2D-DPN mice reached the top with a value of 5 for BCS (obese) and therefore a significant increase in BSA, BMI and Lee index respect to CTL-NOM ($p< 0.001$). CuAqE treatment failed to modify the previous parameters, due to the degree of obesity present in the mice (Table 1).

We finally succeeded in generating DM in mice via MLD-STZ or HFD-DIO leading to persistent hyperglycemia. We then evaluated relevant traits that are generated such as neuropathic pain, that are modified such as PAC and that are overactivated such as aldose reductase in DPN.

3.2 Effect of CuAqE on neuropathic pain in DPN mice

Neuropathic pain is a complex, chronic pain state accompanied by tissue injury and nerve damage. To assess allodynia as a painful response to a normally non-noxious or innocuous stimulus in DPN mice. We decided to focus on determining allodynia punctate (touch-triggered) by manually applying von Frey monofilaments of varying strengths. Pain-like behaviors evoked by mechanical stimulation were obtained by two different methods in DPN mice. Figure 3 shows details of PWT. We examined DPN model on pain assays at 20 weeks for T1D-DPN and 44 weeks for T2D-DPN. DPN mice displayed a decrease in mechanical PWT compared with CTL-NOM ($p<0,001$).

CuAqE treatment mice did display a difference in mechanical PWT, between before and post-treatment values. CuAqE produced an increase in mechanical PWT after 8 weeks treatment.

Table 1. Body Composition and pain parameters in DPN murine models with phyto-pharmacotherapeutic monitoring of CuAqE. Lee index, Body surface area (BSA), Body mass index (BIM), Condition scoring (BCS), Pain and distress assessment score and Mouse grimace scale (MGS) in C57BL/6 male mice that were treated with CuAqE. Values represent means ± SD of each group (n=5). Statistical analysis was performed using one-way ANOVA with Bonferroni's Multiple comparisons test. *p<0,001 vs CTL-NOM. [a] p<0,001 vs T1D-DPN or T2D-DPN. + Data shown as median.

	Body Composition parameters					
	Lee index	**BSA (cm^2)**	**BMI (kg/m^2)**	**BCS +**	**Pain and Distress+**	**MGS**
T1D-DPN model						
CTL-NOM	0.435±0.010	98.40±1.33	4.50±0.13	3	1	1.4±0.70
CTL-CuAqE	0.434±0.014	98.00±3.12	4.47±0.05	3	2	1.5±0.53
T1D-DPN	0.425±0.012	88.13±1.58*	4.24±0.20*	2	0	8.1±0.74*
T1D-DPN-CuAqE	0.420±0.016	91.52±2.08*	4.32±0.14	3	1	3.5±0.53*[a]
T2D-DPN model						
CTL-NOM	0.410±0.007	95.21±0.96	4.31±0.03	3	0	0.8±0.79
CTL-CuAqE	0.412±0.007	96.14±1.09	4.30±0.05	3	0.5	1.0±0.82
T2D-DPN	0.482±0.005*	152.17±1.61*	6.05±0.04*	5	2	6.4±1.17*
T2D-DPN-CuAqE	0.476±0.009*	149.68±1.41*	5.95±0.12*	5	1	3.2±0.63*[a]

Assessing Pain and Distress in Mice	Value
Pain and distress assessment: Normal; well groomed; alert; active; good condition; asleep or calm; normal appetite	0
Mild or anticipated pain and distress: Not well groomed; awkward gait; slightly hunched; looks at wound or pulls away when area touched; mildly agitated	1
Moderate pain and distress: rough hair coat; dirty incision; squinted eyes; moves slowly; walks hunched and/or slowly; depressed or moderately agitated; slight dehydration; pruritic; restless; uncomfortable; not eating or drinking	2
Severe pain and distress: Very rough hair coat; eyes sunken (severe dehydration); slow to move or non-responsive when coaxed; hunched; large abdominal mass; dyspnea; self-mutilating; violent reaction to stimuli or when approached	3

Mouse grimace scale (MGS)
Facial features (action units): Facial expressions in mice indicating pain and/or distress include squinted eyes, contracted skin around nose and ears pulled back. Not present=0 Moderate=1 Severe=2
Orbital tightening is narrowing of the orbital area, with a tightly closed eyelid or an eye squeeze (denoted by wrinkle around eye).
Nose bulge is a rounded extension of skin visible on the bridge of the nose.
Cheek bulge refers to convex appearance of the cheek muscle (between eye and whiskers) from its baseline position.
Ear position: refers to ears pulled apart and back from their baseline position or featuring vertical ridges that form owing to tips of ears being drawn back.
Whisker change: is movement of whiskers from their baseline position either backward, against the face or forward, as if standing on end; whiskers may also clump together piloerection.

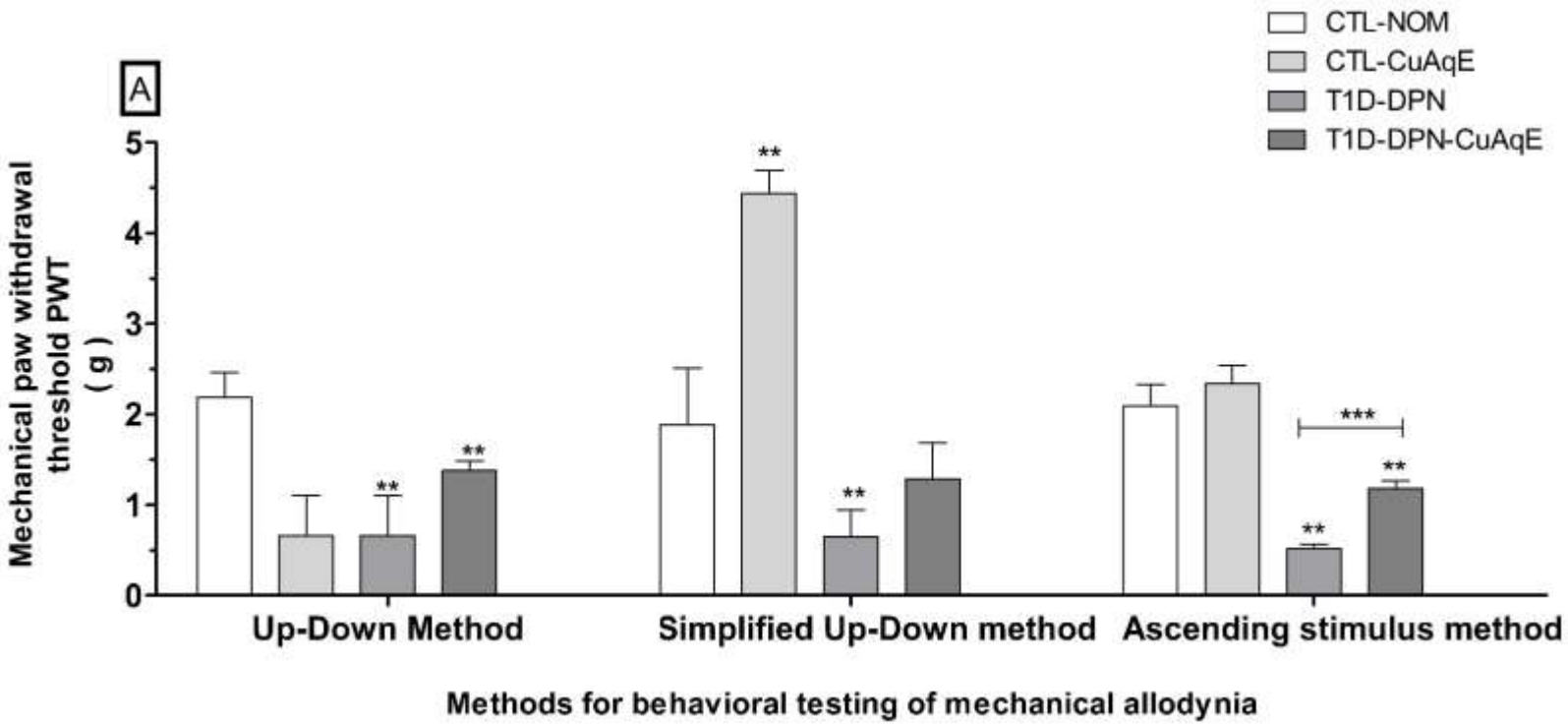
A
CTL-NOM
CTL-CuAqE
T1D-DPN
T1D-DPN-CuAqE
Mechanical paw withdrawal threshold PWT (g)
0
1
2
3
4
5
**
**
**
**
***
**
Up-Down Method
Simplified Up-Down method
Ascending stimulus method
Methods for behavioral testing of mechanical allodynia

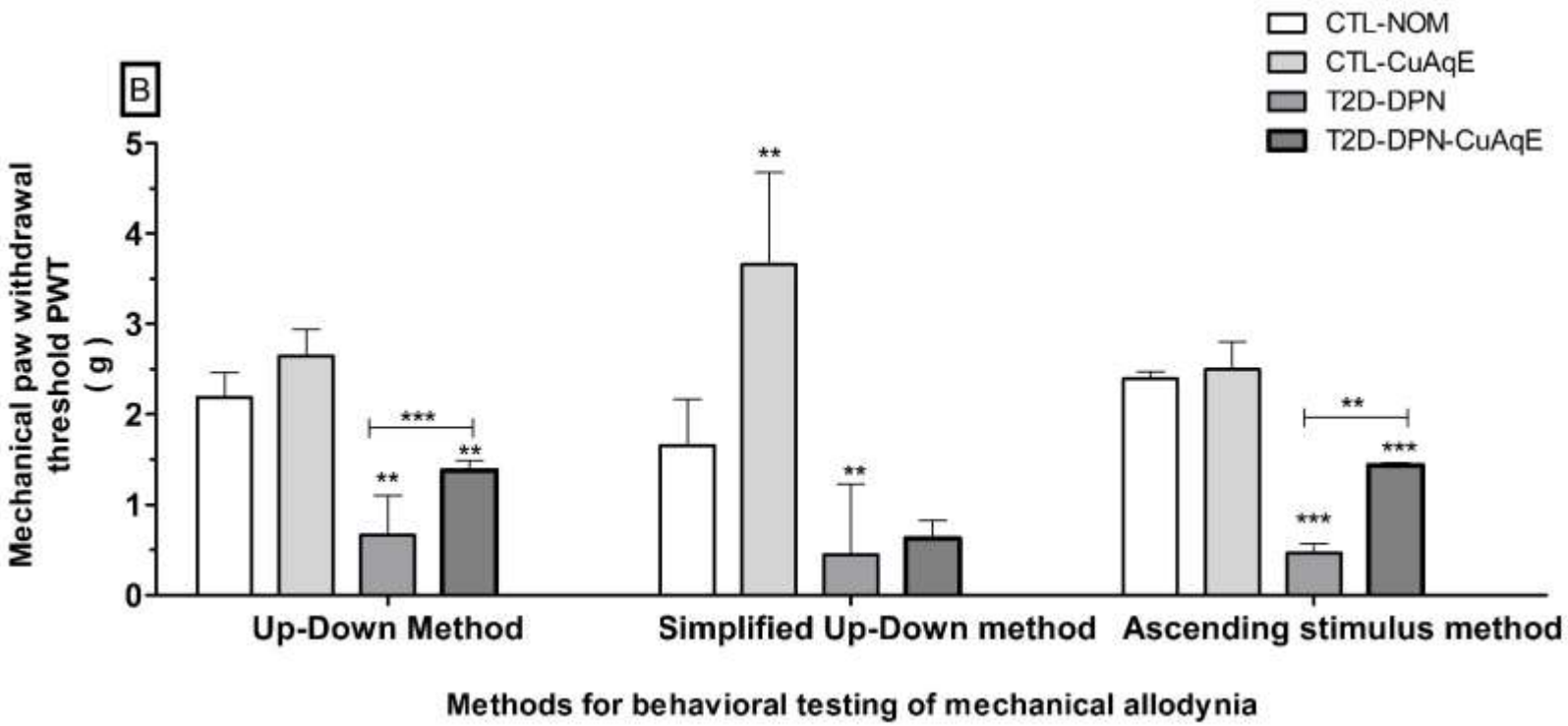

Figure 3. Paw Withdrawal Threshold (PWT) in DPN murine model with phyto-pharmacotherapeutic monitoring of CuAqE.

PWT (g) during mechanical allodynia assessment with von Frey filaments in C57BL/6 male mice that were treated with CuAqE for 8 weeks. (A) in T1D-DPN model and (B) in T2D-DPN model. Values represent means ± SD of each group (n=5). Statistical analysis was performed using one-way ANOVA with Bonferroni's Multiple comparisons test. **p<0,001 vs CTL-NOM. *** p<0,001 vs CTL-T1D or CTL-T2D.

CuAqE-induced increase in mechanical PWT was not significantly greater or equal than CTL-NOM. Alternatively, CuAqE treated mice differ in MGS scores, as they produced MGS attenuation relative to DPN mice associated with neuropathic pain in the rodent by up to 50% ($p < 0.001$) (Table 1).

3.3 Effect of CuAqE on CAP in DPN mice

We analyzed the CAP evoked in sensory SU nerves to observe the electrophysiological effect of CuAqE in DPN model mice (Figure 4). CAP increased gradually in size according to the intensity of the electrical stimulus applied, reaching its maximal amplitude at two times the stimulus threshold (2T).

As illustrated in Figure 5, area CAPs evoked in diabetic SU nerves at 8 weeks in T1D-DPN and T2D-DPN monitoring showed significant differences with respect to control nerves. Since it is clearly observed a decrease in average area on both nerves ($p < 0.001$). Indicating a reduction of the gross neural response at 2x threshold levels in C57BL/6 mice. While at CuAqE tends to increase in area in DPN mice, there are no significant differences. Main effects of treatment on CAP duration are showed in Figure 6. In the T1D-DPN mice there were no differences, but in T2D-DPN mice showed a significant increase respect to CTL-NOM ($p < 0.001$). While that CuAqE treatment did not change CAP latency across 8 weeks. Likewise, CAP Width of DPN mice was greater than that control mice ($p < 0.001$), but CuAqE treatment animals did not differ significantly from either DPN controls or CTL-NOM (Figure 7).

Respect to NCV there are no differences in the T1D-DPN model, however in T2D-DPN we observed a significant decrease in NCV compared with CTL-NOM ($p < 0.001$). CuAqE has no positive effect (Figure 8). Regarding the stimulus threshold, the analysis showed significant main effects of decreasing the threshold in both DPN models compared to the CTL-NOM ($p < 0.001$). CuAqE treatment had a positive but non-significant interaction in both DPN models (Figure 9).

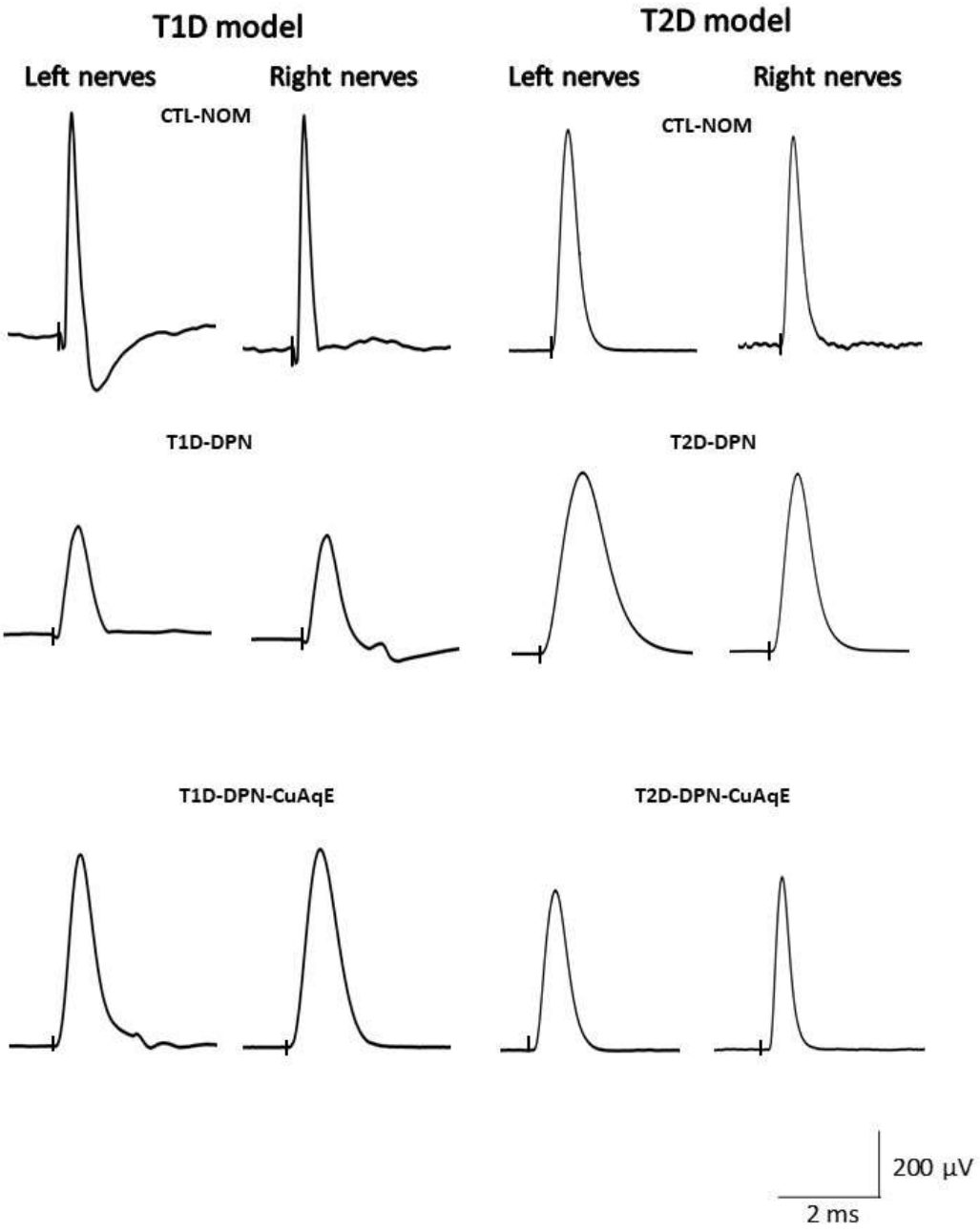

Figure 4. **Compound Action Potentials (CAPs) recorded in SU nerves from DPN murine model with phyto-pharmacotherapeutic monitoring.** Average recordings of CAP evoked with stimulus current pulses two times threshold applied to SU nerves in C57BL/6 male mice that were treated with CuAqE for 8 weeks.

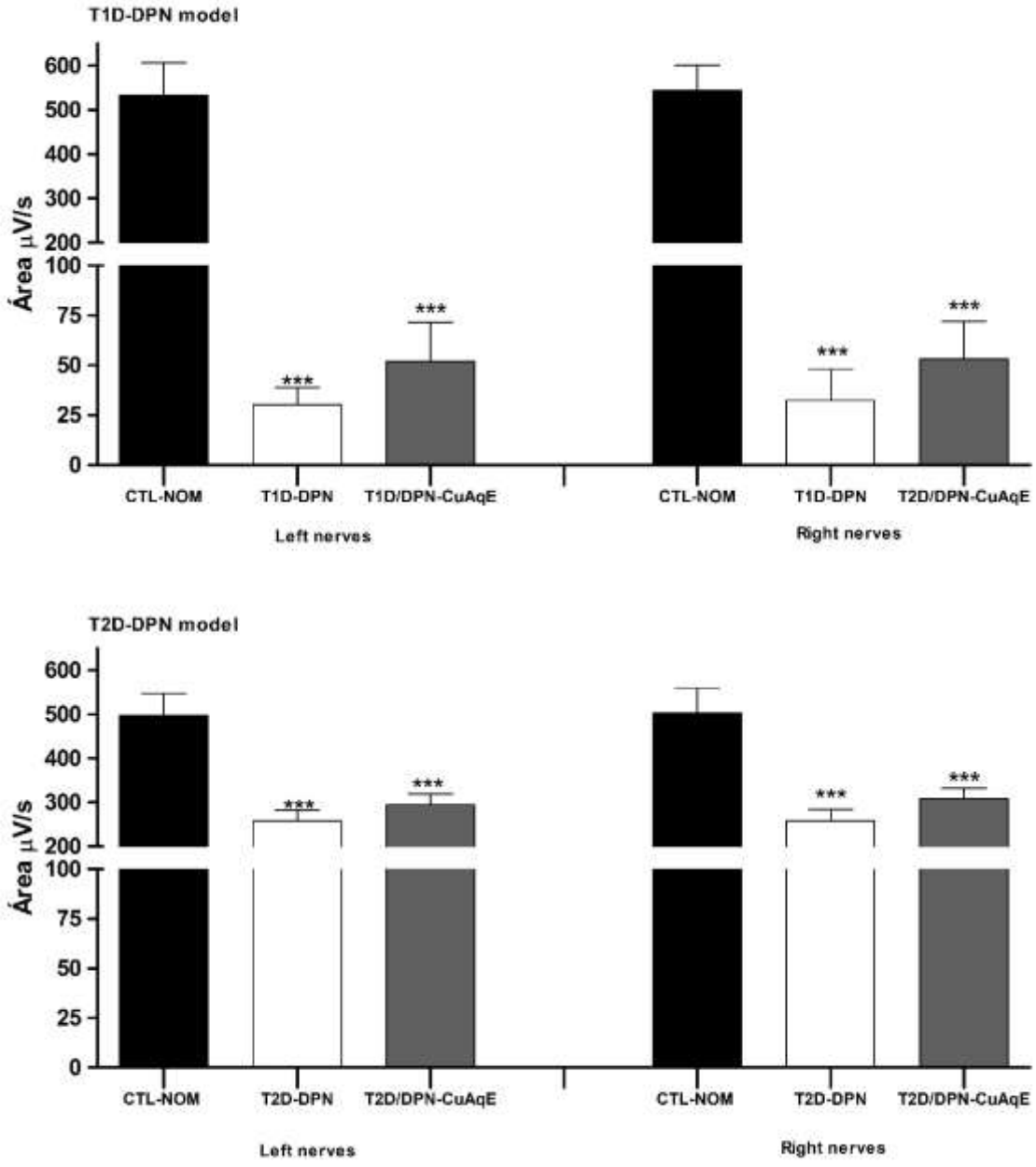

Figure 5. **CAP area recorded in SU nerves of DPN murine model with phyto-pharmacotherapeutic monitoring of CuAqE.** CAP area (µV/s) determined in C57BL/6 male mice that were treated with CuAqE for 8 weeks. Values represent means ± SD of each group (n=5). Statistical analysis was performed using one-way ANOVA with Tukey's multiple comparisons test. ***p<0,001 vs CTL-NOM.

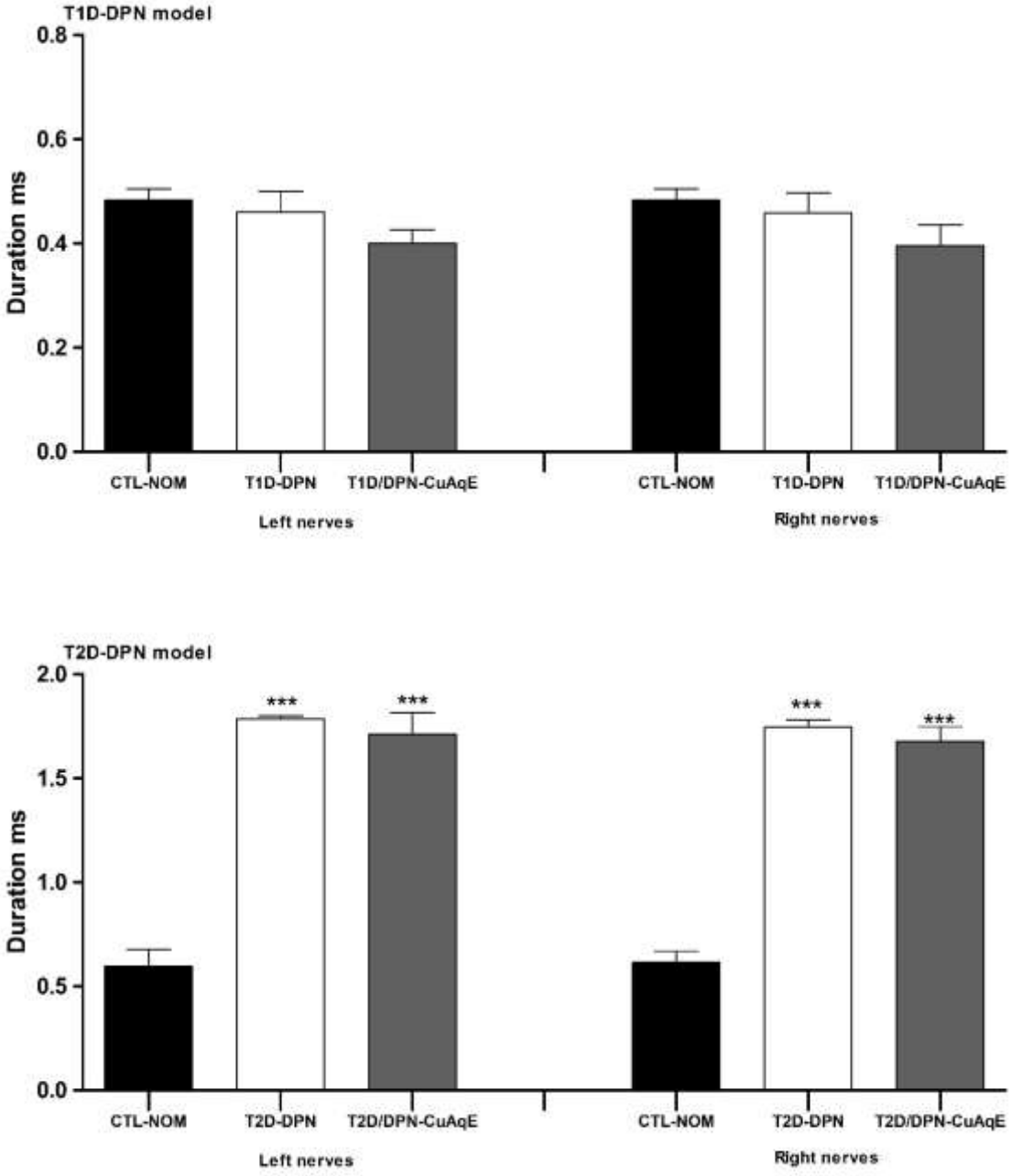

Figure 6. **CAP duration recorded in SU nerves of DPN murine model with phyto-pharmacotherapeutic monitoring of CuAqE.** Latency (ms) determined in C57BL/6 male mice that were treated with CuAqE for 8 weeks. Values represent means ± SD of each group (n=5). Statistical analysis was performed using one-way ANOVA with Tukey's multiple comparisons test. ***p<0,001 vs CTL-NOM.

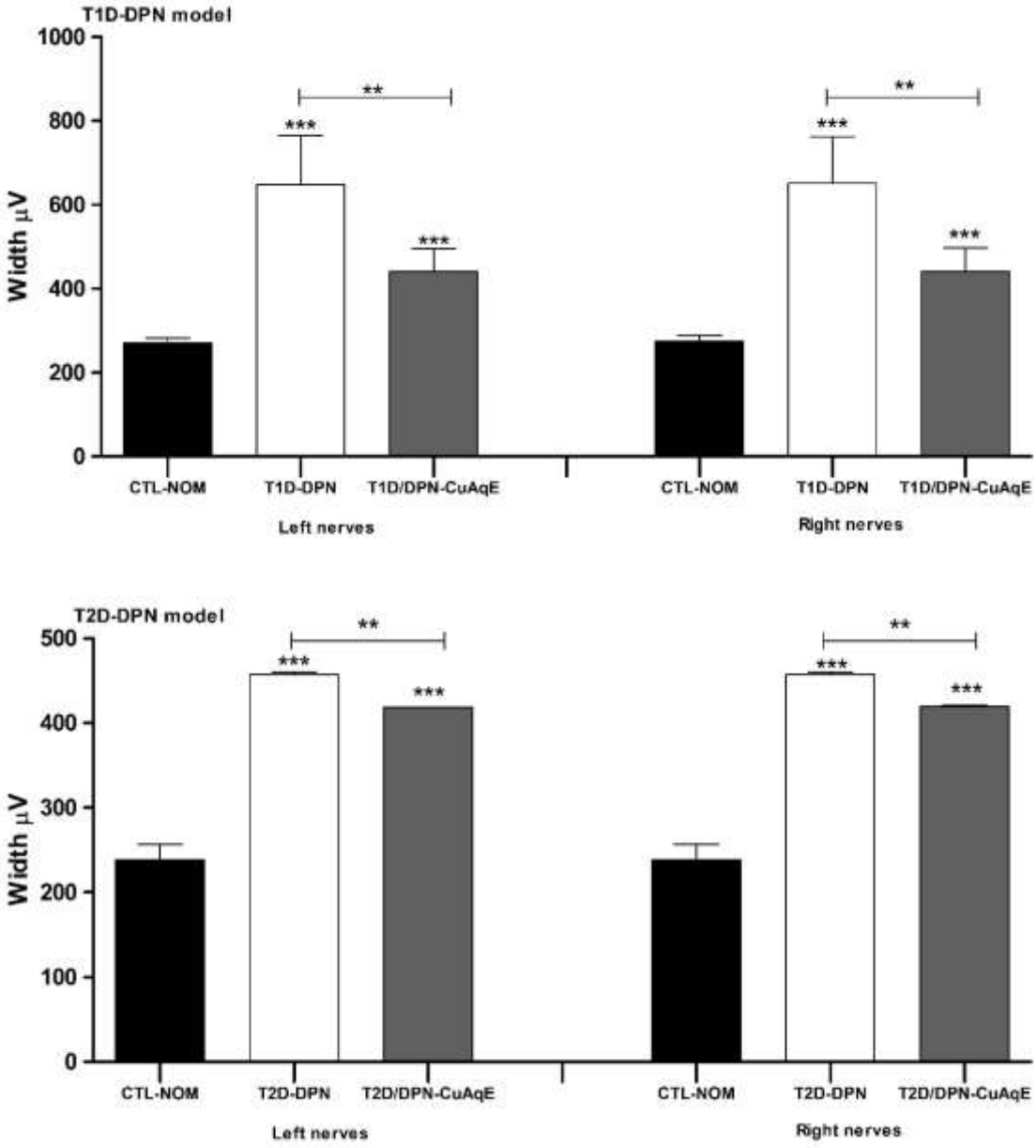

Figure 7. **CAP amplitude recorded in SU nerves of DPN murine model with phyto-pharmacotherapeutic monitoring of CuAqE**. Width (µV) determined in C57BL/6 male mice that were treated with CuAqE for 8 weeks. Values represent means ± SD of each group (n=5). Statistical analysis was performed using one-way ANOVA with Tukey's multiple comparisons test. ***p<0,001 vs CTL-NOM. ** p<0,001 vs CTL-T1D or CTL-T2D.

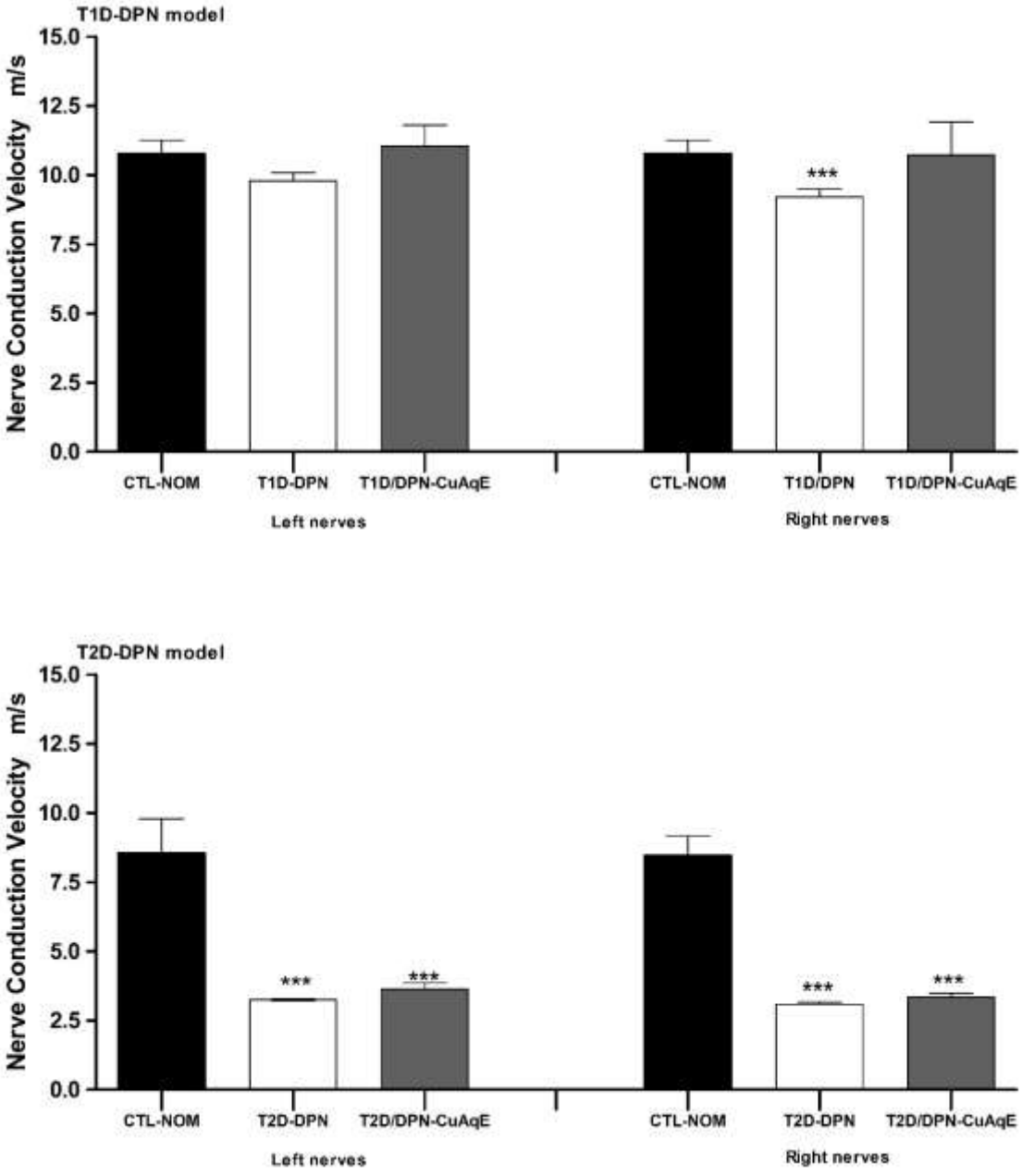

Figure 8. **Nerve Conduction Velocity in SU nerves of DPN murine model with phyto-pharmacotherapeutic monitoring of CuAqE**. NVS (m/s) determined in C57BL/6 male mice that were treated with CuAqE for 8 weeks. Values represent means ± SD of each group (n=5). Statistical analysis was performed using one-way ANOVA with Tukey's multiple comparisons test. ***p<0,001 vs CTL-NOM.

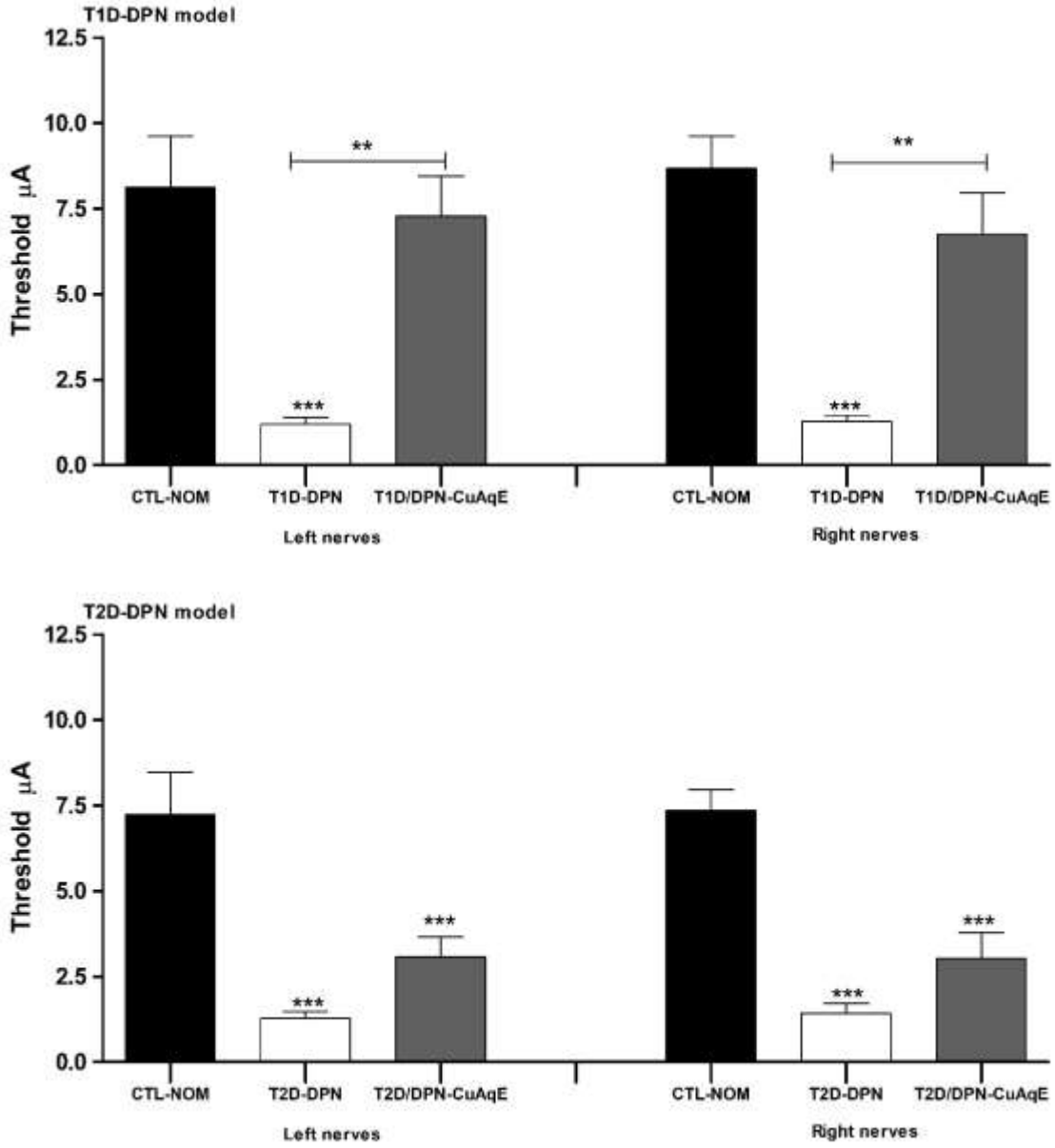

Figure 9. **CAP stimulus threshold recorded in SU nerves of DPN murine model with phyto-pharmacotherapeutic monitoring of CuAqE**. Threshold (µA) determined in C57BL/6 male mice that were treated with CuAqE for 8 weeks. Values represent means ± SD of each group (n=5). Statistical analysis was performed using one-way ANOVA with Tukey's multiple comparisons test. ***p<0,001 vs CTL-NOM. ** p<0,001 vs CTL-T1D or CTL-T2D.

3.4 Determination of AKR1B1 levels

Concentration of AKR1B1 as ascertain antioxidant effect was measured at end of DPN induction period y CuAqE treatment end point. Table 2 depicts an increase in this oxidative stress biomarker. For T1D-DPN increase was 1.9-fold in nervous tissue ($p<0,001$) and without any change in plasma, compared to CTL-NOM. CuAqE treatment significantly inhibits enzyme activity by 26.5% in T1D-DPN-CuAqE ($p<0,001$) in nervous tissue.

In the case of T2D-DPN there is an increase in both nervous tissue and plasma, 2.21 and 0.5 times respectively compared to CTL-NOM ($p<0,001$). CuAqE treatment has a significant inhibitory activity on aldose reductase of more than 50% in T2D-DPN-CuAqE both in nervous tissue and plasma ($p<0,001$).

4. Discussion

4.1 Generation of DPN in DM mice model

Using an MLD-STZ or HFD-DIO in C57BL/6 mice creates a higher level of FBG. T1D-DPN or T2D-DPN were considered diabetics because hyperglycemia progressed showed FBG exceeded 250 mg/dL after MLD-STZ (8 weeks) or DIO-HFD (44 weeks), respectively. FBG in T1D-DPN were significantly higher compared to T2D-DPN.

We have previously demonstrated the hypoglycemic effect of CuAqE in diabetic mouse models. Continue to observe this pharmacotherapeutic activity in this study. Thus, in T1D-DPN-CuAqE allowing glycemic control during the treatment time with CuAqE.

For T2D-DPN-CuAqE indicates that good glucose metabolic control was maintained with high efficacy and optimal hypoglycemic efficiency. This effect may be due to phenolic compounds from plants of *Asteraceae* family to which *Calea urticifolia* belongs. Since they have been reported to have hypoglycemic activity (Ribnicky et. al., 2014).

Table 2. Concentration of Aldose Reductase in DPN murine models with phyto-pharmacotherapeutic monitoring of CuAqE. Aldo-keto reductase family 1, member B1 (aldose reductase, Akr1b1) in C57BL/6 male mice that were treated with CuAqE. Values represent means ± SD of each group (n=10). Statistical analysis was performed using one-way ANOVA with Bonferroni's Multiple comparisons test. * p<0,001 vs CTL-NOM. [a] p<0,001 vs CTL-T1D or CTL-T2D.

ALDOSE REDUCTASE (AKR1B1) NG/ML

T1D MODEL	Left nerve	Right nerve	Plasma levels
CTL-NOM	213.9± 8.1	214.0± 6.4	335.4±58.2
CTL-CUAQE	169.7±18.4	172.5±17.1	335.9±45.9
T1D-DPN	642.1±38.5*	632.2±36.0*	338.0±45.4
T1D-DPN-CUAQE	468.6±27.2*[#]	464.5±23.0*[#]	341.3±51.4
T2D MODEL	**Left nerve**	**Right nerve**	**Plasma levels**
CTL-NOM	276.1±17.9	273.2±17.5	376.1±36.1
CTL-CUAQE	239.5±12.1	241.0±13.9	377.8±42.6
T2D-DPN	733.5±30.3*	877.2±72.1*	564.1± 9.1*
T2D-DPN-CUAQE	382.6±25.9*[#]	385.2±33.4*[#]	527.9± 8.4*[#]

MLD-STZ or HFD-DIO diet in C57BL/6 mice is a model to study the pathogenesis of neuropathic changes that develop in TD1-DPN or TD2-DPN with marked hyperglycemia, as well as others metabolic disorders (Yako et. al. 2023; Stino et. al., 2020). Neuropathic changes are caused by hyperglycemia in both models (Obrosova et. al., 2007; Obrosov et. al., 2017; Umbaugh et. al., 2022; Eid et. al. 2023).

As metabolic disorders (DM) and neuropathy phenotype (DPN) are mimic in these model mice, are useful model to test efficacy of potential therapies such as to evaluate the therapeutic effect of medicinal plants (Watcho et. al., 2011; Yang et. al., 2022; Lucarini et. al., 2019) or drugs against DPN (Chandrasekaran et. al., 2024; Xu, et. al., 2023).

4.2 Effect of CuAqE on neuropathic pain in DPN mice

Pain is an unpleasant sensory and emotional experience associated with actual or potential tissue damage (IASP, 2025). In the long term, it can develop into a debilitating condition (chronic pain) such as neuropathic pain. Despite the validity of the anthropomorphizing of pain in mice and certainly using nociception as the ability to detect a potentially harmful stimulus. No test can measure pain in mice directly.

Accurately and promptly assessing pain in experimental animals is extremely important to avoid unnecessary suffering of the animals and to enhance the reproducibility of experiments. Care in the research facility and ensuring the psychological well-being of research mice is an integral part. Because mice have many behavioral needs that if not met can negatively impact their behavior, physical health, and usefulness for research.

A mouse behavior management plan was implemented through monitoring of mice based on the Guide for the Care and Use of Laboratory Animals (Bloomsmith et. al., 2018). With CuAqE treatment, however, pain thresholds are significantly reduced, according to MGS. It is therefore tempting to speculate that the reduction in facial expression of pain reflects an effect of this medicinal plant on neuropathic pain.

In these experiments to generate DPN and thus neuropathic pain, C57BL/6 mouse strain was used. It has been reported that baseline MGS scores may differ between strains and thus show different pain sensitivities in behavioral assays due to differences in nociceptor expression. In support of this, male C57BL/6 mice have been found to have significantly lower baseline MGS scores than C3H or CD-1 mice from an animal welfare perspective. This is important when evaluating medicinal plants in DPN models (Onuma, et. al., 2024).

Additionally, we used emotional experience in male C57BL/6 mice presumed unpleasant neuropathic pain with two indirect methods to quantify and assess pain-like behaviors such as hind paw withdrawal from a stimulus. Furthermore, the mice took up to 30-45 minutes to acclimatize to the cage before the test was performed (data not shown). We thought this was due to the stress of daily administration of the treatments. However, it has been reported that mice can take up to an hour or more to acclimatize (Deuis & Vetter, 2017).

In the present study, CuAqE produced an increase in the mechanical allodynia induced on DPN mice. Even so, we propose one approach to evaluate circadian variations in biologic functions such as gene expression and protein synthesis in diabetic mice with the purpose of effects of pharmacotherapy with CuAqE effective and tolerance. The expression and function of some types of proteins that regulate susceptibility to drugs and their pharmacokinetics were previously reported to change in a circadian time-dependent manner (Akamine, et. al., 2015).

The intensity of pain in diabetic neuropathy varies in a circadian time-dependent manner. It is well there are differences in circadian properties of pain hypersensitivity in T1D-DPN and T2D-DPN mice. Polyol pathway-induced accumulation of sorbitol in the sciatic nerve modulates circadian properties of diabetes-induced neuropathic pain

hypersensitivity in diabetic mice. In T2D-DPN this accumulation has significant diurnal oscillation (Akamine, et. al., 2018).

CuAqE could be used for the prevention of DPN, since the medicinal plant inhibits aldose reductase activity and suppresses sorbitol synthesis via the polyol pathway. As observed, CuAqE prevented a drastic decrease in PWT in diabetic mice and reduced aldose reductase activity and therefore accumulation of sorbitol in peripheral nerve cells.

4.3 Effect of CuAqE on CAP in DPN mice

In order to analyze the effect of CuAqE in to generate and propagate action potentials in isolated nerves of diabetic mice. We analyzed electrophysiological parameters of CAP responses evoked in the in vitro sural nerve preparation. We found an important reduction in area both models and only increased duration T2D-DPN model of SU nerve-CAP compared with that recorded in control nerves.

These results confirm development of DNP in both diabetic mouse models therefore disrupt myelination and consequently were apparent electrophysiological characteristics altered of mice sensory SU nerve. In summary, the electrophysiological characteristics of the CAP (area, duration, width, threshold and NCV) are modified in both DPN models compared to the control. CuAqE tries to correct these alterations, perhaps due to the severe neuropathic damage as a consequence of the prolonged progression time of the DPN, but it does not manage to do so within the treatment time.

Especially because of developmental time of DM during which cellular mechanisms that underlie such alterations are likely to operate. According to the later, we assume that alterations observed in T1D-DPN model mice of the CAPs recorded in the sural nerves of diabetic mice at 8 weeks after STZ injection days are mainly due to hyperglycemia instead of a neurotoxic effect of STZ (Quiroz-González, et. al., 2016).

Evoked CAPs in this assay are associated with activation of large-diameter, highly-myelinated, and fast-conducting primary somatosensory neurons. Known as Aβ low-threshold mechanoreceptors (Aβ-LTMRs), which normally mediate tactile, discriminative touch, and vibration sensation (Gautam, et. al., 2024). Mediate mechanical hyperalgesia of DPN. CAPs are all-or-nothing events, thus a decrease in the AUC of a CAP evoked by a single electrical pulse represents a decrease in the number of axons conducting a CAP (Nair, et. al., 2023).

However, CuAqE was unable to fully modulate the electrophysiological parameters of PAC, so it is necessary to venture to further explore the effect of this medicinal plant on DPN as a strategy aimed at preventing the progression of DSPN. CuAqE was shown to be a metabolic regulator of FBG in DM, which is one of the targets in holistic management of DPN. There are very few investigations focused on studying the effect of medicinal plants on CAP (Leal-Cardoso et. al., 2004) and study of CAP in DPN since research regularly focuses on electrophysiological evidence of sensory and motor nerve dysfunction (O'Brien et. al., 2014).

Nevertheless, there is evidence suggesting differences in the generation of DPN by T1D and T2D in the inhibition of downstream signaling pathways, biomarker gene expression and degree of deterioration and density of nerve fibers (Sloan & Tesfaye, 2021). Therefore, it is necessary to continue evaluating CuAqE with this work perspective.

4.3 Effect of CuAqE in aldose reductase concentrations on DPN mice

Reported that more and more people support the use of medicinal plant therapy and transition from synthetic drugs to herbal therapies for DPN (Arora et. al., 2021; Tiwari et. al., 2019 and Bilal et. al., 2018). Based on the high compliance of patients towards herbal medicines and the promising efficacy shown by natural antioxidants in the management of DPN (Borgonetti & Galeotti, 2023). In the present work, we investigated capability of CuAqE, at antioxidant dose, to modulate aldose reductase activity in DPN

mice. Agreeing that it has an important inhibitory activity in this key enzyme for the pathophysiology of DNP (Gupta et. al., 2024 and Thakur et. al., 2021).

Otherwise, DPN is well known as one of the severe complications of DM. The development of DPN partially attributes to hyperglycemia and accumulation of sorbitol in neuronal cells due to aldose reductase which is a part of the polyol pathway. Because inhibition of sorbitol dehydrogenase leads to development of the neuropathy in diabetes, aldose reductase is believed as one of the main factors to induce diabetic neuropathy (Gumede et.al., 2022 and Sato, et. al., 2015).

Polyol pathway is one of the more promising targets for diabetic neuropathy, particularly through aldose reductase inhibitor drugs. In our DNP model there was an increase in aldose reductase levels in SU nerve which shows hyperglycemia-induced oxidative stress contributed to DPN pathogenesis. CuAqE was shown to be an aldose reductase inhibitor as it prevents its activation through its antioxidant capacity, indicating that CuAqE could reduce the diabetes-induced oxidative stress and contribute in functional, biochemical and structural recovery of peripheral nerves.

Moreover, inhibition of aldose reductase in T1D mice for inhibitor drug like as Fidarestat, reduced oxidative stress in peripheral nerves and markedly protected mice from diabetes-induced functional deficits (Ho, et. al., 2006). CuAqE could be a potential phytomedicine that inhibits aldose reductase, but its effect in in vitro models and its possible mechanism of action in DPN remain to be explored.

4.4 Final considerations of effect CuAqE in DPN mice

DPN is usually difficult to treat because etiology is heterogeneous and the underlying pathophysiology is complex. Recently, various medicinal plants have been reported effective for the management of DPN as an alternative therapy (Borgonetti & Galeotti, 2023; Lee et. al., 2022; Singh, et. al., 2017; Garg & Adams, et. al., 2012). Most of the

naturally occurring secondary metabolites such as flavonoids, terpenoids, alkaloids bear complicated architectural skeletons and often exhibit diverse biological activities.

These secondary metabolites through their antioxidant potential, which helps in the modulation of DPN (Singh, et. al., 2017). Antioxidant compounds have been reported for CuAqE so it could have potential as an alternative medicine in DPN by modulating the oxidative stress and inflammatory cytokine (Torres, et. al., 2016). Besides for Mexican medicinal plants of the same family, hypoglycemic and antinociceptive effects have been reported (Raafat et. al., 2016).

However, there are evaluations with different perspectives to evaluate medicinal plants with an alternative therapy approach for DPN but they are more directed towards histological or molecular studies (pathophysiology) via Targeting of molecular mechanisms triggering DPN (Ebrahimi et. al., 2019). Mainly in Polyol pathway looking for agonists of aldose reductase by molecular docking (Chavhan et. al., 2025; Gakpey et. al., 2025; Kausar et. al., 2025). Therefore, CuAqE can be explored as a potential aldose reductase inhibitor for pharmacological intervention and management of various neuropathies. Some other research focuses on the management of non-diabetic neuropathy such as chemotherapy-induced neuropathy with medicinal plants (Santos et. al., 2022; Lee et. al., 2021; Liu et. al., 2019; Oveissi et. al., 2019; Wu et. al., 2019; Schloss et. al., 2017).

In parallel, the effect of CuAqE on foot baths can be evaluated in patients with DPN and glycemic management in a controlled trial (Huang et. al., 2024; Fan et. al., 2018) or oral administration (Meizhen et. al., 2023; Zhang et. al., 2020; Zhang et. al., 2019; Jin et. al., 2017) to provide an evidence-based complementary therapeutic approach for treatment of DPN. Further research on the plant's effect in DPN is needed to choose useful alternatives that can shed information in a beneficial direction, given that the molecular and action mechanisms by which CuAqE may intervene in the improvement

of DPN are not yet understood as well as the plants of traditional Chinese medicine (Chen et. al., 2013; Chen & Liu et. al., 2011).

5. Conclusions

In conclusion, present findings showed efficacy of CuAqE in attenuating DNP symptoms without inducing impairment in health and welfare of experimental animals. This activity was produced at dose of 11mg/kg and appears to be related to the capability of extract and of its main constituent's phenolic compounds may be due to the combination of antioxidant, anti-inflammatory and neuroprotective effects by modulating oxidative and pro-inflammatory responses, might CuAqE represent interesting candidate for DNP management.

6. References

1. Adamson Barnes, N. S., Mitchell, V. A., Kazantzis, N. P., & Vaughan, C. W. (2016). Actions of the dual FAAH/MAGL inhibitor JZL195 in a murine neuropathic pain model. British journal of pharmacology, 173(1), 77–87. https://doi.org/10.1111/bph.13337
2. Ahmadzadeh, A. M., Pourali, G., Mirheidari, S. B., Shirazinia, M., Hamedi, M., Mehri, A., Amirbeik, H., Saghebdoust, S., Tayarani-Najaran, Z., Sathyapalan, T., Forouzanfar, F., & Sahebkar, A. (2024). Medicinal Plants for the Treatment of Neuropathic Pain: A Review of Randomized Controlled Trials. Current pharmaceutical biotechnology, 25(5), 534–562. https://doi.org/10.2174/1389201024666230714143538
3. Akamine, T., Koyanagi, S., Kusunose, N., Hashimoto, H., Taniguchi, M., Matsunaga, N., & Ohdo, S. (2015). Dosing time-dependent changes in the analgesic effect of pregabalin on diabetic neuropathy in mice. The Journal of pharmacology and experimental therapeutics, 354(1), 65–72. https://doi.org/10.1124/jpet.115.223891
4. Akamine, T., Kusunose, N., Matsunaga, N., Koyanagi, S., & Ohdo, S. (2018). Accumulation of sorbitol in the sciatic nerve modulates circadian properties of

diabetes-induced neuropathic pain hypersensitivity in a diabetic mouse model. Biochemical and biophysical research communications, 503(1), 181–187. https://doi.org/10.1016/j.bbrc.2018.05.209

5. Alemán-Contreras, R., Gómez-Díaz, R. A., Noyola-García, M. E., Mondragón-González, R., Wacher, N., & Ferreira-Hermosillo, A. (2024). Utility of Fasting C-Peptide for the Diagnostic Differentiation of Patients with Type 1, Type 2 Diabetes, MODY, and LADA. Life (Basel, Switzerland), 14(5), 550. https://doi.org/10.3390/life14050550
6. Arora, K., Tomar, P. C., & Mohan, V. (2021). Diabetic neuropathy: an insight on the transition from synthetic drugs to herbal therapies. Journal of diabetes and metabolic disorders, 20(2), 1773–1784. https://doi.org/10.1007/s40200-021-00830-2
7. Attal, N., & Bouhassira, D. (2021). Advances in the treatment of neuropathic pain. Current opinion in neurology, 34(5), 631–637. https://doi.org/10.1097/WCO.0000000000000980
8. Bello-Chavolla, O. Y., Antonio-Villa, N. E., Fermín-Martínez, C. A., Fernández-Chirino, L., Vargas-Vázquez, A., Ramírez-García, D., Basile-Alvarez, M. R., Hoyos-Lázaro, A. E., Carrillo-Larco, R. M., Wexler, D. J., Manne-Goehler, J., & Seiglie, J. A. (2022). Diabetes-Related Excess Mortality in Mexico: A Comparative Analysis of National Death Registries Between 2017-2019 and 2020. Diabetes care, 45(12), 2957–2966. https://doi.org/10.2337/dc22-0616
9. Beshyah, S. A., Jayyousi, A., Al-Mamari, A. S., Shaaban, A., Ozairi, E. A., Nafach, J., Jallo, M. K. I., Khader, S., & Evans, M. (2024). Current Perspectives in Pre- and Diabetic Peripheral Neuropathy Diagnosis and Management: An Expert Statement for the Gulf Region. Diabetes therapy: research, treatment and education of diabetes and related disorders, 15(12), 2455–2474. https://doi.org/10.1007/s13300-024-01658-8
10. Bilal, M., Iqbal, M. S., Shah, S. B., Rasheed, T., & Iqbal, H. M. N. (2018). Diabetic Complications and Insight into Antidiabetic Potentialities of Ethno- Medicinal

Plants: A Review. Recent patents on inflammation & allergy drug discovery, 12(1), 7–23. https://doi.org/10.2174/1872213X12666180221161410

11. Bloomsmith, M. A., Perlman, J. E., Hutchinson, E., & Sharpless, M. (2018). Behavioral Management Programs to Promote Laboratory Animal Welfare. In R. H. Weichbrod (Eds.) et. al., Management of Animal Care and Use Programs in Research, Education, and Testing. (2nd ed., pp. 63–82). CRC Press/Taylor & Francis. https://doi.org/10.1201/9781315152189-5
12. Bonin, R. P., Bories, C., & De Koninck, Y. (2014). A simplified up-down method (SUDO) for measuring mechanical nociception in rodents using von Frey filaments. Molecular pain, 10, 26. https://doi.org/10.1186/1744-8069-10-26
13. Borgonetti, V., & Galeotti, N. (2023). Honokiol-Rich Magnolia officinalis Bark Extract Attenuates Trauma-Induced Neuropathic Pain. Antioxidants (Basel, Switzerland), 12(8), 1518. https://doi.org/10.3390/antiox12081518
14. Burkholder, T., Foltz, C., Karlsson, E., Linton, C. G., & Smith, J. M. (2012). Health Evaluation of Experimental Laboratory Mice. Current protocols in mouse biology, 2, 145–165. https://doi.org/10.1002/9780470942390.mo110217
15. Chandrasekaran, K., Najimi, N., Sagi, A. R., Yarlagadda, S., Salimian, M., Arvas, M. I., Hedayat, A. F., Kevas, Y., Kadakia, A., Kristian, T., & Russell, J. W. (2024). NAD+ Precursors Reverse Experimental Diabetic Neuropathy in Mice. International journal of molecular sciences, 25(2), 1102. https://doi.org/10.3390/ijms25021102
16. Chavhan, A. B., Kola, H., Bobba, B., Verma, Y. K., & Verma, M. K. (2025). In-silico study and in-vitro validations for an affinity of mangiferin with aldose reductase: Investigating potential in tackling diabetic retinopathy. Computational biology and chemistry, 114, 108281. https://doi.org/10.1016/j.compbiolchem.2024.108281
17. Chen, W., Zhang, Y., & Liu, J. P. (2011). Chinese herbal medicine for diabetic peripheral neuropathy. *The Cochrane database of systematic reviews*, (6), CD007796. https://doi.org/10.1002/14651858.CD007796.pub2

18. Chen, W., Zhang, Y., Li, X., Yang, G., & Liu, J. P. (2013). Chinese herbal medicine for diabetic peripheral neuropathy. The Cochrane database of systematic reviews, 2013(10), CD007796. https://doi.org/10.1002/14651858.CD007796.pub3
19. Cole, J. B., & Florez, J. C. (2020). Genetics of diabetes mellitus and diabetes complications. Nature reviews. Nephrology, 16(7), 377–390. https://doi.org/10.1038/s41581-020-0278-5
20. Deuis, J. R., Dvorakova, L. S., & Vetter, I. (2017). Methods Used to Evaluate Pain Behaviors in Rodents. Frontiers in molecular neuroscience, 10, 284. https://doi.org/10.3389/fnmol.2017.00284
21. Ebrahimi, F., Farzaei, M. H., Bahramsoltani, R., Heydari, M., Naderinia, K., & Rahimi, R. (2019). Plant-derived medicines for neuropathies: a comprehensive review of clinical evidence. Reviews in the neurosciences, 30(6), 671–684. https://doi.org/10.1515/revneuro-2018-0097
22. Eid, S. A., Rumora, A. E., Beirowski, B., Bennett, D. L., Hur, J., Savelieff, M. G., & Feldman, E. L. (2023). New perspectives in diabetic neuropathy. Neuron, 111(17), 2623–2641. https://doi.org/10.1016/j.neuron.2023.05.003
23. Elafros, M. A., Andersen, H., Bennett, D. L., Savelieff, M. G., Viswanathan, V., Callaghan, B. C., & Feldman, E. L. (2022). Towards prevention of diabetic peripheral neuropathy: clinical presentation, pathogenesis, and new treatments. The Lancet. Neurology, 21(10), 922–936. https://doi.org/10.1016/S1474-4422(22)00188-0
24. Fan, G., Huang, H., Lin, Y., Zheng, G., Tang, X., Fu, Y., Wei, H., Zhao, L., Liu, Z., Wang, M., Wang, S., Li, Q., Fang, Z., Zhou, Y., Dai, F., & Qiu, X. (2018). Herbal medicine foot bath for the treatment of diabetic peripheral neuropathy: protocol for a randomized, double-blind and controlled trial. Trials, 19(1), 483. https://doi.org/10.1186/s13063-018-2856-4
25. Faselis, C., Katsimardou, A., Imprialos, K., Deligkaris, P., Kallistratos, M., & Dimitriadis, K. (2020). Microvascular Complications of Type 2 Diabetes Mellitus.

Current vascular pharmacology, 18(2), 117–124. https://doi.org/10.2174/1570161117666190502103733

26. Faselis, C., Katsimardou, A., Imprialos, K., Deligkaris, P., Kallistratos, M., & Dimitriadis, K. (2020). Microvascular Complications of Type 2 Diabetes Mellitus. Current vascular pharmacology, 18(2), 117–124. https://doi.org/10.2174/1570161117666190502103733
27. Feldman, E. L., Nave, K. A., Jensen, T. S., & Bennett, D. L. H. (2017). New Horizons in Diabetic Neuropathy: Mechanisms, Bioenergetics, and Pain. Neuron, 93(6), 1296–1313. https://doi.org/10.1016/j.neuron.2017.02.005
28. Gakpey, M. E. L., Aidoo, S. A., Jumah, T. A., Hanson, G., Msipa, S., Mbaoji, F. N., Bukola, O., Tjale, P. C., Sangare, M., Tebourbi, H., & Awe, O. I. (2025). Targeting aldose reductase using natural African compounds as promising agents for managing diabetic complications. Frontiers in bioinformatics, 5, 1499255. https://doi.org/10.3389/fbinf.2025.1499255
29. Garg, G., & Adams, J. D. (2012). Treatment of neuropathic pain with plant medicines. Chinese journal of integrative medicine, 18(8), 565–570. https://doi.org/10.1007/s11655-012-1188-6
30. Gautam, M., Yamada, A., Yamada, A. I., Wu, Q., Kridsada, K., Ling, J., Yu, H., Dong, P., Ma, M., Gu, J., & Luo, W. (2024). Distinct local and global functions of mouse Aβ low-threshold mechanoreceptors in mechanical nociception. Nature communications, 15(1), 2911. https://doi.org/10.1038/s41467-024-47245-0
31. Goyal R, Singhal M, Jialal I. Type 2 Diabetes. [Updated 2023 Jun 23]. In: StatPearls [Internet]. Treasure Island (FL): StatPearls Publishing; 2025 Jan-. Available from: https://www.ncbi.nlm.nih.gov/books/NBK513253/
32. Gumede, N., Ngubane, P., & Khathi, A. (2022). Assessing the risk factors for myocardial infarction in diet-induced prediabetes: myocardial tissue changes. BMC cardiovascular disorders, 22(1), 350. https://doi.org/10.1186/s12872-022-02758-8
33. Gupta J. K. (2024). The Role of Aldose Reductase in Polyol Pathway: An Emerging Pharmacological Target in Diabetic Complications and Associated

Morbidities. Current pharmaceutical biotechnology, 25(9), 1073–1081. https://doi.org/10.2174/1389201025666230830125147

34. Ho, E. C., Lam, K. S., Chen, Y. S., Yip, J. C., Arvindakshan, M., Yamagishi, S., Yagihashi, S., Oates, P. J., Ellery, C. A., Chung, S. S., & Chung, S. K. (2006). Aldose reductase-deficient mice are protected from delayed motor nerve conduction velocity, increased c-Jun NH2-terminal kinase activation, depletion of reduced glutathione, increased superoxide accumulation, and DNA damage. Diabetes, 55(7), 1946–1953. https://doi.org/10.2337/db05-1497
35. Huang, H. Y., Lin, Y. P., Wei, H., Fu, Y., Zhou, Y. H., Fang, Z. H., Qiu, X. T., Wang, M., Li, Q. B., Li, S. S., Wang, S. D., Dai, F., Liu, Z. J., Zhao, L., Wen, J. X., Wu, L. Y., Zeng, H. Y., Zhang, J. M., Lu, Q. Y., He, L., … Fan, G. J. (2024). Effect and Safety of Herbal Medicine Foot Baths in Patients with Diabetic Peripheral Neuropathy: A Multicenter Double-Blind Randomized Controlled Trial. Chinese journal of integrative medicine, 30(3), 195–202. https://doi.org/10.1007/s11655-024-3900-8
36. Huerta-Reyes, M., Tavera-Hernández, R., Alvarado-Sansininea, J. J., & Jiménez-Estrada, M. (2022). Selected Species of the Cucurbitaceae Family Used in Mexico for the Treatment of Diabetes Mellitus. Molecules (Basel, Switzerland), 27(11), 3440. https://doi.org/10.3390/molecules27113440
37. International Association for the Study of Pain, IASP. (2025). Pain Terms, A Current List with Definitions and Notes on Usage" in Classification of Chronic Pain, Second Edition, IASP Task Force on Taxonomy, edited by H. Merskey and N. Bogduk, IASP Press, Seattle, ©1994. pp 209-214. https://www.iasp-pain.org/resources/terminology/
38. Jin, D., Huang, W. J., Meng, X., Yang, F., Zheng, Y. J., Bao, Q., Zhang, M. Z., Yang, Y. N., Ni, Q., Lian, F. M., & Tong, X. L. (2017). Chinese herbal medicine TangBi Formula treatment of patients with type 2 diabetic distal symmetric polyneuropathy disease: study protocol for a randomized controlled trial. Trials, 18(1), 631. https://doi.org/10.1186/s13063-017-2345-1

39. Kausar, M. A., Anwar, S., Elagib, H. M., Parveen, K., Hussain, M. A., Najm, M. Z., Nair, A., & Kar, S. (2025). GC-MS Profiling of Ethanol-Extracted Polyherbal Compounds from Medicinal Plant (Citrullus colocynthis, Curcuma longa, and Myristica fragrans): In Silico and Analytical Insights into Diabetic Neuropathy Therapy via Targeting the Aldose Reductase. Current issues in molecular biology, 47(2), 75. https://doi.org/10.3390/cimb47020075
40. Langford, D. J., Bailey, A. L., Chanda, M. L., Clarke, S. E., Drummond, T. E., Echols, S., Glick, S., Ingrao, J., Klassen-Ross, T., Lacroix-Fralish, M. L., Matsumiya, L., Sorge, R. E., Sotocinal, S. G., Tabaka, J. M., Wong, D., van den Maagdenberg, A. M., Ferrari, M. D., Craig, K. D., & Mogil, J. S. (2010). Coding of facial expressions of pain in the laboratory mouse. Nature methods, 7(6), 447–449. https://doi.org/10.1038/nmeth.1455
41. Leal-Cardoso, J. H., Moreira, M. R., da Cruz, G. M., de Morais, S. M., Lahlou, M. S., & Coelho-de-Souza, A. N. (2004). Effects of essential oil of Alpinia zerumbet on the compound action potential of the rat sciatic nerve. Phytomedicine : international journal of phytotherapy and phytopharmacology, 11(6), 549–553. https://doi.org/10.1016/j.phymed.2003.07.008
42. Lee, C. W., Jin, J. S., Kwon, S., Jin, C., Cho, S. Y., Park, S. U., Jung, W. S., Moon, S. K., Park, J. M., Ko, C. N., & Cho, K. H. (2022). Are herbal medicines alone or in combination for diabetic peripheral neuropathy more effective than methylcobalamin alone? A systematic review and meta-analysis. Complementary therapies in clinical practice, 49, 101657. https://doi.org/10.1016/j.ctcp.2022.101657
43. Lee, J. H., Kim, N., Park, S., & Kim, S. K. (2021). Analgesic effects of medicinal plants and phytochemicals on chemotherapy-induced neuropathic pain through glial modulation. Pharmacology research & perspectives, 9(6), e00819. https://doi.org/10.1002/prp2.819
44. Liu, Y. P., Shao, S. J., & Guo, H. D. (2020). Schwann cells apoptosis is induced by high glucose in diabetic peripheral neuropathy. Life sciences, 248, 117459. https://doi.org/10.1016/j.lfs.2020.117459

45. Liu, Y., May, B. H., Zhang, A. L., Guo, X., Lu, C., Xue, C. C., & Zhang, H. (2019). Integrative Herbal Medicine for Chemotherapy-Induced Peripheral Neuropathy and Hand-Foot Syndrome in Colorectal Cancer: A Systematic Review and Meta-Analysis. Integrative cancer therapies, 18, 1534735418817833. https://doi.org/10.1177/1534735418817833
46. Lovic, D., Piperidou, A., Zografou, I., Grassos, H., Pittaras, A., & Manolis, A. (2020). The Growing Epidemic of Diabetes Mellitus. Current vascular pharmacology, 18(2), 104–109. https://doi.org/10.2174/1570161117666190405165911
47. Lucarini, E., Pagnotta, E., Micheli, L., Parisio, C., Testai, L., Martelli, A., Calderone, V., Matteo, R., Lazzeri, L., Di Cesare Mannelli, L., & Ghelardini, C. (2019). Eruca sativa Meal against Diabetic Neuropathic Pain: An H2S-Mediated Effect of Glucoerucin. Molecules (Basel, Switzerland), 24(16), 3006. https://doi.org/10.3390/molecules24163006
48. Lucía, C. A., Jacqueline, B. R., Alberto, B. L., David, B. A., & Beatriz, R. A. (2021). Actualized inventory of medicinal plants used in traditional medicine in Oaxaca, Mexico. Journal of ethnobiology and ethnomedicine, 17(1), 7. https://doi.org/10.1186/s13002-020-00431-y
49. Meizhen, Z., Xiaohui, H., Yiting, T., Yupeng, C., Puyu, H. E., Liming, Z., Bing, P., & Qing, N. I. (2023). Efficacy and safety of Buyang Huanwu decoction for diabetic peripheral neuropathy: a systematic review and Metaanalysis. Journal of traditional Chinese medicine = Chung i tsa chih ying wen pan, 43(5), 841–850. https://doi.org/10.19852/j.cnki.jtcm.20230802.002
50. Montoya, A., Gallardo-Rincón, H., Silva-Tinoco, R., García-Cerde, R., Razo, C., Ong, L., Stafford, L., Lenox, H., & Tapia-Conyer, R. (2023). Type 2 diabetes epidemic in Mexico. Burden of disease 1990-2021 analysis and implications for public policies. Epidemia de diabetes tipo 2 en México. Análisis de la carga de la enfermedad 1990-2021 e implicaciones en la política pública. Gaceta medica de Mexico, 159(6), 474–486. https://doi.org/10.24875/GMM.M24000835

51. Nair, S. S., Pavelkova, N., Murphy, C. M., Kollarik, M., & Taylor-Clark, T. E. (2023). Action potential conduction in the mouse and rat vagus nerve is dependent on multiple voltage-gated sodium channels (NaV1s). Journal of neurophysiology, 130(3), 684–693. https://doi.org/10.1152/jn.00041.2023
52. O'Brien, P. D., Sakowski, S. A., & Feldman, E. L. (2014). Mouse models of diabetic neuropathy. ILAR journal, 54(3), 259–272. https://doi.org/10.1093/ilar/ilt052
53. Obrosov, A., Shevalye, H., Coppey, L. J., & Yorek, M. A. (2017). Effect of tempol on peripheral neuropathy in diet-induced obese and high-fat fed/low-dose streptozotocin-treated C57Bl6/J mice. Free radical research, 51(4), 360–367. https://doi.org/10.1080/10715762.2017.1315767
54. Obrosova, I. G., Ilnytska, O., Lyzogubov, V. V., Pavlov, I. A., Mashtalir, N., Nadler, J. L., & Drel, V. R. (2007). High-fat diet induced neuropathy of pre-diabetes and obesity: effects of "healthy" diet and aldose reductase inhibition. Diabetes, 56(10), 2598–2608. https://doi.org/10.2337/db06-1176
55. Onuma, K., Watanabe, M., & Sasaki, N. (2024). The grimace scale: a useful tool for assessing pain in laboratory animals. Experimental animals, 73(3), 234–245. https://doi.org/10.1538/expanim.24-0010
56. Oveissi, V., Ram, M., Bahramsoltani, R., Ebrahimi, F., Rahimi, R., Naseri, R., Belwal, T., Devkota, H. P., Abbasabadi, Z., & Farzaei, M. H. (2019). Medicinal plants and their isolated phytochemicals for the management of chemotherapy-induced neuropathy: therapeutic targets and clinical perspective. Daru : journal of Faculty of Pharmacy, Tehran University of Medical Sciences, 27(1), 389–406. https://doi.org/10.1007/s40199-019-00255-6
57. Previtali S. C. (2021). Peripheral Nerve Development and the Pathogenesis of Peripheral Neuropathy: the Sorting Point. Neurotherapeutics : the journal of the American Society for Experimental NeuroTherapeutics, 18(4), 2156–2168. https://doi.org/10.1007/s13311-021-01080-z
58. Quiroz-González S, Rodríguez-Torres EE, Segura-Alegría B, Pereyra-Venegas J, Lopez-Gomez RE, Jiménez-Estrada I. (2016). Detrended fluctuation analysis

of compound action potentials recorded in the cutaneous nerves of diabetic rats. Chaos Solitons Fract 83:223–233. https://doi.org/10.1016/j.chaos.2015.12.011

59. Raafat, K., Wurglics, M., & Schubert-Zsilavecz, M. (2016). Prunella vulgaris L. active components and their hypoglycemic and antinociceptive effects in alloxan-induced diabetic mice. Biomedicine & pharmacotherapy = Biomedecine & pharmacotherapie, 84, 1008–1018. https://doi.org/10.1016/j.biopha.2016.09.095
60. Ribnicky, D. M., Roopchand, D. E., Poulev, A., Kuhn, P., Oren, A., Cefalu, W. T., & Raskin, I. (2014). Artemisia dracunculus L. polyphenols complexed to soy protein show enhanced bioavailability and hypoglycemic activity in C57BL/6 mice. Nutrition (Burbank, Los Angeles County, Calif.), 30(7-8 Suppl), S4–S10. https://doi.org/10.1016/j.nut.2014.03.009
61. Santos, W. B. D. R., Guimarães, J. O., Pina, L. T. S., Serafini, M. R., & Guimarães, A. G. (2022). Antinociceptive effect of plant-based natural products in chemotherapy-induced peripheral neuropathies: A systematic review. Frontiers in pharmacology, 13, 1001276. https://doi.org/10.3389/fphar.2022.1001276
62. Sato, D., Kusunoki, M., Shinzawa, G., Feng, Z., Nishina, A., & Nakamura, T. (2015). Effects of aldose reductase inhibitor on microneurographically assessed peripheral sympathetic nerve activity in rats. Autonomic neuroscience: basic & clinical, 193, 69–73. https://doi.org/10.1016/j.autneu.2015.08.005
63. Schloss, J., Colosimo, M., & Vitetta, L. (2017). Herbal medicines and chemotherapy induced peripheral neuropathy (CIPN): A critical literature review. Critical reviews in food science and nutrition, 57(6), 1107–1118. https://doi.org/10.1080/10408398.2014.889081
64. Selvarajah, D., Kar, D., Khunti, K., Davies, M. J., Scott, A. R., Walker, J., & Tesfaye, S. (2019). Diabetic peripheral neuropathy: advances in diagnosis and strategies for screening and early intervention. The lancet. Diabetes & endocrinology, 7(12), 938–948. https://doi.org/10.1016/S2213-8587(19)30081-6

65. Singh, H., Bhushan, S., Arora, R., Singh Buttar, H., Arora, S., & Singh, B. (2017). Alternative treatment strategies for neuropathic pain: Role of Indian medicinal plants and compounds of plant origin-A review. Biomedicine & pharmacotherapy = Biomedecine & pharmacotherapie, 92, 634–650. https://doi.org/10.1016/j.biopha.2017.05.079
66. Sloan, G., Selvarajah, D., & Tesfaye, S. (2021). Pathogenesis, diagnosis and clinical management of diabetic sensorimotor peripheral neuropathy. Nature reviews. Endocrinology, 17(7), 400–420. https://doi.org/10.1038/s41574-021-00496-z
67. Stino, A. M., Rumora, A. E., Kim, B., & Feldman, E. L. (2020). Evolving concepts on the role of dyslipidemia, bioenergetics, and inflammation in the pathogenesis and treatment of diabetic peripheral neuropathy. Journal of the peripheral nervous system : JPNS, 25(2), 76–84. https://doi.org/10.1111/jns.12387
68. Tang, W. H., Martin, K. A., & Hwa, J. (2012). Aldose reductase, oxidative stress, and diabetic mellitus. Frontiers in pharmacology, 3, 87. https://doi.org/10.3389/fphar.2012.00087
69. Thakur, S., Gupta, S. K., Ali, V., Singh, P., & Verma, M. (2021). Aldose Reductase: a cause and a potential target for the treatment of diabetic complications. Archives of pharmacal research, 44(7), 655–667. https://doi.org/10.1007/s12272-021-01343-5
70. Tiwari, R., Siddiqui, M. H., Mahmood, T., Bagga, P., Ahsan, F., & Shamim, A. (2019). Herbal Remedies: A Boon for Diabetic Neuropathy. Journal of dietary supplements, 16(4), 470–490. https://doi.org/10.1080/19390211.2018.1441203
71. Torres-Rodríguez, M. L., García-Chávez, E., Berhow, M., & de Mejia, E. G. (2016). Anti-inflammatory and anti-oxidant effect of *Calea urticifolia* lyophilized aqueous extract on lipopolysaccharide-stimulated RAW 264.7 macrophages. Journal of ethnopharmacology, 188, 266–274. https://doi.org/10.1016/j.jep.2016.04.057
72. Umbaugh, D. S., Maciejewski, J. C., Wooten, J. S., & Guilford, B. L. (2022). Neuronal Inflammation is Associated with Changes in Epidermal Innervation in

High Fat Fed Mice. Frontiers in physiology, 13, 891550. https://doi.org/10.3389/fphys.2022.891550

73. Watcho, P., Stavniichuk, R., Ribnicky, D. M., Raskin, I., & Obrosova, I. G. (2010). High-fat diet-induced neuropathy of prediabetes and obesity: effect of PMI-5011, an ethanolic extract of Artemisia dracunculus L. Mediators of inflammation, 2010, 268547. https://doi.org/10.1155/2010/268547
74. Watcho, P., Stavniichuk, R., Tane, P., Shevalye, H., Maksimchyk, Y., Pacher, P., & Obrosova, I. G. (2011). Evaluation of PMI-5011, an ethanolic extract of Artemisia dracunculus L., on peripheral neuropathy in streptozotocin-diabetic mice. International journal of molecular medicine, 27(3), 299–307. https://doi.org/10.3892/ijmm.2011.597
75. Wu, B. Y., Liu, C. T., Su, Y. L., Chen, S. Y., Chen, Y. H., & Tsai, M. Y. (2019). A review of complementary therapies with medicinal plants for chemotherapy-induced peripheral neuropathy. Complementary therapies in medicine, 42, 226–232. https://doi.org/10.1016/j.ctim.2018.11.022
76. Xu, J. W., Xu, X., Ling, Y., Wang, Y. C., Huang, Y. J., Yang, J. Z., Wang, J. Y., & Shen, X. (2023). Vincamine as an agonist of G-protein-coupled receptor 40 effectively ameliorates diabetic peripheral neuropathy in mice. Acta pharmacologica Sinica, 44(12), 2388–2403. https://doi.org/10.1038/s41401-023-01135-1
77. Yako, H., Niimi, N., Takaku, S., & Sango, K. (2023). Advantages of omics approaches for elucidating metabolic changes in diabetic peripheral neuropathy. Frontiers in endocrinology, 14, 1208441. https://doi.org/10.3389/fendo.2023.1208441
78. Yang, J., Wei, Y., Zhao, T., Li, X., Zhao, X., Ouyang, X., Zhou, L., Zhan, X., Qian, M., Wang, J., & Shen, X. (2022). Magnolol effectively ameliorates diabetic peripheral neuropathy in mice. Phytomedicine : international journal of phytotherapy and phytopharmacology, 107, 154434. https://doi.org/10.1016/j.phymed.2022.154434

79. Yang, K., Wang, Y., Li, Y. W., Chen, Y. G., Xing, N., Lin, H. B., Zhou, P., & Yu, X. P. (2022). Progress in the treatment of diabetic peripheral neuropathy. Biomedicine & pharmacotherapy = Biomedecine & pharmacotherapie, 148, 112717. https://doi.org/10.1016/j.biopha.2022.112717
80. Zempoalteca, R., Porras, M. G., Moreno-Pérez, S., Ramirez-Funez, G., Aguirre-Benítez, E. L., González Del Pliego, M., Mariscal-Tovar, S., Mendoza-Garrido, M. E., Hoffman, K. L., Jiménez-Estrada, I., & Melo, A. I. (2018). Early postnatal development of electrophysiological and histological properties of sensory sural nerves in male rats that were maternally deprived and artificially reared: Role of tactile stimulation. Developmental neurobiology, 78(4), 351–362. https://doi.org/10.1002/dneu.22561
81. Zhang, X., Wang, H., Zhang, Y., Liu, Y., Wang, Z., Du, Q., & Xie, C. (2020). Danggui Sini decoction for treating diabetic peripheral neuropathy: A protocol of systematic review and meta-analysis of randomized controlled trials. Medicine, 99(21), e20482. https://doi.org/10.1097/MD.0000000000020482
82. Zhang, Y., Gong, G., Zhang, X., Zhou, L., Xie, H., Tian, Y., & Xie, C. (2019). Huangqi Guizhi Wuwu decoction for diabetic peripheral neuropathy: Protocol for a systematic review. Medicine, 98(31), e16696. https://doi.org/10.1097/MD.0000000000016696
83. Zheng, Y., Ley, S. H., & Hu, F. B. (2018). Global aetiology and epidemiology of type 2 diabetes mellitus and its complications. Nature reviews. Endocrinology, 14(2), 88–98. https://doi.org/10.1038/nrendo.2017.151
84. Zhu, J., Hu, Z., Luo, Y., Liu, Y., Luo, W., Du, X., Luo, Z., Hu, J., & Peng, S. (2024). Diabetic peripheral neuropathy: pathogenetic mechanisms and treatment. Frontiers in endocrinology, 14, 1265372. https://doi.org/10.3389/fendo.2023.1265372

7. CONCLUSIONES GENERALES

Finalmente, proporcionamos directrices para el diseño experimental de DM en ratones para la evaluación de plantas medicinales como lo fue con *Calea urticifolia*, las cuales pueden servir como herramientas para investigar la influencia farmacológica en el metabolismo de la glucosa cuando se administran concomitantemente plantas medicinales y fármacos convencionales.

El uso de medicamentos herbales (solos o en combinación con medicamentos alopáticos) para tratar los síntomas de la diabetes es común en México. Actualmente, existen al menos 800 plantas mexicanas que se utilizan para tratar la diabetes. Desafortunadamente, solo unas pocas de estas especies han sido analizadas para confirmar su eficacia como agentes antidiabéticos.

En esta investigación, *Calea urticifolia* demostró la capacidad de reducir la glucosa en sangre en ratones diabéticos machos C57BL/6, con lo cual se valida su actividad como un agente fitoterapéutico hipoglucemiante. Además, para el tratamiento de la DM, se necesitan nuevos agentes hipoglucemiantes o combinaciones de fármacos con fitoquímicos y/o preparados herbarios con eficacia terapéutica y menos efectos secundarios. En este estudio, nos centramos en las interacciones de la combinación de *Calea urticifolia* con OAD; aun así, es necesario profundizar en los procesos de ADME.

En comparación con los efectos farmacológicos observados con los OAD´s, se obtienen mejores resultados con OAD´s/CuAqE debido a la presencia de diversos compuestos bioactivos de la planta que pueden actuar en sinergia, actuando sobre las mismas o diferentes vías para reducir la glucosa que los OAD´s. Posteriormente, se demostró la eficacia de *Calea urticifolia* para atenuar los síntomas de DNP sin afectar la salud ni el bienestar de los animales de experimentación.

Ambos efectos, hipoglucemiante y neuroprotector se produjeron con una dosis de 11 mg/kg y parece estar relacionada con la capacidad del extracto y de los compuestos fenólicos, los cuales son su principal componente. Esto podría deberse a la combinación de efectos antioxidantes, antiinflamatorios y neuroprotectores al modular las respuestas oxidativas y proinflamatorias.

Considerando que la DM es una enfermedad crónica multifactorial, se necesita más investigación para comprender mejor el posible mecanismo de la acción hipoglucemiante de esta planta, explorando el efecto de CuAqE en la producción hepática de glucosa, la absorción intestinal de glucosa y la captación periférica de glucosa en el tejido muscular y adiposo.

En concreto, los hallazgos experimentales obtenidos proporcionan un enfoque terapéutico complementario basado en la evidencia para el tratamiento de la DM y de su complicación microvascular mas común que es la DPN.

8. REFERENCIAS GENERALES

1. Acosta-Recalde, Patricia, Zully Vera, Gladys, Morinigo, Macarena, Maidana, Gladys Mabel, & Samaniego, Lourdes. (2018). Uso de plantas medicinales y fitoterápicos en pacientes con Diabetes Mellitus tipo 2. Memorias del Instituto de Investigaciones en Ciencias de la Salud, 16(2), 6-11. https://doi.org/10.18004/mem.iics/1812-9528/2018.016(02)06-011.
2. Batiha, G. E., Al-Kuraishy, H. M., Al-Gareeb, A. I., Alruwaili, M., AlRuwaili, R., Albogami, S. M., Alorabi, M., Saad, H. M., & Simal-Gandara, J. (2023). Targeting of neuroinflammation by glibenclamide in Covid-19: old weapon from arsenal. Inflammopharmacology, 31(1), 1–7. https://doi.org/10.1007/s10787-022-01087-8
3. Cole, J. B., & Florez, J. C. (2020). Genetics of diabetes mellitus and diabetes complications. Nature reviews. Nephrology, 16(7), 377–390. https://doi.org/10.1038/s41581-020-0278-5.

4. Dalsgaard, N. B., Gasbjerg, L. S., Helsted, M. M., Hansen, L. S., Hansen, N. L., Skov-Jeppesen, K., Hartmann, B., Holst, J. J., Vilsbøll, T., & Knop, F. K. (2023). Acarbose diminishes postprandial suppression of bone resorption in patients with type 2 diabetes. Bone, 170, 116687. https://doi.org/10.1016/j.bone.2023.116687.
5. LaMoia, T. E., & Shulman, G. I. (2021). Cellular and Molecular Mechanisms of Metformin Action. Endocrine reviews, 42(1), 77–96. https://doi.org/10.1210/endrev/bnaa023.
6. Lebovitz H. E. (2019). Thiazolidinediones: the Forgotten Diabetes Medications. Current diabetes reports, 19(12), 151. https://doi.org/10.1007/s11892-019-1270-y
7. O'Neill, S. M., Kenny, L. C., Khashan, A. S., West, H. M., Smyth, R. M., & Kearney, P. M. (2017). Different insulin types and regimens for pregnant women with pre-existing diabetes. The Cochrane database of systematic reviews, 2(2), CD011880. https://doi.org/10.1002/14651858.CD011880.pub2
8. Picó-Guzmán, F. J., Martínez-Montañez, O. G., Ruelas-Barajas, E., & Hernández-Ávila, M. (2022). Estimación del impacto económico por complicaciones cardiovasculares y de diabetes mellitus 2019-2028 [The estimated economic impact of cardiovascular and diabetes mellitus complications 2019-2028]. Revista medica del Instituto Mexicano del Seguro Social, 60(Suppl 2), S86–S95.
9. Rodríguez Bolaños, R.deL., Reynales Shigematsu, L. M., Jiménez Ruíz, J. A., Juárez Márquezy, S. A., & Hernández Ávila, M. (2010). Costos directos de atención médica en pacientes con diabetes mellitus tipo 2 en México: análisis de microcosteo [Direct costs of medical care for patients with type 2 diabetes mellitus in Mexico micro-costing analysis]. Revista panamericana de salud publica = Pan American journal of public health, 28(6), 412–420. https://doi.org/10.1590/s1020-49892010001200002.
10. Rosenstock, J., Allison, D., Birkenfeld, A. L., Blicher, T. M., Deenadayalan, S., Jacobsen, J. B., Serusclat, P., Violante, R., Watada, H., Davies, M., & PIONEER

3 Investigators (2019). Effect of Additional Oral Semaglutide vs Sitagliptin on Glycated Hemoglobin in Adults With Type 2 Diabetes Uncontrolled With Metformin Alone or With Sulfonylurea: The PIONEER 3 Randomized Clinical Trial. JAMA, 321(15), 1466–1480. https://doi.org/10.1001/jama.2019.2942.

11. Salas-Zapata, L., Palacio-Mejía, L. S., Aracena-Genao, B., Hernández-Ávila, J. E., & Nieto-López, E. S. (2018). Costos directos de las hospitalizaciones por diabetes mellitus en el Instituto Mexicano del Seguro Social [Direct service costs of diabetes mellitus hospitalisations in the Mexican Institute of Social Security]. Gaceta sanitaria, 32(3), 209–215. https://doi.org/10.1016/j.gaceta.2016.06.015.
12. Torres-Vanda, M., & Gutiérrez-Aguilar, R. (2023). Mexican Plants Involved in Glucose Homeostasis and Body Weight Control: Systematic Review. Nutrients, 15(9), 2070. https://doi.org/10.3390/nu15092070.
13. World Health Organization (WHO) WHO Guidelines on Safety Monitoring of Herbal Medicines in Pharmacovigilance Systems. World Health Organization; Geneva, Switzerland: 2004. https://www.who.int/publications/i/item/9241592214.

9. ANEXOS

9.1 Participación con presentación de trabajo de investigación


UASLP
CONACYT
MÉXICO
La Universidad Autónoma de San Luis Potosí a través
de la Secretaría de Investigación y Posgrado otorga el presente
Reconocimiento
a Edgar Omar Segura Esparragoza
Por su participación como Ponente en la
XXV
ANIVERSARIO
SEMANA NACIONAL
DE CIENCIA Y TECNOLOGÍA
DESASTRES NATURALES:
TERREMOTOS Y HURACANES


UASLP
Universidad Autónoma
de San Luis Potosí
SECRETARÍA DE
INVESTIGACIÓN
Y POSGRADO
La Universidad Autónoma de San Luis Potosí, a través de la Secretaría de Investigación y Posgrado,
otorga el presente
RECONOCIMIENTO
a Edgar Omar Segura Esparragoza
Por su participación como Ponente en la Semana Estatal de Ciencia y Tecnología realizada del
21 al 25 de octubre de 2019.
"Siempre Autónoma. Por mi Patria Educaré"
SEMANA ESTATAL
DE CIENCIA Y
TECNOLOGÍA

9.2 Participación como asistente


La Universidad Autónoma de Baja California

agradece a

MC. Edgar Omar Segura Esparragoza

Por su asistencia al 1er FORO INTERNACIONAL:
"Investigación Básica y Aplicada de Productos Naturales"

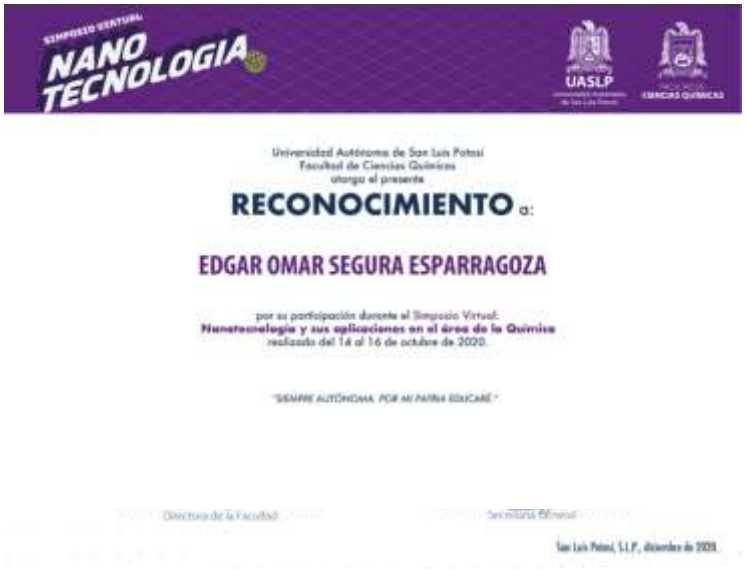
NANO TECNOLOGIA

UASLP

Universidad Autónoma de San Luis Potosí
Facultad de Ciencias Químicas
otorga el presente

RECONOCIMIENTO a:

EDGAR OMAR SEGURA ESPARRAGOZA

por su participación durante el Simposio Virtual:
Nanotecnología y sus aplicaciones en el área de la Química
realizado del 14 al 16 de octubre de 2020.


ENCUENTRO
BIOTEC
2020
EL CAMINO AL MAÑANA

El Instituto Tecnológico de Monterrey campus Laguna
en conjunto con la Sociedad de Alumnos de Bioingeniería

Otorga el presente reconocimiento a:

EDGAR OMAR SEGURA ESPARRAGOZA

Por su asistencia al quinto "ENCUENTRO BIOTEC 2020".
Llevado a cabo los días 11 y 12 de Noviembre de 2020.

Tecnológico de Monterrey


CENIT

2° FORO NACIONAL DE CIENCIAS FARMACÉUTICAS

"A favor de una cultura farmacéutica en México"

La Red Mexicana de Investigación Preclínica y Desarrollo Farmacéutico
otorga la presente

CONSTANCIA

A: Edgar Omar Segura Esparragoza

Por haber asistido al *"SEGUNDO FORO NACIONAL DE CIENCIAS FARMACÉUTICAS"* del 26 al 28 de noviembre de 2020 en modalidad virtual con una duración de 24 horas.

Presidente de la REMDEF

Director del Centro Nayarita de Innovación y Transferencia de Tecnología A.C.

Coordinadora del Cuerpo Académico UAN-CA-302

Asistentes 2° Foro Nacional de Ciencias Farmacéuticas REMDEF

LA SUSCRITA SECRETARIA ACADÉMICA DE LA FACULTAD DE CIENCIAS QUÍMICAS, DEPENDIENTE DE LA UNIVERSIDAD AUTÓNOMA DE SAN LUIS POTOSÍ.

HACE CONSTAR

Que el (la) M.C. Edgar Omar Segura Esparragoza, asistió a la **"15ª Reunión de Aseguramiento de la Calidad y Actualización en tópicos de Obesidad y Diabetes"**, que se llevó a cabo el 29 de Febrero de 2020, como parte del Programa de Evaluación Externa de la Calidad de esta Facultad con 5 horas de valor curricular, con el auspicio del Colegio Mexicano de Ciencias de Laboratorio Clínico, A.C. y la International Federation of Clinical Chemistry and Laboratory Medicine.

Para los usos y fines legales que al (la) interesado (a) convengan, se extiende la presente **CONSTANCIA**, a los 29 días del mes de febrero del dos mil veinte.

"SIEMPRE AUTÓNOMA. POR MI PATRIA EDUCARÉ"

Dra. Sandra Elizabeth Cervantes Niño
SECRETARIA ACADÉMICA

SALUD

Comisión Coordinadora de Institutos Nacionales de Salud y Hospitales de Alta Especialidad
Dirección General de la Coordinación de Hospitales Federales de Referencia
La Unidad Médico Quirúrgica Juárez Centro a través de la Coordinación de Capacitación, Educación y Desarrollo y la Coordinación para la Promoción y Aplicación de la Ciencia y la Tecnología de la Universidad Autónoma de San Luis Potosí, otorgan la presente constancia a

M.C.F.B. EDGAR OMAR SEGURA ESPARRAGOZA

Por su participación como ASISTENTE en el curso:

"Localización de venas, tomo de muestra sanguínea, tamiz neonatal y de orina - Guías CLSI y Recomendaciones EFNL-COLABIOCLI"

De la Unidad Médico Quirúrgica Juárez Centro

San Luis Potosí, los días 14 y 15 de junio 2019.

Colegio Potosino de Químicos Farmacobiólogos, A.C.
Afiliado a la
Federación Nacional de Químicos Clínicos, CONAQUIC A.C.

OTORGAN LA PRESENTE

CONSTANCIA

A:

MCFB. Edgar Omar Segura Esparragoza

Por su participación como ASISTENTE del TALLER:

Control de Calidad en el Diagnóstico por el Laboratorio de las Parasitosis Intestinales

Realizado los días 21 y 22 de Febrero en la ciudad de San Luis Potosí, S.L.P.
Con un valor de 15 horas crédito
San Luis Potosí, SLP. a 22 de Febrero del 2020

10. CARTA DE ACEPTACIÓN Y PORTADA DEL ARTÍCULO

Atena
Editora

DECLARAÇÃO DE PUBLICAÇÃO

A Atena Editora, especializada na publicação de livros, revistas internacionais e coletâneas de artigos científicos em todas as áreas do conhecimento, com sede na cidade de Ponta Grossa-PR, declara que após avaliação cega pelos pares, membros do nosso Conselho Editorial, o artigo intitulado "PROTECTIVE EFFECT OF AQUEOUS EXTRACT OF CALEA URTICIFOLIA IN A MOUSE MODEL OF DIABETIC NEUROPATHY", de autoria de "Edgar Omar Segura Esparragoza, Ismael Jiménez Estrada, Erika García-Chávez, foi aprovado e publicado na revista "International Journal of Biological and Natural Sciences (ISSN 2764-1813)", sob ISSN 2764-1813 e DOI 10.22533/at.ed.813362304079.

Agradeço a escolha pela Atena Editora como meio de transmitir ao público científico e acadêmico o trabalho e parabenizo os autores pela publicação.

Reitero protestos de mais elevada estima e consideração.

Ponta Grossa, 26 de março de 2024

Prof.ª Antonella Carvalho de Oliveira
Doutora em ensino de ciência e tecnologia
Editora Chefe
ATENA EDITORA
PREFIXO EDITORIAL ISBN 97865
PREFIXO EDITORIAL DOI 10.22533

Rua Antônio Rodrigues Teixeira Júnior,122
Ponta Grossa – PR
CEP: 84.015-490
contato@atenaeditora.com.br
www.atenaeditora.com.br

v. 3, n. 6, 2023

International Journal of Biological and Natural Sciences

PROTECTIVE EFFECT OF AQUEOUS EXTRACT OF CALEA URTICIFOLIA IN A MOUSE MODEL OF DIABETIC NEUROPATHY

Edgar Omar Segura Esparragoza
Posgrado en Ciencias Farmacobiológicas, Facultad de Ciencias Químicas, Universidad Autónoma de San Luis Potosí, México.
0009-0009-1830-8197

Ismael Jiménez Estrada
Centro de Investigación y Estudios Avanzados del Instituto Politécnico Nacional, Ciudad de México, México.
0000-0003-2751-3554

Erika García-Chávez
Instituto de Investigación de Zonas Desérticas. Universidad Autónoma de San Luis Potosí, México.
0000-0001-7155-4121